WESTPORT
TECHNOLOGY CENTER INTERNATIONAL

Cementing Technology

DT-97-151 April 1998

DEA 87
FINAL CONCLUSIONS

By:
F. Sabins
T. Edwards
K. Stringer

Westport Technology Center International
6700 Portwest Drive
Houston, Texas 77024
(281) 560-4666
(713) 864-9357 (Fax)
www.westport1.com

Sponsored by: JIP Sponsors
W.O# H09196H000

PERFORMANCE STUDIES OF MUD CONVERTED TO CEMENT DEA-87 FINAL CONCLUSIONS

Introduction

The first phase of DEA-87, "Performance Studies of Drilling Mud Converted to Cement" was a Joint Industry Project (JIP) of 16 industry participants and the Gas Research Institute (GRI). The emphasis of Phase I focused on several key issues associated with Blast Furnace Slag (BFS)/Mud technology. These issues are: gas migration simulating geo-pressured reservoirs; the thermal and chemical stability of the BFS/Mud system under hostile environments, including temperature and CO_2, using a flow loop and galvanic corrosion cells; dimensional stability during hydration, including total hydration volume reduction; and testing the mechanical properties of both BFS/Mud and Portland cements. The mechanical tests included triaxial compressive strength, tensile strength and long term creep. These tests results provided a look at some of the applications and capabilities of the BFS/Mud systems but were not comprehensive.

Phase II testing built on the results of Phase I, but focused primarily on areas and slurry compositions not addressed in Phase I. This included a minor focus on additional tests similar to those conducted in Phase I, but at different conditions and with variations in the slurries. The major focus of Phase II was in other applications of the BFS/Mud systems, BFS-Cement, or BFS by itself in comparison to Portland cement slurries. The first portion of Phase II was a literature search on the hydration of BFS. The second portion of Phase II testing was gas leakage tests simulating geo-pressured reservoirs with various slurry compositions. These tests were conducted both for short term gas migration and long term leakage. The third portion tests the ability of various systems to seal gas in an annular configuration over long time periods with applied high stress.

Gas Migration Testing Procedures:

The test procedures for conducting the gas migration tests were as follows:

1. Fill the model up with water and heat it to the BHCT.
2. Mix approximately 4 gal of the test slurry in a 5 gal bucket.
3. Heat the slurry up to the BHCT while continuously stirring the slurry under low shear.
4. Condition the slurries for one hour.
5. Pump the slurry into the model until good returns from the top of the model are observed.
6. Open valves for water column on top of the cement and gas pressure.
7. Maintain 1.7 psi differential between hydrostatic pressure and the gas pressure.
8. Increase Temperature of the model from BHCT to BHST.
9. Maintain the BHST for the entire testing time.
10. Record the following data:
    a. Temperature of the Model
    b. Pore pressure at several locations in the model (one at the gas entry point, and one at 6 feet from the bottom).
    c. Amount of Gas entering the model (first 48 hours).
    d. Amount of Gas flowing out of the model
11. At the end of the testing period evaluate the path of gas flow

Testing conditions were as follows:
Bottom Hole Circulating Temperature (BHCT) = 126°F
Bottom Hole Static Temperature (BHST) = 152°F
8000 Ft Casing Job with 0.9°F/100 ft Gradient

Phase I - Portland and BFS Cement Mix Formulations:

• Cement #1
Portland Cement + 1.0% D160 + 2.0% Bentonite + 0.2% D65 at 16.5 ppg

• Cement #2
Portland Cement + 0.6% Halad-344 + 2.0% Bentonite + 0.2% CFR3 at 16.5 ppg

• BFS / Mud #1
12.5 ppg Dispersed mud + 5 ppb Sodium Hydroxide + 10 ppb Sodium Carbonate + 0 ppb CLS (Unical) + 350 ppb Blast Furnace Slag (Blue Circle) at 15.6 ppg

• BFS / Mud #2
12.5 ppg PHPA mud + 5 ppb Sodium Hydroxide + 10 ppb Sodium Carbonate + 1 ppb CLS (Unical) + 350 ppb Blast Furnace Slag (Blue Circle) at 15.6 ppg

Phase II - Portland and Dispersed Mud BFS Cement Mix Formulations:

- Test/Slurry No. 1
  Portland Class "H" Cement + 4.0% Bentonite + 1.0% Fluid loss Additive + 0.15% Dispersant at 15.6 ppg

- Test/Slurry No. 2
  Dispersed Mud diluted from 12.5 ppg to 10.5 ppg, 4 ppb Sodium Hydroxide, 0 ppb Sodium Carbonate, 1 ppb Dispersant (Unical), 367.56 ppb Blast Furnace Slag, Final Density of 15.6 ppg.

- Test/Slurry No. 3
  Dispersed Mud diluted from 12.5 ppg to 10.5 ppg, 4 ppb Sodium Hydroxide, 4 ppb Sodium Carbonate, 1 ppb Dispersant (Unical), 359.68 ppb Blast Furnace Slag, Final Density of 15.6 ppg.

- Test/Slurry No. 4
  Dispersed Mud diluted from 12.5 ppg to 10.5 ppg, 4 ppb Sodium Hydroxide, 8 ppb Sodium Carbonate, 2 ppb Dispersant (Unical), 351.60 ppb Blast Furnace Slag, Final Density of 15.6 ppg.

- Test/Slurry No. 5
  Dispersed Mud diluted from 12.5 ppg to 10.5 ppg, 4 ppb Sodium Hydroxide, 12 ppb Sodium Carbonate, 2.5 ppb Dispersant (Unical), 343.76 ppb Blast Furnace Slag, Final Density of 15.6 ppg.

- Test/Slurry No. 6
  PHPA Mud diluted from 12.5 ppg to 10.5 ppg, 4 ppb Sodium Hydroxide, 0 ppb Sodium Carbonate, 3 ppb Dispersant (Unical), 362 ppb Blast Furnace Slag, Final Density of 15.6 ppg.

- Test/Slurry No. 7
  PHPA Mud diluted from 12.5 ppg to 10.5 ppg, 4 ppb Sodium Hydroxide, 4 ppb Sodium Carbonate, 3.5 ppb Dispersant (Unical), 354 ppb Blast Furnace Slag, Final Density of 15.6 ppg.

- Test/Slurry No. 8
  PHPA Mud diluted from 12.5 ppg to 10.5 ppg, 4 ppb Sodium Hydroxide, 8 ppb Sodium Carbonate, 3.5 ppb Dispersant (Unical), 346 ppb Blast Furnace Slag, Final Density of 15.6 ppg.

- Test/Slurry No. 9
  PHPA Mud diluted from 12.5 ppg to 10.5 ppg, 4 ppb Sodium Hydroxide, 12 ppb Sodium Carbonate, 3.5 ppb Dispersant (Unical), 343.76 ppb Blast Furnace Slag, Final Density of 15.6 ppg.

Phase II - Special BFS Cement Mix Formulations:

• Special BFS Cement Mix #1
PHPA (12.5 ppg diluted to 10.5 ppg) + 5.52 lbs/bbl Sodium Hydroxide (NaOH) + 13.81 lbs/bbl Sodium Tripoly Phosphate ($Na_5P_3O_{10}$) + 314.3 ppb Blast Furnace Slag

• Special BFS Cement Mix #2
PHPA (12.5 ppg diluted to 10.5 ppg) + 4.43 lbs/bbl Sodium Hydroxide (NaOH) + 11.07 lbs/bbl Hydrated Lime + 1.85 lbs/bbl Dispersant + 314.3 ppb Blast Furnace Slag

• Special BFS Cement Mix #3
PHPA (12.5 ppg diluted to 10.5 ppg) + 4.43 lbs/bbl Sodium Hydroxide (NaOH) + 11.07 lbs/bbl Sodium Carbonate (Na_2CO_3) + 2 gal/bbl NRJ1428 Water-Borne Acetone Formaldehyde Resin + 314.3 ppb Blast Furnace Slag

The Final Cementing Density was ≈15.2 lbs/gal for all three compositions.

Phase I - Summary and Conclusions

The following conclusions were presented in the final report for Phase I.

1. A reliable gas migration model was developed that can be used to test and compare the abilities of various cementing systems as to their effectiveness of preventing gas migration.

2. Gas Migration for the BFS systems tested in this program exhibited similar physical characteristic in some respects and different in others.

a. Initially the BFS slurries utilizing the dispersed mud and the PHPA mud provided a pressure drop and similar volumes of gas that entered the matrix as did the Portland cement system.

b. Both of the BFS systems tested did not maintain a seal to gas in the hydration times between 12 hours and 36 hours. A significant amount of gas was able to channel through the cement.

3. With the slurries tested in this study the hydration volume reduction of the slag per unit of volume was 1.5 times the volume reduction of Portland cement.

4. For the BFS compositions used in this study, three out of eleven BFS samples showed comparable tensile strengths with Portland. The average tensile strength of Portland cement was 436 psi compared to 290 psi in the three PHPA prepared BFS. However, eight out of the eleven BFS samples failed at lower than 15 psi tensile stress.

5. The compressive strength of Portland cement was found to be approximately 15% greater than BFS with dispersed mud. The Portland cement also displayed a brittle-ductile transition, while BFS displayed only brittle behavior. The shear strength of Portland cement was slightly greater than BFS. Shear strength increased with increasing confining stress in the Portland cement, but remained constant in the BFS.

6. Long-term creep tests demonstrated all three systems exhibited axial "creep" phenomena over a 38 day period. Axial strain did not reach equilibration after 38 days. The axial strain rates of all the samples were low, but the BFS rates were approximately 50% lower than the Portland. Total axial strains after this time were between 1% - 1.5%. None of the samples failed as a result of the "creep" response.

7. Attempts to compare fracture toughness failed because of the inability to extract BFS specimens from their molds. All ten BFS samples broke apart upon removal, while the Portland samples did survive extraction from their molds.

8. It was found that the flowloop, coupled with Inductively Coupled Plasma Spectroscopy (ICP) measurements, could effectively determine dissolution rates of BFS and Portland Cement under the chosen test conditions; temperature, partial pressure of CO_2 and flow velocity.

9. If the BFS cement systems (40% by weight slag) are normalized for available reactive calcium with Portland cement (72% by weight cement) the conversion rate should be considered the same.

10. Below 20 ft/sec dissolution rates of the three samples were insensitive to flow velocity but became flow-dependent at 25 ft/sec. Temperature affected the dissolution to a less degree. However under a nitrogen blanket BFS-dispersed mud dissolved more rapidly than the others. All three test variables (temperature, flow velocity and CO_2) affected the dissolution rates of the cement and BFS systems to a different degree. Among them 200 psi CO_2 was the strongest factor, accelerating dissolution of the three cements, followed by temperature and flow velocity.

Phase II Summary

The following is a summary of conclusions from both Phase I and Phase II.

1. The gas migration model design and test procedures has evolved into a system that produces sensitive, reliable and accurate comparative gas migration results.

2. The gas migration model at the stated test conditions allowed the measurement of several key parameters on the test systems:
a. Pressure drop with time
b. Time of gas entry into the cemented column
c. Real time rate of gas entry
d. Final set bulk permeability of the cemented column

3. The annular seal test device has provided a reliable way to test the long term seal of various cement systems under high stress conditions.

Short Term Gas Migration

1. Several Portland Cement Systems were used as the standard for comparing the Slag-Mix Systems. All of the Portland cement Systems tested had a low amount of gas that entered during the tests and the resultant set bulk permeability to gas was low. (Generally below 50 md)

2. The Slag-Mix utilizing the dispersed mud was difficult to test in the gas migration model due to a small amount of gas that was generated from the system. However the Slag-Mix using the dispersed mud indicated reasonable control of gas migration at activator levels of 4/0, 4/4, and 4/8 ppb (sodium hydroxide/sodium carbonate).

3. The dispersed Slag-Mix system with activator levels of 4/8 produced a high bulk permeability to gas.

4. The PHPA Slag-Mix slurries exhibited abilities similar to the Portland Cement to control gas at low concentrations of activator. At high levels of activator, anything above 4/0, the PHPA Slag-Mix exhibited poor control of gas migration on all tests run in this project.

5. The absence of Sodium Carbonate decreases volume of gas entering the slurry.

6. Increasing the concentration of Sodium Carbonate in the PHPA system allows gas entry to occur earlier, as shown below..

System	Gas Entry @ (minutes)
4/0	1100
4/4	400
4/8	350
4/12	200

7. The Special BFS Cement:
Mix #1 - Did not perform well in preventing gas migration from occurring in the model.
Mix #2 - Did perform well in preventing gas migration from occurring in the model.
Mix #3 - Prevented gas migration in the short term, but did not in the long term.

Annular Seal - Test Models

The test models are a 2 3/8" pipe (1.90" inside diameter) inside a 5" pipe (4" inside diameter) 2 1/2' long (see schematic 2).

Annular Seal - Test Procedures

1. The slurries will be mixed in a one gallon mixer at room temperature.
2. The models annulus will be filled with slurry and placed in an oven and heated to BHST.
3. After curing for a period of over 72 hours the pressure stress test will be conducted.
   a. Stress inside of center casing to preset pressure value for 5 minutes
   b. Release the pressure inside the center casing and measure the flow rate of gas through the models cemented annulus with 50 psi gas pressure for 5 minutes.
   c. Increase the pressure inside the center casing and repeat steps a and b.
   d. Repeat steps c up to safety pressure limit of inside center casing.

Annular Seal - Summary and Conclusions

The following is a summary of conclusions from both Phase I and Phase II.

1. The bulk permeability of the models indicates that the Portland cement system maintained a tight seal to gas for up to 28 days even when pressures of 10,000 psi was placed on the inside of the casing.

2. The 4/0 and 4/12 dispersed BFS Cement systems did not produce an adequate long term seal. Both systems allowed a substantial amount of gas to flow even before any stress was placed inside the casing.

3. The bulk permeability of the models indicates that the Portland cement and the 4/0 PHPA BFS Cement system maintained a tight seal to gas even when pressures of 10,000 psi was placed on the inside of the casing. But the 4/12 PHPA BFS Cement system allowed a substantial amount of gas to flow even before any stress was placed inside the casing.

4. The bulk permeability of the system indicates the Special BFS Cement Mix #2 (with Hydrated Lime) maintained a tight seal to gas up to 28 days even when pressures up to 10,000 psi was placed on the inside casing.

5. Special BFS Cement Mix #3 (with Water-Borne Acetone Formaldehyde Resin) system also maintained a tight seal to gas until 28 days at which time measurement showed a substantial amount of gas to flow relative to earlier measurements.

Literature Survey

A literature survey was also conducted and the results were reported in Progress Report No. 3.

WESTPORT
TECHNOLOGY CENTER INTERNATIONAL

DT-97-151 November 1997

DEA 87 - Phase II
Progress Report No. 5

By:

F. Sabins
T. Edwards
K. Stringer
L. Graham

Westport Technology Center International
6700 Portwest Drive
Houston, Texas 77024
(281) 560-4666
(713) 864-9357 (Fax)
www.westport1.com

Prepared for: DEA 87 Members
WO#H09196H000

DEA 87 PHASE 2
PROGRESS REPORT NO. 5

OBJECTIVE

The objective of this project was to test and compare Blast Furnace Slag (BFS) Cements with Portland Cement in two testing scenarios. The tests conducted were gas migration and annular sealing. This report summarizes the results of Phase II test data conducted on the Special BFS Cement Mix Formulation slurry designs. These Special BFS Cement Mix tests were designed with a lower density than those previously tested in this project. These Special BFS Cement Mix slurries were also designed to have non-progressive gel strengths.

SECTION I - GAS MIGRATION TESTS

This section will outline the gas migration testing results obtained on the Special BFS Cement Mix Formulations using PHPA mud. The gas migration test cell used in the testing is shown in schematic 1. The results for tests conducted are shown in plots 1a, b through 3a, b in the Appendix. In order for the data to be analyzed, each test result is shown in two charts. The first chart (plot a) shows the data in the first 1500 to 1600 minutes. The next chart (plot b) shows the data collected during the entire test time (2 to 7 days). The chart legend shows seven variables in two groups. The top group is graphed along the primary y-axis, the bottom group is graphed along the secondary y-axis. The top group contains the yellow line of the Top heise (psi), the red line for the Bottom heise (psi), and the black line for the Gas In (psi). The bottom group contains the green line for the Gas In (cc's), the blue line for the Gas Out (liters), and the aqua line for the actual Slurry temperature (°F), and the brown line for the Athena temperature (°F). The Athena temperature controller listed on each chart shows the model / pipe control temperature. This Athena temperature as

well as the actual slurry temperature is shown on each plot only as reference to the temperature conditions of the test. The Gas In (cc's), or gas inlet volume, can only be measured up to approximately 1700 to 1800 cc's. Although the actual volume of gas that could enter the model was unlimited, the measurement system would stop measuring after this 1800 cc volume.

Testing Procedures for Seven Day Tests:

Testing conditions were as follows:
Bottom Hole Circulating Temperature (BHCT) = 126°F
Bottom Hole Static Temperature (BHST) = 152°F
8000 Ft Casing Job with 0.9°F/100 ft Gradient

The mud compositions used in the testing was as follows:

Nondispersed System (PHPA)
Sea Water
10.0 ppb Prehydrated Bentonite
1.5 ppb PHPA
2.0 ppb CMS
0.5 ppb PAC-L
NaOH to pH 9.5
Barite to 12.5 ppg
30.0 ppb Rev Dust
Density = 12.5 #/gal
Fluid Loss = 3.6 cc's/30 min.

The test procedures for conducting the gas migration tests were as follows:

1. Fill the model up with water and heat it to the BHCT.
2. Mix approximately 4 gal of the test slurry in a 5 gal bucket.
3. Heat the slurry up to the BHCT while continuously stirring the slurry under low shear.
4. Condition the slurries for one hour.
5. Pump the slurry into the model until good returns from the top of the model are observed.
6. Open valves for water column on top of the cement and gas pressure.
7. Maintain 1.7 psi differential between hydrostatic pressure and the gas pressure.
8. Increase Temperature of the model from BHCT to BHST.
9. Maintain the BHST for the entire testing time.
10. Record the following data:
    a. Temperature of the Model
    b. Pore pressure at several locations in the model (one at the gas entry point, and one at 6 feet from the bottom).
    c. Amount of Gas entering the model (first 48 hours).
    d. Amount of Gas flowing out of the model
11. At the end of the testing period evaluate the path of gas flow

The Special BFS Cement Mix Formulations:

Special BFS Cement Mix #1: PHPA (12.5 ppg diluted to 10.5 ppg) + 5.52 lbs/bbl Sodium Hydroxide (NaOH) + 13.81 lbs/bbl Sodium Tripoly Phosphate ($Na_5P_3O_{10}$) + 314.3 ppb Blast Furnace Slag

Special BFS Cement Mix #2: PHPA (12.5 ppg diluted to 10.5 ppg) + 4.43 lbs/bbl Sodium Hydroxide (NaOH) + 11.07 lbs/bbl Lime + 1.85 lbs/bbl Dispersant + 314.3 ppb Blast Furnace Slag

Special BFS Cement Mix #3: PHPA (12.5 ppg diluted to 10.5 ppg) + 4.43 lbs/bbl Sodium Hydroxide (NaOH) + 11.07 lbs/bbl Sodium Carbonate (Na_2CO_3) + 2 gal/bbl NRJ1428 Resin + 314.3 ppb Blast Furnace Slag

The Final Cementing Density was ≈15.2 lbs/gal for all three compositions.

Laboratory Test Results

The laboratory design test results on each of the Special BFS Cement Mix Formulations tested with the PHPA mud is shown in Table 1.

All the slurries had similar properties. The data for the Portland Cement system is shown for comparison purposes only. Thickening time and Ultrasonic Cement Analyzer (UCA) charts are in the Appendix at the end of this report.

Table 1
Slurry Test Data

Slurry	Portland	Special BFS Cement Mix #1	Special BFS Cement Mix #2	Special BFS Cement Mix #3
Thick Time (Hrs:min)	2:11	3:07	3:01	2:12
Free Fluid @ 80°F (% by vol.)	0	0	0	0
Free Fluid @ 126°F (% by vol.)	0	0	0	0
Fluid Loss (cc's / 30 min.)	69	334	242	228
UCA (50 psi) (500 psi) (24 hrs)	5:04 6:36 2820	4:36 5:02 1800	2:54 3:58 950	2:30 4:02 1071
Rheology (600 rpm (300 rpm) Gel Str.) (10":10")	300+ 164 5: 17	103 60 13 : 15	139 67 4 : 25	300+ 165 52 : 55

Gas Migration Test Results:

Below is the summary of the tests conducted and a description of the data generated for each test. All of the plots are in the Appendix at the end of this report.

- Test / Special BFS Cement Mix #1 - Plot #1a, b
  Composition: PHPA Mud diluted from 12.5 ppg to 10.5 ppg, 5.52 ppb Sodium Hydroxide, 13.81 ppb Sodium Tripoly Phosphate, 314.3 ppb Blast Furnace Slag, Final Density of 15.22 ppg.

  Test Comments: From plot 1a the gas entry started at 88 minutes and the gas out of the model was observed at 218 minutes. The gas flow continued for the entire 7 day testing period. A total of over 1800 cc's of gas entered the model. This is the maximum amount of gas that the gas entry set up can deliver. Plot 2b shows that a total gas out about 74300 cc was observed throughout the testing period. The Top Heise developed mechanical problems and quit reading data to the computer shortly after 200 minutes.

- Test / Special BFS Cement Mix #2- Plot #2a, b
  Composition: PHPA Mud diluted from 12.5 ppg to 10.5 ppg, 4.43 ppb Sodium Hydroxide, 11.07 ppb Hydrated Lime, 1.85 ppb Dispersant (Unical), 314.3 ppb Blast Furnace Slag, Final Density of 15.17 ppg.

  Test Comments: Plot 2a shows that the gas entry and exit from the model started about 400 minutes continued for the entire 7 day testing period. Plot 2b shows that a total of about 800 cc's of gas was measured out of the model during the entire 7 day testing program.

- Test / Special BFS Cement Mix #3 - Plot #3a, b

  Composition: PHPA Mud diluted from 12.5 ppg to 10.5 ppg, 4.43 ppb Sodium Hydroxide, 11.07 ppb Sodium Carbonate, 2 gal/bb NRJ1428 Water-Borne Acetone Formaldehyde Resin, 314.3 ppb Blast Furnace Slag, Final Density of 15.13 ppg.

  Test Comments: In this case, plot 3a shows that the gas entry and exit from the model was just before 200 minutes. Plot 3b indicates that only 68 cc's of gas was measured out of the model during the entire testing period. The pressures indicated a sharp increase at 7500 minutes.

Permeability Measurements:

Tables 2, 3, and 4 summarizes the bulk permeability to gas that was observed and calculated in each of the tests. After the test models completed the seven day (just over 2 days for Special BFS Cement Mix #1) testing period, the flow rate was measured at the top of the models. With the BHST being maintained the models were cut at one foot intervals starting from the top. A special adapter was made to capture the cross-sectional flow of gas through the model at each cut location so flow rate could be measured. Equation 1 was used to calculate the bulk permeability.

Equation 1:

$$k = (q_{sc}\, P_{sg}\, T\, Z\, m\, L) \setminus (3.164\, T_{sg}\, A\, (P_1^2 - P_2^2))$$

where:

k = Permeability, darcy

q_{sc} = Volumetric Flow rate of Gas, SCF/Day

P_{sg} = Standard Pressure, psia

T = Temperature , °R

Z = Z factor

m = Viscosity, cp

L = Length, ft
T_{sg} = Standard Temperature, °R
A = Flowing Area, ft^2
P_1 = High pressure, psi
P_2 = Low pressure, psi

The flow rate q is taken from the inlet gas volumetric flow rate and then adjusted to standard temperature and pressure. These measurements were taken with the model at the test temperature at 5 minute intervals up to 10 minutes.

The matrix permeability was low but the bulk permeability was high because of the flow of gas through the micro channel at the cement / pipe interface.

Table 2
Summary of Flow Rate & Bulk Permeability to Gas
Special BFS Cement Mix #1

Photograph Cut	Length from Gas Inlet (ft)	Pressure (psi)	Flow Rate (cc's / min)	BulK Perm (md)
	10	7.54	62.4	684
A	9	7.55	70.0	690
B	8	31.76	108.6	137
C	7	24.37	65.6	107
D	6	24.38	376	527
E	5	24.31	740.4	868
F	4	24.25	1124	1059
G	3	24.19	1694	1201
H	2	24.07	2898	1379
I	1	7.43	971	1084

Table 3
Summary of Flow Rate & Bulk Permeability to Gas
Special BFS Cement Mix #2

Photograph Cut	Length from Gas Inlet (ft)	Pressure (psi)	Flow Rate (cc's/min)	Bulk Perm (md)
	10	31.3	0.1	0.21
A	9	31.3	0.1	0.10
B	8	31.3	0.0	0.00
C	7	31.3	0.0	0.00
D	6	31.3	0.1	0.06
E	5	31.3	0.2	0.16
F	4	31.3	1.5	0.95
G	3	31.3	2.4	1.16
H	2	31.3	8.0	2.58
I	1	31.3	568	91.6

Table 4
Summary of Flow Rate & Bulk Permeability to Gas
Special BFS Cement Mix #3

Photograph Cut	Length from Gas Inlet (ft)	Pressure (psi)	Flow Rate (cc's/min)	Bulk Perm (md)
	10	31.09	8.4	13.68
A	9	31.11	25.8	37.78
B	8	30.86	46.8	61.66
C	7	31.25	62.0	70.13
D	6	31.24	91.8	89.04
E	5	31.22	103.6	83.82
F	4	31.23	104.2	67.41
G	3	31.21	115.4	56.05
H	2	31.21	124.0	40.15
I	1	31.17	320.0	51.91

Mapping Gas Flow Channels in Models

The model was cut in one foot intervals from the top down. Photos of the cuts of each gas migration tests are shown in figures 1 through 3 in the Appendix. The top cut is identified as Cut A down through Cut I on the bottom. The nitrogen pressure applied to the bottom of the model throughout the gas migration test was continuously maintained through out the cutting process. The temperature on the model was maintained at 152°F BHST through out the cutting process. Immediately after the cut had been made the exposed facial surface was wetted with soapy water. Any gas through the model was identified by the formation of bubbles. If the gas was from between the inner pipe wall and the outer cement surface the area was marked with a grease pen enclosing the area of

bubbles. If the gas was coming through the matrix of cement the area was circled.

The group photo is laid out in the following pattern. A straight line was draw down the outside of the model, the model was cut in one foot sections and each section was orientated in the same position as cut from the model and photographed.

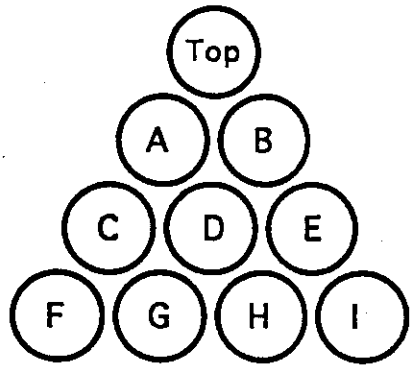

SECTION 2 - DIMENSIONAL STABILITY

OBJECTIVE

The objective of this portion of Phase II is to measure the plastic state shrinkage, total volume reduction and the "gas tightness" of BFS and Portland cement systems by way of the Cement Hydration Analyzer. No slurries were tested in this section. It was recommended by the committee members that due to the limited data obtained in Phase I with this testing that no work would be performed in Phase II.

SECTION 3 - ANNULAR SEALING TEST

OBJECTIVE

The objective of this portion of the project was to test the ability of various BFS systems, and Portland Cement systems, to seal gas in an annular configuration. Well conditions simulating high stress was modeled. The flow rate of dry gas was measured in a full scale annular seal model containing several different slurries for periods up to 28 days. Additionally, the same models will investigate the ability of the systems to seal gas flow in the annulus under high stress conditions.

The tested composition was the following:

- Portland Class H cement + 1.0% Fluid Loss Additive + Bentonite + Dispersant at a Density of 15.6 #/gal
  Bentonite was used to meet design criteria for the cement slurry.

- The slurries tested in this section were Special BFS Cement Mix #2 and Special BFS Cement Mix #3.

(Only three slurries could be tested and one had to be the Portland Cement comparison. Because the Special BFS Cement Mix #1 did not perform well in the gas migration model, it was the one that was chosen to be eliminated in this testing.)

Test Models

The test models are a 2 3/8" pipe (1.90" inside diameter) inside a 5" pipe (4" inside diameter) 2 1/2' long (see schematic 2).

Test Procedures

1. The slurries will be mixed in a one gallon mixer at room temperature.
2. The models annulus will be filled with slurry and placed in an oven and heated to BHST.
3. After curing for a period of over 72 hours the pressure stress test will be conducted.
   a. Stress inside of center casing to preset pressure value for 5 minutes
   b. Release the pressure inside the center casing and measure the flow rate of gas through the models cemented annulus with 50 psi gas pressure for 5 minutes.
   c. Increase the pressure inside the center casing and repeat steps a and b.
   d. Repeat steps c up to safety pressure limit of inside center casing.

Table 5, 6 and 7 summarizes the data for the slurries tested. After the first set of flow rate measurements following the initial curing time period the models were maintained at temperature. Flow rate measurements were taken at two, three, and four weeks. The initial flow rate (0 psi) was measured for a base line at each of these time periods. The models were pressurized to 10,000 psi for five minutes and the pressure was released, then flow rates were measured again.

Measurement of Bulk Permeability

The bulk permeability of the models were calculated from the flow data using Equation 1. Table 5 and Table 6 indicates that the Portland cement and the Special BFS Cement Mix #2 system maintained a tight seal to gas even when after pressures up to 10,000 psi was placed on the inside of center casing for five minutes and then released. Table 7 indicated that the Special BFS Cement Mix #3 system also maintained a tight seal to gas until 28 days at which time measurement showed a substantial amount of gas to flow relative to earlier measurements. The calculated bulk permeability however did not change much with increasing stress on the inside of the center casing.

After the test period was concluded each model was cut in half and gas flow through the cemented annulus was reestablished. The gas flow path was marked on the cut surface of the model which was then photographed. The photographs of each cut model are shown in figures 4, 5, and 6 in the Appendix.

Table 5
Portland Cement System

Pressure of Gas (psi)	Time (days)	Inside Stress Pressure (psi)	Flow rate (cc's / min)	Bulk Perm (md)
50	4	0	15.6	0.83
50	4	1000	25.8	1.37
50	4	2000	28.0	1.48
50	4	3000	29.4	1.56
50	4	4000	27.2	1.44
50	4	5000	29.8	1.58
50	4	6000	30.2	1.60
50	4	7000	32.0	1.69
50	4	8000	30.4	1.61
50	4	9000	35.6	1.88
50	4	10000	38.4	2.03
50	14	0	14.0	0.74
50	14	10000	32.0	1.69
50	21	0	23.6	1.25
50	21	10000	39.4	2.09
50	28	0	26.2	1.39
50	28	10000	29.8	1.58

Table 6
Special BFS Cement Mix #2

Pressure of Gas (psi)	Time (days)	Inside Stress Pressure (psi)	Flow rate (cc's / min)	Bulk Perm (md)
50	4	0	2.9	0.16
50	4	1000	7.4	0.39
50	4	2000	6.6	0.35
50	4	3000	6.9	0.36
50	4	4000	5.8	0.31
50	4	5000	12.6	0.67
50	4	6000	18.8	0.99
50	4	7000	18.6	0.98
50	4	8000	22.2	1.17
50	4	9000	41.0	2.17
50	4	10000	51.8	2.74
50	14	0	21.0	1.11
50	14	10000	36.4	1.93
50	21	0	10.8	0.57
50	21	10000	54.2	2.87
50	28	0	24.0	1.27
50	28	10000	62.1	3.29

Table 7
Special BFS Cement Mix #3

Pressure of Gas (psi)	Time (days)	Inside Stress Pressure (psi)	Flow rate (cc's / min)	Bulk Perm (md)
50	4	0	1638	87
50	4	1000	2076	110
50	4	2000	2362	125
50	4	3000	2203	117
50	4	4000	2648	140
50	4	5000	2588	137
50	4	6000	2610	138
50	4	7000	2740	145
50	4	8000	3192	169
50	4	9000	3150	167
50	4	10000	2680	142
50	14	0	370	20
50	14	10000	2246	119
50	21	0	316	17
50	21	10000	1050	56
50	28	0	22440	1188
50	28	10000	24500	1297

Appendix

Schematic 1 - Gas Migration Model
Schematic 2 - Annular Seal Model

Plot 1a - Gas Migration Test With Special BFS Cement Mix #1 System (Short Time)
Plot 1b - Gas Migration Test With Special BFS Cement Mix #1 System (Entire Test Time)

Plot 2a - Gas Migration Test With Special BFS Cement Mix #2 System (Short Time)
Plot 2b - Gas Migration Test With Special BFS Cement Mix #2 System (Entire Test Time)

Plot 3a - Gas Migration Test With Special BFS Cement Mix #3 System (Short Time)
Plot 3b - Gas Migration Test With Special BFS Cement Mix #3 System (Entire Test Time)

Figure 1a-j: Cross Section Cuts of Gas Migration Model (Special BFS Cement Mix #1 System)

Figure 2a-j: Cross Section Cuts of Gas Migration Model (Special BFS Cement Mix #2 System)

Figure 3a-j: Cross Section Cuts of Gas Migration Model (Special BFS Cement Mix #3 System)

Figure 4 - Cross Section Cut of Annular Sealing Model (Portland Cement)

Figure 5 - Cross Section Cut of Annular Sealing Model (Special BFS Cement Mix #2 System)

Figure 6 - Cross Section Cut of Annular Sealing Model (Special BFS Cement Mix #3 System)

Thickening Time and Ultrasonic Cement Analyzer charts

Schematic 1

DEA-87 PHASE II

GAS MIGRATION MODEL

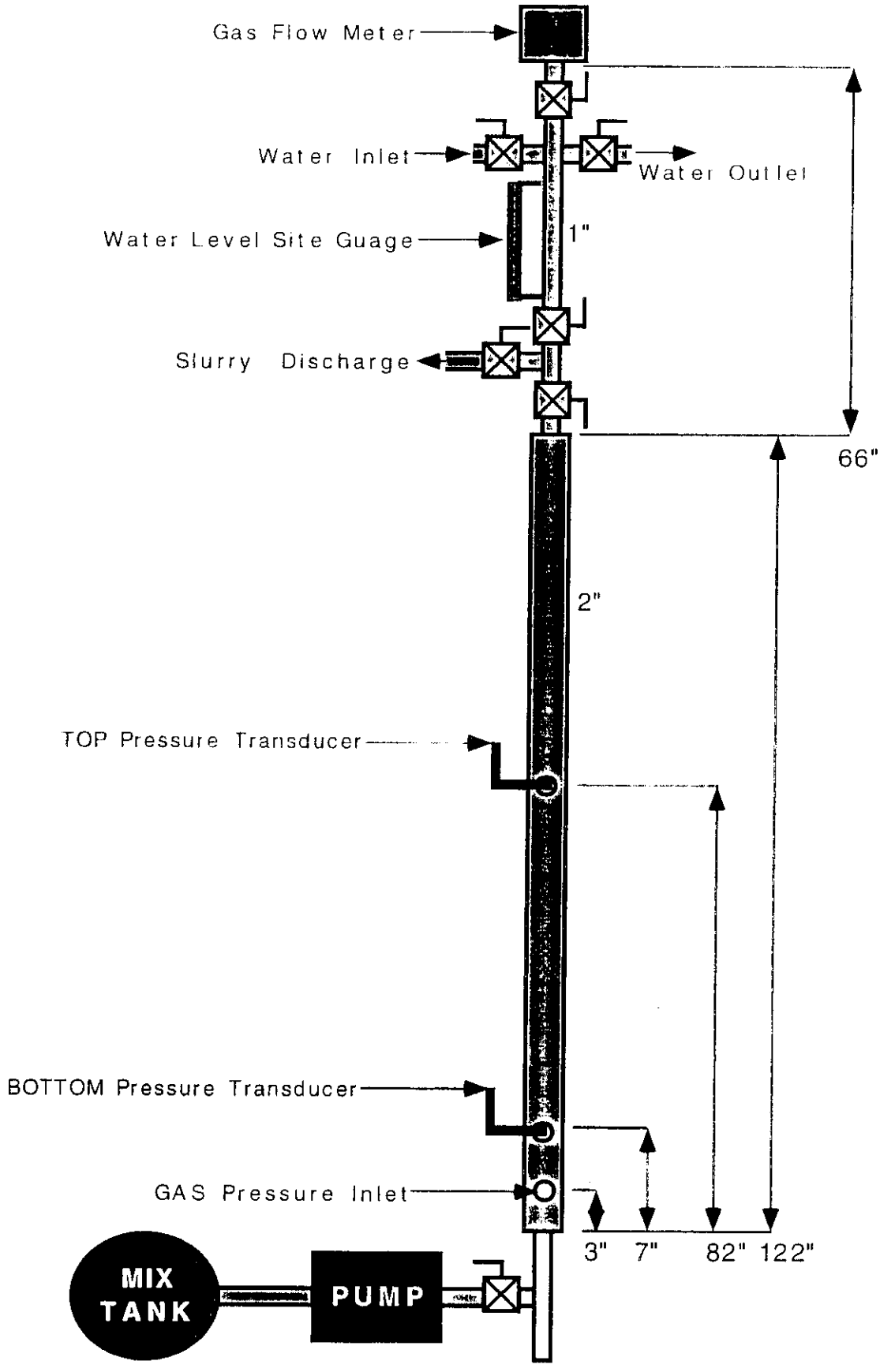

DATA ACQUISITION

ITRI

Schematic 2

ANNULAR SEALING TEST SCHEMATIC

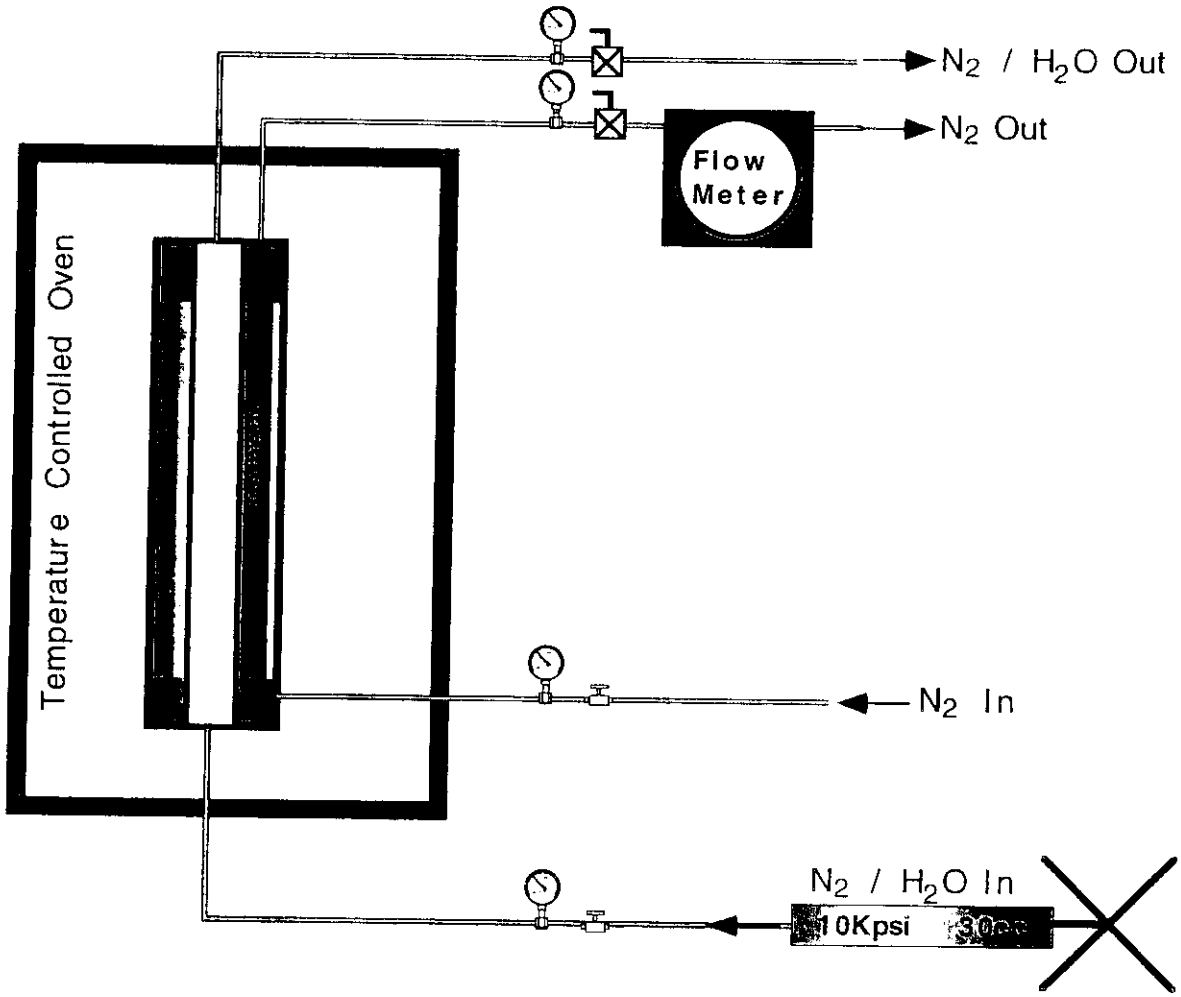

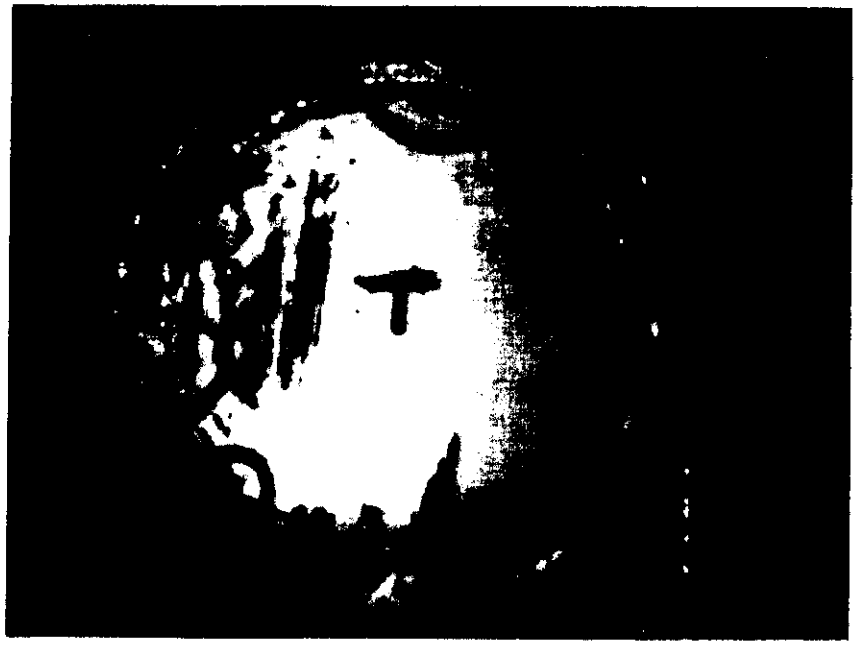

Figure 1a: Special BFS Cement Mix #1 - Cut A

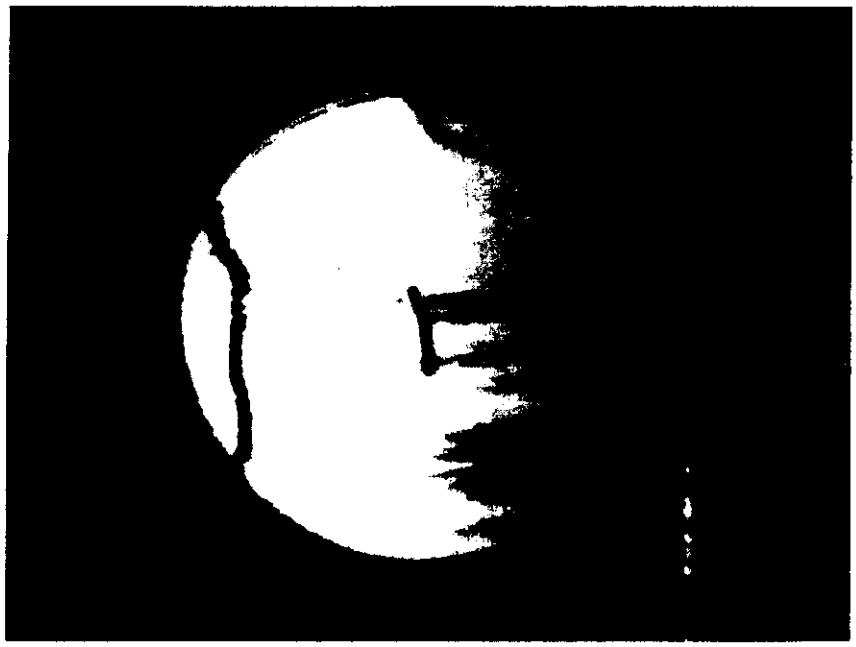

Figure 1b: Special BFS Cement Mix #1 - Cut B

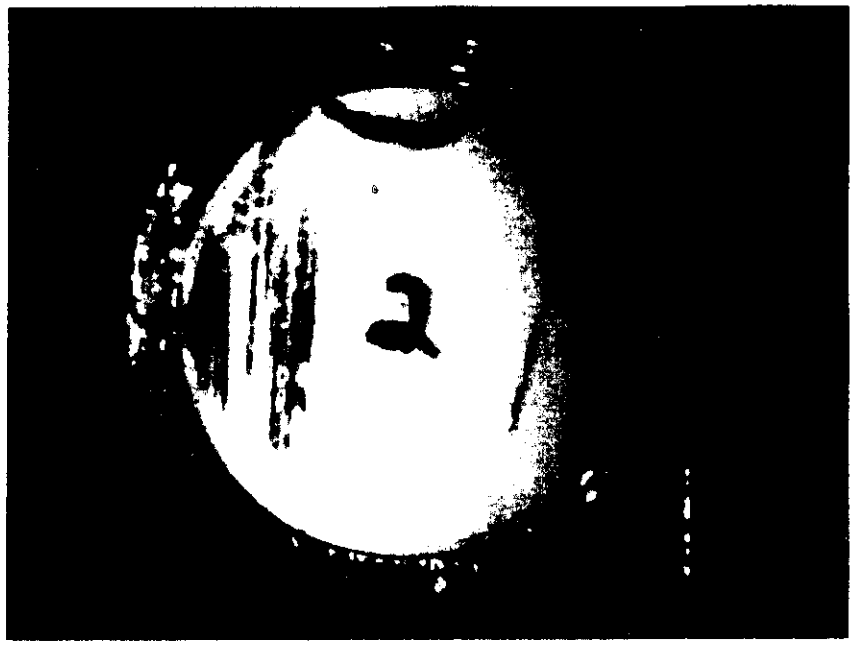

Figure 1c: Special BFS Cement Mix #1 Cut C

Figure 1d: Special BFS Cement Mix #1 Cut D

Figure 1e: Special BFS Cement Mix #1 - Cut E

Figure 1f: Special BFS Cement Mix #1 - Cut F

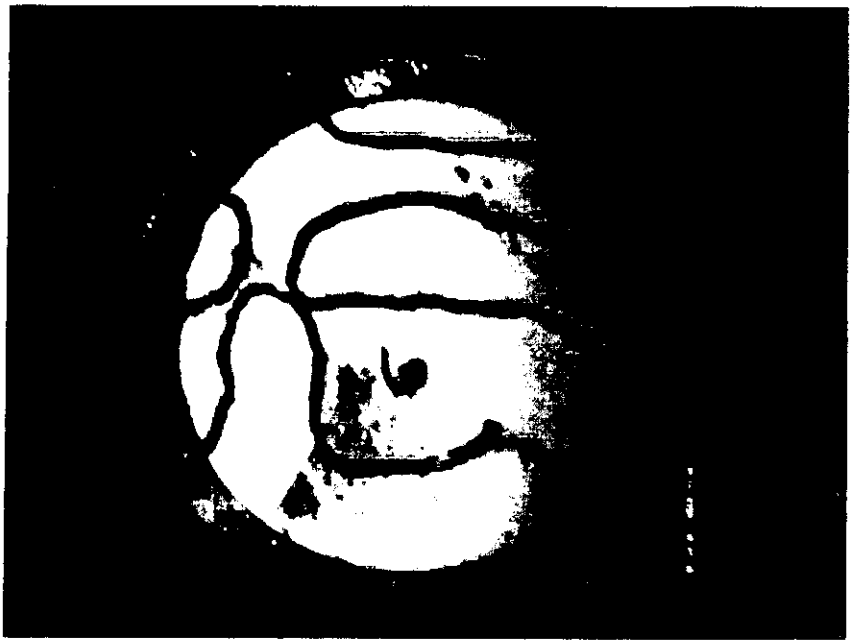

Figure 1g: Special BFS Cement Mix #1 - Cut G

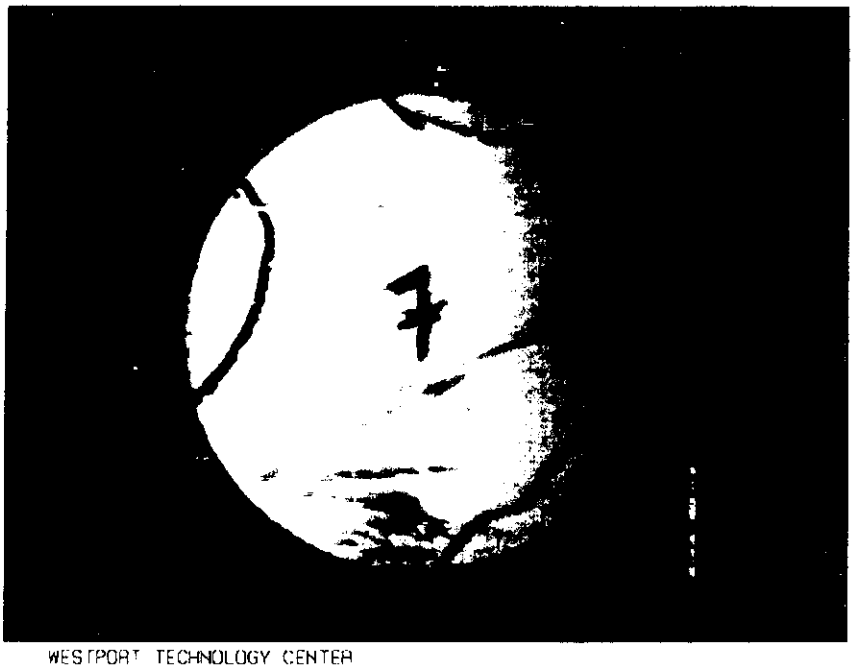

Figure 1h: Special BFS Cement Mix #1 - Cut H

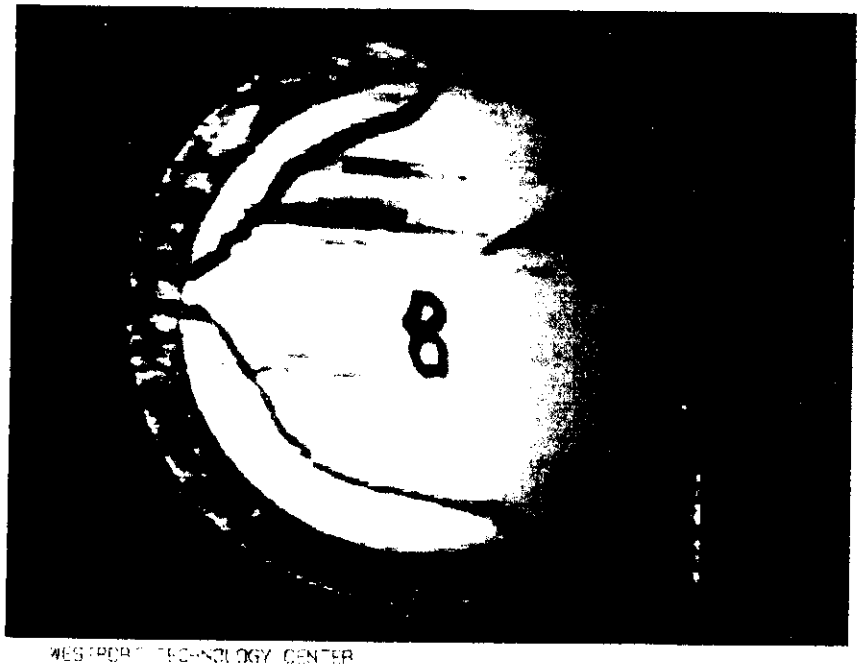

Figure 1i: Special BFS Cement Mix #1 - Cut I

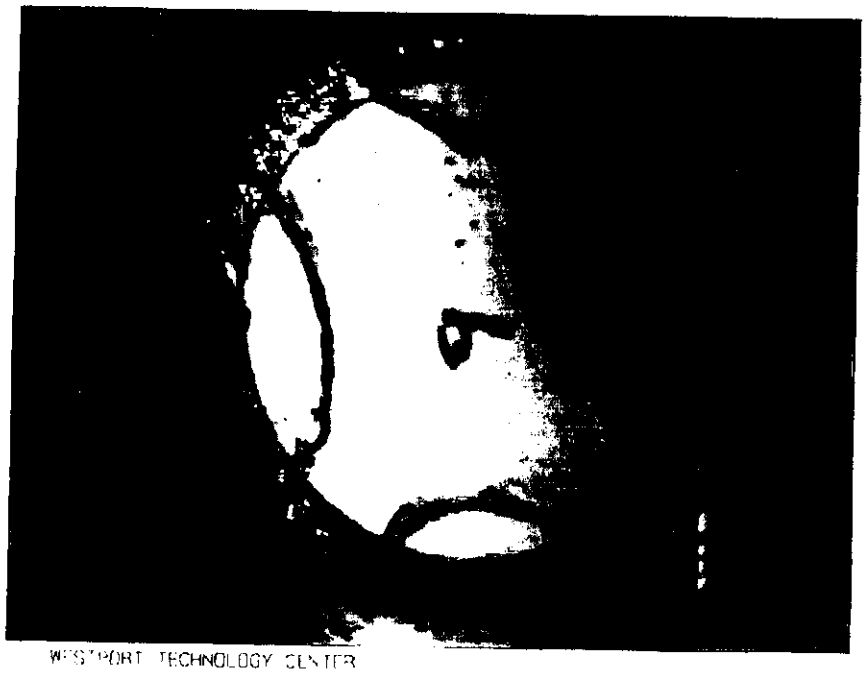

Figure 1j: Special BFS Cement Mix #1 - Cut J

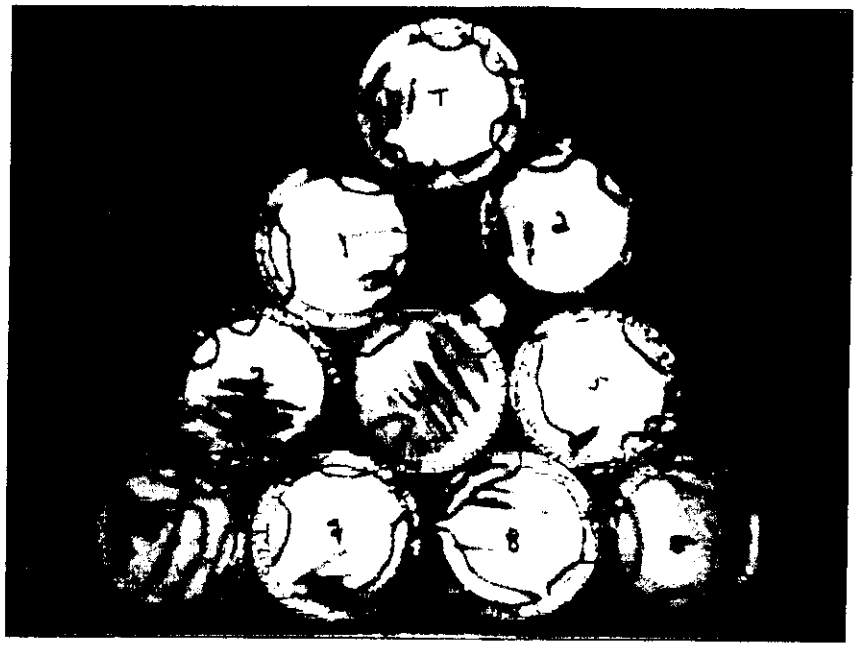

Figure 1k - Special BFS Cement Mix # 1 - Cuts A through J

Figure 2c: Special BFS Cement Mix #2 - CutC

Figure 2d: Special BFS Cement Mix #2 - Cut D

Figure 2e: Special BFS Cement Mix #2 - Cut E

Figure 2f: Special BFS Cement Mix #2 - Cut F

Figure 2g: Special BFS Cement #2 - Cut G

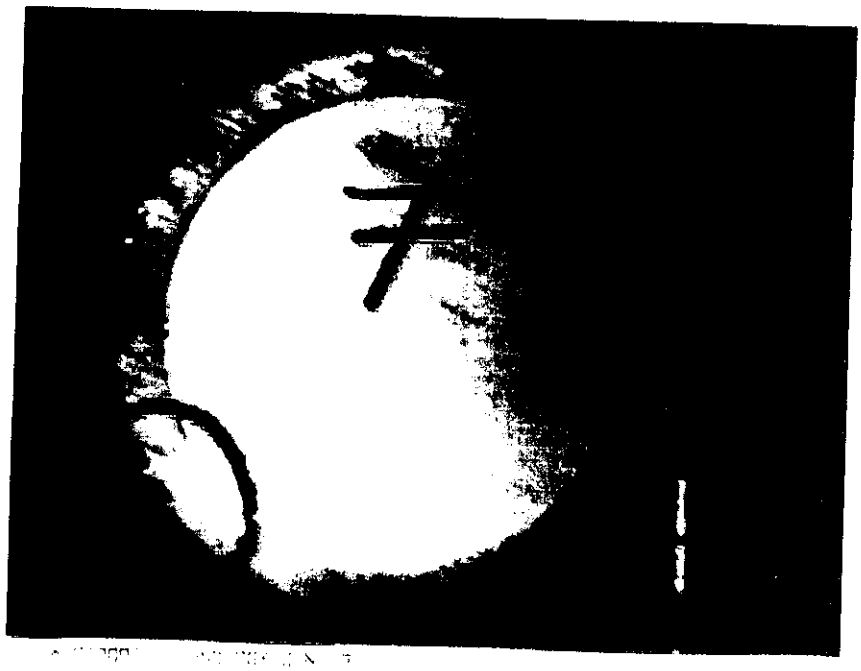

Figure 2h: Special BFS Cement Mix #2 - Cut E

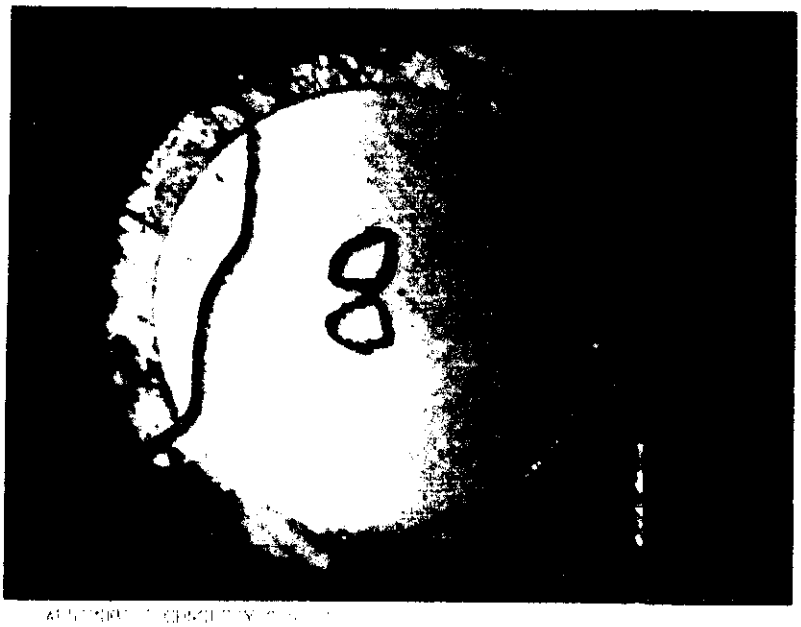

Figure 2i: Special BFS Cement Mix #2 - Cut I

Figure 2j: Special BFS Cement Mix #2 - Cut J

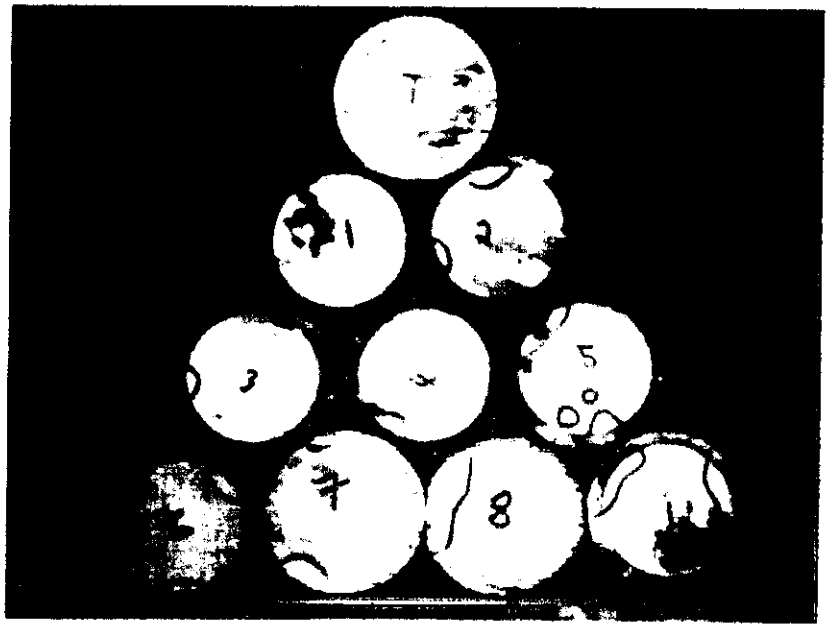

Figure 2k - Special BFS Cement Mix #2 - Cuts A through J

Figure 3a: Special BFS Cement Mix #3 - Cut A

Figure 3b: Special BFS Cement Mix #3 - Cut B

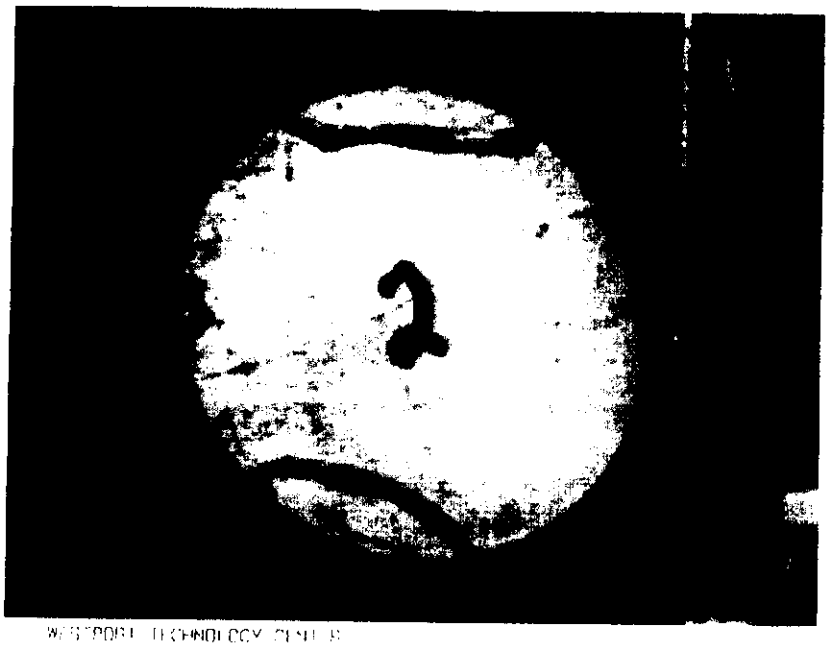

Figure 3c: Special BFS Cement Mix #3 - Cut C

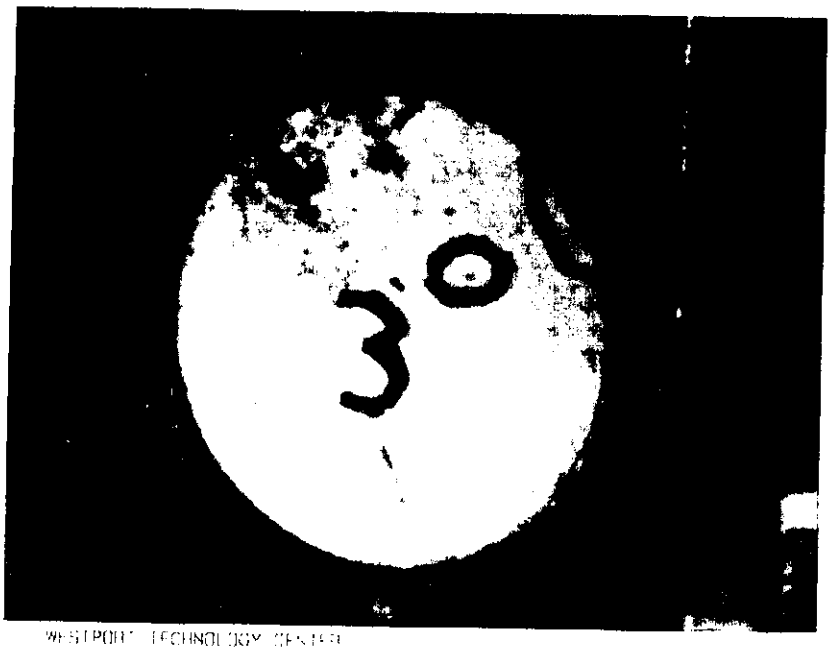

Figure 3d: Special BFS Cement Mix #3 - Cut D

Figure 3e: Special BFS Cement Mix #3 - Cut E

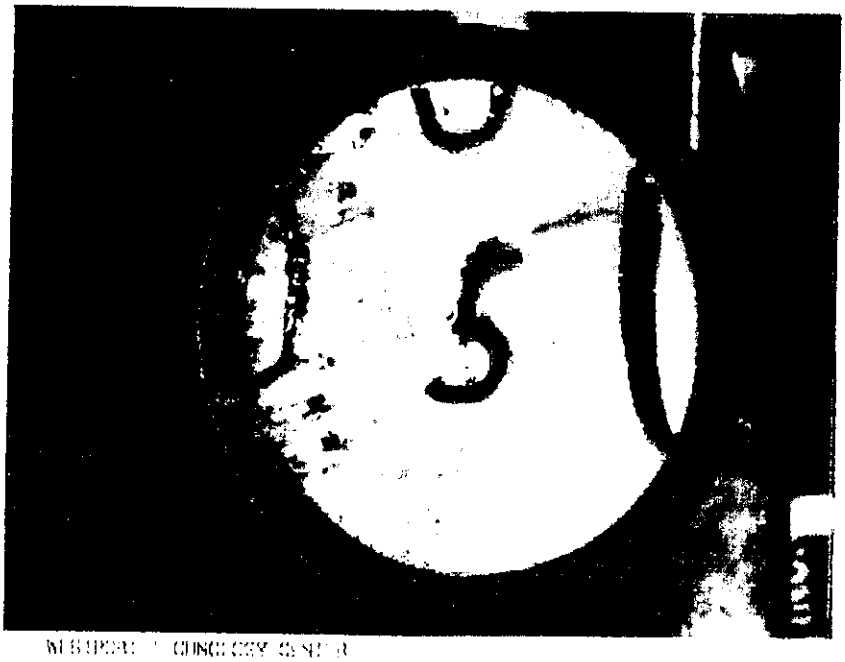

Figure 3f: Special BFS Cement Mix #3 - Cut F

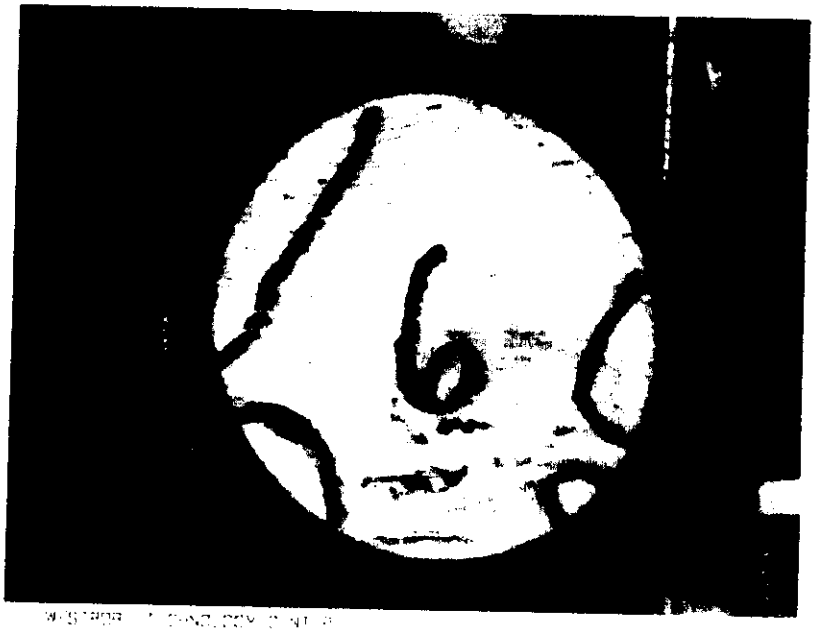

Figure 3g: Special BFS Cement Mix #3 - Cut G

Figure 3h: Special BFS Cement Mix #3 - Cut H

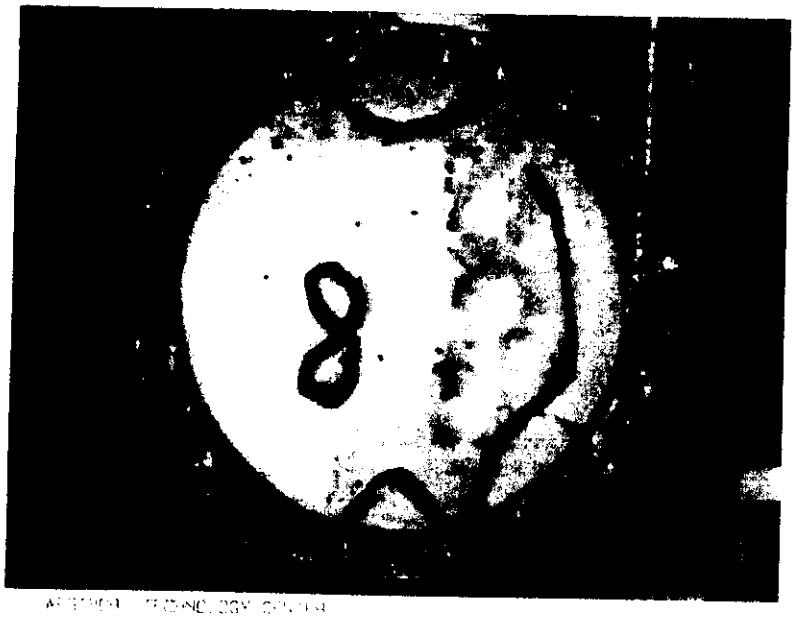

Figure 3i: Special BFS Cement Mix #3 - Cut I

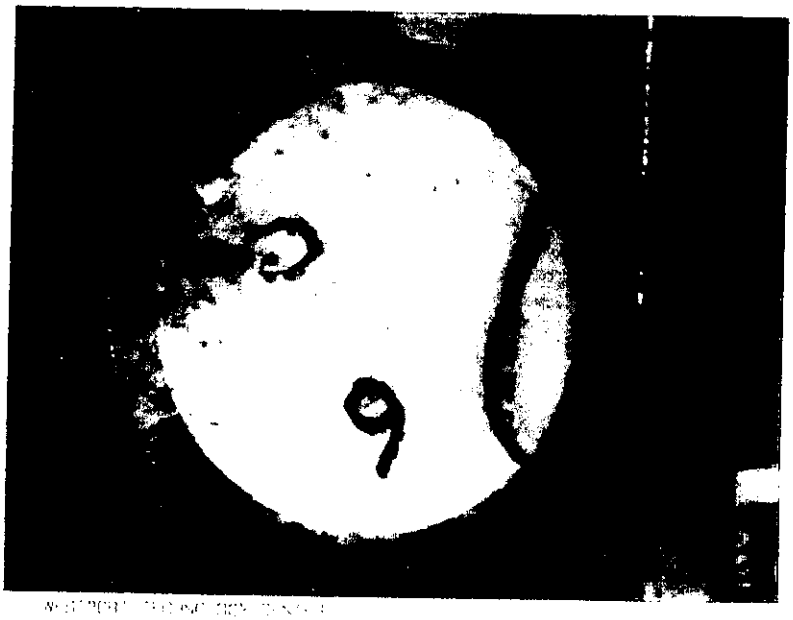

Figure 3j: Special BFS Cement Mix #3 - Cut J

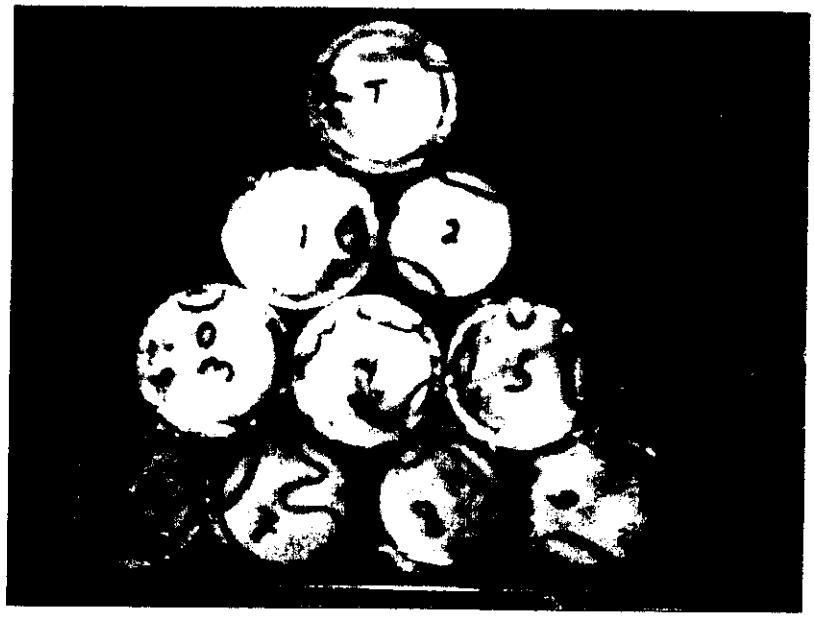

Figure 3k - Special BFS Cement Mix #3 - Cuts A through J

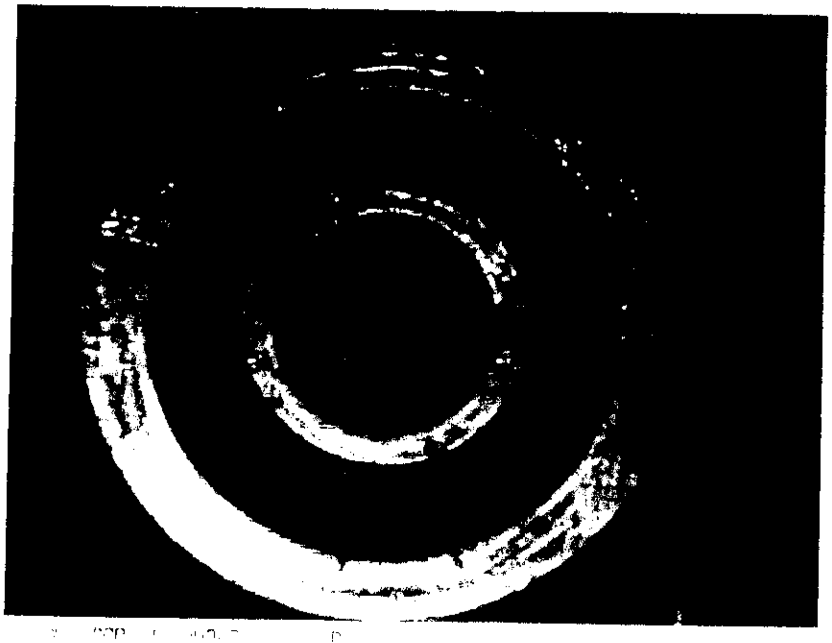

Figure 4: Portland Cement Annular Seal

Figure 5: Special BFS Cement Mix #2 - Annular Seal

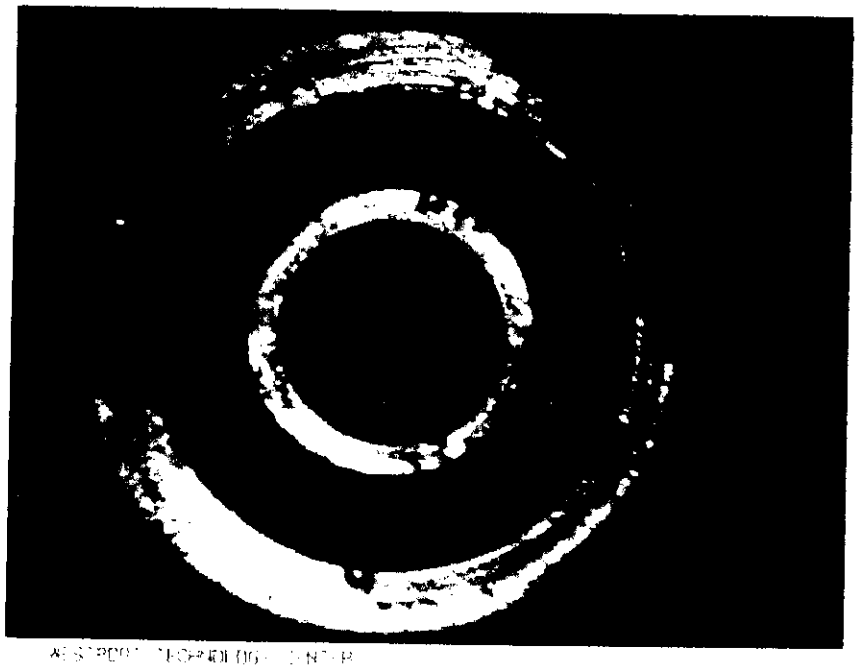

Figure 6: Special BFS Cement Mix #3 - Annular Seal

DEA-87 Phase II

Special BFS Cement Mix #2 — Thickening Time

3:01 (181') to 100 Bc

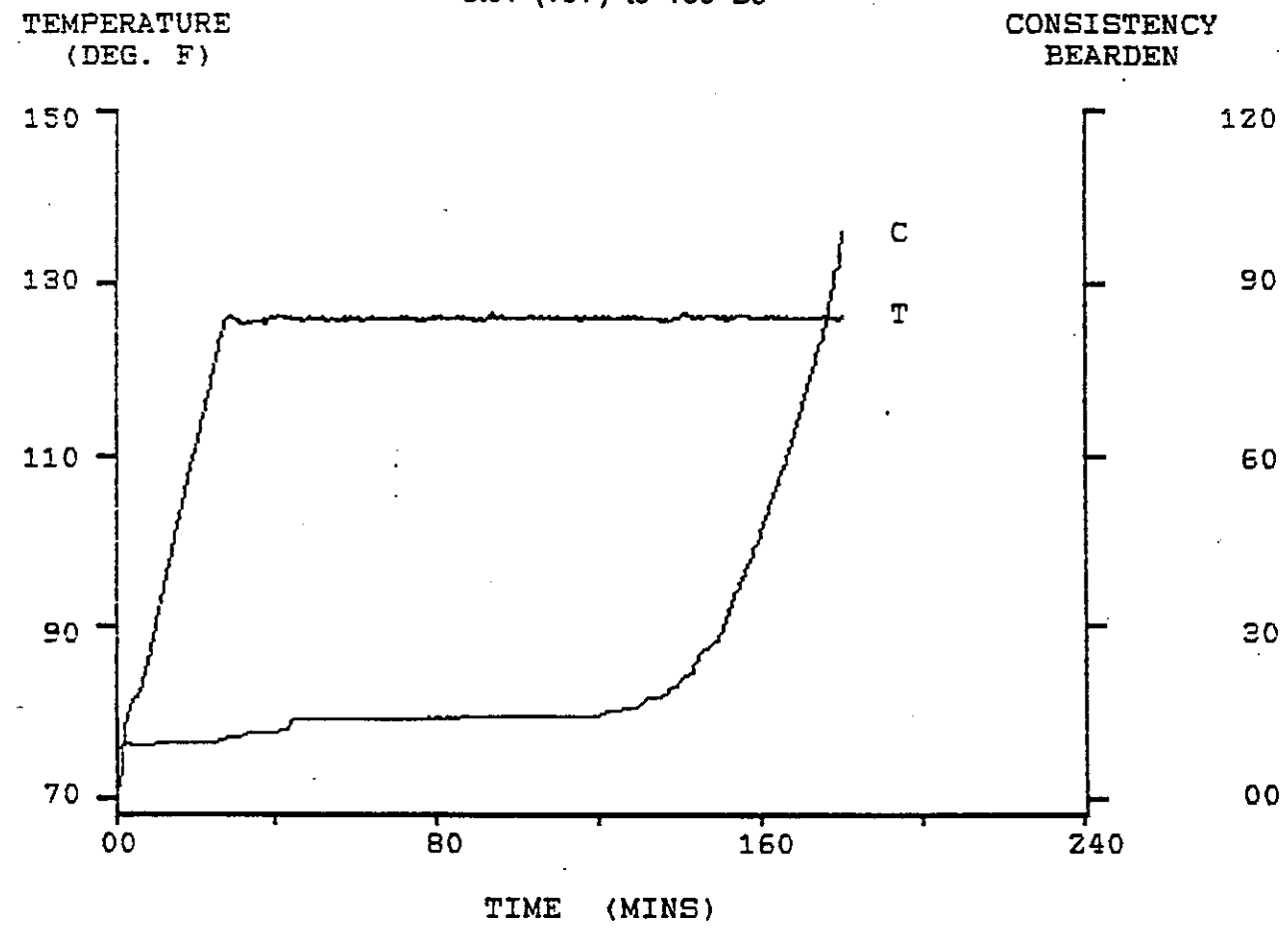

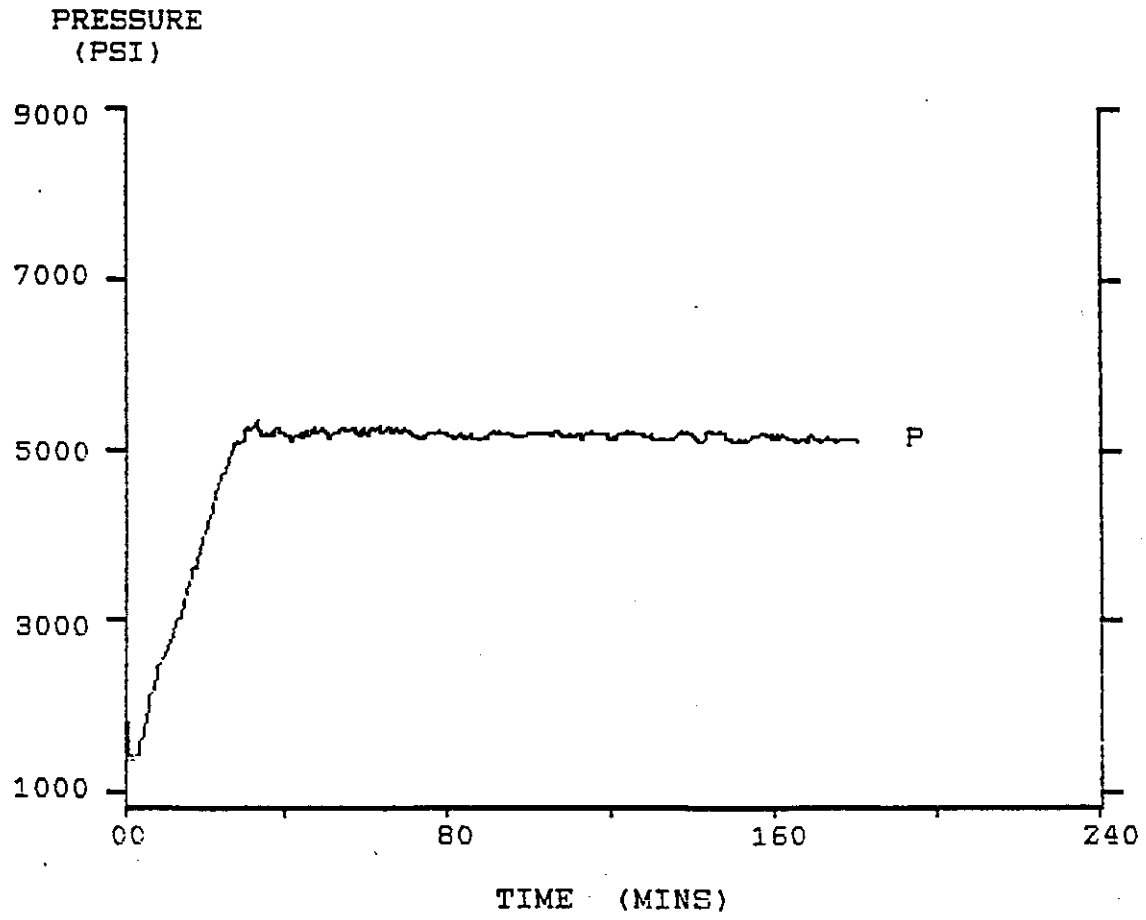

DEA-87 Phase II

Special BFS Cement Mix #3 – Thickening Time

2:12 (132') to 100 Bc

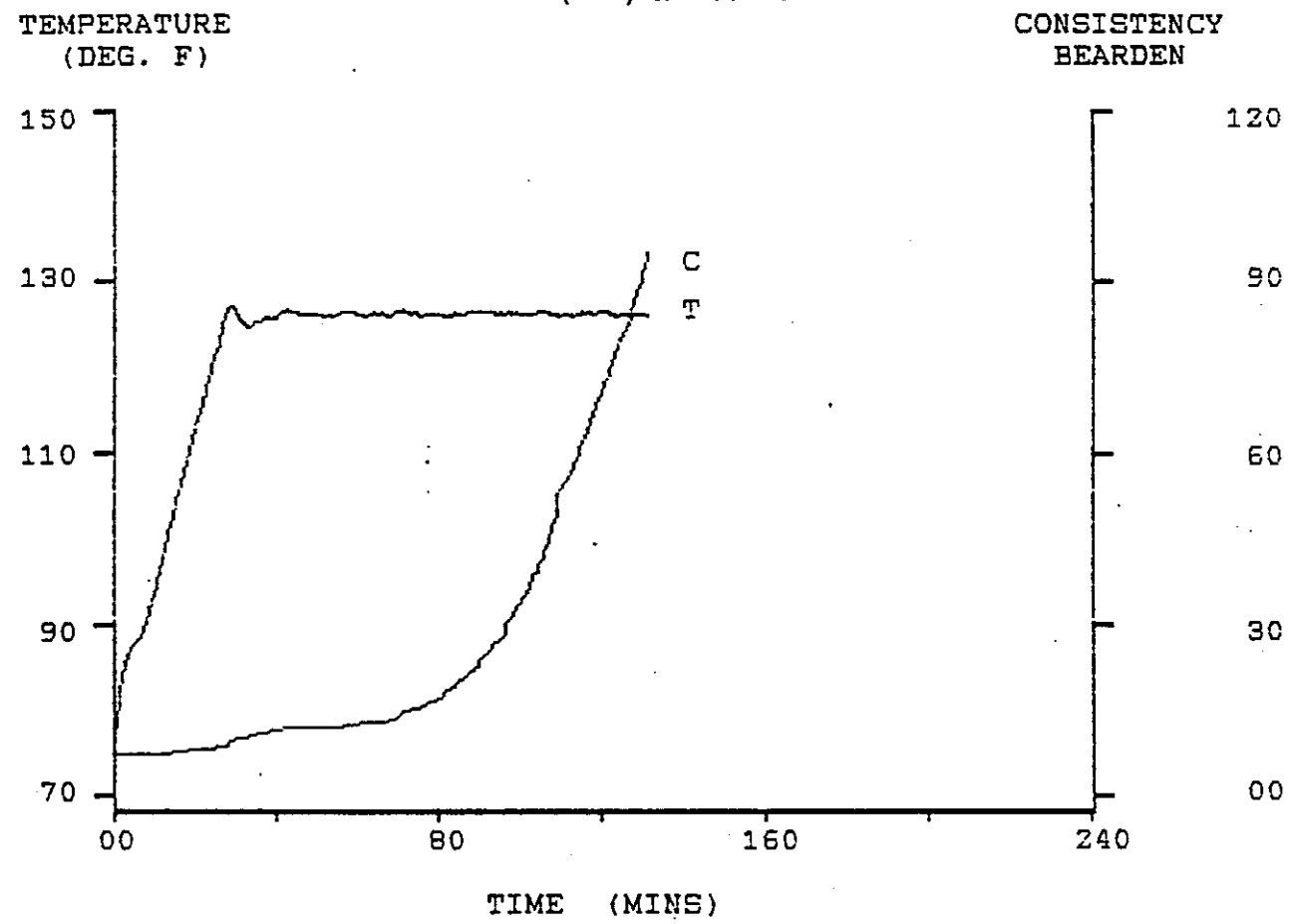

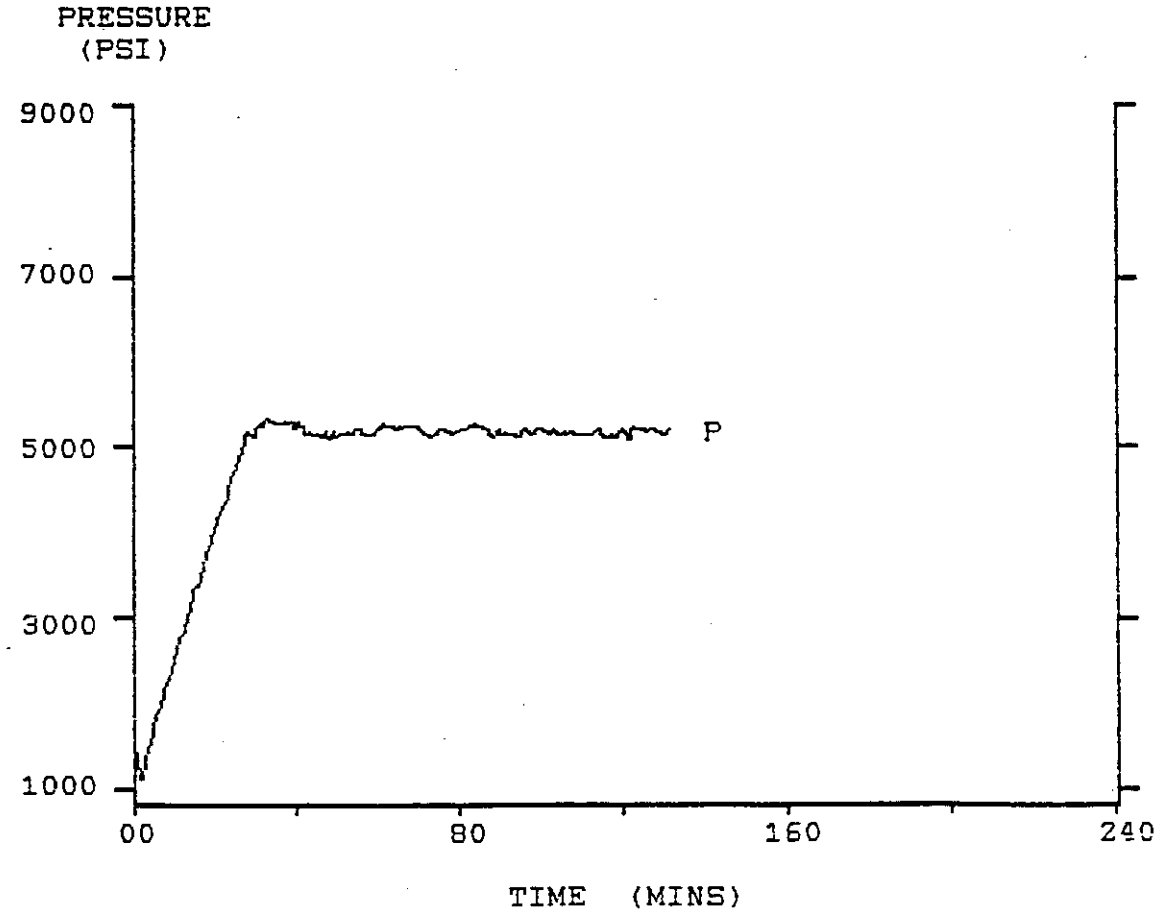

PROJECT NO.: DEA-87 Phase II
DATE: 01/22/97
PRESSURE: 3000 PSI
TEMPERATURE: 152°F BHST

ULTRASONIC CEMENT ANALYZER
HALLIBURTON SERVICES

INITIAL SET:	50	@	4: 36
STRENGTH 1 :	500	@	5: 02
STRENGTH 2 :	19999		
CURR. STR. :	2274	@	69: 47

CEMENT: Special BFS Cement Mix#1: 12.5 ppg PHPA diluted to 10.5 ppg + 5.52 lb/bbl Sodium Hydroxide + 13.81 lb/bbl Sodium Tripoly Phosphate + 314.3 ppb Blast Furnace Slag at 15.2 ppg

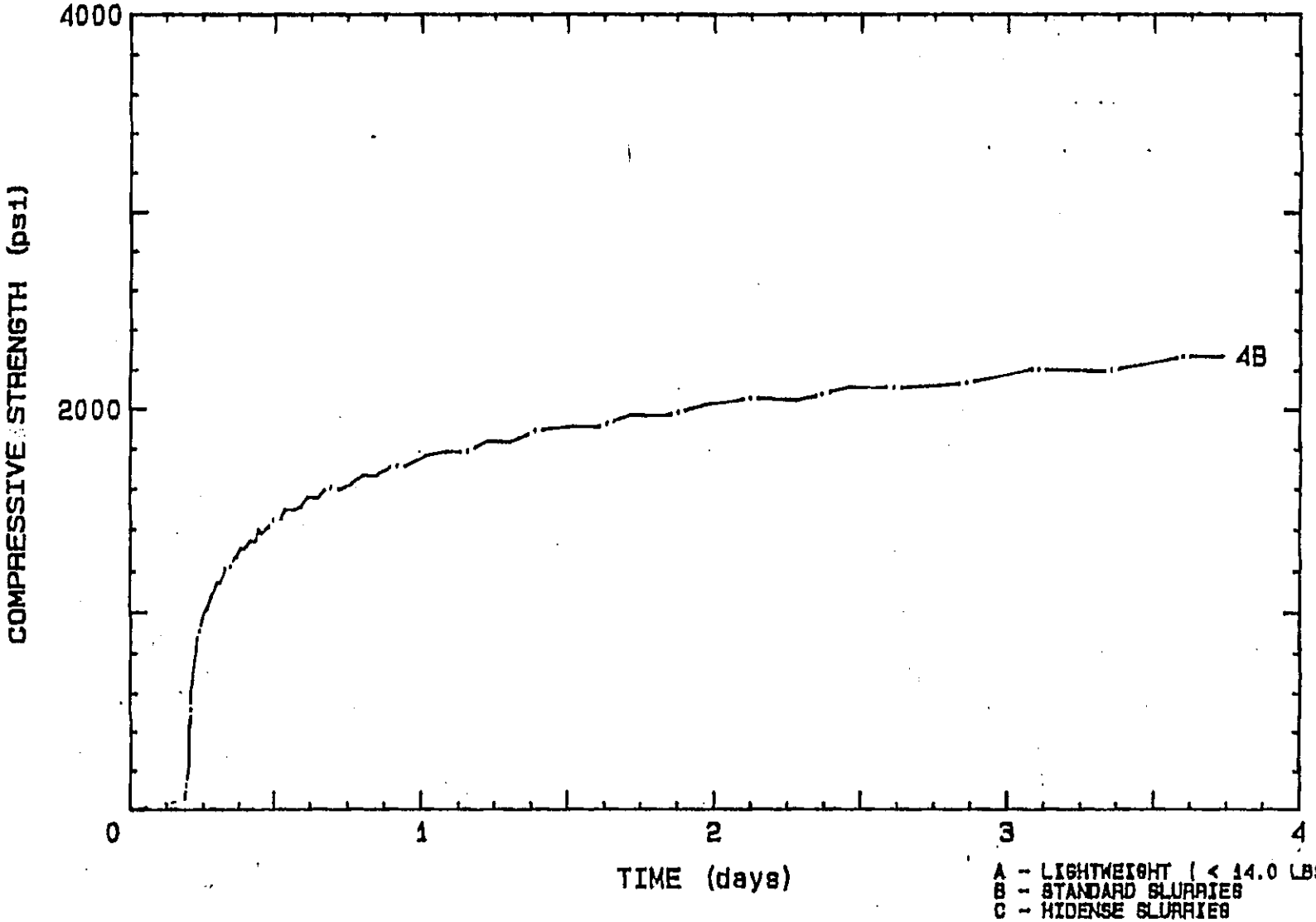

PROJECT NO.: DEA-87 Phase II
DATE: 05/16/97
PRESSURE: 3000 PSI
TEMPERATURE: 152°F BHST

ULTRASONIC CEMENT ANALYZER
WESTPORT TECHNOLOGY

INITIAL SET:	50	@	2:54
STRENGTH 1 :	500	@	3:58
STRENGTH 2 :	19999		
CURR. STR. :	950	@	24:03

Special BFS Cement Mix #2:
CEMENT: 12.5 ppg PHPA diluted to 10.5 ppg + 4.43 lb/bbl Sodium Hydroxide + 11.07 lb/bbl Lime + 1.85 lb/bbl Dispersant + 314.3 ppb Blast Furnace Slag at 15.2 ppg

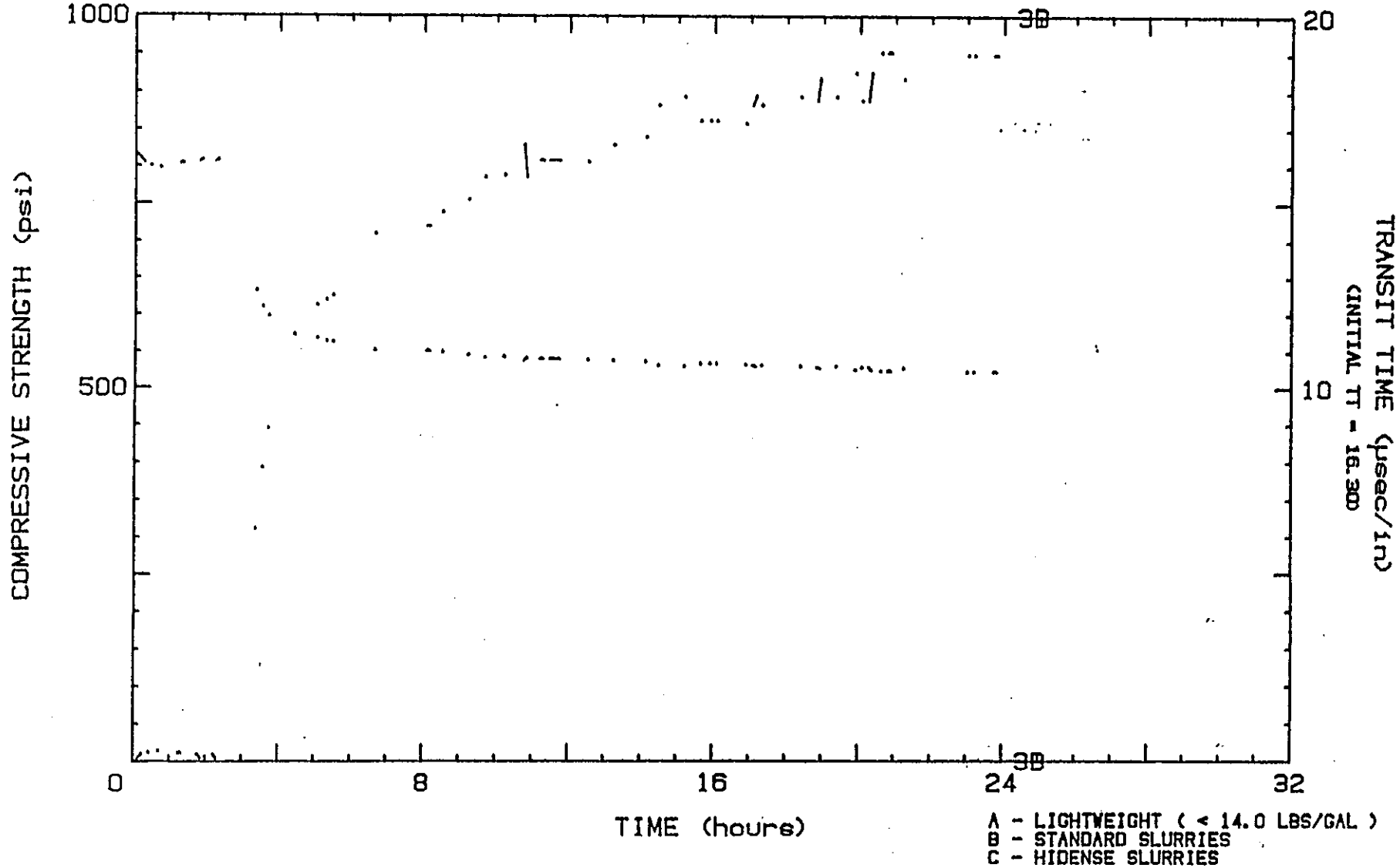

A - LIGHTWEIGHT (< 14.0 LBS/GAL)
B - STANDARD SLURRIES
C - HIDENSE SLURRIES

PROJECT NO.: DEA-87 Phase II
DATE: 09/04/97
PRESSURE: 3000 PSI
TEMPERATURE: 152°F BHST

ULTRASONIC CEMENT ANALYZER
WESTPORT TECHNOLOGY

INITIAL SET:	50	@	2:30
STRENGTH 1 :	500	@	4:02
STRENGTH 2 :	19999		
CURR. STR. :	1071	@	25:16

CEMENT: Special BFS Cement Mix #3:
12.5 ppg PHPA diluted to 10.5 ppg + 4.43 lb/bbl Sodium Hydroxide + 11.07 lb/bbl Sodium Carbonate + 2 gal/bbl NBJ-1428 Resin + 314.3 ppb Blast Furnace Slag at 15.2 ppg

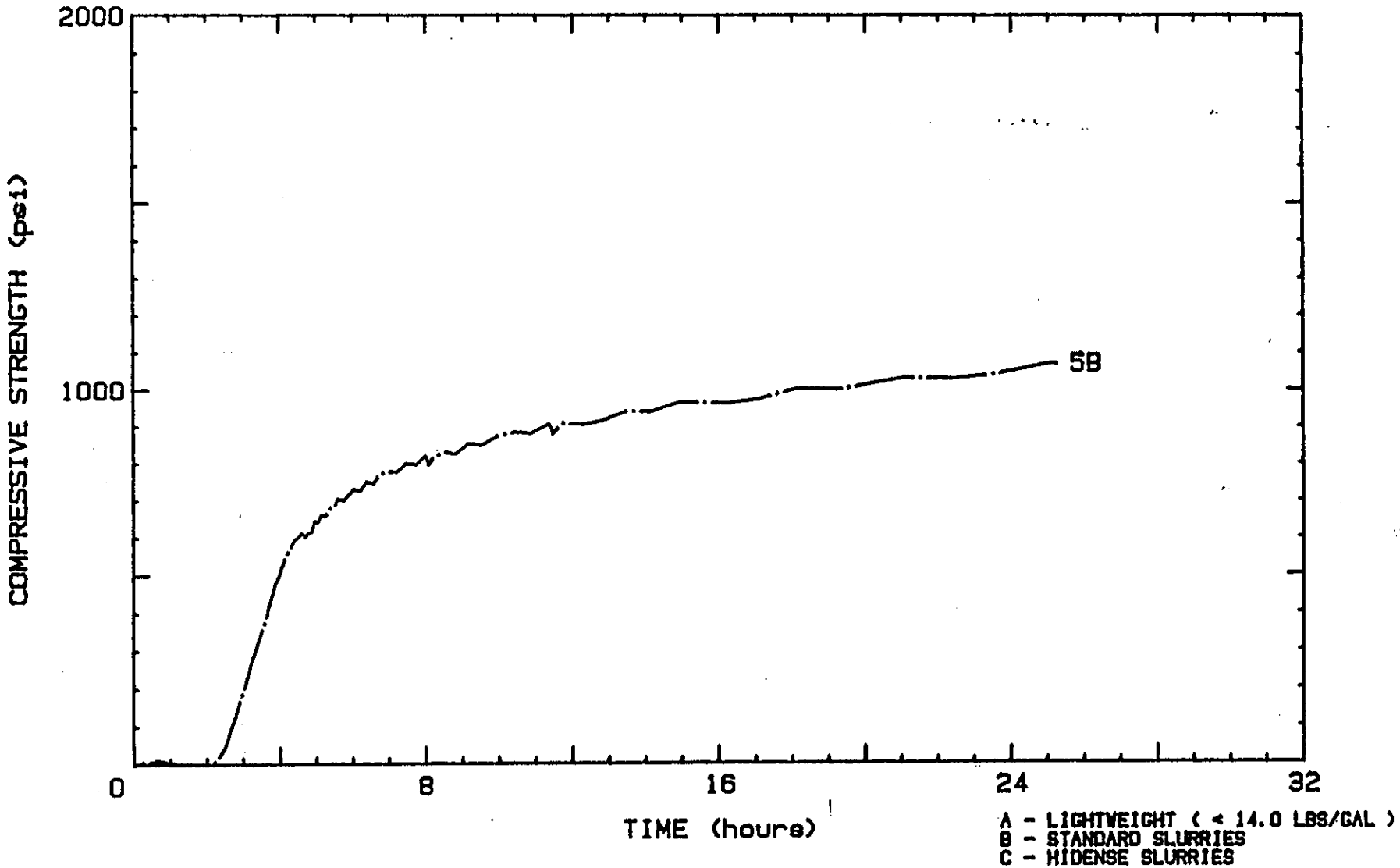

A - LIGHTWEIGHT (< 14.0 LBS/GAL)
B - STANDARD SLURRIES
C - HIDENSE SLURRIES

IIT RESEARCH INSTITUTE
WESTPORT TECHNOLOGY CENTER INTERNATIONAL

DRILLING TECHNOLOGIES

WTCI-96-184 August 1996

DEA-87, PHASE II
PROGRESS REPORT NO. 4

By:

F. Sabins, T. Edwards, & K. Stringer

Westport Technology Center International
6700 Portwest Drive
Houston, Texas 77024
(713) 560-4666
(713) 864-9357 (Fax)
www.westport1.com

Sponsored by: DEA-87 Joint Industry Project
W.O.#: H009196H000

Approved by:
D. B. Young

DEA 87 PHASE 2
PROGRESS REPORT NO. 4

OBJECTIVE

The objective of this project is to test and compare Blast Furnace Slag Cements with Portland Cement in two testing scenarios. These tests were performed: gas migration tests and annular sealing tests. The dimensional stability tests were not performed for this report. This report summarizes the initial data conducted on the cement and slags.

SECTION I - GAS MIGRATION TESTS

This section will outline the gas migration testing results obtained on the PHPA Slag Cements. The gas migration test cell used in the testing is shown in schematic 1. The results for tests conducted so far as shown in plots 1a, b through 4a, b in the Appendix. In order for the data to be analyzed easier each test result was plotted into two plots. The first plot (plot a) shows the data in the first 1000 to 1500 minutes. The next plot (plot b) shows the data collected during the entire test time (over 7 days in most cases).

Testing Procedures for Seven Day Tests:

Testing conditions were as follows:
BHCT = 126°F
BHST = 152°F
8000 Ft Casing Job with 0.9°F/100 ft Gradient

The mud compositions used in the testing was as follows:

Nondispersed System (PHPA)
Sea Water
10.0 ppb PH Bentonite
1.5 ppb PHPA
2.0 ppb CMS
0.5 ppb PAC-L
NaOH to pH 9.5
Barite to 12.5 ppg
30.0 ppb Rev Dust
Density = 12.5 #/gal

The Final Cementing Density was 15.6 #/gal for all compositions.
The cement composition tested was the following:

- Portland Class H cement + 1.0% Fluid Loss Additive + Bentonite + Dispersant at a Density of 15.6 #/gal

Bentonite was used to meet design criteria for the cement slurry.

The test procedures for conducting the gas migration tests were as follows:

1. Fill the model up with water and heat it to the BHCT.
2. Mix approximately 4 gal of the test slurry in a 5 gal bucket.
3. Heat the slurry up to the BHCT while continuously stirring the slurry under low shear.
4. Condition the slurries for one hour.
5. Pump the slurry into the model until good returns from the top of the model are observed.
6. Open valves for water column on top of the cement and gas pressure.
7. Maintain 1.7 psi differential between hydrostatic pressure and the gas pressure.
8. Increase Temperature of the model from BHCT to BHST.
9. Maintain the BHST for the entire testing time.

10. Record the following data:
    a. Temperature of the Model
    b. Pore pressure at several locations in the model (one at the gas entry point, and one at 6 feet from the bottom).
    c. Amount of Gas entering the model (first 48 hours).
    d. Amount of Gas flowing out of the model
11. At the end of the testing period evaluate the path of gas flow

Schematic 1

DEA-87 PHASE II

GAS MIGRATION MODEL

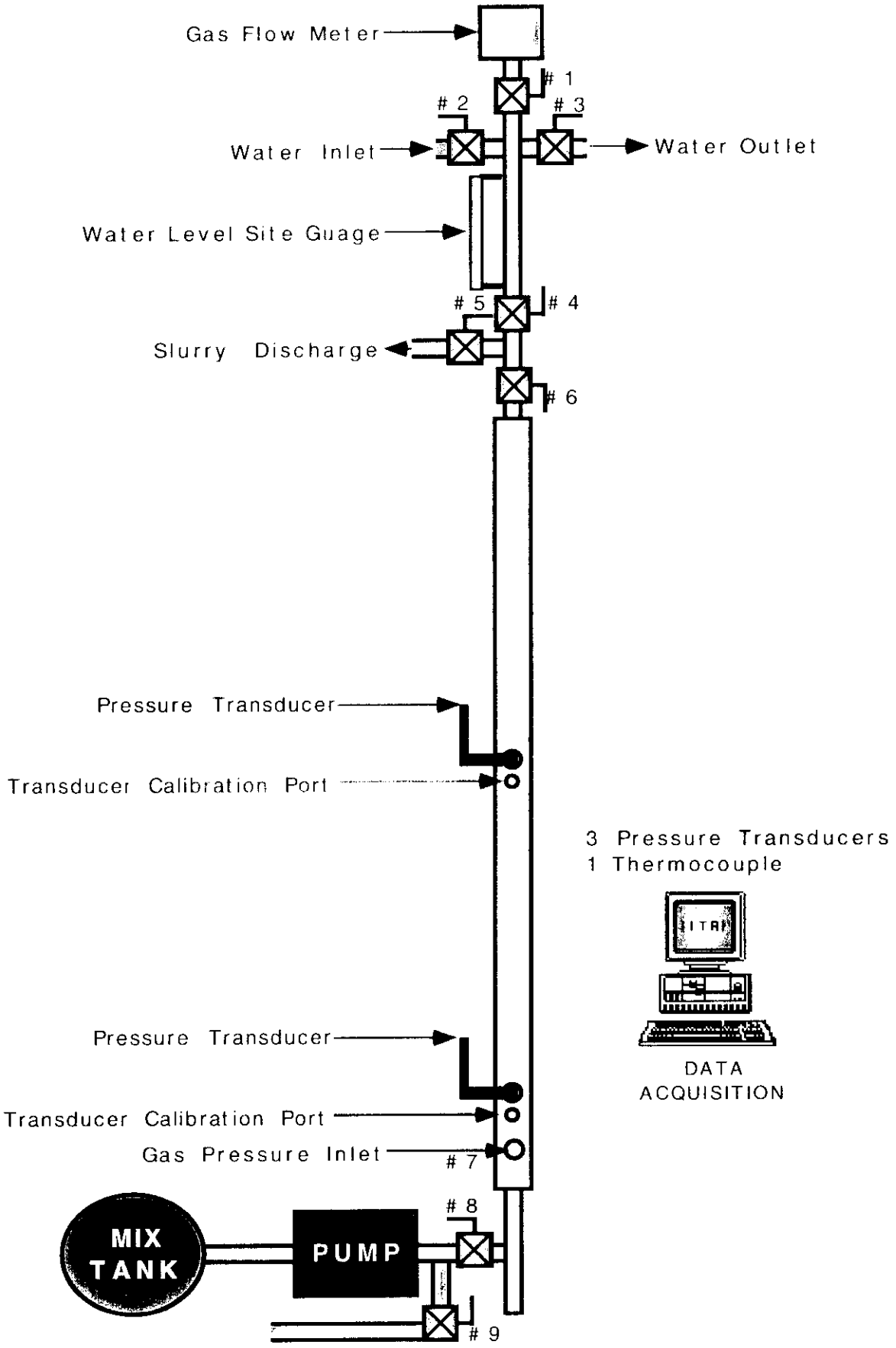

Laboratory Test Results

The laboratory design test results on each of the slurries tested for the PHPA systems is shown in Table 1.

All the slurries had similar properties. The data for the Portland Cement system is shown for comparison purposes only.

Table 1
Slurry Test Data

Slurry	1 Portland	6 PHPA 4/0	7 PHPA 4/4	8 PHPA 4/8	9 PHPA 4/12
Thick Time Hrs:min	2:11	2:41	3:35	3:34	3:03
Free Water cc's	0	0	0	0	0
UCA					
50 psi	5:04	3:03	3:35	3:42	2:43
500 psi	6:36	4:04	3:55	3:53	2:55
24 hrs	2820	1100	1400	1530	1696
Rheology					
600	300+	300+	300+	300+	235
300	164	150	100	141	119
10":10"	5:17	4:7	5:11	5:14	5:14

Seven Day Gas Migration Test Results:

Below is the summary of the tests conducted and a description of the data generated for each test. All of the plots are in the Appendix at the end of this report.

- Test/Slurry No. 6 - plot #1a,b
  Composition: PHPA Mud diluted from 12.5 ppg to 10.5 ppg, 4 ppb Sodium Hydroxide, 0 ppb Sodium Carbonate, 3 ppb Dispersant (Unical), 362 ppb Blast Furnace Slag, Final Density of 15.6 ppg.

  Test Comments: From plot 1a the gas entry started about 1100 minutes and the gas out of the model was observed shortly thereafter. The gas rate in and the gas rate out continued for the entire 7 day testing period. Plot 2b shows that a total of about 5500 cc of gas was observed throughout the testing period.

- Test/Slurry No. 7- plot #2a,b
  Slurry No. 3
  PHPA Mud diluted from 12.5 ppg to 10.5 ppg, 4 ppb Sodium Hydroxide, 4 ppb Sodium Carbonate, 3.5 ppb Dispersant (Unical), 354 ppb Blast Furnace Slag, Final Density of 15.6 ppg.

  Test Comments: Plot 2a shows that the gas entry was much quicker with the 4/4 slurry than the 4/0 slurry. Gas into the model started about 400 minutes and gas was observed shortly after. Plot 2b shows that a total of about 50 liters of gas was measured coming out of the model during the entire 7 day testing program.

- Test/Slurry No. 8 - plot #3a,b
  Slurry No. 4
  PHPA Mud diluted from 12.5 ppg to 10.5 ppg, 4 ppb Sodium Hydroxide, 8 ppb Sodium Carbonate, 3.5 ppb Dispersant (Unical), 346 ppb Blast Furnace Slag, Final Density of 15.6 ppg.

Test Comments: In this case, plot 3a shows that the gas entry into the model was about 350 minutes and the gas out shortly after. Plot 4b indicates that 110 liters of gas was measured out of the model during the entire testing period.

- Test/Slurry No. 9 - plot #4a,b
  Slurry No. 5
  PHPA Mud diluted from 12.5 ppg to 10.5 ppg, 4 ppb Sodium Hydroxide, 12 ppb Sodium Carbonate, 3.5 ppb Dispersant (Unical), 343.76 ppb Blast Furnace Slag, Final Density of 15.6 ppg.

  Test Comments: This slurry allowed gas to enter the model in about 200 minutes. This is the shortest time observed in all of PHPA testing (see plot 5a). The total amount of gas that was measured through the model was over 400 liters (see plot 5b)

Permeability Measurements:

Tables 2, 3, 4 and 5 summarizes the bulk permeability to gas that was observed and calculated in each of the tests. Bulk Permeability were calculated from Cutting the Model. Once the test models were through the seven day testing, they were then cut up into one foot sections. A special adapter was made to capture the cross-sectional flow of gas through the model. Equation 1 was used to calculate the bulk permeability.

Equation 1:

$$k = (q_{sc} P_{sg} T Z \mu L) \setminus (3.164 T_{sg} A (P_1^2 - P_2^2))$$

where:

k = Permeability, darcy

q_{sc} = Volumetric Flow rate of Gas, SCF/Day

P_{sg} = Standard Pressure, psia

T = Temperature , °R

Z = Z factor

μ = Viscosity, cp

L = Length, ft

T_{sg} = Standard Temperature, °R

A = Flowing Area, ft^2

P_1 = High pressure, psi

P_2 = Low pressure, psi

The flow rate q is taken from the inlet gas volumetric flow rate and then adjusted to standard temperature and pressure. These measurements were taken with the model at the test temperature at 5 minute intervals up to 15 minutes.

Table 2
Summary of Bulk Permeability to Gas
4/0 PHPA

Pressure (psi)	Length from Gas Inlet (ft)	Perm (m)
8.6	10	8.2
	9	6.9
	8	--
	7	--
	6	--
	5	12.5
	4	13.6
	3	21.1
	2	23.7
	1	18.8

Table 3
Summary of Bulk Permeability to Gas
PHPA 4/4

Pressure (psi)	Length from Gas Inlet (ft)	Perm (md)
8.6	10	215
	9	286
	8	294
	7	315
	6	355
	5	334
	4	323
	3	426
	2	421
	1	658

Table 4
Summary of Bulk Permeability to Gas
PHPA 4/8

Pressure (psi)	Length from Gas Inlet (ft)	Perm (md)
8.6	10	382
	9	654
	8	605
	7	769
	6	1270
	5	1427
	4	1452
	3	1421
	2	1269
	1	3288

Table 5
Summary of Bulk Permeability to Gas
PHPA 4/12

Pressure (psi)	Length from Gas Inlet (ft)	Perm (md)
8.6	10	776
	9	2724
	8	2980
	7	3149
	6	4300
	5	6311
	4	7609
	3	9955
	2	20610
	1	13491

Mapping Gas Flow Channels in Models

The model was cut in one foot intervals from the top down. Photos of the cuts of each gas migration tests are shown in figures 1 through 4 in the Appendix. The top cut is identified as Cut A down through Cut I on the bottom. The nitrogen pressure applied to the bottom of the model throughout the gas migration test was continuously maintained through out the cutting process. The temperature on the model was maintained at 152°F BHST through out the cutting process. Immediately after the cut had been made the exposed facial surface was wetted with soapy water. Any gas through the model was identified by the formation of bubbles. If the gas was from between the inner pipe wall and the outer cement surface the area was marked with a grease pen enclosing the area of bubbles. If the gas was coming through the matrix of cement the area was circled.

The group photo is laid out in either of the following patterns. Orientation of each piece is in a straight line.

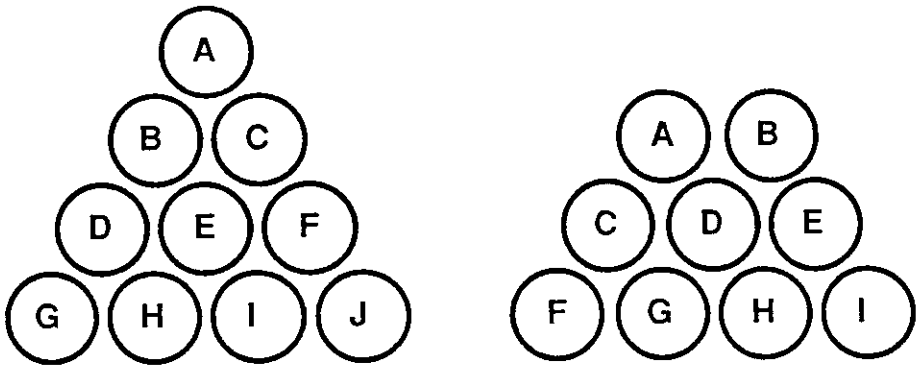

SECTION 2 - DIMENSIONAL STABILITY

OBJECTIVE

The objective of this portion of Phase II is to measure the plastic state shrinkage, total volume reduction and the "gas tightness" of BFS and Portland cement systems by way of the Cement Hydration Analyzer. No slurries were tested in this section. It is recommended that due to the limited data obtained with this testing that no future work should be performed.

SECTION 3 - ANNULAR SEALING TEST

OBJECTIVE

The objective of this portion of the project is to test the ability of various BFS systems, and Portland Cement systems, to seal gas in an annular configuration. Well conditions simulating high stress will be modeled. The flow rate of dry gas will be measured in a full scale annular model containing several different slurries for periods up to 28 days. Additionally, the same model will investigate the ability of the systems to seal gas flow in the annulus under high stress conditions.

The slurries tested in this section will be the same ones used in section 2 and 3.

Test Models

The test models are a 2 3/8" pipe (1.90" inside diameter) inside a 5" pipe (4" inside diameter) 2 1/2' long (see schematic 2). Three different slurries were tested for a pressure stress test only.

Test Procedures

1. The slurries will be mixed in a one gallon mixer at room temperature.
2. The models will be filled with slurry and placed in an oven and heated to BHST.
3. After curing for a period of over 72 hours the pressure stress test will be conducted.
   a. Stress inside of casing to preset value for 5 minutes
   b. Release the pressure inside the casing and measure the flow rate of gas through the model with 50 psi gas pressure for 5 minutes.
   c. Increase the pressure inside the casing and repeat steps a and b.
   d. Repeat steps c up to safety pressure limit of inside casing.
4. After curing for a period of over 72 hours the temperature stress test was to be conducted. These tests however were not conducted on the samples. The procedure was to do the following:
   a. Circulated room temperature water inside the 2 3/8 " casing for 5 minutes.

b. Continually measure the flow rate of gas through the annulus with 50 psi pressure.
c. Increase temperature to 175 °F and repeat steps a and b.
d. Increase temperature to 200 °F and repeat steps a and b.

Table 6, 7 and 8 summarizes the data for the slurries tested.

Schematic 2

ANNULAR SEALING TEST SCHEMATIC

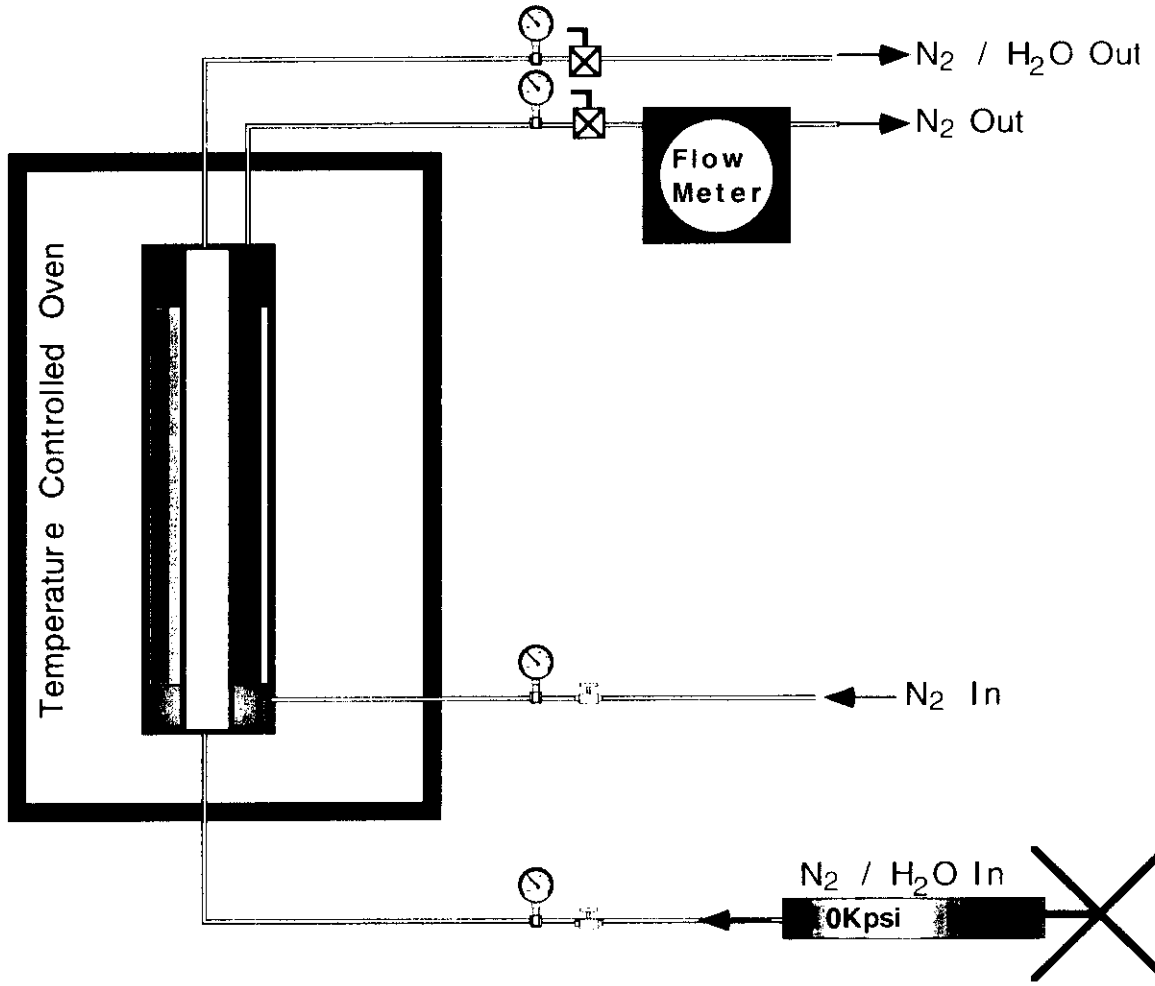

Measurement of Bulk Permeability

The bulk permeability of the models were calculated from the flow data using Equation 1. Table 6 and Table 7 indicates that the Portland cement and the 4/0 PHPA system maintained a tight seal to gas even when pressures of 10,000 psi was placed on the inside of the casing. Table 8 however, indicated that the 4/12 PHPA BFS system allowed a substantial amount of gas to flow even before any stress was placed inside the casing. The calculated bulk permeability however did not change much with increasing stress on the inside casing.

A cut of each of the models is shown in figures 5 ,6 and 7 in the Appendix.

Table 6
Portland Cement System

Pressure of Gas (psi)	Time (days)	Pressure inside casing (psi)	Flow rate (l/5 min)	Perm (md)
50	3	0	0	0
50	3	1000	0	0
50	3	2000	2	0.11
50	3	3000	2	0.11
50	3	4000	2	0.11
50	3	5000	2	0.11
50	3	6000	2.6	0.14
50	3	7000	2.2	0.14
50	3	8000	14	0.74
50	3	9000	20	1.06
50	3	10000	30	1.59
50	14	0	12	0.64
50	14	10000	72	3.81
50	21	0	12	0.64
50	21	10000	42	2.22
50	28	0	10	0.53
50	28	10000	39	2.06

Table 7
BFS System (4/0)

Pressure of Gas (psi)	Time (days)	Pressure inside casing (psi)	Flow rate (l/min)	Perm (md)
50	3	0	0	0
50	3	1000	2	0.11
50	3	2000	2	0.11
50	3	3000	4	0.21
50	3	4000	4	0.21
50	3	5000	2	0.11
50	3	6000	11	0.58
50	3	7000	13.4	0.71
50	3	8000	20	1.06
50	3	9000	26	1.38
50	3	10000	40	2.12
50	14	0	152	8.04
50	14	10000	173	9.16
50	21	0	194	10.27
50	21	10000	230	12.2
50	28	0	88	4.66
50	28	10000	222	11.75

Table 8
BFS System (4/12)

Pressure of Gas (psi)	Time (days)	Pressure inside casing (psi)	Flow rate (l/min)	Perm (md)
50	3	0	7.16	379
50	3	1000	10.4	550
50	3	2000	12.68	671
50	3	3000	14.3	757
50	3	4000	15.66	829
50	3	5000	16.6	879
50	3	6000	17.2	910
50	3	7000	17.56	929
50	3	8000	15.6	826
50	3	9000	16.0	847
50	3	10000	16.8	889
50	14	0	17.0	900
50	14	10000	18.54	981
50	21	0	18.98	1004
50	21	10000	20.58	1089
50	28	0	19.0	1005
50	28	10000	18.2	963

Appendix

Plot 1 a - Gas Migration Test With 4/0 BFS System (Short Time)
Plot 1 b - Gas Migration Test With 4/0 BFS System (Entire Test Time)

Plot 2 a - Gas Migration Test With 4/4 BFS System (Short Time)
Plot 2 b - Gas Migration Test With 4/4 BFS System (Entire Test Time)

Plot 3 a - Gas Migration Test With 4/8 BFS System (Short Time)
Plot 3 b - Gas Migration Test With 4/8 BFS System (Entire Test Time)

Plot 4 a - Gas Migration Test With 4/12 BFS System (Short Time)
Plot 4 b - Gas Migration Test With 4/12 BFS System (Entire Test Time)

Figure 1a-j: Cross Section Cuts Of Gas Migration Model (4/0 BFS System)

Figure 2a-j: Cross Section Cuts Of Gas Migration Model (4/4 BFS System)

Figure 3a-j: Cross Section Cuts Of Gas Migration Model (4/8 BFS System)

Figure 4a-j: Cross Section Cuts Of Gas Migration Model (4/12 BFS System)

Figure 5 - Cross Section Cut Of Annular Sealing Model (Portland Cement)

Figure 6 - Cross Section Cut Of Annular Sealing Model (4/0 BFS System)

Figure 7 - Cross Section Cut Of Annular Sealing Model (4/12 BFS System)

Plot 1a

PHPA 4 / 0

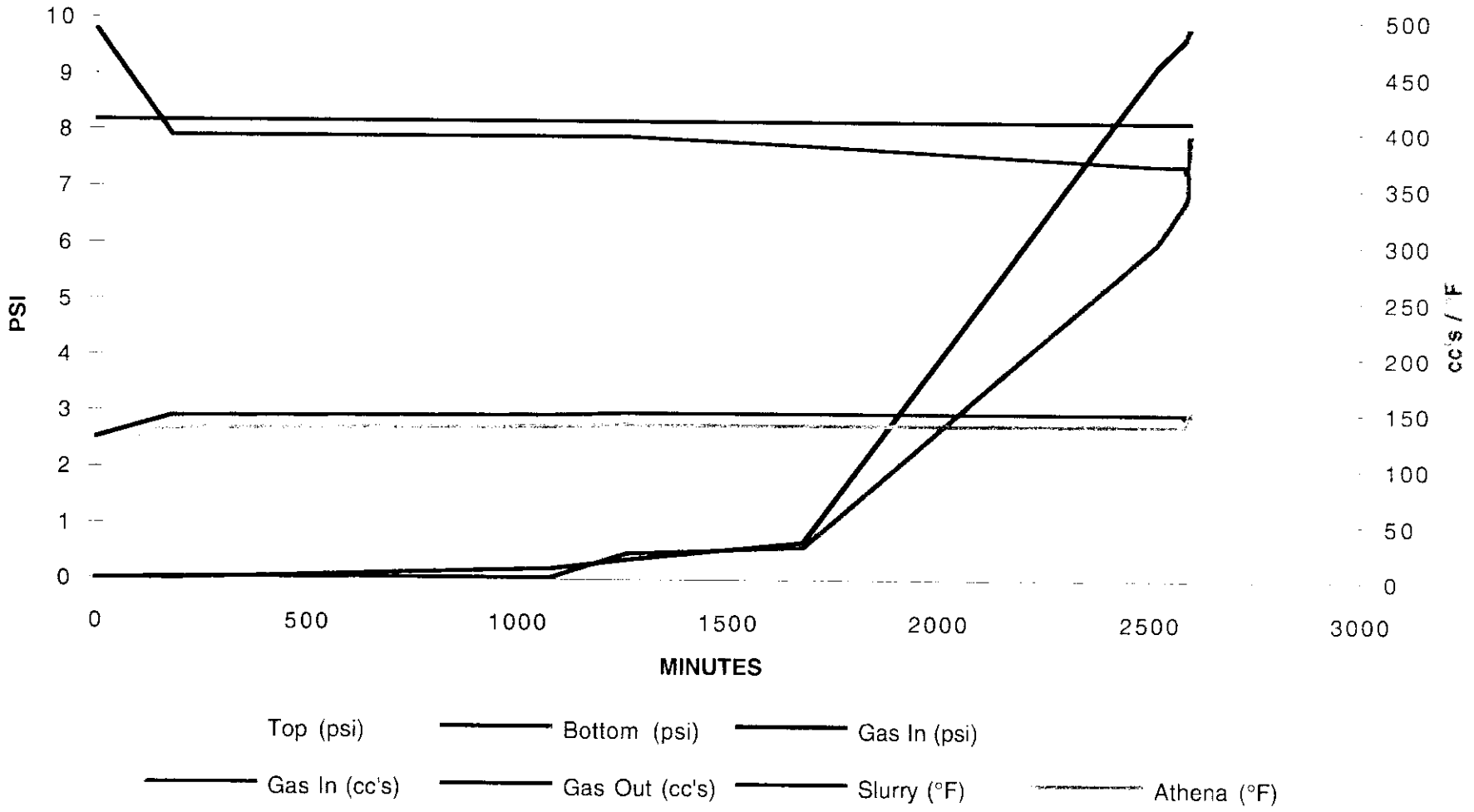

Plot 1b

PHPA 4 / 0

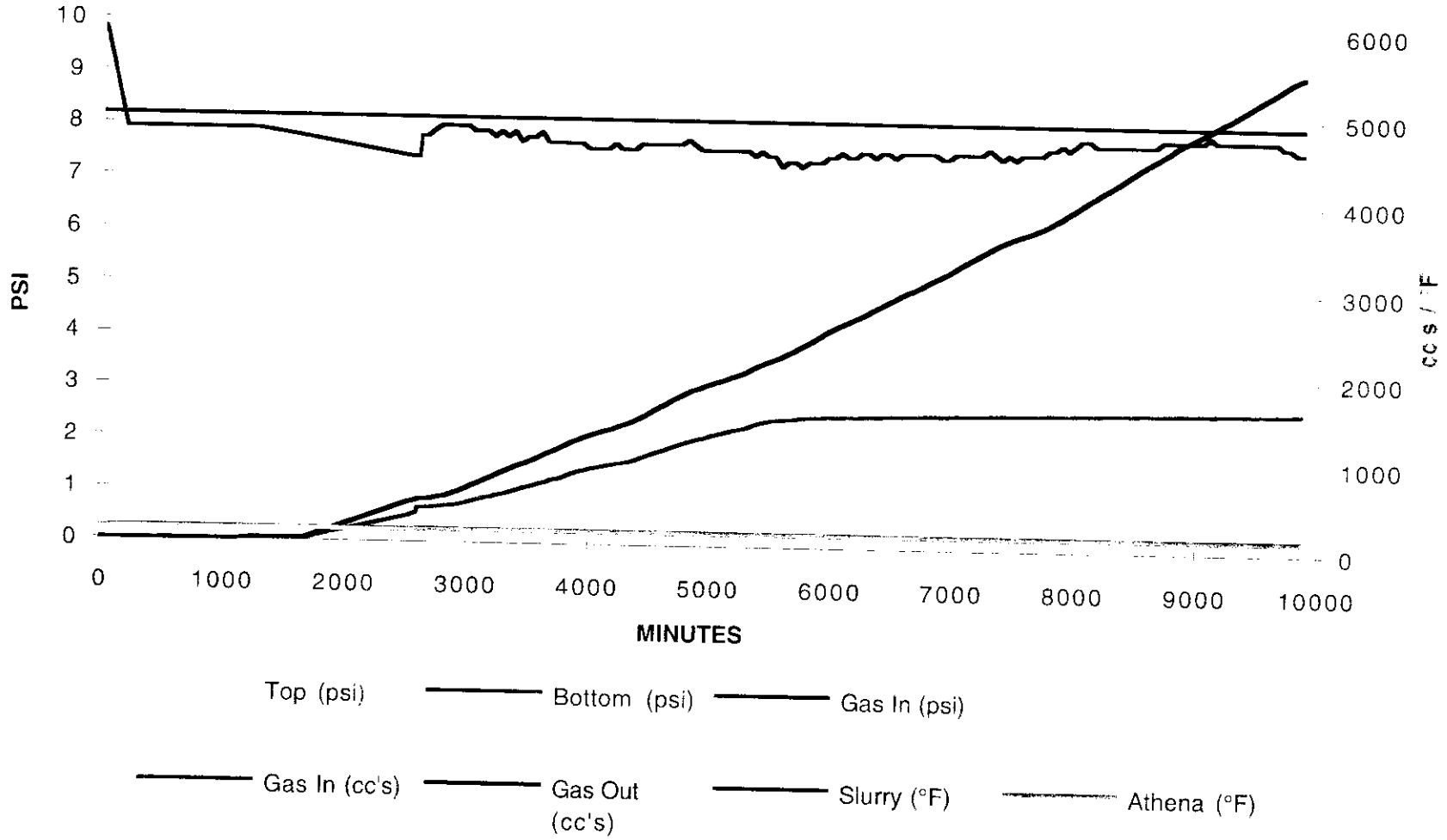

Plot 2a

PHPA 4 / 4

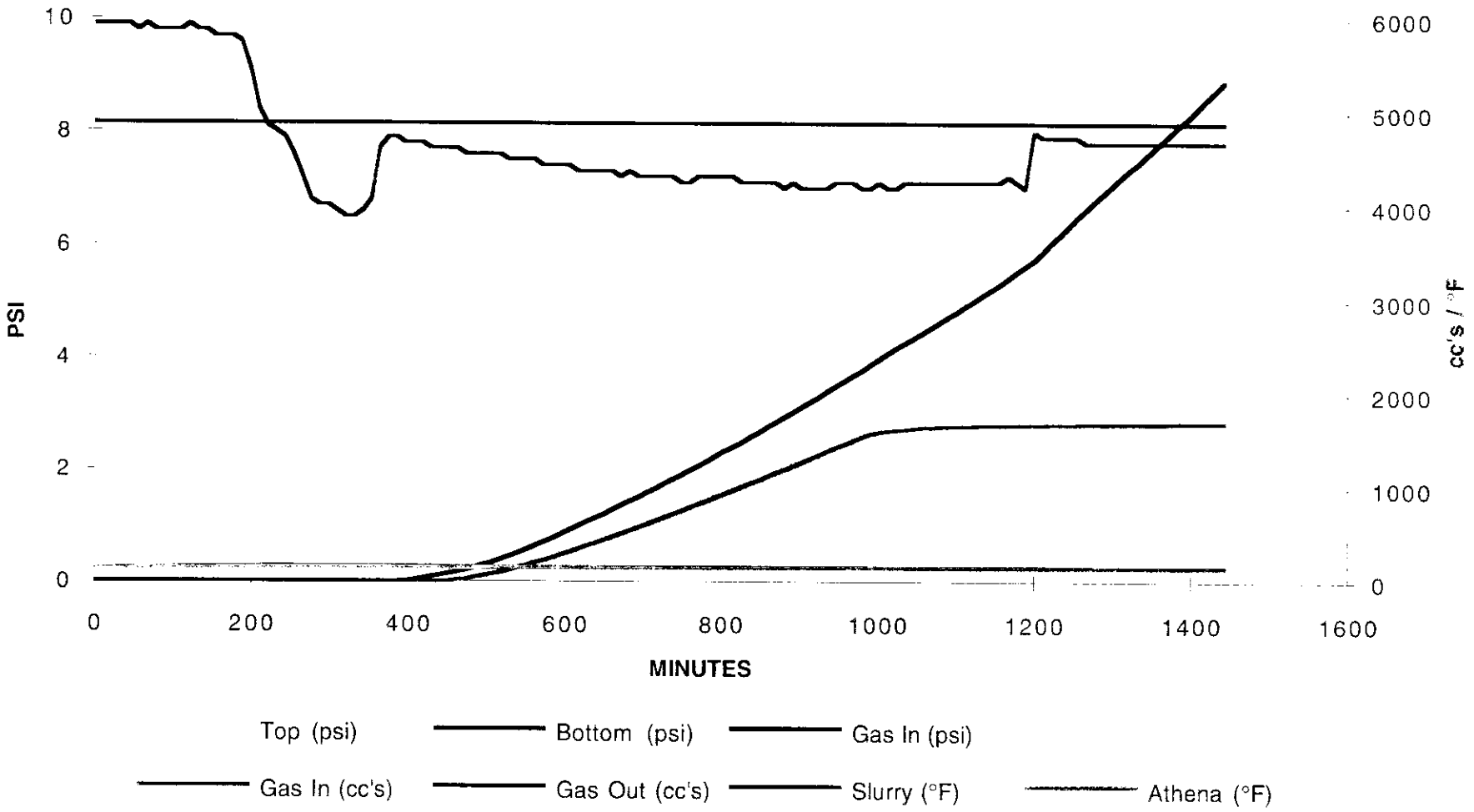

Plot 2b

PHPA 4 / 4

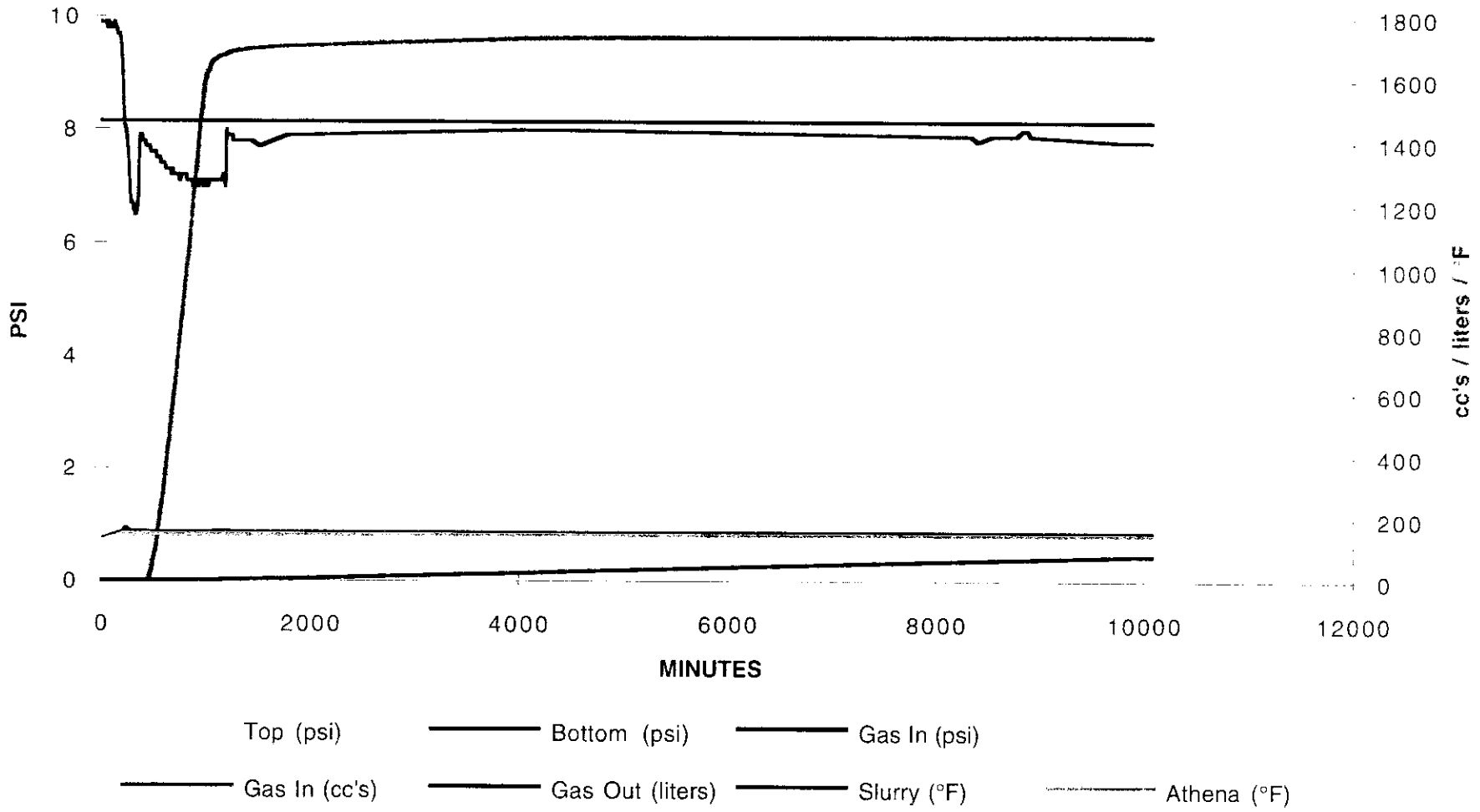

Plot 3a

PHPA 4 / 8

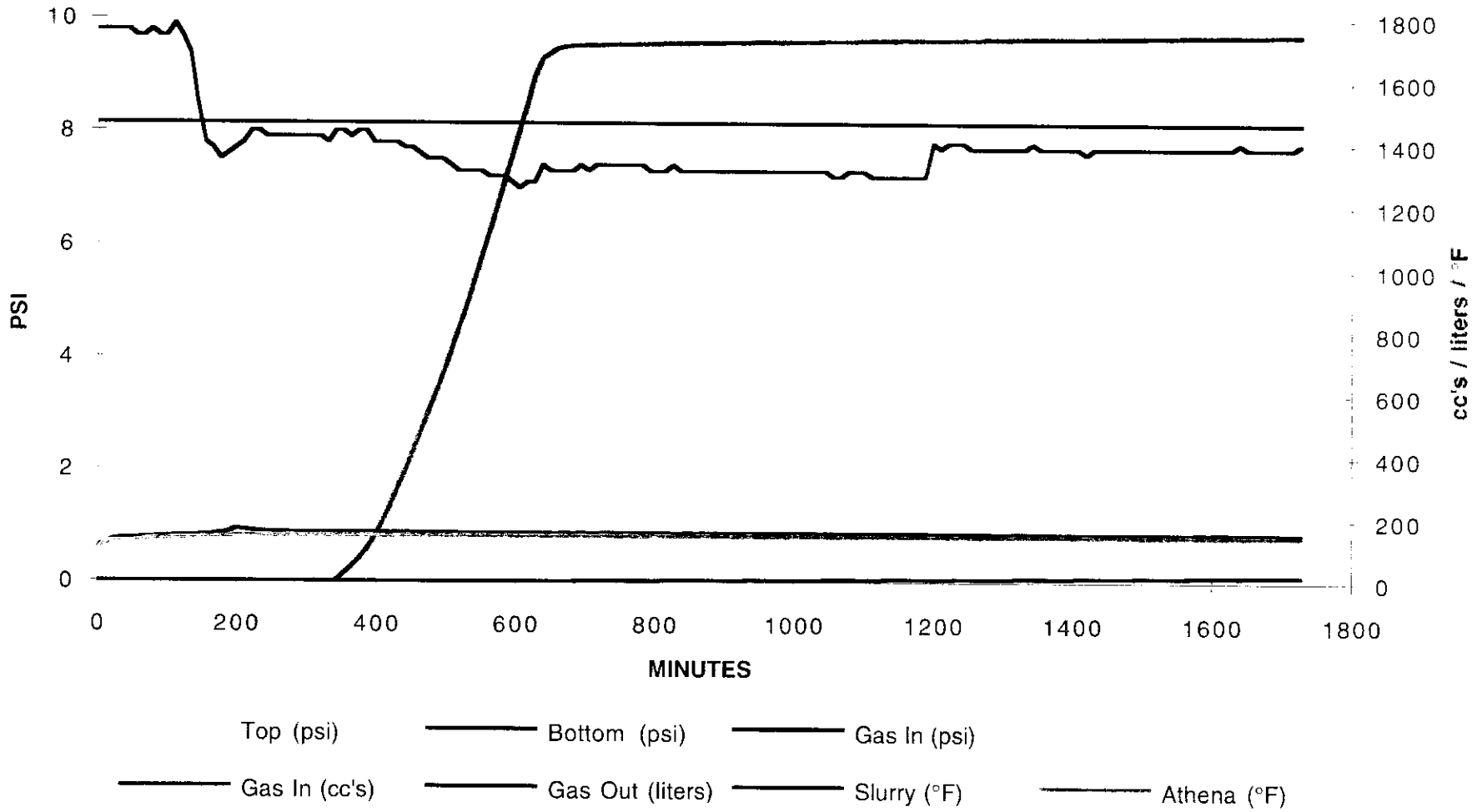

Plot 3b

PHPA 4 / 8

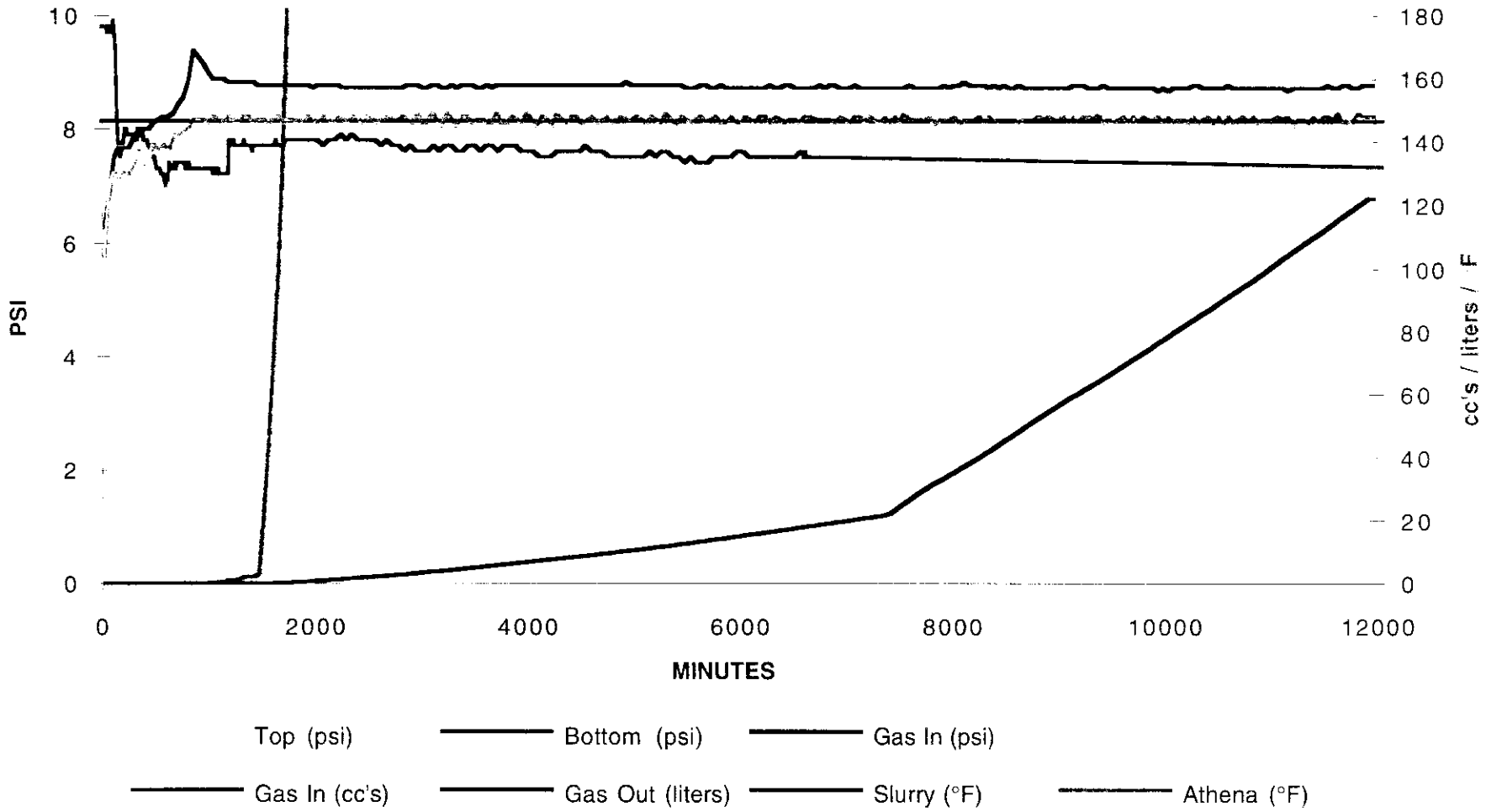

Plot 4a

PHPA 4 / 12

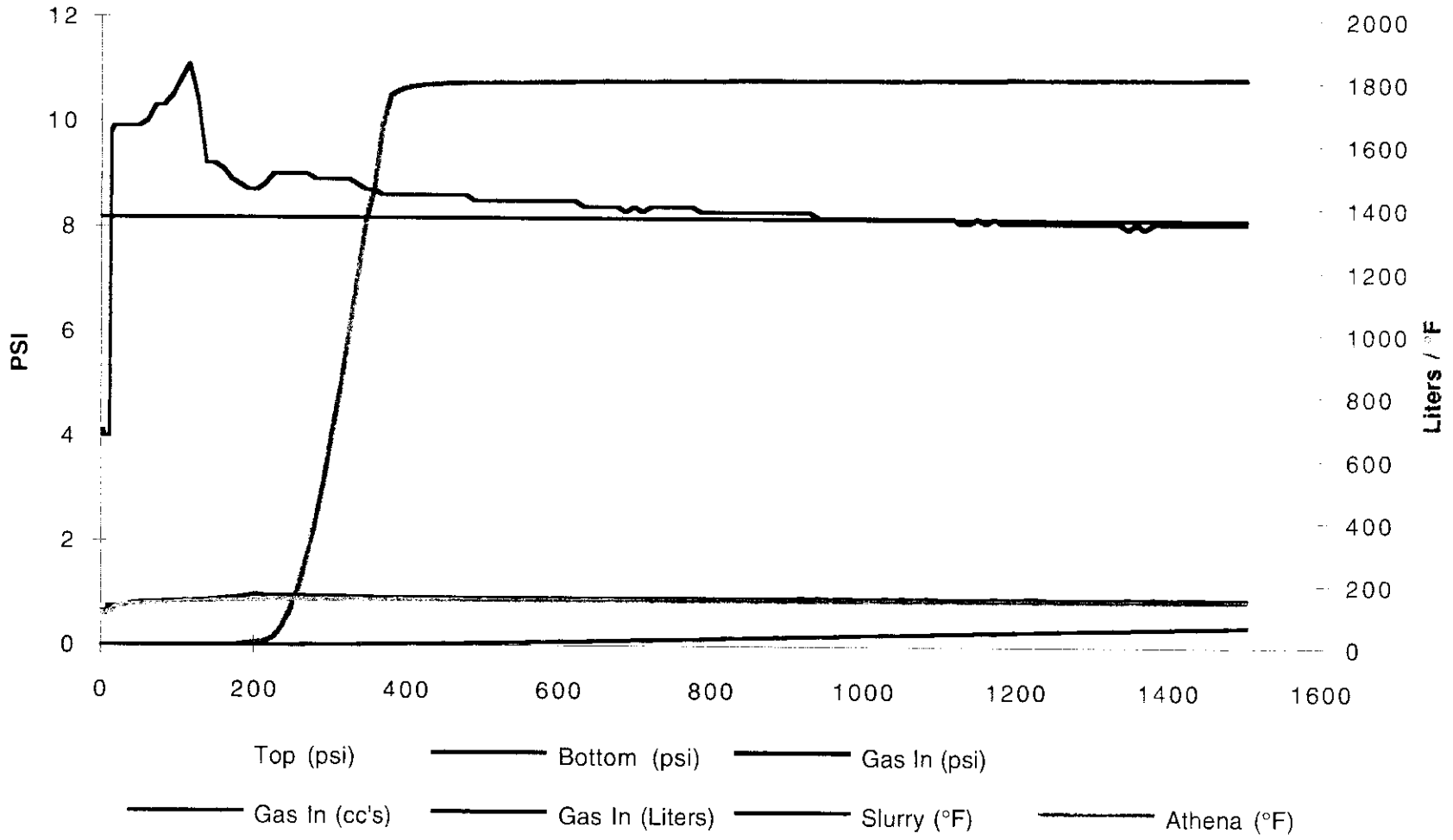

Plot 4b

PHPA 4 /12

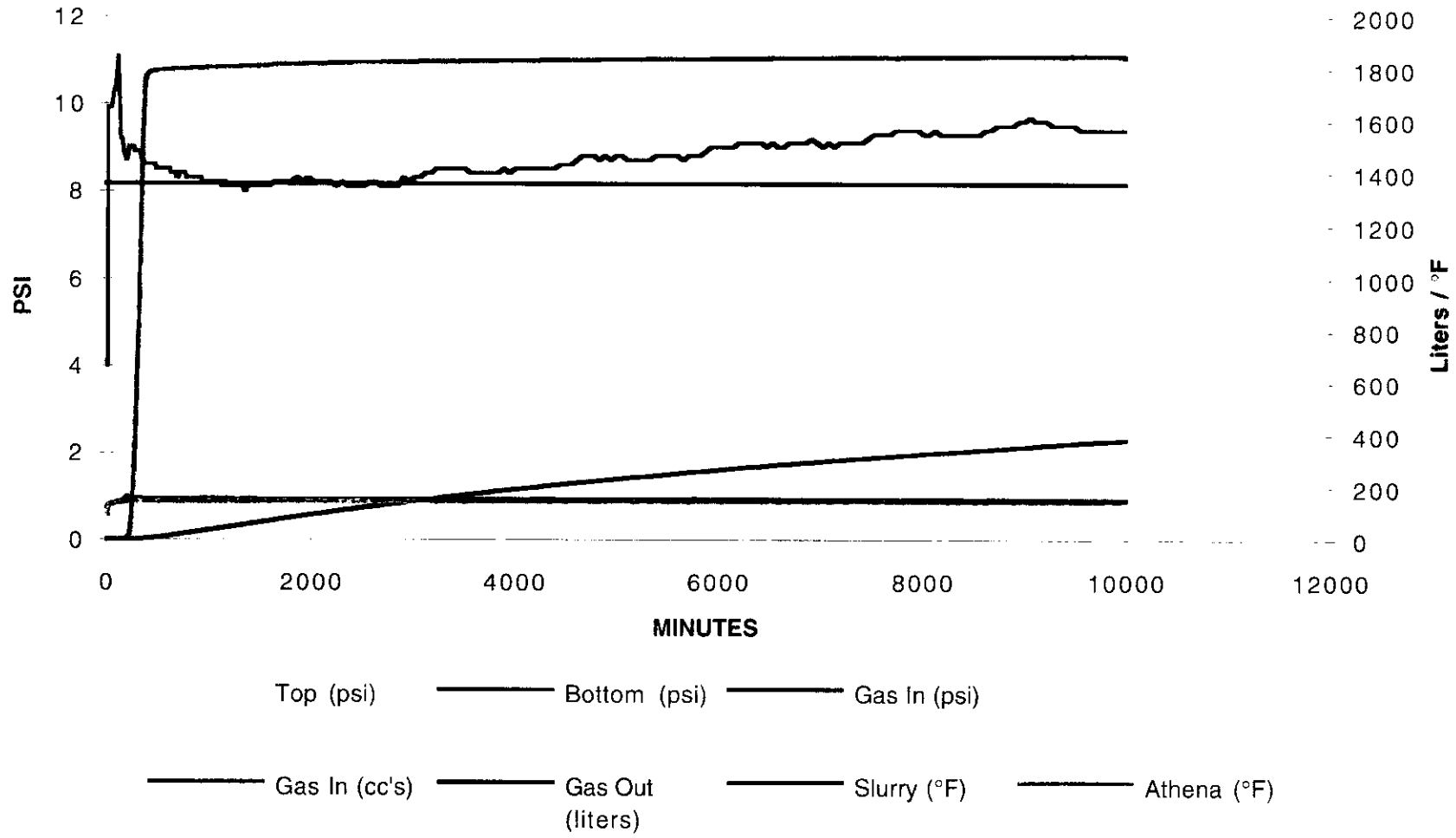

Figure 1a: PHPA 4 / 0 BFS - Cut A

Figure 1b: PHPA 4 / 0 BFS - Cut B

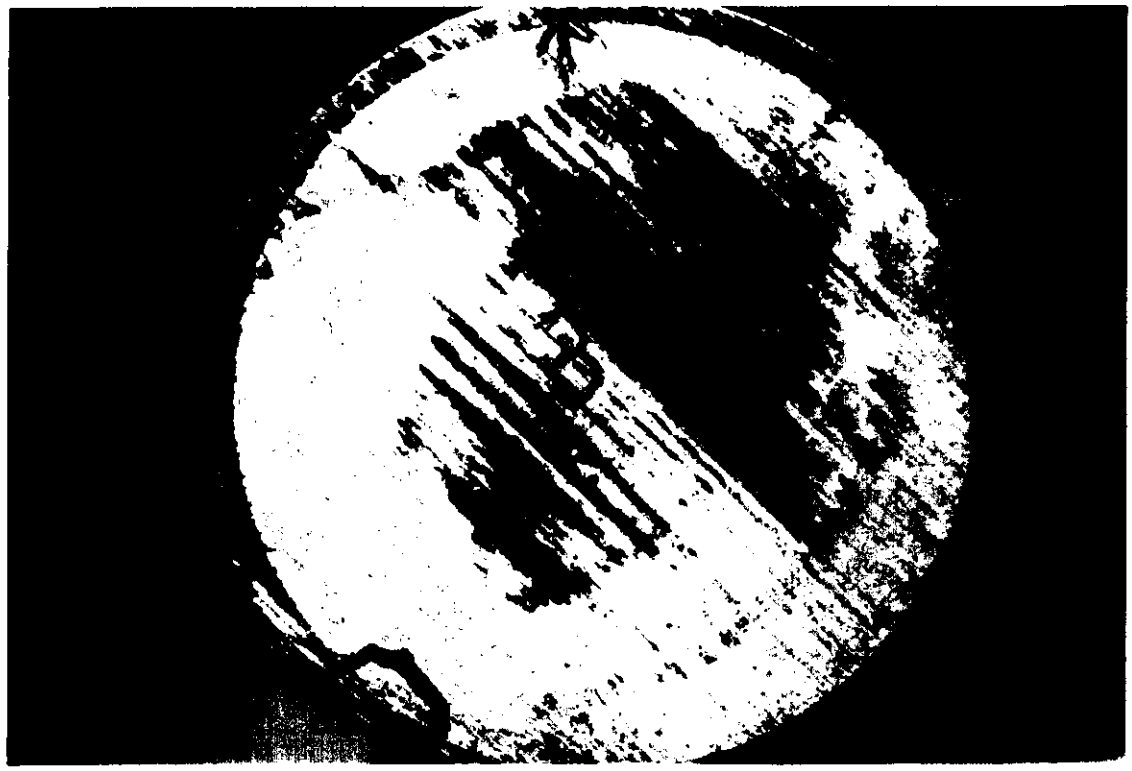

Figure 1c: PHPA 4 / 0 BFS - Cut C

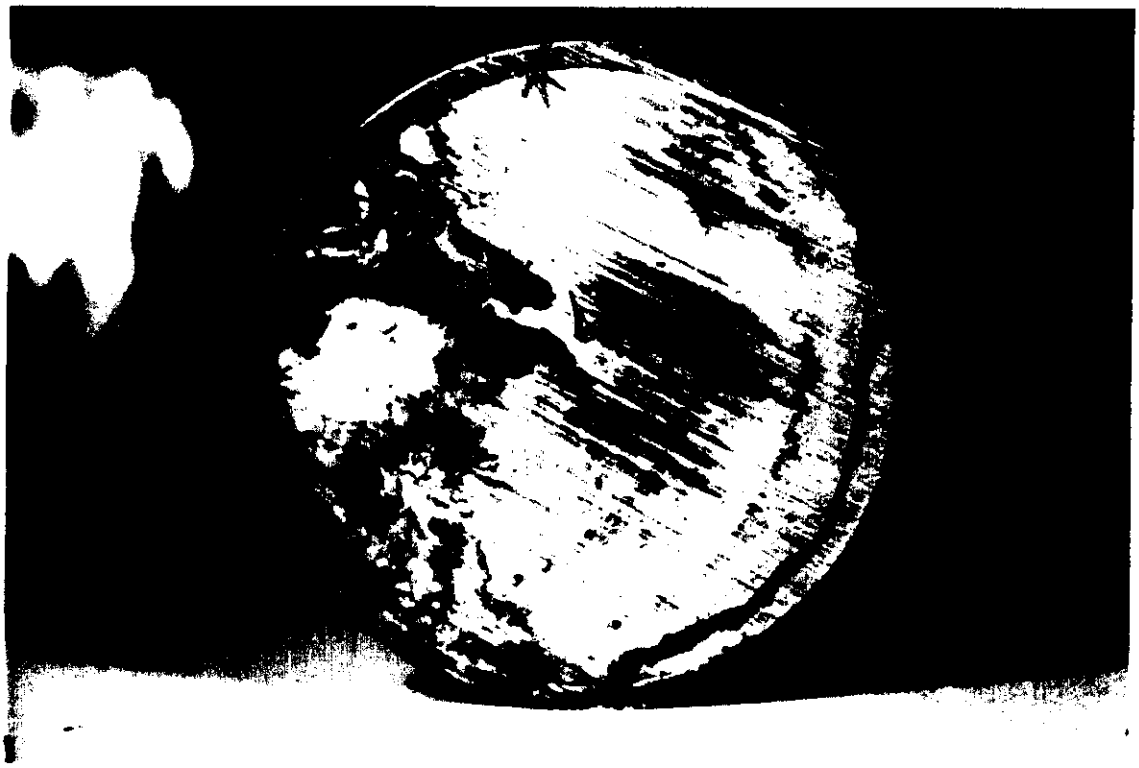

Figure 1d: PHPA 4 / 0 BFS - Cut D

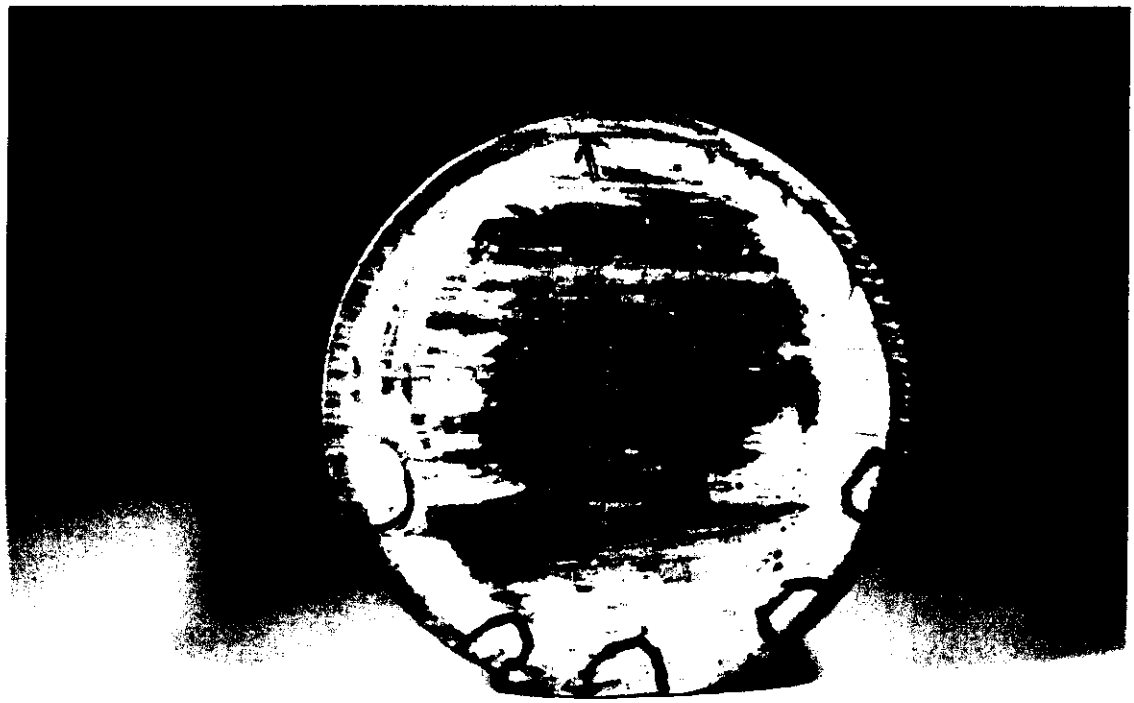

Figure 1e: PHPA 4 / 0 BFS - Cut E

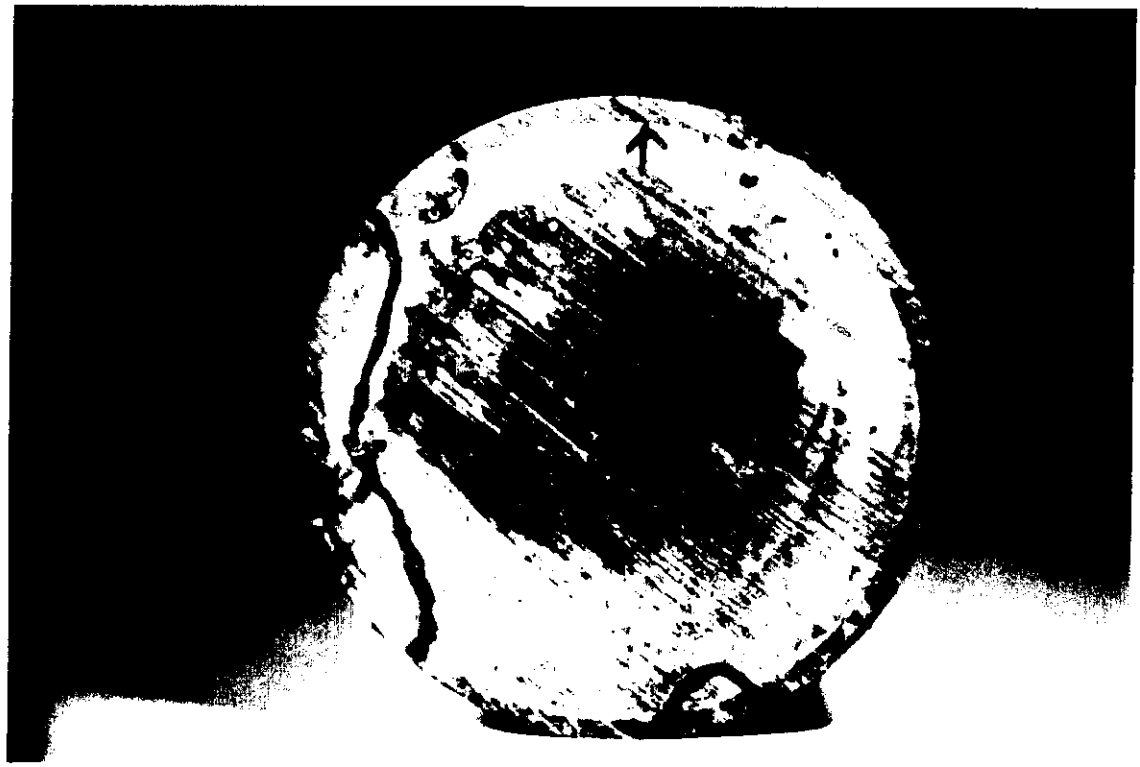

Figure 1f: PHPA 4 / 0 BFS - Cut F

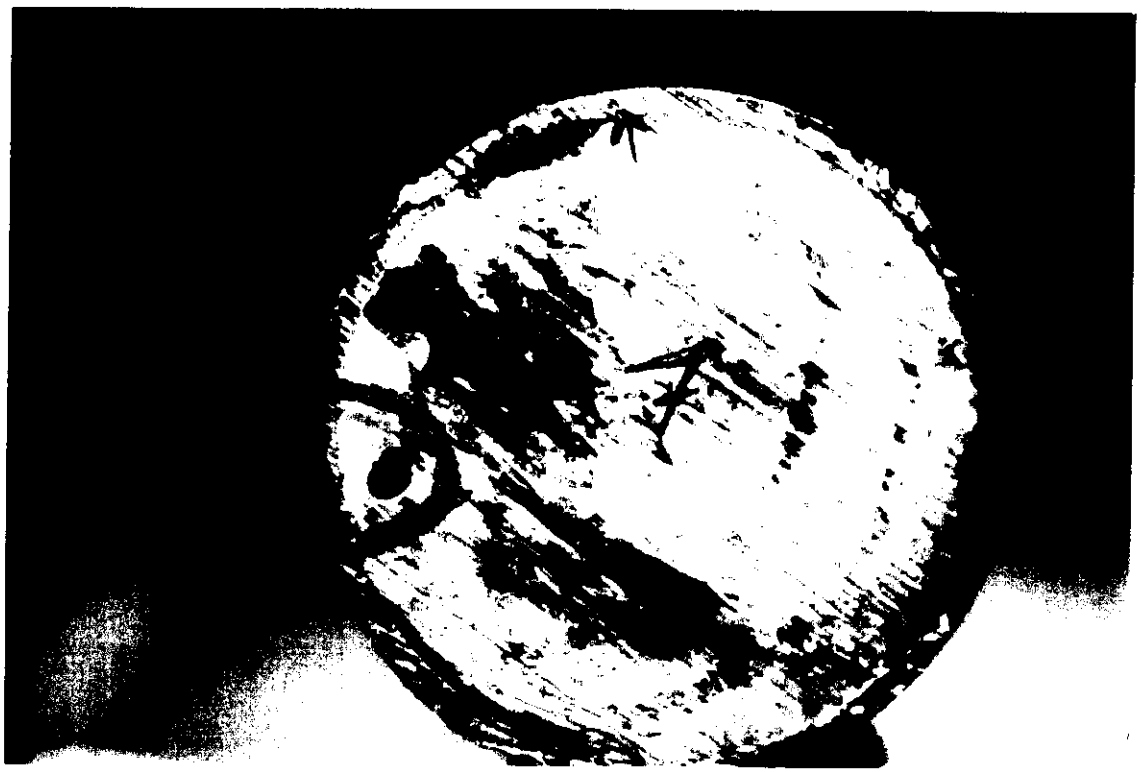

Figure 1g: PHPA 4 / 0 BFS - Cut G

Figure 1h: PHPA 4 / 0 BFS - Cut H

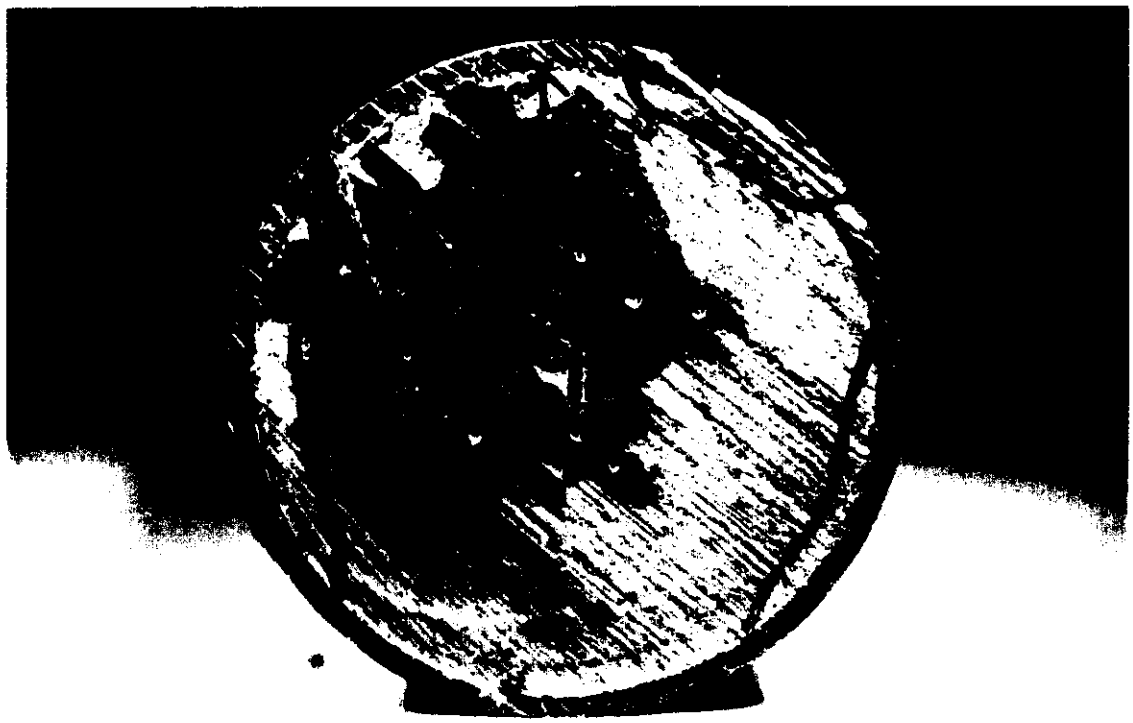

Figure 1i: PHPA 4 / 0 BFS - Cut I

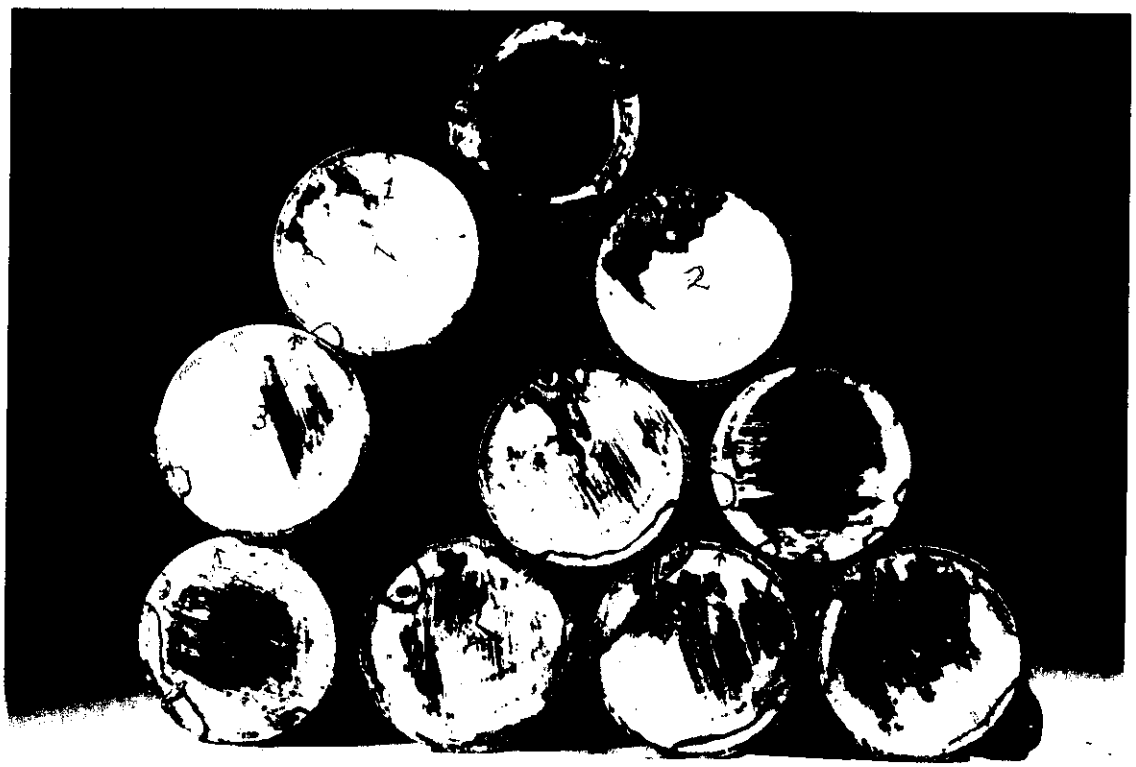

Figure 1j: PHPA 4 / 0 BFS - Cuts A through I

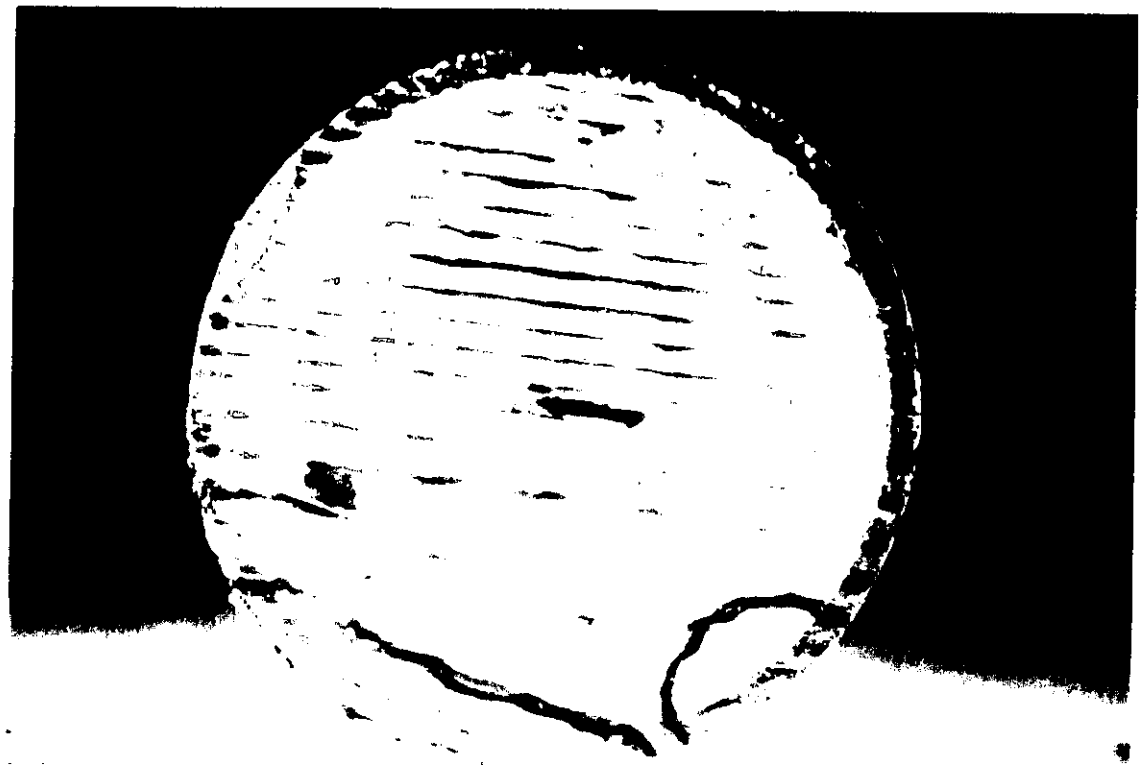

Figure 2a: PHPA 4 / 4 BFS - Cut A

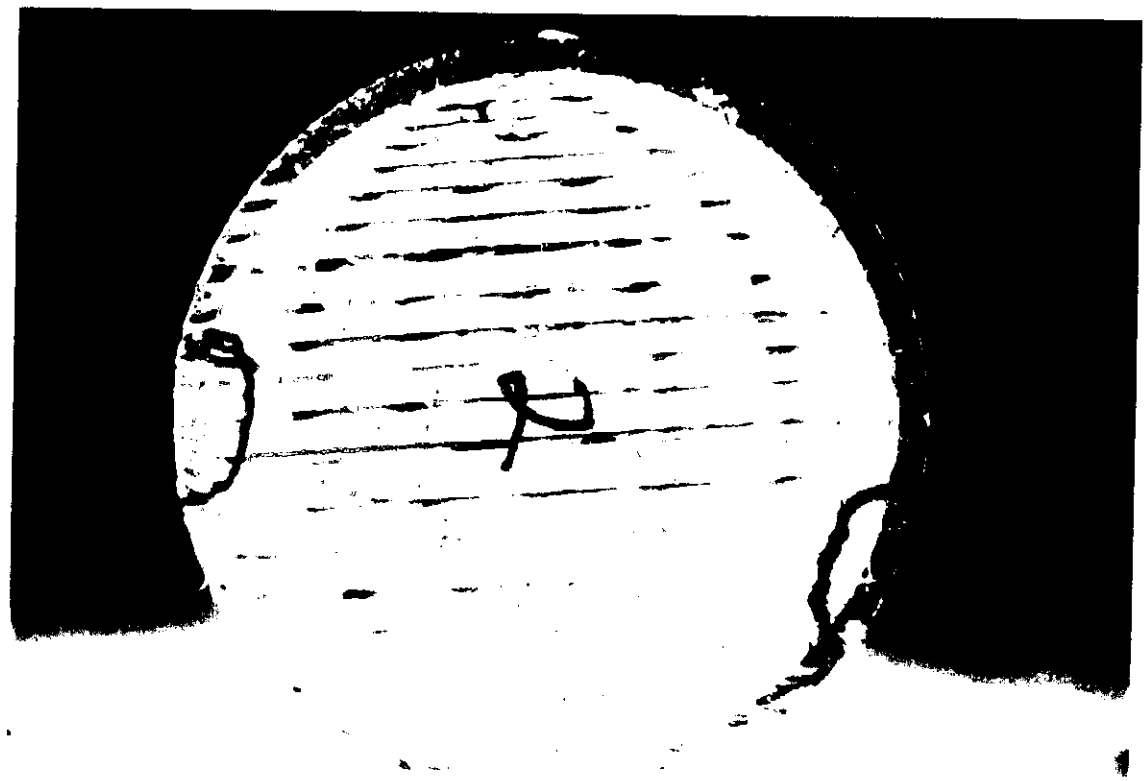

Figure 2b: PHPA 4 / 4 BFS - Cut B

Figure 2c: PHPA 4 / 4 BFS - Cut C

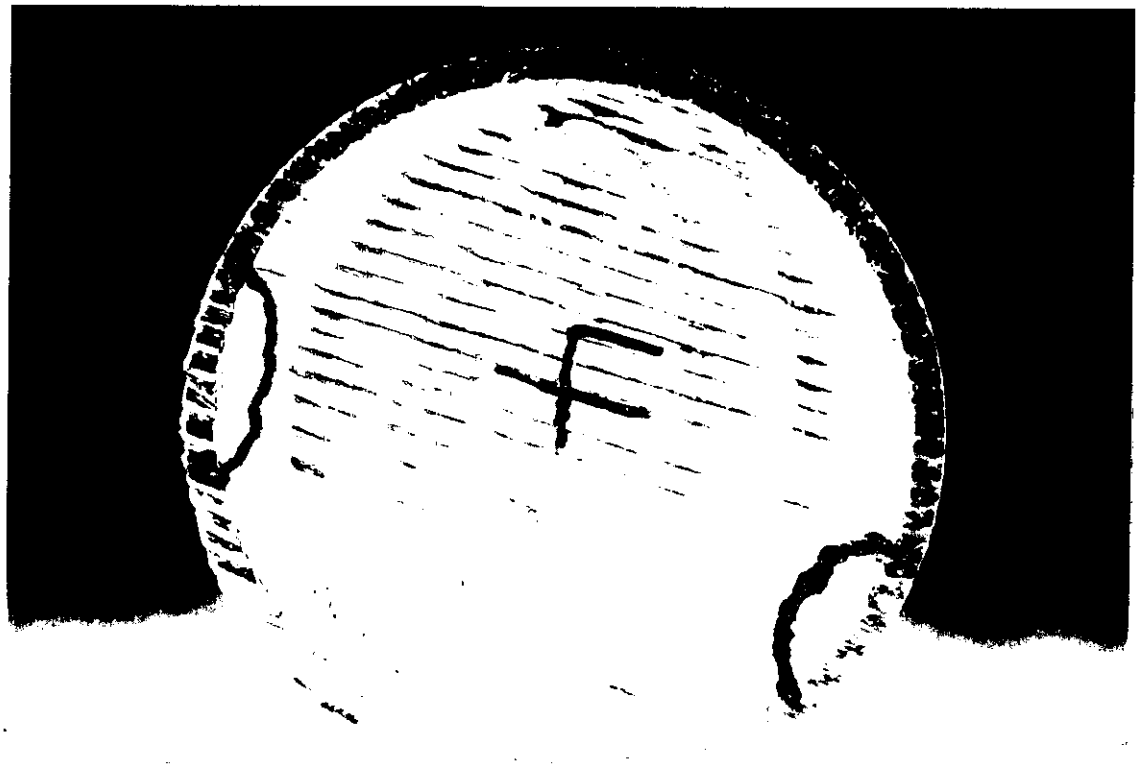

Figure 2d: PHPA 4 / 4 BFS - Cut D

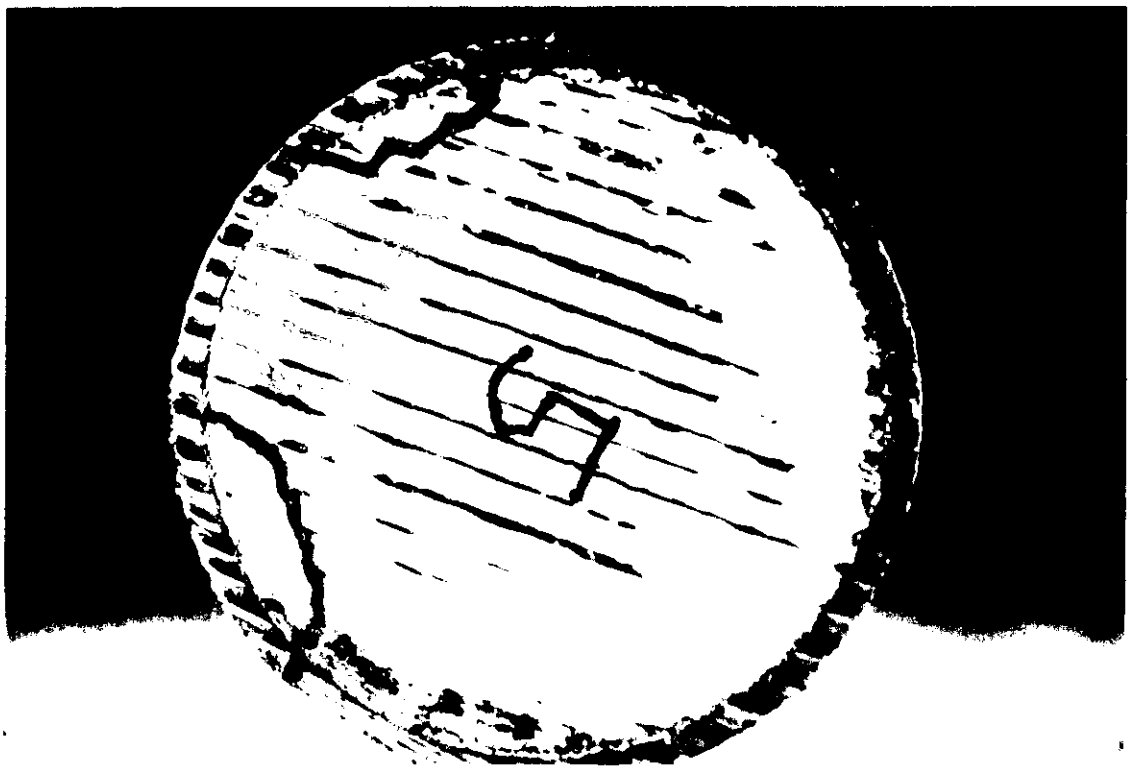

Figure 2e: PHPA 4 / 4 BFS - Cut E

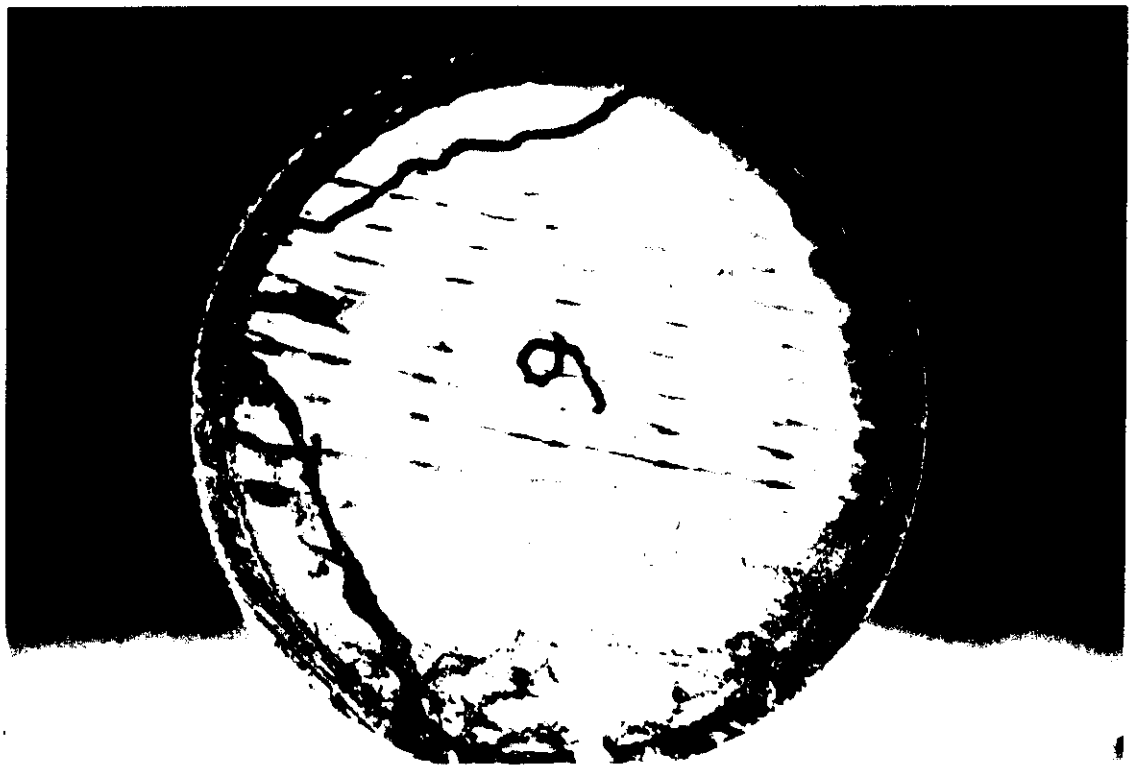

Figure 2f: PHPA 4 / 4 BFS - Cut F

Figure 2g: PHPA 4 / 4 BFS - Cut G

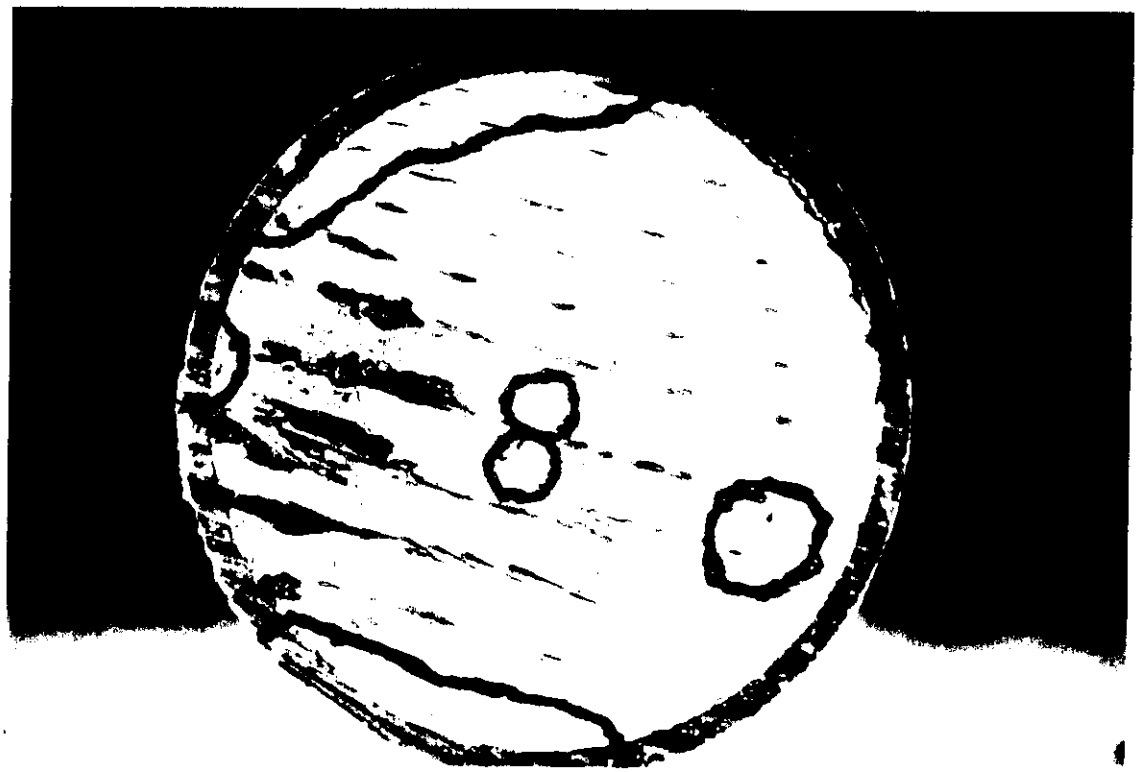

Figure 2h: PHPA 4 / 4 BFS - Cut H

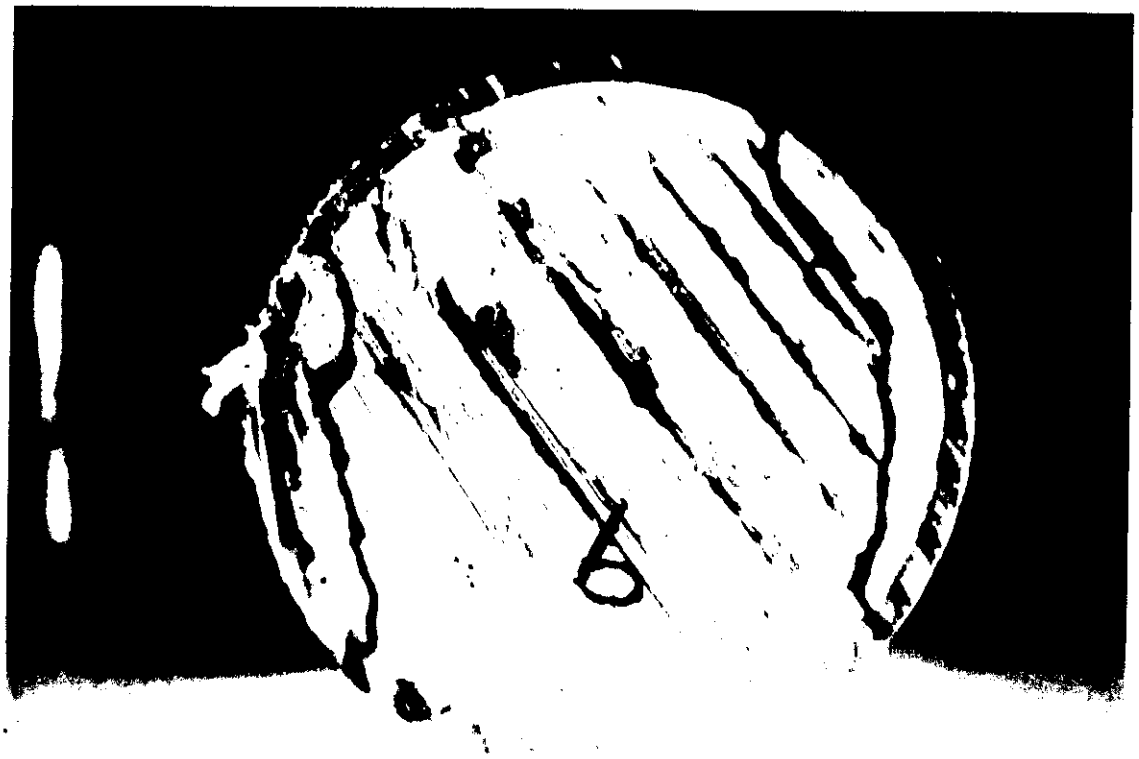

Figure 2i: PHPA 4 / 4 BFS - Cut I

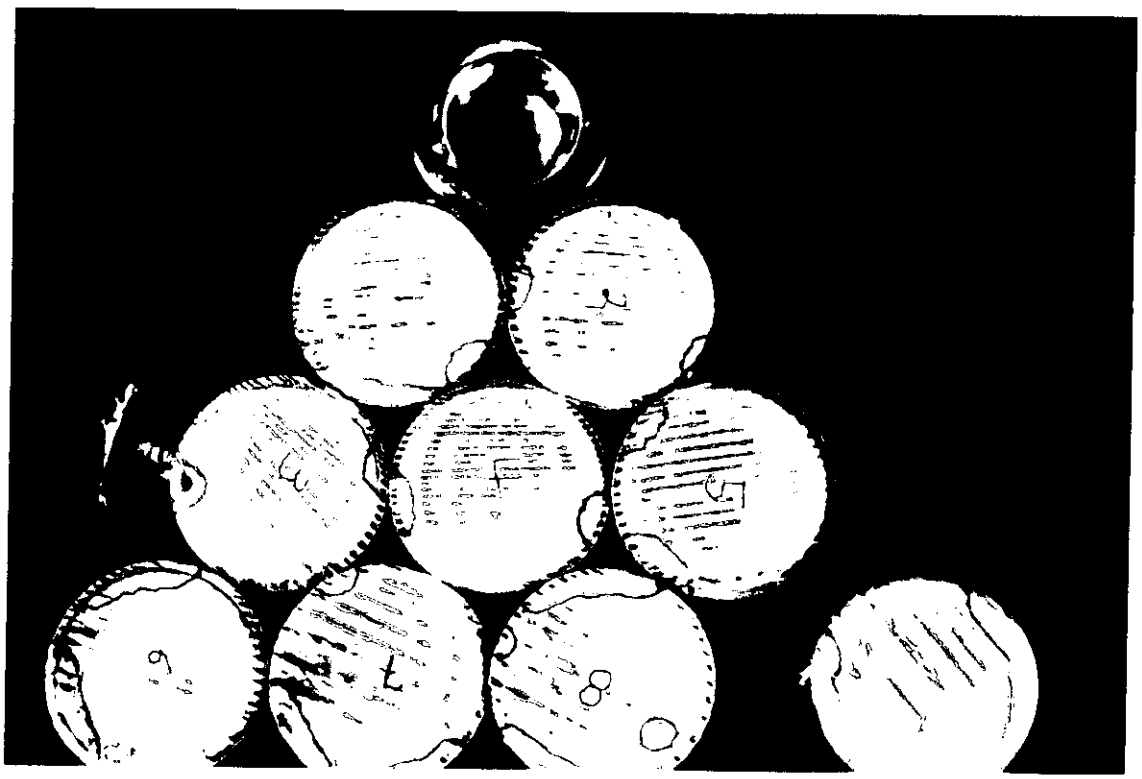

Figure 13j: PHPA 4 / 4 BFS - Cuts A through I

Figure 3a: PHPA 4 / 8 BFS - Cut A

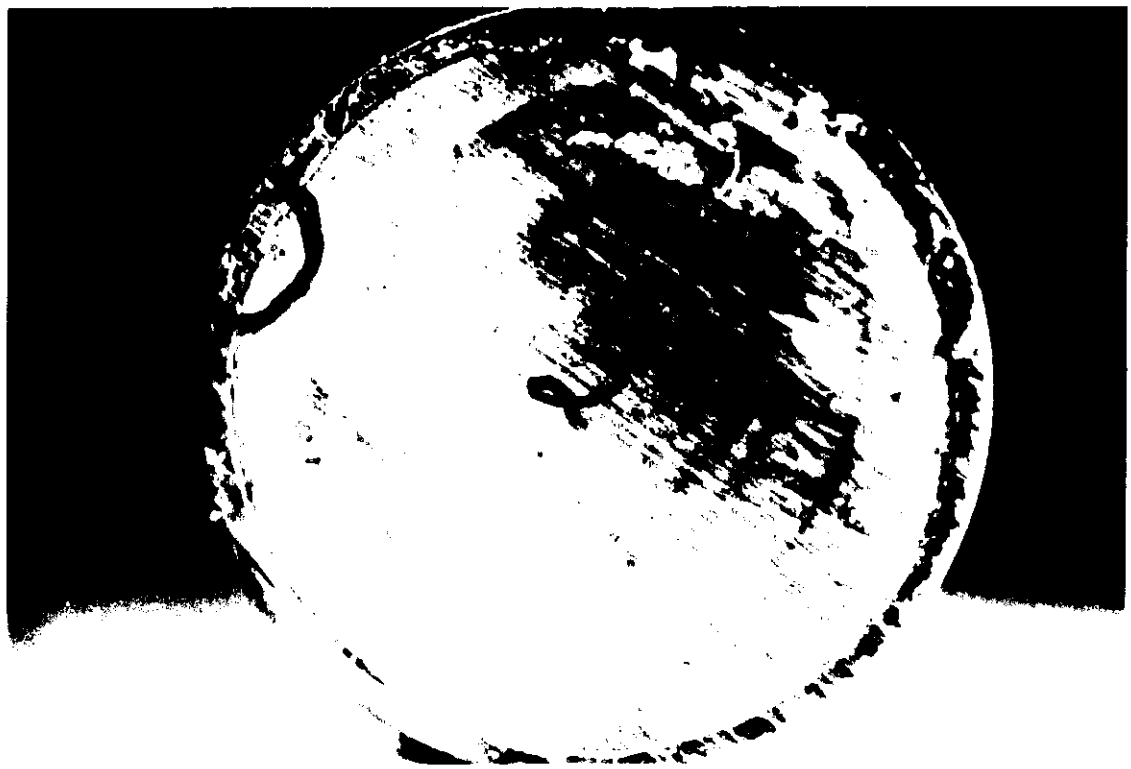

Figure 3b: PHPA 4 / 8 BFS - Cut B

Figure 3c: PHPA 4 / 8 BFS - Cut C

Figure 3d: PHPA 4 / 8 BFS - Cut D

Figure 3e: PHPA 4 / 8 BFS - Cut E

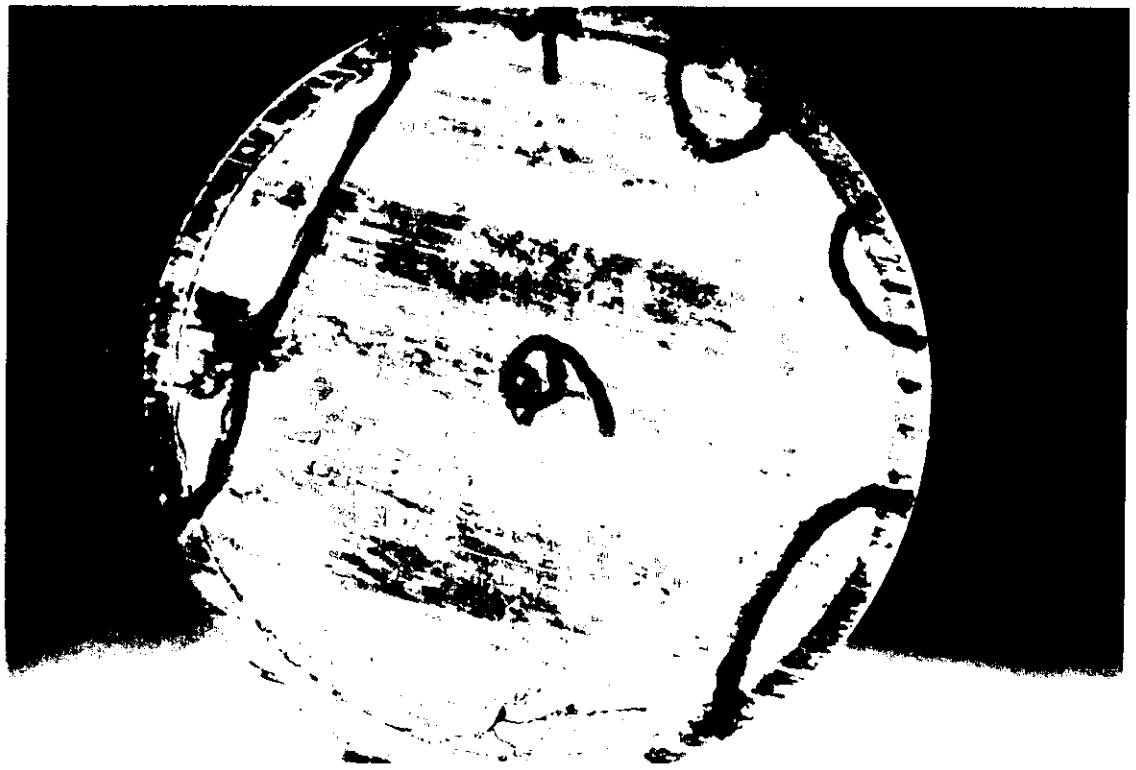

Figure 3f: PHPA 4 / 8 BFS - Cut F

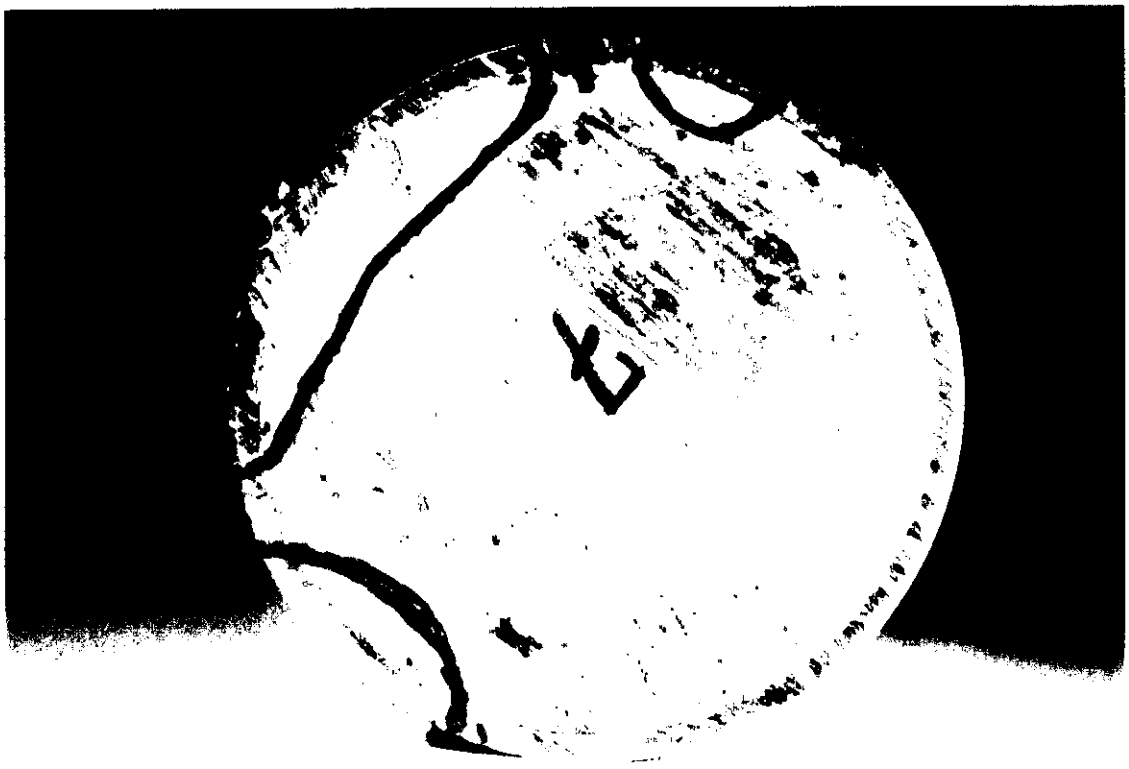

Figure 3g: PHPA 4 / 8 BFS - Cut G

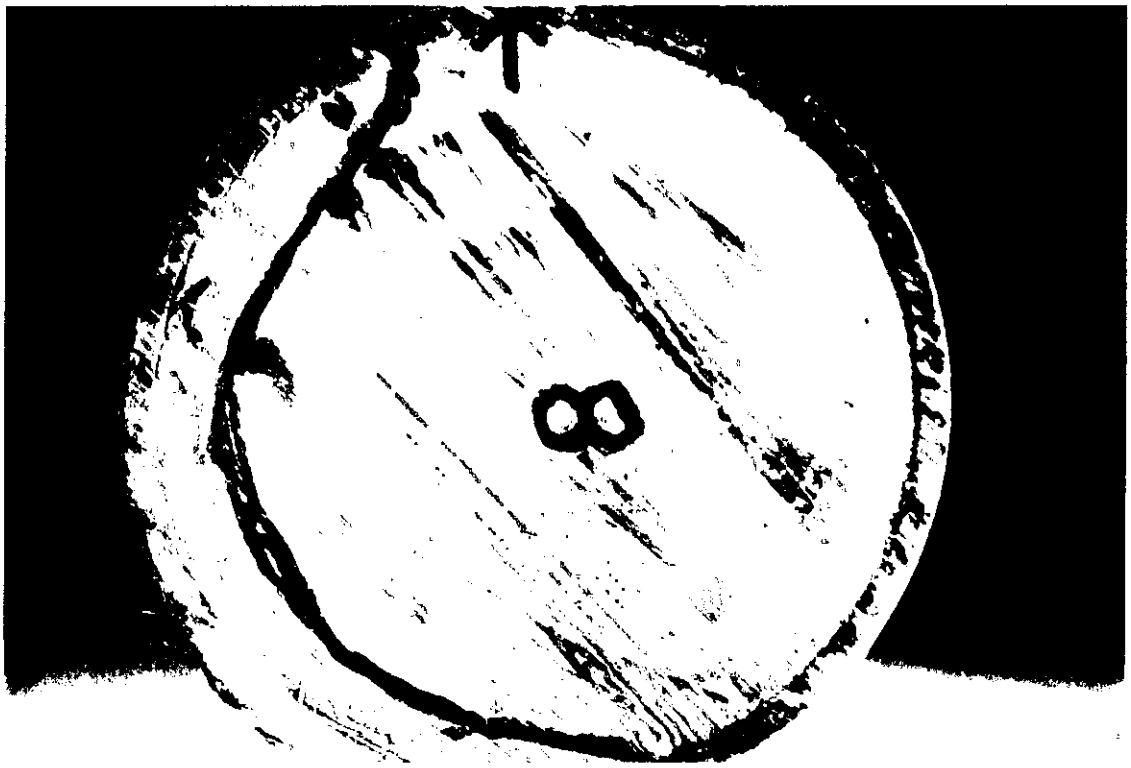

Figure 3h: PHPA 4 / 8 BFS - Cut H

Figure 3i: PHPA 4 / 8 BFS - Cut I

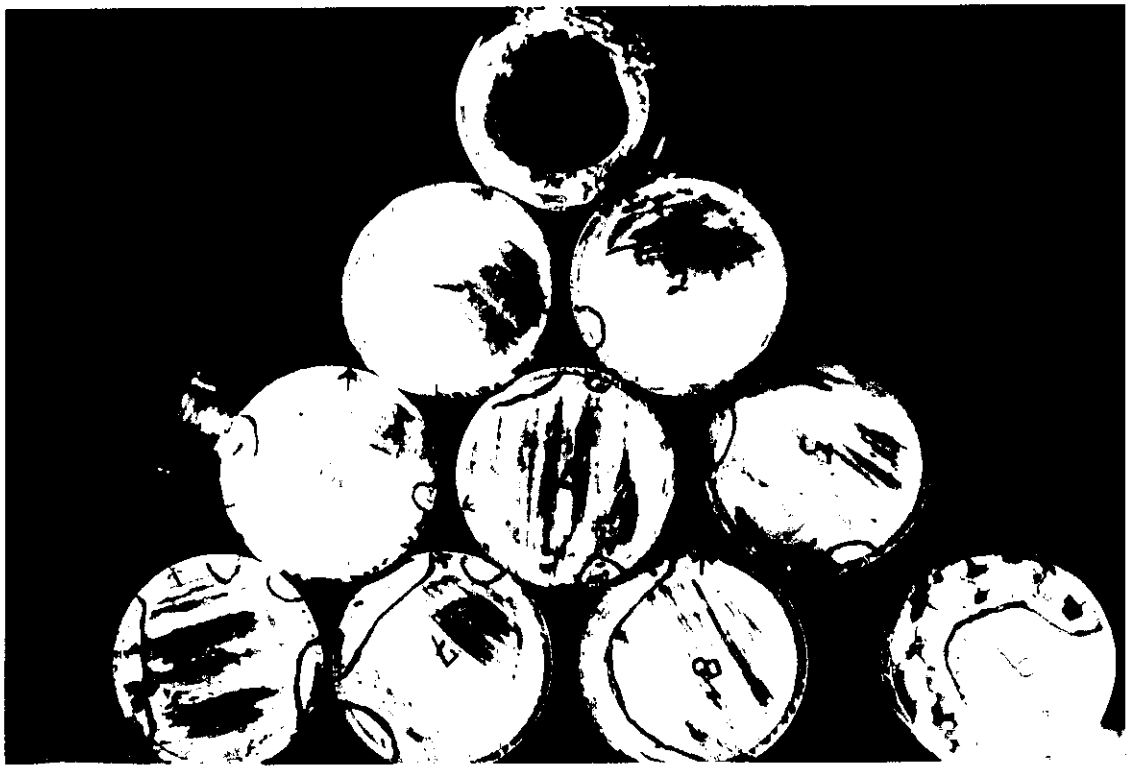

Figure 13j: PHPA 4 / 8 BFS - Cuts A through I

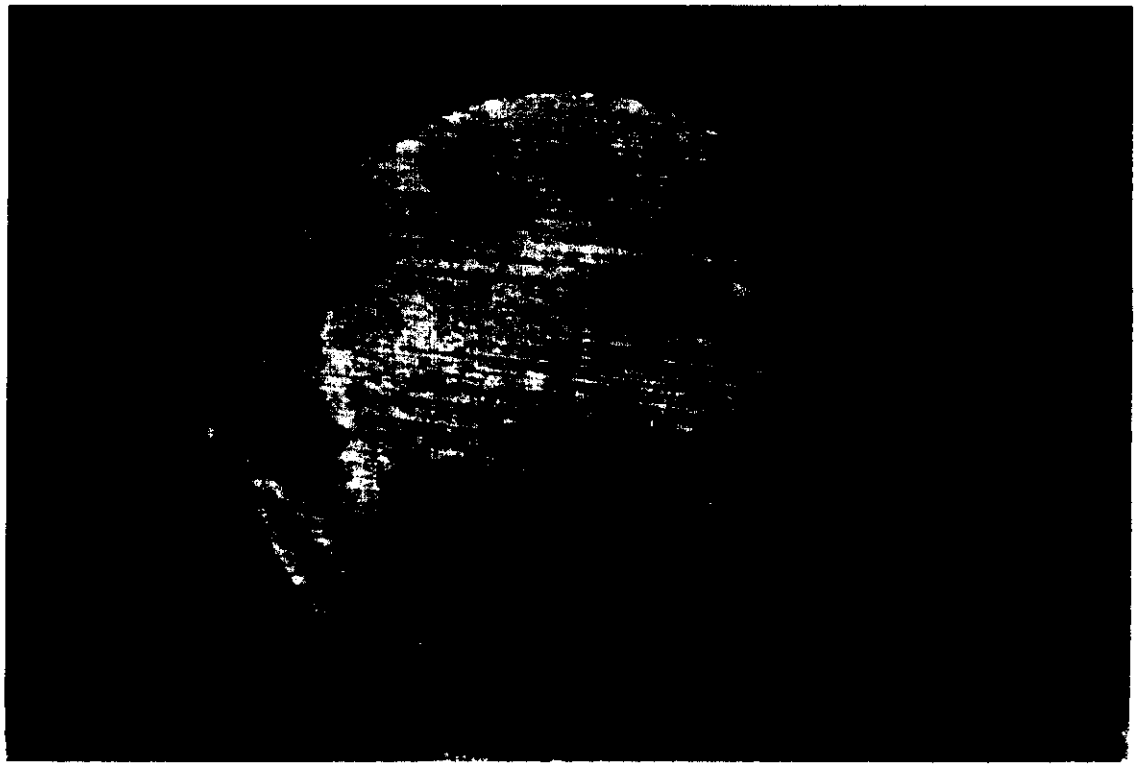

Figure 4a: PHPA 4 / 12 BFS - Cut A

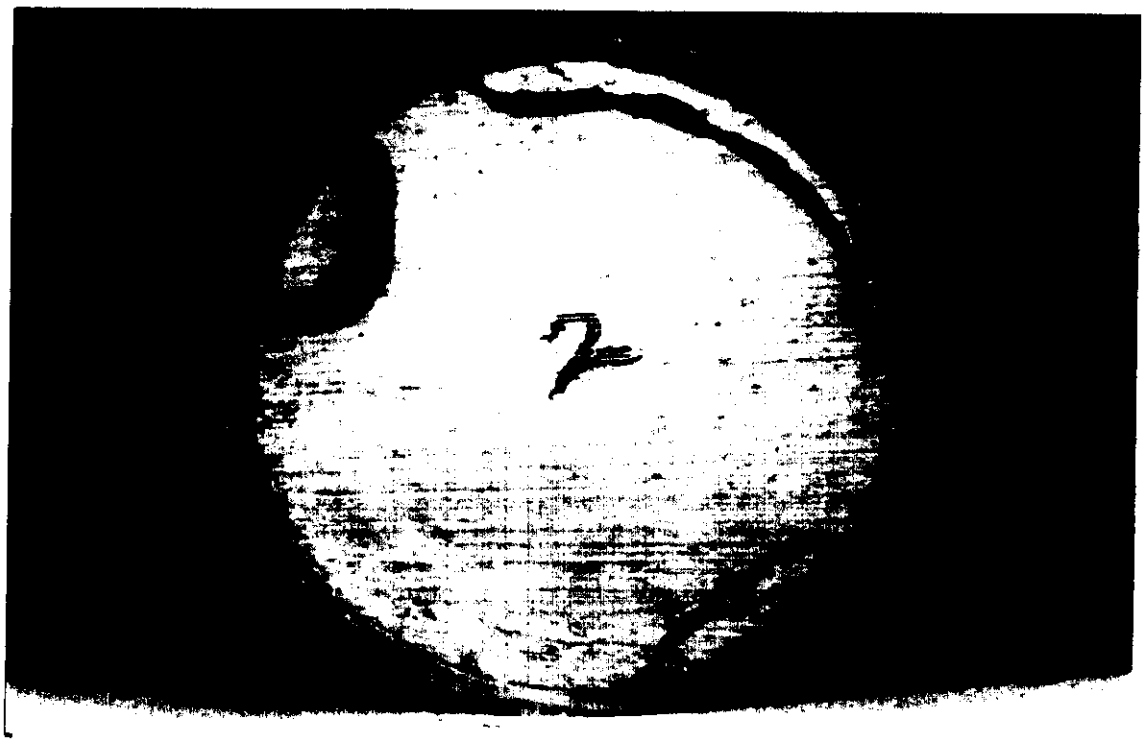

Figure 4b: PHPA 4 / 12 BFS - Cut B

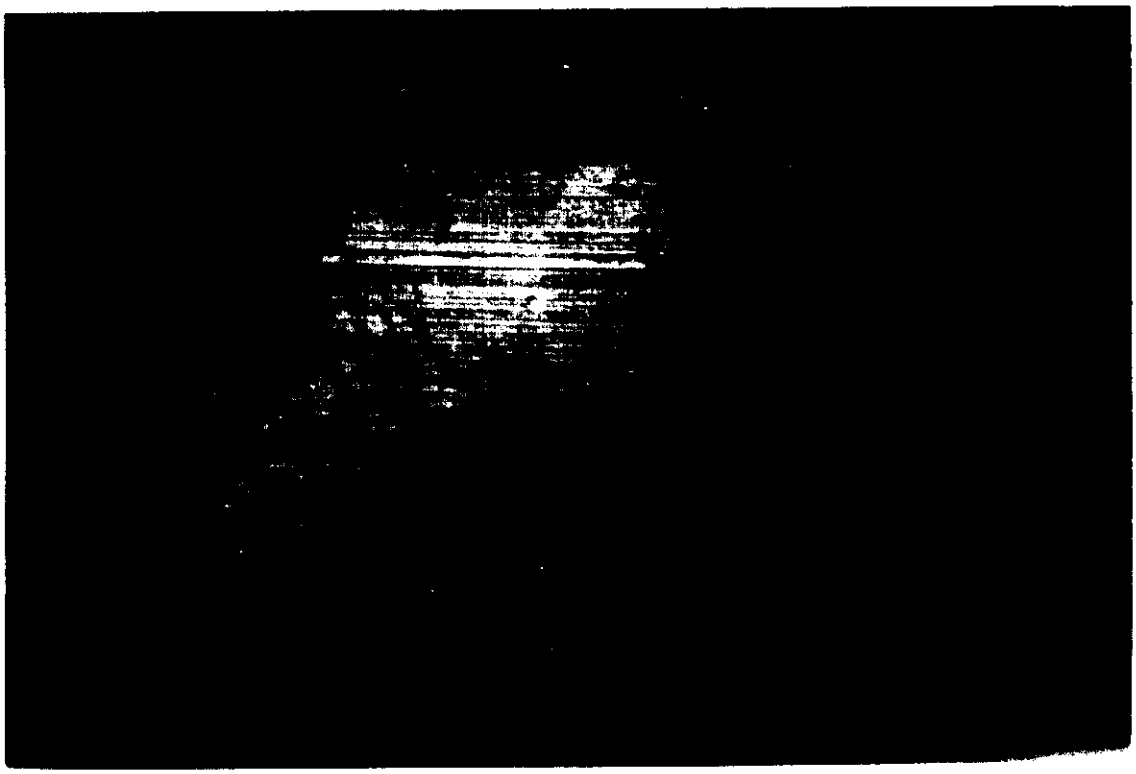

Figure 4c: PHPA 4 / 12 BFS - Cut C

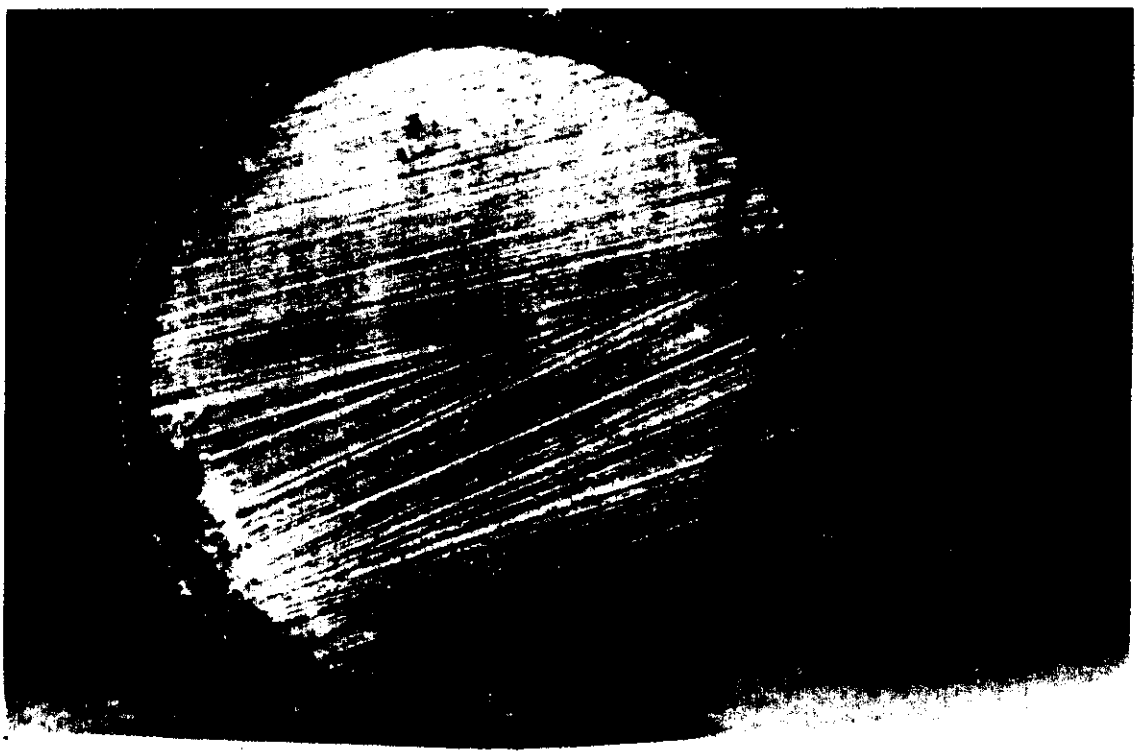

Figure 4d: PHPA 4 / 12 BFS - Cut D

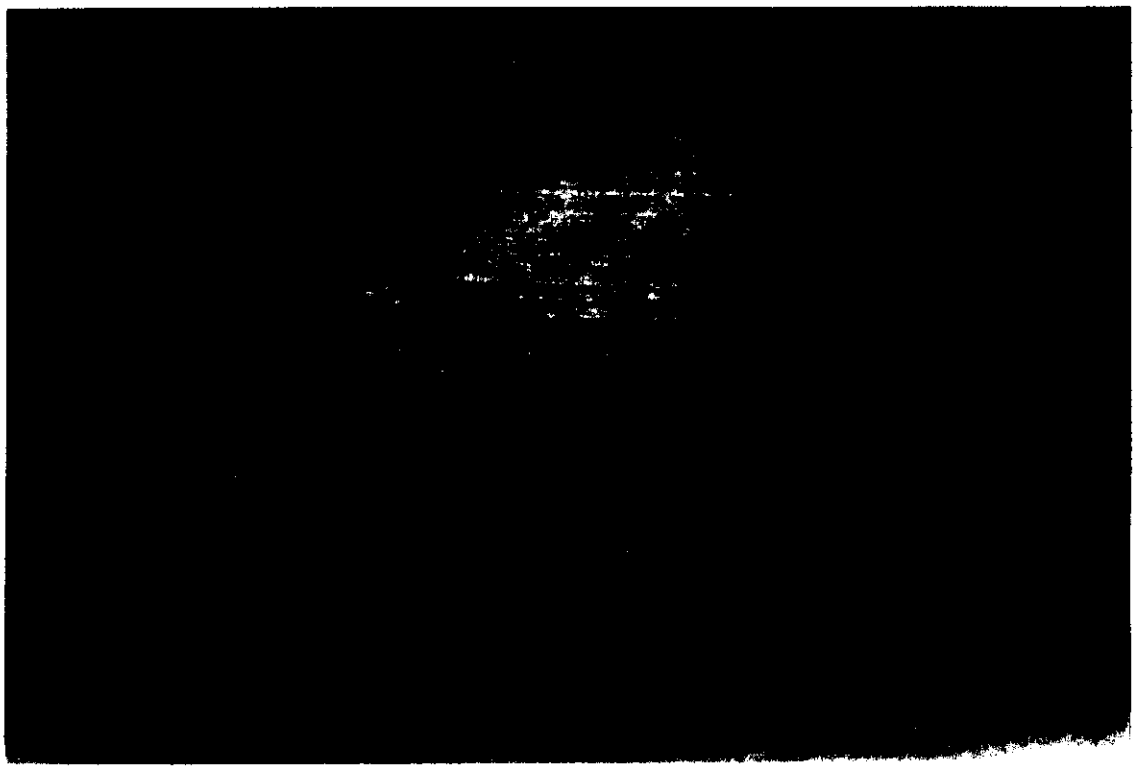

Figure 4e: PHPA 4 / 12 BFS - Cut E

Figure 4f: PHPA 4 / 12 BFS - Cut F

Figure 4g: PHPA 4 / 12 BFS - Cut G

Figure 4h: PHPA 4 / 12 BFS - Cut H

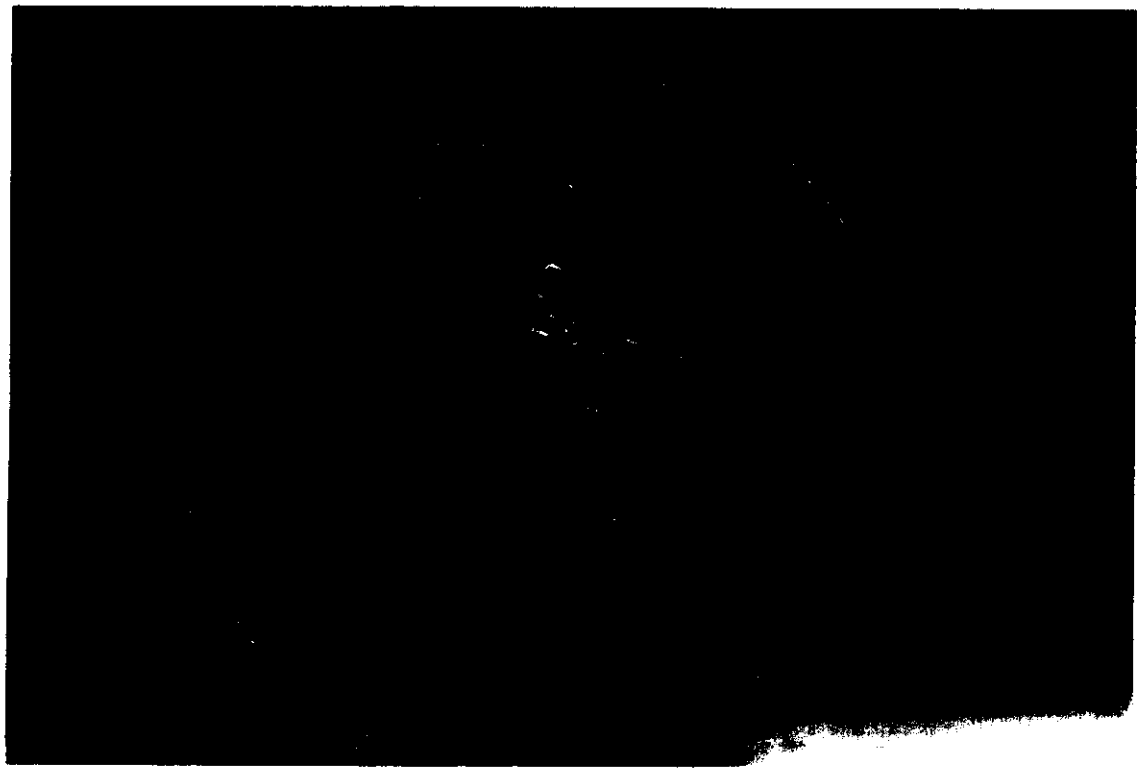

Figure 4i: PHPA 4 / 12 BFS - Cut I

Figure 13j: PHPA 4 / 12 BFS - Cuts A through I

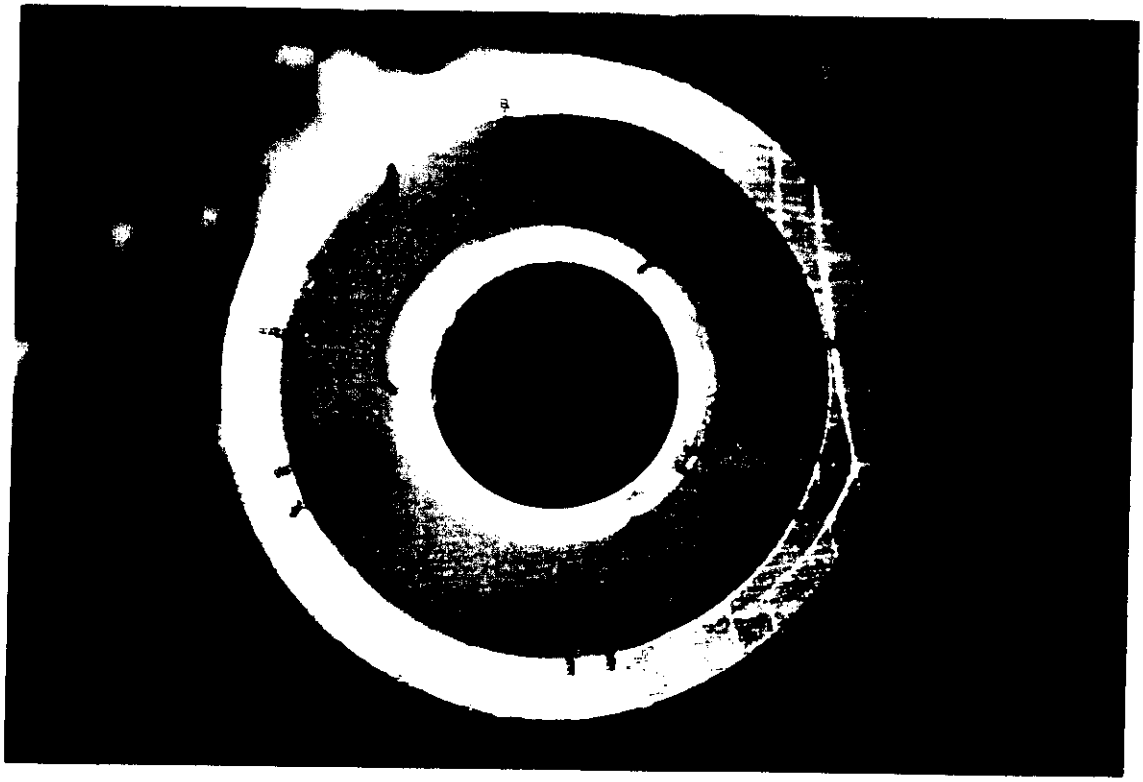

Figure 5: Portland Cement Annular Seal

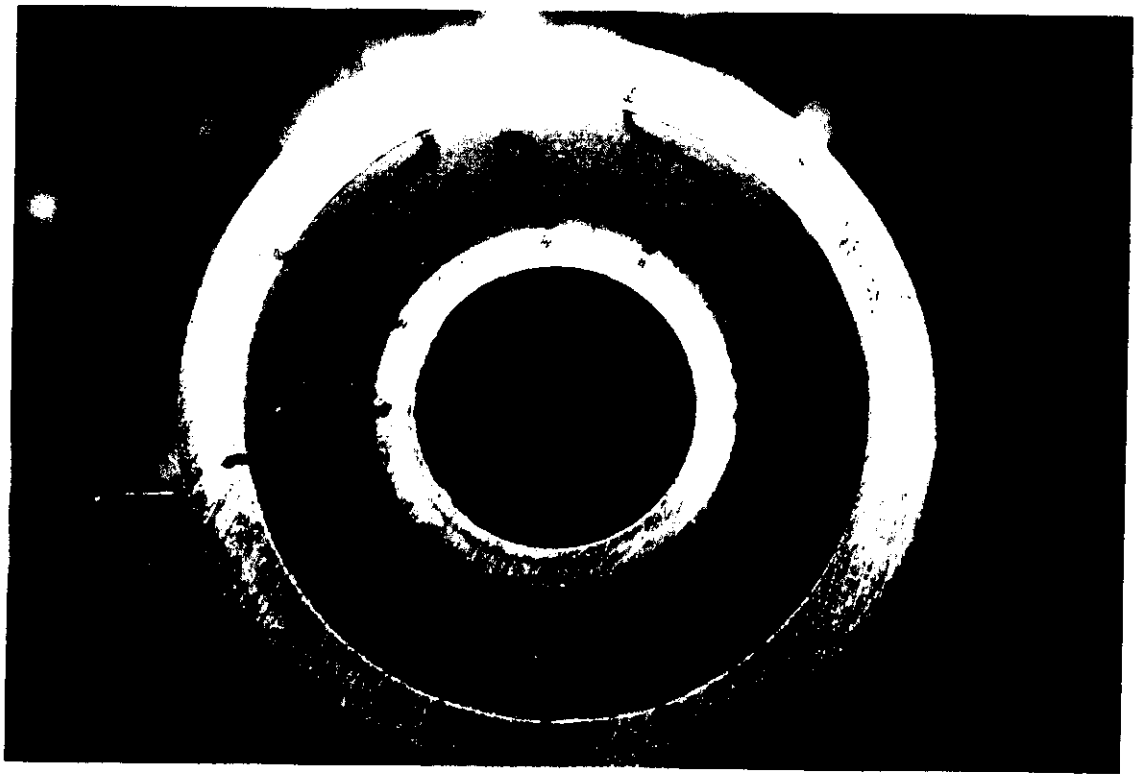

Figure 6: PHPA 4 / 0 BFS Annular Seal

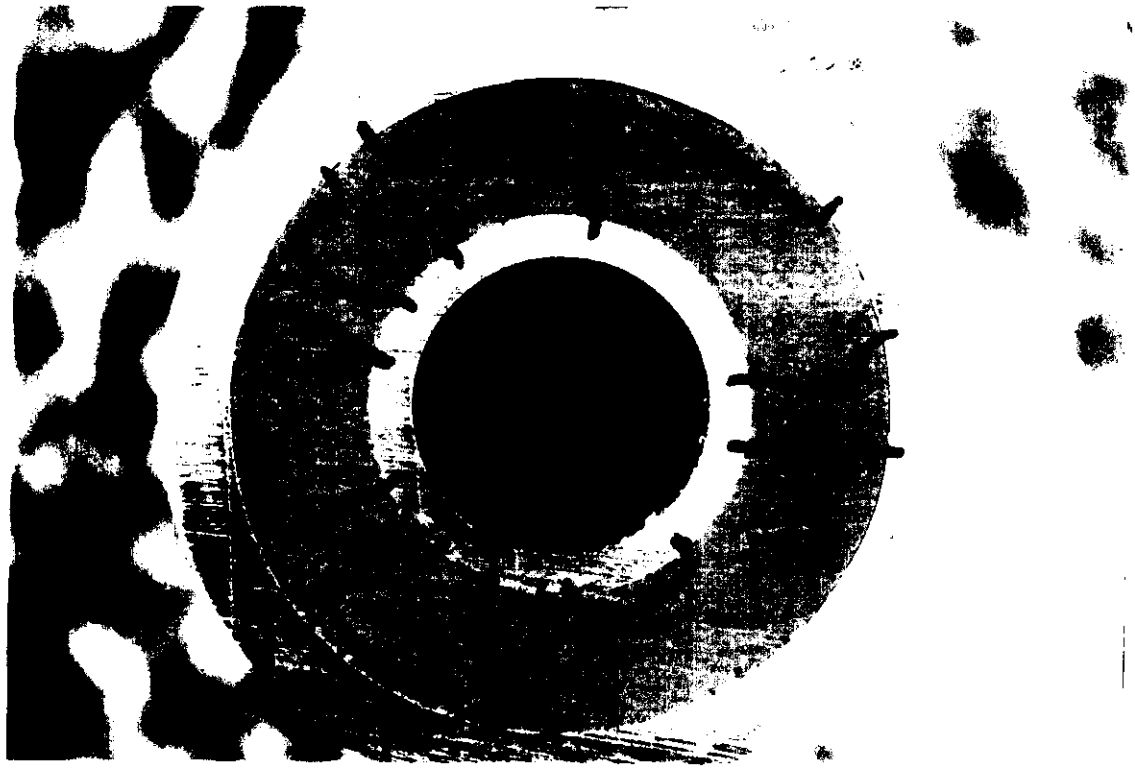

Figure 7: PHPA 4 / 12 BFS Annular Seal

IIT RESEARCH INSTITUTE
WESTPORT TECHNOLOGY CENTER INTERNATIONAL

DRILLING TECHNOLOGIES

WTCI-96-134 June 1996

DEA-87, Phase II
Progress Report No. 3
Literature Survey and Analysis

By:
F. Sabins

Work by:
R. Caenn

Westport Technology Center International
6700 Portwest Drive
Houston, Texas 77024
(713) 560-4666
(713) 864-9357 (Fax)
www.westport1.com

Sponsored by: DEA-87 Joint Industry Project
W.O.#: H09196H000

Approved by:
D. B. Young

OBJECTIVE

The objective of this work is a detailed literature search on the hydration mechanics of Blast Furnace Slag (BFS). The cement construction industry has used BFS for a variety of applications for many years. Several "non-petroleum" papers have been written on various aspects of BFS. These papers were thoroughly investigated in order to gain a more complete understanding of the BFS/Mud system's:

a. gelling and settling characteristics, and
b. slag cement chemistry

This information is desired to gain insight into the key issue of using BFS in drilling fluids.

Conclusions

From review of all of the papers available in the literature the following conclusions and observations can be made:

1. Almost all of the BFS used in the construction industry is in conjunction with Portland Cement.
2. BFS is used with Portland Cement because of the enhanced properties provided by the mixture i.e. mixability, rheology and compressive strengths.
3. In construction applications (which is generally atmospheric conditions) the BFS by itself exhibits excessive cracking and shrinkage but under steam conditions (which is more like the petroleum application) the cement systems exhibit only minor shrinkage and cracking.
4. Activation of the BFS system is the critical parameter that effects the shrinkage and cracking.
5. A wide variety of activators are available to activate the BFS used in the petroleum applications. Some of the more useful activators that can be used in addition to Sodium Hydroxide and Sodium Bicarbonate are: Sodium Silicate, Hydrated Lime, Lithium Salts, and some Flyashes.

Introduction

Comprehensive literature searches were undertaken to find relevant public information on the use of blast furnace slags (BFS) in the cement construction industry. The sources used for the searches were:

- University of Tulsa - Petroleum Abstracts
- American Chemical Society - CCS Reference Center
- Engineering Information, Inc. - Compendex Plus

This analysis of the survey focuses on the non-petroleum cement technology using blast furnace slags. It is divided into four sections:

1. General Information - Historical data, manufacturing processes, cement industry uses, and general information .
2. Chemistry - Current knowledge on the chemical process, structures, and by-products of BFS usage.
3. Physical Properties - Reported physical properties of BFS, with emphasis on cracking and shrinkage.
4. Activators - Published reports on the various methods used to activate BFS and BFS/Portland Cement mixes.

BFS use in the oilfield has primarily been as a stand alone cementitious material mixed with drilling fluids. However, the cement construction industry has for some time only been using BFS mixed with Portland cement (OPC). Very limited information is available for BFS by itself. Rather than limit the information available it was decided to look at all of the applications of BFS whether by itself or in conjunction with Portland cement to see what useful information can be obtained. Most of the work reported in the literature has been with BFS/OPC mixes which is reflected in this report.

The complete literature survey listing is shown in the Appendix.

General Information

The American Concrete Institute (ACI) issued a report in 1987 that is a comprehensive look at ground granulated BFS (GGBFS), also referred to as granulated or glassy BFS (GBFS), in the construction industry[1]. The ACI report primarily addresses the use of GBFS as a separate material added along with ordinary Portland cement (OPC) to produce concrete. The report also only considered GBFS derived from the smelting of iron ores, so the information in the report only applies to those particular BFS types. The report is, however, an excellent overview of BFS manufacture and use. The following general information paragraphs summarize the information in this report, with a few additions from other publications.[2,3]

Definitions

Blast-Furnace Slag -- *The non-metallic product, consisting essentially of silicates and aluminosilicates of calcium and other bases, that is developed in a molten condition simultaneously with iron in a blast furnace.*

Granulated Blast-Furnace Slag -- *The glassy, granular material formed when molten blast-furnace slag is rapidly chilled, as by immersion in water.*

History

GBFS was used as a cementitious material in the late 1700s and through the 1800s. The first reported production of an OPC/BFS cement was in Germany in 1892 and in the USA in 1896. During World War II, and other times of cement shortages, BFS/OPC blends were produced by intergrinding 25 to 40 percent GBFS with the clinker. These cements performed well but were slow in gaining their ultimate strength. By 1982, however, only about 1 to 2 percent of the total hydraulic cement supply has been of the BFS type. Since the 1950s slag has been used as a separate cementitious material added at the concrete mixer. Separation of the grinding of BFS and OPC has these advantages:

- each material is ground to its optimum fineness for better quality control
- the proportions are adjusted while mixing to suit particular needs
- better storage properties

Manufacture

BFS is a by-product of the pig iron manufacturing process. Iron ores are reduced in blast furnaces to iron oxide and then to molten iron by using coke and limestone. Iron collects at the bottom of the furnace while the slag residue floats on top. The composition of the BFS is dependent on the nature of the ore, the chemical composition of the additives, the size and efficiency of the oven, and the type of iron being made[3]

If the molten BFS is cooled slowly a dense solid material is formed. This material is crushed and sized according to the ultimate use of the slag, i.e., concrete aggregate, road construction, etc. Rapid cooling produces products such as expanded slag, light weight filler material, and granulated slag, a glassy material that can be made in a variety of particle sizes. Rapid cooling by quenching with water is the most common process for granulating slags[1].

Specifications

ASTM C 989 specifies three strength grades for GBFS. The grades are based on a *Slag-Activity Index* (SAI), which relates the average compressive strength of slag-cement mortar cubes to the average compressive strength of reference cement mortar cubes. The SAI is influenced by the cement mortar used. In addition, to the strength requirements the GBFS specifications also have limits on residue, sulfur content, and sulfate content. Canada has two BFS specifications, CSA A 363, Cementatious Hydraulic Slag, and CSA A 23.5, Supplemental Cementing Materials and Their Use in Concrete Construction. Blends of GBFS and cements are covered by ASTM C 595. Three types of blends are addressed:

- slag-modified Portland cement, < 25% BFS.
- Portland-BFS cement, 25—70% BFS.

- slag cement, > 70% BFS.

Mixing and Handling

BFS in the bulk form should be handled like other cementitious materials. Make sure it is clearly marked since BFS can have appearances similar to OPC. No special mixing procedures are necessary with BFS, although correct proportioning is essential to obtaining the final properties in the concrete[1]. Several investigators reported that BFS/OPC mixes had improved workability and placeability characteristics than without the slag. The rheology is different with slag, indicating better particle dispersion and higher fluidity of the pastes and mortars, with and without water-reducing admixtures. Increased slump was also found with BFS/OPC mortars. This may have some benefit in oil industry. In some specific slurries, however, most of rheology of the slurries are controlled by addition of dispersant and application temperatures.

An increase in the time of setting over Portland cement is usually the case in BFS mixtures. The degree to which the set time is effected is determined by:

- curing temperature
- proportions used
- water to cementitious material ratio
- Portland cement characteristics

The time to initial setting is typically extended by one-half to one hour at temperatures around 73°F, with little to no change at temperatures above 85°F. Significant retardation has been noticed at low temperatures, but this can be offset with accelerators.

The strength and rate of strength development varies greatly with curing conditions, BFS proportion, and BFS type. In general, however, most BFS/OPC concretes exhibit reduced strengths. Also, when a BFS concrete has been optimized for compressive strength, they generally yield a higher modulus of rupture after aging beyond 7 days. This may be due to the increased denseness of the paste.[1]

BFS has been used in a variety of ratios with OPC. The ACI report[1] suggests the following ratios:

Ready Mix Applications - In warm weather with an active BFS product, 50/50 mixture or in cold weather and with less active BFS - 20-30% slag. For special ready mix applications: sulfate resistance or low temperature rise - 50/50 ratio and for early strength development - <50% BFS.

Precast Applications - for accelerated mixtures, 40-60% BFS; In normal precast applications, the addition of BFS results in a lower 1-day strength.

No-Slump Applications - BFS additions give increased workability and reduced water demand, resulting in a concrete with greater density and strength.

Mortars and Grouts - BFS improves the strength, permeability, flow and cohesive characteristics.

Additives

In general, standard OPC additives have been used for accelerating or retarding BFS/OPC mixes, with the exception of using caustic soda to activate the BFS. The following are summaries of some of the products used in these mixes.

Accelerators - alkali additives in general accelerate the performance of BFS/OPC mixes.
Grind Size - The grind size is important to optimize reactivity and strength development; palletized BFS requires a greater amount of NaOH for activation.
Initial pH - Higher initial pHs are important for early hydration

Chemistry

Oxides of silica, Alumina, lime, and magnesia constitute about 95% of the total oxides in granulated BFS. The range of chemical constituents found in BFS from the USA and Canada in weight percentages are given in the following table:

Table 1

Weight Percentages of Various Materials in Slag

Material	Weight %
SiO2	32—42
Al2O3	7—17
CaO	29—42
S	0.7—2.2
Fe2O3	0.1—1.5
MnO	0.2—1.0

Compared to OPC, GBFS hydrates very slowly when initially mixed into water. A small immediate reaction occurs, releasing calcium and aluminum ions. For this reason, GBFS is usually treated with alkali salts or OPC to speed up the hydration. The hydration of GBFS with OPC or alkali salts depends on the breakdown and dissolution of the glassy slag structure by hydroxyl ions released by the OPC. GBFS consumes calcium hydroxide to form calcium silicate hydrate. GBFS can also be hydrated without adding OPC by using alkali hydroxides alone. The ACI report stated that there is general agreement that the hydration product formed from GBFS and Portland cement is the same as that formed from OPC, that is, calcium-silicate hydrate.

Hydration

Slag hydration differs from OPC in many aspects. Slag is a homogeneous material (glass) with a uniform reactive surface [4]. Clinker powder is composed of small areas of various minerals with different solubility's and reactivates. While the reaction of clinker is highly exothermic and the hydrated product is built from a needle-like structure, slag and water is only slightly exothermic and is built from a homogeneous mass. To reach high early strength in a slag mix, the particles need to be very close. This can accomplished by reducing the water content. The hydrated slag is more dense in character and develops a more orderly structure. Alkalies effect slag hydration by causing ion exchange and condensation reactions. No formation of $Ca(OH)_2$ occurs during slag hydration.[5]

Sulfides

BFS also contains soluble sulfides which effects the electrochemical potential of BFS/OPC mixtures and may play a role in steel passivation. Macphee[6] suggests that the reducing components of BFS impedes the formation of oxidized passive layers on steel in contact with BFS/OPC pastes. On the other hand, Shkolnick[7] reports that water cooling during slag manufacture causes desulphurization of the BFS which results in some loss of its hydration activity. There were no reported incidences of Sulfide gases being evolved from BFS mixes.

Physical Properties

A large number of papers have dealt with the physical properties of BFS/OPC or BFS/alkali mixtures. In general, BFS and BFS/OPC concretes have compression strengths similar to OPC, but may have less flexural strength than OPC depending on the mixture and nature of the BFS, OPC, and aggregate.

Micro-Cracks and Shrinkage

Of interest to oilfield users are the reports on microfractures and shrinkage of the hydrated BFS cements. One paper by Anderson and Gram published in 1987 by the Nordic Concrete

Federation dealt specifically with BFS by itself. They found that shrinkage in an air dried, alkali-activated slag was up to twice as much as that of OPC. Steam curing (curing under 100% humidity conditions at temperatures greater than 212 °F) however, generally reduced the amount of shrinkage. Thin sections of their test specimens showed a large number of micro cracks in the slag paste as compared to a BFS/OPC mix. A finer grind BFS had fewer micro-cracks and both the air dried and steam dried samples showed the same crack pattern. The following are the conclusions published in their paper.[8]

Alkali-activation is a very efficient way to activate granulated blast furnace slags especially in combination with steam curing. A steam-cured activated slag mortar can achieve a flexural strength above 10Mpa and a compressive strength above 50 mPa after no more than 8 hours.

The setting time for slags with a fineness (Blaine) up to 530 m2/kg is of the same magnitude as for ordinary Portland cement.

The shrinkage of air-cured slag mortars is much higher than (often twice as high) the shrinkage of air-cured OPC mortars.

Steam curing reduces the shrinkage to levels comparable with OPC mortars.

Studies of thin sections have shown that alkali-activated slag develops an extensive number of micro cracks. These micro cracks may influence the durability of the material in a negative way. Further research activities should be concentrated on finding countermeasures against the development of micro cracks.

Hakkinen[9] reported that the rate of carbonation and the gas permeability was high in alkali activated BFS/OPC mixes, evidently proceeding along microcracks, but that the strength of the slag concrete increased by about 50%. Metso[10] reported microcracks in two different types of slags, probably due to shrinkage. The two types of slags had very different alkali-aggregate reactions at the same activation levels. Kutti[11] reported that the amount and type of silica gel formed governs the shrinkage properties of a slag concrete.

Special Properties

Kaushal[12] stated that a high rate of heat evolution is detrimental to the physical properties of concrete. They observed thermal cracking in samples that had the highest rate. Their work showed that slag is less effective at reducing heat evolution than either aggregate or fly ash.

Onabolu[13] looked at the steel/concrete interface in reinforced concretes containing slag and exposed to seawater. Their conclusions were:

- the presence of CaOH at the interface affords sufficient corrosion protection
- slag containing concretes have better durability in sea water than OPC.

Mueller[14] reported that BFS/OPC blends *have fluid loss, free fluid, and compressive strength properties comparable to, and under some conditions more favorable than, Portland Cement.* This of course is highly dependent on the type of mud utilized and the amount of activator.

Activators

NaOH is the primary activator for BFS and BFS/OPC mixes. Isozaki[5] reports that only a few wt. percent of NaOH is optimum for activation. They also report that sodium lignosulfonate is effective as a superplasticizer (dispersant) for NaOH activated BFS cement but the formal concentrates of b-naphthalene sodium sulfonate does not work.

Metso[15] and others[16] looked at activating BFS with several different chemicals and blends of the chemicals. The following are their findings:

Table 2

Various Activators and Their Effect on BFS

Activator	Effect
OPC, Cement Clinker	Very high activation effect, especially for high cement content.
NaOH	Very good activation effect.
Ash of Sulfite Sludge	Activates finer slag moderately.
Fly Ash	Poorer activation.
$Ca(OH)_2$	Moderate activation, dosage under 1.0% positive.
Na2CO3, Na2SiO3, Alumina Cement	Activation effect poor or even nil.
HCl, CaSO4, phosphogypsum, CaCl2	No activation effect.
Gypsum + Cement	Good activation effect
Phosphogypsum + NaOH	Good activation effect, demoulding period had to be increased.
Gypsum + NaOH	Poorer activating effect than with gypsum/cement mix.
Cement + NaOH	Good activation effect, but not better than cement or NaOH alone.
Ash of Sulfite Sludge + NaOH	Moderate activation effect, demoulding period had to be increased.
Fly Ash + NaOH	Good activation effect.
Na2CO3 + NaOH	Very good activation effect.
Various Lithium Salts	Moderate activation effect
F-admixture*	Much higher activation than the others.

*A modified lignosulfonate, primarily sodium based.

Shi[17] reported that, in general, the ability of the various chemicals tested to activate BFS/OPC mixes is, from highest to lowest, NaOH, Na2SiO3, Na2CO3, Na3PO4, NaF, Na2HPO4. Blends with Sodium Silicate[18] showed improved compressive and flexural strength over OPC, but shrinkage strains were higher.

Also of interest, Shi[17] reported that due to the high variations in different slag products, the ASTM C1073 test procedure is not suitable for activation evaluation of BFS and BFS mixes.

References Used

The following papers were used to develop this summary.

1. ACI Committee 226, "F-Ground Granulates Blast-Furnace Slag as a Cementiteous Constituent in Concrete," American Concrete Institute, Jan 1988, Vol. 226, pp. 1-15.
2. Spellman, Louis U., "Use of Blast Furnace Slag as a Cementitious Component: New Profit Opportunity for steel and cement companies," Mining Congress Journal, April 1982.
3. Jain, U.C., "Blast Furnace Slag--Processing and Utilisation," Cement Quarterly Journal of the Cement Manufacturing Association - India, July-Sept 1981, Vol 14, No. 4, pp. 23-30.
4. Talling, Bob, "Accelerated Hardening of Slag when Used as an Active Binder," Proceedings of ACI Symposium, 1985, pp. 143-159.
5. Isozaki, S. Iwamota and Nakagawa K., "Some Properties of Alkali Activated Slag Cement" Proceedings, 8th ICCC, Rio de Janiero, 2986, Vol 5, pp 395-399.
6. Macphee, D.E.; Cao, H.T., "Theoretical description of the impact of blast furnace slag (BFS) on steel passivation in concrete," Magazine of Concrete Research, 1993, Vol 45, No. 162.
7. Shkolnick, Y. Sh., "Physiochemical Principals of the Hydraulic Activity of Blast Furnace Slags," Proceedings, 8th ICCC, Rio de Janiero, 1986, Vol 4, pp.133-136.
8. Andersson, Ronny; Graham, Hans-Erik, "Properties of Alkali Activated Slag Concrete," Nordic Conrete Research, pp. 7-18."
9. Häkkinen, Tarja, "The Permeability of High Strength Blast Furnace Slag Concrete," Nordic Concrete Research, 1992, No. 10, pp. 55-66
10. Metso, J., "The Alkali Reaction of Alkali-activated Finnish Blast Furnace Slag," Silicates Industriels, 1982, Vol 4-5, pp. 123-127.
11. Kutti, T., "Hydration Products of Alkali Activated Slag," 9th International Congress on the Chemistry of Cement.
12. Kaushal, S.; Roy D.M.; Licastro, P.H., "Heat of Hydration and Charaterization of Reaction Products of Adiabatically Cured Fly Ash and Slag Mixtures," pp.87-97.
13. Onabolu, O.A.; Pratt, P.L., "The Effect of Blast Furnace Slag on The Microstructure of the Cement Past/Steel Interface," Material Research Symposium Proceedings, 1988, Vol 113.

14. Mueller, D.T.; DiLullo, G.; Hibbler, J.; Kelly, P., "Portland Cement--Blast Furnace Slag Blends in Oil Well Cementing Applications," SPE 30153, pp.1-4.
15. Metso, J.; Kajaus, E., " Activation of Blast Furnace Slag by Some Inorganic Materials," Publ. SP-Am. Concrete Institute, 79 (Fly Ash) Vol 2, pp.1059-1073.
16. Stark, D., Morgan, B., Okamoto, P. "Eliminating or Minimizing Alkali-Silica Reactvity," Strategic Highway Research Program, National Reseach Council Washington, DC 1993.
17. Shi, Caijun; Day, Robert L., "Early Hydration Characteristics of Alkali-Slag Cements," submitted to Cement and Concrete Research.
18. Douglas, E.; Bilodeau, A.; Malhotra, V.M., "Properties and Durability of Alkali-Activated Slag Concrete," ACI Materials Journal, Sept-Oct 1992, Vol 89, No. 5, pp. 509-516.
19. Shi, Caijun; Day, Robert L., "Some Questions Concerning the ASTM Standard Test Method For Hydraulic Activity of Ground Slag By Reaction With Alkali (ASTM C1073-91)," submitted to Cement, Concrete & Aggregate.

Appendix - Literature Search

The following is a list of references found from the complete literature search. Copies of these papers are available on request.

20. Benge, O.G.; Webster W.W., "Blast Furnace Slag Slurries may have limits for Oil Field Use," Oil & Gas Journal, July 18, 1994, pp. 41-49.
21. Benge, O.G.; Webster W.W., "Evaluation of Blast Furnace Slag Slurries for Oilfield Application," SPE 27449, pp. 169-180.
22. Brooks, Fred; Lang, Willaim J.; Daves, Thomas W., "An Advanced Injection System Designed to Activate Blast Furnace Slag Cement," SPE 28712, pp. 277-288.
23. Cowan, K.M.; Hale, A.H.; Nahm, J.J., "Conversion of Drilling Fluids to Cements With Blast Furnace Slag: Performance Properties and Applications for Well Cementing," SPE 24575.
24. Daimon, M., "Sous-Theme III-2 Mécanisme et Cinétique de l'Hydration du Ciment au Latier," Rapports Principaux, Paris 1980, Vol 1, pp. III-2/1 - 2/8.
25. Daube, Jean; Bakker, Robert, "Portland Blast-Funace Slag Cement: A Review," Blended Cement, pp. 5-14.
26. Dawson, D.M.; Briggs, A., "Effects of Hydrosttic Pressure on the Integrity of Concrete Part II. Preliminary studies on Monolithic Blast Furnace Slag/Cement Under Simulated Sea Disposal Conditions," UKAEA Atomic Energy Research Establishment, Jan 1986.
27. Dunston, Edwin R. Jr., "A Strength Model for Concretes Containing Fly Ash, Blast Furnce Slag and Silica Fume," Materials Research Society Symposium Proceedings, Vol 65, pp. 235-241.
28. Feng, Q.L.; Glasser, F.P., "Microstructure, Mass Transport and Densification of Slag Cement Pastes," Materials Research Society Symposium Proceedings, 1990, Vol 178, pp. 57-65.

29. Feng, Q.L.; Lachowski, E.E.; Glasser, F.P., "Densification and Migration of Ions in Blast Furnace Slag-Portland Cement Pastes," Material Research Society Symposium Proceedings, 1989, Vol 136, pp.263-272.
30. Forss, Bengt, "F-Cement, a New Low-Porosity Slag Cement," Silicates Industriales, 1983, Vol 3, pp. 79-82.
31. Glasser, F.P.; Diamond, S.; Roy D.M., "Hydration Reactions in Cement Pastes Incorporating Fly Ash and other Pozzolanic Materials," Materials Research Society Symposium Proceedings, 1987, Vol 85, pp. 167-186.
32. Glukhovskji, V; Zaitsev, Yy.; Pakhomov, V., "Slag-Alkaline Cements and Concretes-Structure, Properties, Technological and Economic Aspects of the Use," Silicates Industriales, 1983, pp. 197-201.
33. Glukovsky, V.D.; Rostocskaja, G.S.; Rumyna G.V., "High Strength Slag-Alkailine Cements," 7th International Congr. Chem. Cem., 1980, Vol 3, pp. V.164-V.168.
34. Häkkin, Tarja, "The Influence of Slag Content On the Microstructure, Permeability and Mechnaical Propertis of Concrete, Part I," Cement and Concrete Research, 1993, Vol 23, pp. 407-421.
35. Häkkin, Tarja, "The Influence of Slag Content On the Microstructure, Permeability and Mechnaical Propertis of Concrete, Part II," Cement and Concrete Research, 1993, Vol 23, pp. 518-530.
36. Häkkinen, Tarja, "The Microstructure of High Strength Blast Furnace Slag Concrete," pp.67-82.
37. Häkkinen, Tarja; Pyy, Hannu; Koskinen, Pertti, "Microstructural and Permeability Properties of Alkali-activated Slag Concrete," Technical Research Centre of Finland, Research Reports, 1987.
38. Harrison, A.M.; Winter, N.B.; Taylor, H.F.W., "Microstructure and Micro Chemistry of Slag Cement Pastes," Material Research Soc. Symposium Proceedures, Oct 24, 1986, Vol 86, pp. 199-209.
39. Hogan, F.J.; Meusel, J.W., "Evaluation for durability and Strength Development of a Ground Granulated Blast Furnace Slag," Cement, Concrete and Aggregates, CCAGDP, Summer 1981, Vol 3, No. 1, pp. 40-52.
40. Hwang, Chao-Lung; Lin, Chao-Yin, "Strength Development of Blended Blast-Furnace Slag-Cement Mortars," Journal of the Chineese Institute of Engineers, 1986, Vol 9, No. 3, pp.233-239.
41. Hwang, C.L.; Yao, H.L.; Lee, H.J.; Lee, R.J., "A Study of Slag Cement--Bentonite Slurry," International Conference on Soil Mechanics and Foundation Engineering, Rio de Janiero, 1989, Vol 3, pp. 1499-1502.
42. Idorn, Gunnar M.; Roy, Della M., "Factors Affecting the Durability of Concrete and the benefits of Using Blast-Furnace Slag Cement," Cement, Concrete and Aggragates, Summer

1984, Vol 6, No. 1, pp. 3-10.

43. Javanmardi, Kazem; Flodberg, Ken D.; Nahm, James J., "Mud to Cement Technology Proven in Offshore Drilling Project," Oil & Gas Journal, Feb. 15, 1993, pp. 49-57.
44. Jumppanen, Ulla-Maija; Deiderichs, Ulrich; Hinrichsmeyer, Konrad, "Material Properties of F-Concrete at High Temperatures," Technical Research Centre of Finland, Research Reports, 1986.
45. Kukko, Heikki; Mannonen, Risto, "Chemical and Mechanical Properties fo Alkali-Activated Blast Furnace Slag (F-Concrete)," Nordic Concrete Research, Vol 1,pp. 16.1-16.16.
46. Kutti, Tomas; Malinski, Roman; Srebnik, Mieczyslaw, "Investigation of Mechanical Properties and Structure of Alkali Activated Blast--Furnace Slag Mortars," Silicates Industriels, 1982-6, pp. 149-153.
47. Lewis, Donald, W., "Blast-Furnace Slag as a Mineral Admixture for Concrete," Concrete Construction, 1982, Vol 27, No. 5, pp. 448-449.
48. Malolepsky, Jan, "Activation of Synthetic Melilite Slags by Alkalies," Proceedings 8th ICCC, Rio de Janiero, 1986, Vol 4, pp. 104-107.
49. Malolepsky, Jan; Deja, Jan, "The Influence of Curing Conditions of the Mechanical Properties of Alkali Activated Slag Binders," Silicates Industriels, 1988, pp.179-186.
50. Massidda, L.; Sanna, U., "Steam Curing Hydration of Compacts of Blastfurnace Slag Activated by Lime, Cement and Gypsum," Silicates Industriales, 1983-3, pp. 55-60.
51. Mukherjee, Provat Kumar, "Absorption of Activators by Blast Furnace Slag During Hydration," Indian Ceramics, August 1985, Vol 28, No. 5, pp. 99-102.
52. Mukherjee, Provat Kumar, "Effects of Parameters on Activation of Blast Furnace Slag During Hydration," Indian Ceramics, Aug 1985, pp.102-106.
53. Mueller, D.T.; Dickerson, J.P., "Blast Furnace Slag Technology: Features, Limitations, and Practical Applications," SPE 28475, pp.117-129.
54. Nahm, J.J.; Javanmardi, Kazem; Cowan K. M.; Hale, A. H., "Slag Mix Conversion Cementing Technology: Reduction of Mud Disposal Volumes and Management of Rig-Site Drilling Wastes," SPE 25988, pp. 443-451.
55. Nahm, J.J., "Literature Review on the Physical Characteristics and Corrosion Potential of Steel of Portland--Slag Cements," Technical Information Report BRC-3215, pp.1-12.
56. Piot, Bernard, "Le Procédé SLAG-MIX: des scories de haut fourneau mélangées à la boue pour cimentar les puits."
57. Purdon, A.O., "The Action of Alkalies on Blast-Furnace Slag," Journal of the Society of Chemical Industry, Sept 1940, Vol LIX, pp.191-202.
58. Richardson, I.G.; Groves, G.W., "Microstructure and Microanalysis of Hardened Cement Pastes Involving Ground Granulated Blast-Furnace Slag," Journal of Materials Science 27, 1992, pp. 6204-6212.
59. Richardson, I.G.; Groves, G.W., " Models for the Composition and Structure of Calcium

Silicate Hydrate (C-S-H) Gel in Hardened Tricalcium Silicate Pastes," Cement and Concrete Research, 1992, Vol 22, pp.1001-1010.

60. Richardson, I.G.; Rodger, S.A.; Groves, G.W., "The Microstructure of ggbfs/OPC Hardened Cement Pastes and Some Effects of Leaching," Materials Research Society Symposium Proceedings, 1990, Vol 176, pp. 63-74.
61. Rogourd, M.; Thomassin J.H.; Ballif, P.; Touray, J.C., "Blast-Furnace Slag Hydration, Surface Analysis," Cement and Concrete Reasearch, 1983, Vol 13, pp. 549-556.
62. Roy, D.M.; Idorn, G.M., " Development of Structure and Properties of Blast Furnace Slag Cements," International Conference on Slag and Blended Cements, Birmingham, AL, Feb 18-19, 1982, pp. i-39.
63. Roy, DM.; Parker, K.M., "Microstructures and Properties of Granulated Slag-Portland Cement Blends at Normal and Elevated Temperatures," SP 79-21, pp. 397-414.
64. Roy, Della M.; White, Elizabeth L.; Nakagawa, Zenbe-e, "Effects of Early Heat of Hydration and Exposure to Elevated Temperatures on Properties of Mortars and Pastes with Slag Cement," Temperature Effects of Concrete, American Society of Testing and Materials, 1985, pp.150-167.
65. Saasen, Arilid; Salmelid, Bjarne; Blomberg, Nils; Hansen, Karsten; Young, S.P.; Justness, Harald, "The Use of Blast Furnace Slag in North Sea Cementing Applications," SPE 28821, pp.143-153.
66. Sauman, Z., "Influence of Fluorides and Silicofluorides on the Hydration of Cement," Proceedings of the 8th ICC, Rio de Janiero, 1986, Vol II, pp. 1345-13[4]8.
67. Shi, Cajun; Day, Robert L., "Alkali-Slag Cements for the Immobilization of Radioactive Wastes."
68. Shi, Caijun; Day, Robert L.; Wu, Xuequan; Tang, Mingshu, "Comparison of the Microstructure and Performance of Alkali-Salg and Portland Cement Pastes," 9th International Congress on the chemistry of Cement,Vol 111, pp. 298-304.
69. Shi, Caijun; Li, Yinyu "Investigation on some Factors Affecting the Characteristics of Alkali-Phosphorus Slag Cement," Cement and Concrete Research, 1989, Vol 19, pp. 527-533.
70. Shi, Caijun; Li, Y, "Effect of the Modulus of Water Glass on the Activation of Phosphorus Slag," Il Cemento, July-Sept 1989, Vol 86, pp. 161-168.
71. Shi, Caijun; Shen, Xiaodong; Yan, Sheng; Wu, Xuequan; Tang, Mingshu, "Immobilization of Radioactive Wastes with Portland and Alkali-Slag Cement Pastes," Il Cemento, April-June 1994, Vol 91, pp. 97-108.
72. Shi, C.; Tang, X.; Li, Y., "Thermal Activation of Phosphorus Slag," Il Cemento, Oct-Dec 1991, Vol 88, pp. 219-225.
73. Shi, Caijun; Wu, Xuequan; Tang, Mingshu, "Hydration of Alkali-Slag Cements at 150°C," Cement and Concrete Research, 1991, Vol 21, pp. 91-100.
74. Sivasundaram, V.; Malhoitra V.M., "Properties of Concrete Incorporating Low Quantity of

Cement and High Volumes of Ground Granulated Slag," ACI Materials Journal, Nov/Dec 1992, Title #89-M61, pp. 554-563.

75 Smolczyk, H. G., "Sous-Theme III-1 Structure et charatérisation des laitiers," Rapports Principaux, Paris 1980, Vol 1, pp. IOII-1/3 - 2/1.

76. Spellman, L.U., "Granulated Blast Furnace Slag as a Mineral Admixture," Concrete International, Vol 4, No. 7, pp. 66-71.

77. Springenschmid, Rupert; Breitenbhucher, R.; Kaussmann, W., " Cracking Tendency of Concretes with Blastfurnace Slag Cements due to Outflow of heat of Hydration," HEFT, Dec 1987, pp. 817-821.

78. Struble, L.; Diamond, S., "Unstable Selling Behavior of Alkali Silica Gels," Cement and Concrete Research, 1981, Vol 11, pp. 611-617.

79. Talling, Bob; Brandstetr, Jiri, "Present State and Future of Alkali-Activated Slag Concretes," 1989 Trondheim Conference, pp.1519-1545.

80. Teoreanu, I.; Puri, Annemarie, "A Study of Blast Furnace Slag with Sodium Silicate and Sodium Fluorosilicate," Romanian Review of Chemistry, 1972, pp. 17, 3, 471-475.

81. Vehovar, L.; Kuhar, V, "Corrosion of High-Strength Steel in Prestressed Concrete* Containing Calcium Sulphide," Steel/SEM, Feb 20, 1984, pp. 1-9.

82. Wolhuter, C.W.; Turkstra, J.; Morris R.M., "Effect of Calcium Chloride On The Volume Contraction, Non-Evaporable Water Content and Bound Chloride Content of Hydrated Portland Cement and Blast-Furnace Slag," Cement and Concrete Research, 1980, Vol 10, pp. 535-543.

83. Wu, X.; Roy, D.M.; Langton, C.A., "Early Stage Hydration of Slag-Cement," Cement and Concrete Research, 1983, Vol 13, pp. 277-286.

DEA 87 PHASE 2
PROGRESS REPORT NO. 2

OBJECTIVE

The objective of this project is to test and compare Blast Furnace Slag Cements with Portland Cement in three testing scenarios. These tests were performed: gas migration tests, dimensional stability tests and annular sealing tests. This report summarizes the initial data conducted on the cements and slags.

SECTION I - GAS MIGRATION TESTS

This section will outline the gas migration testing results obtained at this point in the test program. The gas migration test cell used in the testing is shown in figure 1. In order for the data to be analyzed easier each test result was plotted into two graphs. The first graph (graph a) shows the data in the first 1000 to 1500 minutes. The next graph (graph b) shows the data collected during the entire test time (over 7 days in most cases). The results for tests conducted so far as shown in figures 2a, b through 6a, b.

Testing Procedures for Seven Day Tests:

Testing conditions were as follows:
BHCT = 126°F
BHST = 152°F
8000 Ft Casing Job with 0.9°F/100 ft Gradient
The mud compositions used in the testing was as follows:

Dispersed System (CLS)	Nondispersed System (PHPA)
Fresh Water	Sea Water
18.0 ppb Bentonite	10.0 ppb PH Bentonite
4.0 ppb Dispersant	1.5 ppb PHPA
2.0 ppb Lignite	2.0 ppb CMS
0.25 ppb XCD	
0.25 ppb PAC-L	0.5 ppb PAC-L
NaOH to pH 10.0	NaOH to pH 9.5
Barite to 12.5 ppg	Barite to 12.5 ppg
30.0 ppb Rev Dust	30.0 ppb Rev Dust
Density = 12.5 #/gal	Density = 12.5 #/gal

The Final Cementing Density was 15.6 #/gal for all compositions.
The cement composition tested was the following:

- Portland Class H cement + 1.0% Fluid Loss Additive + Bentonite + Dispersant at a Density of 15.6 #/gal

Bentonite was used to meet design criteria for the cement slurry.

The test procedures for conducting the gas migration tests were as follows:

1. Fill the model up with water and heat it to the BHCT.
2. Mix approximately 4 gal of the test slurry in a 5 gal bucket.
3. Heat the slurry up to the BHCT while continuously stirring the slurry under low shear.
4. Condition the slurries for one hour.
5. Pump the slurry into the model until good returns from the top of the model are observed.
6. Open valves for water column on top of the cement and gas pressure.
7. Maintain 1.7 psi differential between hydrostatic pressure and the gas pressure.
8. Increase Temperature of the model from BHCT to BHST.
9. Maintain the BHST for the entire testing time.
10. Record the following data:
    a. Temperature of the Model
    b. Pore pressure at several locations in the model (one at the gas entry point, and one at 6 feet from the bottom).

c. Amount of Gas entering the model (first 48 hours).
d. Amount of Gas flowing out of the model

11. At the end of the testing period evaluate the path of gas flow

Laboratory Test Results

The laboratory design test results on each of the slurries tested is shown in Table 1. All the slurries had similar properties. Slurry No. 5 did have some high fann reading but this is expected with the high concentration of activator.

Table 1
Slurry Test Data

Slurry	1 Portland	2 DIS 4/0	3 DIS 4/4	4 DIS 4/8	5 DIS 4/12
Thick Time Hrs:min	2:11	2:05 2:21	2:39 2:02	2:43	2:10
Free Water cc's	0	0	0	0	0
UCA 50 psi 500 psi 24 hrs	5:04 6:36 2820	3:40 3:57 1397	2:47 3:03 1581	3:50 4:00 1600	5:32 5:45 2048
Rheology 600 300 10':10"	300+ 164 5 / 17	300+ 210 8 / 17	300+ 203 14 / --	300+ 148 10 / 26	300+ 300+ 174/220

Seven Day Gas Migration Test Results:

Below is the summary of the tests conducted and a description of the data generated for each test.

- Test/Slurry No. 1 - Figure #2a, b
  Composition: Portland Class "H" Cement + 4.0% Bentonite + 1.0% Fluid loss Additive + 0.15% Dispersant at 15.6 ppg

  Test Comments: This test was the only Portland cement system tested in the gas migration model. The cement maintained the original hydrostatic pressure for up to about 200 minutes and then the pressure started to decrease. When the pressure at the gas entry level decreased to the gas pressure, the gas began to enter the model. A total of over 1500 cc of gas entered the model. The 1500 cc's is the total amount of gas that the gas entry set up could deliver. The total amount of gas volume that could have entered due to hydration volume reduction is about 250 cc. The total test time was in excess of 12,000 minutes and no gas was measured coming out of the model. The measurement system out of the model did not appear to be measuring correctly.

- Test/Slurry No. 2 - Figure #3a,b
  Composition: Dispersed Mud diluted from 12.5 ppg to 10.5 ppg, 4 ppb Sodium Hydroxide, 0 ppb Sodium Carbonate, 1 ppb Dispersant (Unical), 367.56 ppb Blast Furnace Slag, Final Density of 15.6 ppg.

  Test Comments: This slag slurry provided some unusual data. The hydrostatic pressure of the slurry actually increases during the test. This pressure increase was very unlike the data observed in the Portland cement. The pressure increase was do to two things. As the slurry set static in the model the temperature increased to the BHST of 152 °F. The slag slurries have a very low permeability and the temperature increase can cause a small pressure increase. The biggest reason however is that some gas was generated in the slurry as the hydration process proceeds. This evolution of gas is identified two ways. First a sulfur smell was

evident in the set column of cement when cutting it up. Secondly several of the BFS systems showed gas coming out of the model before any gas was measured going in (see test 3 and 4). The gas entry into the setting slag slurry was delayed up to about 1500 minutes. The gas continued to enter the column very slowly until the maximum volume of the gas entry system was reached. The total amount of gas that entered the column was over 1600 cc's. No gas was measured coming out of the model but with over 1600 cc's of gas entry and measurable gas flowing during the cutting process it was assumed that the gas measurement system was malfunctioning.

- Test/Slurry No. 3 - Figure #4a,b
  Slurry No. 3
  Dispersed Mud diluted from 12.5 ppg to 10.5 ppg, 4 ppb Sodium Hydroxide, 4 ppb Sodium Carbonate, 1 ppb Dispersant (Unical), 359.68 ppb Blast Furnace Slag, Final Density of 15.6 ppg.

  Test Comments: This slurry exhibited the largest pressure increases of all of the BFS systems. The pressure increased to 40 psi during the first 400 minutes. The slurry then lost hydrostatic pressure below the gas pressure. It is evident in Figure 4a that some gas was flowing out of the model during the time of the pressure increase. There was approximately 700 cc's of gas that was evolved from the hydration of the slag system as evidenced by the gas out measurements. Only a small amount of gas (only about 100 cc's of gas) entered the model. This may be due to the large pressure increases that occurred in the slag system as it set. However it does appears that some small gas channels were formed in the cement when the model was cut because gas flows were measured. (These post set gas flow tests are discussed in the next section). These flows are probably a result of the generation of the gas by the system and the outside entry of gas into the model.

- Test/Slurry No. 4 - Figure #5a,b
  Slurry No. 4
  Dispersed Mud diluted from 12.5 ppg to 10.5 ppg, 4 ppb Sodium Hydroxide, 8 ppb Sodium Carbonate, 2 ppb Dispersant (Unical), 351.60 ppb Blast Furnace Slag, Final Density of 15.6 ppg.

Test Comments: This test showed very similar result to Test 3. Initially, there was a high pressure generated in the slag slurry as the exit gas volumes of over 450 cc's were accumulated (see Figure 5a). There was however no gas entry into the slurry until 2,600 minutes. The exit gas volume however did not measure any substantial amount of gas out of the top of the model. This indicates that the gas measurement system was not sensitive enough to measure the small rates of gas flowing through the model after the cement was set. The gas rate into the model was 14.0 cc's per minute.

- Test/Slurry No. 5 - Figure #6a,b
  Slurry No. 5
  Dispersed Mud diluted from 12.5 ppg to 10.5 ppg, 4 ppb Sodium Hydroxide, 12 ppb Sodium Carbonate, 2.5 ppb Dispersant (Unical), 343.76 ppb Blast Furnace Slag, Final Density of 15.6 ppg.

  Test Comments: This test also had an small initial increase in pressure, but the magnitude of the pressure increase was much less than test 3 and 4. After the small initial pressure increase the pressure declined to below the gas pressure. At approximately 400 minutes gas began to enter the slag slurry. At approximately 2000 minutes gas was measured at the top of the cement column. Gas continued to flow through the cement column throughout the remainder of the test.

Permeability Measurements:

Table 2 summarizes the bulk permeability to gas that was observed and calculated in each of the tests. Several types of gas flow measurements and/or calculations were performed. Each of the data points in the table used one of the measurement systems described below. The short hand version of the method used in the table is provided in parenthesis at the end of the title of each method.

Method 1: Bulk permeability from the plots ($plot_{in}$ and $plot_{out}$)

This method used the gas entry rate into the model during the test to calculate a bulk permeability to flow. The bulk permeability equation used to calculate the values is the "Steady State Linear Flow of Gases Equation". Equation 1 calculates the bulk permeability to gas assuming that the flow was through the permeability. Although the flow in and through the models was not necessarily through the permeability, this equation can be used for comparison purposes. The equation is as follows:

Equation 1:

$$k = (q_{sc} P_{sg} T Z m L) \setminus (3.164 T_{sg} A (P_1^2 - P_2^2))$$

where:
k = Permeability, darcy
q_{sc} = Volumetric Flow rate of Gas, SCF/Day
P_{sg} = Standard Pressure, psia
T = Temperature , °R
Z = Z factor
m = Viscosity, cp
L = Length, ft
T_{sg} = Standard Temperature, °R
A = Flowing Area, ft^2
P_1 = High pressure, psi
P_2 = Low pressure, psi

If the flow of gas into the model was linear then this method was used to calculate a bulk permeability using equation 1. The flow rate q is taken from the inlet gas volumetric flow rate and then adjusted to standard temperature and pressure. These measurement is taken with the model at the test temperature at 5 minute intervals up to 15 minutes.

Method 2: Bulk Permeability from Ports (ports)

After the seven day testing period the test models were pressurized with gas to measure the flow rate with pressure through several ports in the pipe while the test was

at temperature. The measurements were performed at 10, 6 and 3 foot from the gas source at 5 minutes inverts up to 15 total minutes. The difficulty with these measurements was that the port at the 6 and 3' level was located at the side of the column. This means that the flow channel would have to be in contact with the port for the true bulk permeability. Equation 1 was used to calculated the permeability.

Method 3: Bulk Permeability from Cutting the Model (cut)

Once the test model were through the seven day testing period they were taken down from the stand and let set at room temperature for a period of 2 to 4 weeks. The models were then cut up into approximately one foot sections. Bulk Permeability measurements were taken at 10', 6' and 3' from the bottom gas source at 5 minute intervals up to 15 minutes total time. A special adapter was made to capture the cross-sectional flow of gas through the model. Equation 1 was used to calculate the bulk permeability.

Table 2 shows the summary of results for all of the gas migration test conducted thus far. The pressure of gas inlet in each is provided as well as the length of the cement column from the gas inlet. The pressures vary from that used during the test (8.5 or 8.7 psi) to 20 or 30 psi. The higher pressures were needed in some cases due to the excessive period of time to obtain a stable gas flow rates. Typically the flow rate test lasted only 15 total minutes. In some cases this time was not long enough to obtain a stabilized flow of gas. If the test was conducted at the low pressure but was not conducted long enough a designation is given as NCLE (not conducted long enough). The permeability is calculated from one of the three methods described above. Some of the flows were measured at the test temperature (152 °F) and some were measured at room temperature some time after the seven day test was complete.

Table 2
Summary of Bulk Permeability to Gas

Test	Slurry	Pressure (psi)	Length from Gas Inlet (ft)	Perm (md)
1	Cement	8.7	10	47 ($plot_{in}$)[a]
		8.7	10	NCLE[b]
		8.7	6	51 (cut)
		8.7	3	504 (cut)
2	4/0	8.7	10	3 ($plot_{in}$)[a]
		8.7	6	23 (port)[a]
		8.7	3	13 (port)[a]
3	4/4	8.5	10	131 (cut)[c]
		20	10	116 (cut)
		8.5	6	NCLE[b]
		20	6	132 (cut)
		8.5	3	87 (cut)
		20	3	197 (cut)
4	4/8	8.5	10	110 ($plot_{in}$)[a]
		8.5	10	NCLE[b]
		20	10	NCLE[b]
		30	10	46 (cut)
		8.5	6	NCLE[b]
		20	6	75 (cut)
		8.5	3	NCLE[b]
		20	3	78 (cut)
5	4/12	8.5	10	235 ($plot_{out}$)[a]
		8.5	6	929 (port)[a]
		8.5	3	2233 (port)[a]

Notes for Table 2:

a. These tests were conducted under temperature, while all other test were conducted at room temperature.
b. These tests were "not conducted long enough to measure any gas through the model.
c. This test was conducted for 1500 minutes so a stabilized reading was made.

Mapping Gas Flow Channels in Models

The model was cut in approximately one foot intervals from the top down. The top cut is identified as Cut A down through Cut I or J on the bottom. The nitrogen pressure applied to the bottom of the model throughout the gas migration test was continuously maintained through out the cutting process. The temperature on the model was approximately at the 152°F BHST for the first cut, but decreased through the cutting process. Immediately after the cut has been made the exposed facial surface was wetted with soapy water. Any gas through the model was identified by the formation of bubbles. If the gas was from between the inner pipe wall and the outer cement surface the area was marked with a grease pen enclosing the area of bubbles. If the area was all the way around the inside of the pipe, the pipe wall itself was marked. If the gas was coming through the matrix of cement the area was circled.

The group photo is laid out in the following pattern depending if there were nine or ten cuts. Orientation of each piece is in a straight line.

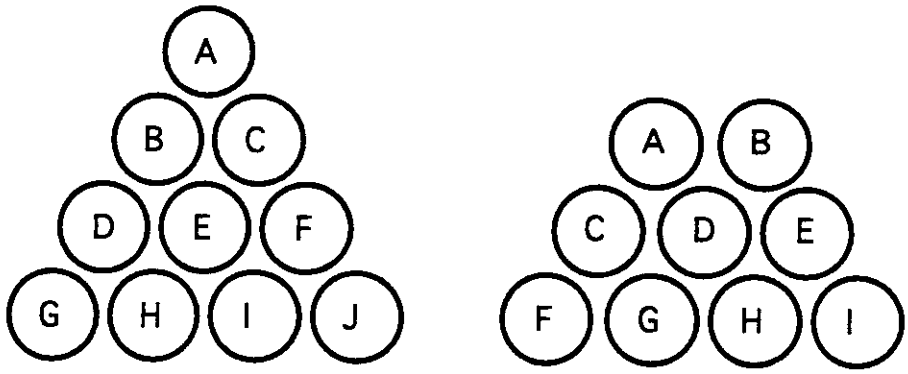

All of the cut models were photographed at the same time, so some of the cracks and chipped out pieces observed in the photographs occurred at a later time. Cracks were not seen immediately after cutting.

SECTION 2 - DIMENSIONAL STABILITY

OBJECTIVE

The objective of this portion of Phase II is to measure the plastic state shrinkage, total volume reduction and the "gas tightness" of BFS and Portland cement systems by way of the Cement Hydration Analyzer. A schematic of the apparatus appears in Figure 7.

Test Procedure

1. Mix the test slurries according to standard procedures.
2. Condition the test slurries for one hour on an atmospheric consistometer. Bring the slurry up to BHCT at the same rate used in Task 2.
3. For low pressure test set the piston pressure at 21.5 bar with a gas pressure of 17.5 bar.
4. Pre- heat the cell to BHCT.
5. Heat the slurry from BHCT to BHST at the same rate as in Task 2.
6. Maintain the test Slurry at BHST for 48 hours.

The following data was taken:

1. Piston movement with time.
2. Temperature and pore pressure of the test slurry.
3. Gas entry into the model with time.

The three slurries tested on the Cement Hydration Analyzer were 1, 2 and 5. Figures 8a, b, and c shows the data for slurry No. 5 while Figure 9a, b, and c shows the test results for slurry No. 2. Figure 10b, c shows the test results for slurry No. 1. No figure 10a was generated. Figures 8a and 9a shows the actual versus theoretical piston pressure and gas pressure. Figures 8b, 9b and 10b shows the top pressure, the piston pressure and the slurry temperature with time. Figures 8c, 9c, and 10c shows the actual piston movement and gas rate in with time.

Table 3 shows a summary of the results of the dimensional stability tests. The 4/12 and the 4/0 slag slurries had a lower measured bulk volume change than did the Portland Cement. The measured values are not the total Bulk and Inner shrinkage but just what is measured in this specific test. These values are dependent on the

geometry of the test vessel as well as applied pressure. The 4/0 slurry had values that were so low that no measurement could be made. This is probably due to the low permeability of the slurry to gas.

Table 3
Bulk Shrinkage and Inner Shrinkage of Three Systems

Test No.	Slurry Composition	% Measured Bulk Volume Change	% Measured Inner Volume Change
1	Dispersed 4/12	????	????
2	Dispersed 4/0	0	0
3	Portland Cement	0.03	3.25

Note: The volume changes for test no. 1 could not be determined from the data supplied. It is estimated that the % Measured Inner Volume Change is 2 to 3%. The missing values will be provided later when the algorithms are obtained.

SECTION 3 - ANNULAR SEALING TEST

OBJECTIVE

The objective of this portion of the project is to test the ability of various BFS systems, and Portland Cement systems, to seal gas in an annular configuration. Well conditions simulating high stress will be modeled. The flow rate of wet and dry gas will be measured in a full scale annular model containing several different slurries for periods up to 28 days. Additionally, the same model will investigate the ability of the systems to seal gas flow in the annulus under high stress conditions.

The slurries tested in this Task will be the same ones used in Task 2 and 3.

Test Models

The test models are a 2 3/8" pipe (1.90" inside diameter) inside a 5" pipe (4" inside diameter) 2 1/2' long (see Figure 10). Three different slurries were tested for a pressure stress test only.

Test Procedures

1. The slurries will be mixed in a one gallon mixer at room temperature.
2. The models will be filled with slurry and placed in an oven and heated to BHST.
3. After curing for a period of over 72 hours the pressure stress test will be conducted.
   a. Stress inside of casing to preset value for 5 minutes
   b. Release the pressure inside the casing and measure the flow rate of gas through the model with 50 psi gas pressure for 5 minutes.
   c. Increase the pressure inside the casing and repeat steps a and b.
   d. Repeat steps c up to safety pressure limit of inside casing.
4. After curing for a period of over 72 hours the temperature stress test was to be conducted. These tests however were not conducted on the samples. An explanation will be provided later. The procedure was to do the following:
   a. Circulated room temperature water inside the 2 3/8 " casing for 5 minutes.
   b. Continually measure the flow rate of gas through the annulus with 50 psi pressure.
   c. Increase temperature to 175 °F and repeat steps a and b.
   d. Increase temperature to 200 °F and repeat steps a and b.

Slurries No.'s 1,2 and 5 were tested in the annular sealing apparatus. Table 3 summarizes the data for slurry No., while table 4 and 5 summarizes the data for slurries 2 and 5 respectively.

Measurement of Bulk Permeability

The bulk permeability of the models were calculated from the flow data using Equation 1. Table 3 indicates that the Portland cement system maintained a tight seal to gas even when pressures of 10,000 psi was placed on the inside of the casing. Table 4 and 5 however, indicate that the Dispersed BFS systems both allowed a substantial amount of gas to flow even before any stress was placed inside the casing. The calculated bulk permeability however did not change much with increasing stress on the inside casing.

Table 3
Portland Cement System

Pressure of Gas (psi)	Time (days)	Pressure inside casing (psi)	Flow rate (l/5 min)	Perm (md)
50	3	0	--	0
50	3	1000	--	0
50	3	2000	--	0
50	3	3000	--	0
50	3	4000	--	0
50	3	5000	--	0
50	3	6000	--	0
50	3	7000	0.18	2.5
50	3	8000	0.19	2.7
50	3	9000	0.24	3.4
50	3	10000	0.33	4.7
50	10	0	0	0
50	17	0	0	0
50	80*	0	0.30	4.7

* This test was conducted at room temperature after 7 days of cooling.

Table 4
BFS System (4/12)

Pressure of Gas (psi)	Time (days)	Pressure inside casing (psi)	Flow rate (l/min)	Perm (md)
50	3	0	3.3	233
50	3	1000	3.3	233
50	3	2000	3.3	233
50	3	3000	3.3	233
50	3	4000	4.2	297
50	3	5000	4.3	304
50	3	6000	4.5	318
50	3	7000	4.6	325
50	3	8000	4.6	325
50	3	9000	5.8	410
50	3	10000	6.3	446
50	10	0	2.0	141
50	10	10000	5.5	388
50	17	0	1.4	99
50	80*	0	7.7	543.2

* This test was conducted at room temperature after 7 days of cooling.

Table 7
BFS System (4/0)

Pressure of Gas (psi)	Time (days)	Pressure inside casing (psi)	Flow rate (l/min)	Perm (md)
50	3	0	5.7	403
50	3	1000	8.5	601
50	3	2000	9.0	636
50	3	3000	9.0	636
50	3	4000	9.0	636
50	3	5000	9.0	636
50	3	6000	9.0	636
50	3	7000	9.2	650
50	3	8000	9.2	650
50	3	9000	9.2	650
50	3	10000	9.2	650
50	10	0	7.0	495
50	10	10000	12.5	884
50	17	0	10.75	760
50	80*	0	10.4	735

* This test was conducted at room temperature after 7 days of cooling.

DEA 87 PHASE 2
PROGRESS REPORT NO. 1

OBJECTIVE:

The objective of this project is to test and compare Blast Furnace Slag Cements with Portland Cement in three testing scenarios. These tests were performed: gas migration tests, dimensional stability tests and annular sealing tests. This report summarizes the initial data conducted on the cements and slags.

SECTION I - GAS MIGRATION TESTS

This section will outline the gas migration testing results obtained for the project so far. The gas migration test cell used in the testing is shown in figure 1. The tests results for tests conducted so far as shown in figures 2 through 6.

Testing conditions were as follows:
BHCT = 126°F
BHST = 152°F
8000 Ft Casing Job with 0.9°F/100 ft Gradient
The mud compositions used in the testing was as follows:

Dispersed System (CLS)	Nondispersed System (PHPA)
Fresh Water	Sea Water
18.0 ppb Bentonite	10.0 ppb PH Bentonite
4.0 ppb Dispersant	1.5 ppb PHPA
2.0 ppb Lignite	2.0 ppb CMS
0.25 ppb XCD	
0.25 ppb PAC-L	0.5 ppb PAC-L
NaOH to pH 10.0	NaOH to pH 9.5
Barite to 12.5 ppg	Barite to 12.5 ppg
30.0 ppb Rev Dust	30.0 ppb Rev Dust
Density = 12.5 #/gal	Density = 12.5 #/gal

The Final Cementing Density was 15.6 #/gal for all compositions.
The cement composition tested was the following:
Portland Class H cement + 1.0% D160 + Bentonite + D65
Density = 15.6 #/gal
Bentonite was used to meet design criteria for the cement slurry. The actual test results on each of the slurries tested is shown in Table 1.

Table 1
Slurry Test Data

slurry	1 Portland	2 DIS 4/0	3 DIS 4/4	4 DIS 4/8	5 DIS 4/12
Thick Time Hrs:min	2:11	2:05 2:21	2:39 2:02	2:43	2:10
Free Water cc's	0	0	0	0	0
UCA 50 psi 500 psi 24 hrs	5:04 6:36 2820	2234 (40:57)	2:47 3:03 1581 2153 (197:04)	3:50 4:00 1600	
Rheology 600 300 10':10"	300+ 164 5 /17	300+ 210 8/17	300+ 203 14/--		300+ 300+ 174/220

The test procedure for conducting the gas migration tests were as follows:

1. Fill the model up with water and heat it to the BHCT.
2. Mix approximately 4 gal of the test slurry in a 5 gal bucket.
3. Heat the slurry up to the BHCT while continuously stirring the slurry under low shear.
4. Condition the slurries for one hour.
5. Pump the slurry into the model until good returns from the top of the model are observed.
6. Open valves for water column on top of the cement and gas pressure.
7. Maintain 1.7 psi differential between hydrostatic pressure and the gas pressure.
8. Increase Temperature of the model from BHCT to BHST.
9. Maintain the BHST for the entire testing time.
10. Record the following data:
    a. Temperature of the Model
    b. Pore pressure at several locations in the model
    c. Amount of Gas entering the model (first 48 hours).
    d. Amount of Gas flowing out of the model
11. At the end of the testing period evaluate the path of gas flow

Below is the summary of the tests conducted.

Figure #2
Slurry No. 1
Portland Class "H" Cement + 4.0% D20 + 1.0% D160 + 0.15% D65 at 15.6 ppg

Note: All of the Dispersed Mud is 12.5 ppg diluted to 10.5 ppg using Fresh Water. The Dispersed Mud System is 18 ppb Bentonite, 4 ppb Dispersant, 2 ppb Lignite, 0.25 ppb XCD, 0.25 ppb PAC-L, Sodium Hydroxide to pH 10.0, Barite to 12.5 ppg, and 30 ppb Rev Dust.

Figure #3
Slurry No. 2
Dispersed Mud diluted from 12.5 ppg to 10.5 ppg, 4 ppb Sodium Hydroxide, 0 ppb Sodium Carbonate, 1 ppb Dispersant (Unical), 367.56 ppb Blast Furnace Slag, Final Density of 15.6 ppg.

Figure #4
Slurry No. 3
Dispersed Mud diluted from 12.5 ppg to 10.5 ppg, 4 ppb Sodium Hydroxide, 4 ppb Sodium Carbonate, 1 ppb Dispersant (Unical), 367.56 ppb Blast Furnace Slag, Final Density of 15.6 ppg.

Figure #5
Slurry No. 4
Dispersed Mud diluted from 12.5 ppg to 10.5 ppg, 4 ppb Sodium Hydroxide, 8 ppb Sodium Carbonate, 2 ppb Dispersant (Unical), 367.56 ppb Blast Furnace Slag, Final Density of 15.6 ppg.

Figure #6
Slurry No. 5
Dispersed Mud diluted from 12.5 ppg to 10.5 ppg, 4 ppb Sodium Hydroxide, 12 ppb Sodium Carbonate, 2.5 ppb Dispersant (Unical), 367.56 ppb Blast Furnace Slag, Final Density of 15.6 ppg.

Table 2 summarizes the bulk permeability to gas that was observed in each of the tests.

Table 2
Bulk Permeability to Gas

Test	Slurry	Pressure (psi)	Length (ft)	Flowrate (cc/min)	Perm (md)
1	Cement	8.7	10	0	0
1	Cement	20	10	0	0
1	Cement	30	10	0.2	0.3
2	DIS 4/0	8.7	10	0.4	3.0
2	DIS 4/0	20	10	0	0
3	DIS 4/4	8.5	10	15.8	131.1
3	DIS 4/4	20	10	42.9	116.3
4	DIS 4/8	8.5	10	0	0
4	DIS 4/8	20	10	0	0
4	DIS 4/8	40	10	27.1	26.2
5	DIS 4/12	8.5	10	26.8	234.7

SECTION 2 - DIMENSIONAL STABILITY

OBJECTIVE

The objective of this portion of Phase II is to measure the plastic state shrinkage, total volume reduction and the "gas tightness" of BFS and Portland cement systems by way of the Cement Hydration Analyzer. A schematic of the apparatus appears in Figure 7.

Test Procedure:

1. Mix the test slurries according to standard procedures.
2. Condition the test slurries for one hour on an atmospheric consistometer. Bring the slurry up to BHCT at the same rate used in Task 2.
3. For low pressure test set the piston pressure at 21.5 bar with a gas pressure of 17.5 bar.
4. Pre- heat the cell to BHCT.
5. Heat the slurry from BHCT to BHST at the same rate as in Task 2.
6. Maintain the test Slurry at BHST for 48 hours.

The following data was taken:

1. Piston movement with time.
2. Temperature and pore pressure of the test slurry.
3. Gas entry into the model with time.

The three slurries tested on the Cement Hydration Analyzer were 1, 2 and 5. Figures 8a, 8b and 8c shows the data for slurry No. 5 while Figure 9a, 9b, and 9c shows the test results for slurry No. 2. The data for Slurry No. 1 will be obtained later and will be distributed to the members.

SECTION 3 - ANNULAR SEALING TEST

OBJECTIVE

The objective of this portion of the project is to test the ability of various BFS systems, and Portland Cement systems, to seal gas in an annular configuration. Well conditions simulating high stress will be modeled. The flow rate of wet and dry gas will be measured in a full scale annular model containing several different slurries for periods up to 28 days. Additionally, the same model will investigate the ability of the systems to seal gas flow in the annulus under high stress conditions.

The slurries tested in this Task will be the same ones used in Task 2 and 3.

Test Models:

The test models are a 2 3/8" pipe inside a 5" pipe 2 1/2' long (see Figure 10). Three different slurries were tested for a pressure stress test only.

Test Procedures:

1. The slurries will be mixed in a one gallon mixer at room temperature.
2. The models will be filled with slurry and placed in an oven and heated to BHST.
3. After curing for a period of over 72 hours the pressure stress test will be conducted.
    a. Stress inside of casing to preset value for 5 minutes
    b. Release the pressure inside the casing and measure the flow rate of gas through the model with 50 psi gas pressure for 5 minutes.
    c. Increase the pressure inside the casing and repeat steps a and b.
    d. Repeat steps c up to safety pressure limit of inside casing.

4. After curing for a period of over 72 hours the temperature stress test was to be conducted. These tests however were not conducted on the samples. An explanation will be provided later. The procedure was to do the following:

a. Circulated room temperature water inside the 2 3/8 " casing for 5 minutes.

b. Continually measure the flow rate of gas through the annulus with 25 psi pressure.

c. Increase temperature to 175 °F and repeat steps a and b.

d. Increase temperature to 200 °F and repeat steps a and b.

Slurries No.'s 1,2 and 5 were tested in the annular sealing apparatus. Table 3 summarizes the data for slurry No., while table 4 and 5 summarizes the data for slurries 2 and 5 respectively.

Table 4
Portland Cement System

Pressure of Gas (psi)	Time (days)	Pressure inside casing (psi)	Flow rate (l/5 min)	Perm (md)
50	3	0	--	0
50	3	1000	--	0
50	3	2000	--	0
50	3	3000	--	0
50	3	4000	--	0
50	3	5000	--	0
50	3	6000	--	0
50	3	7000	0.18	2.5
50	3	8000	0.19	2.7
50	3	9000	0.24	3.4
50	3	10000	0.33	4.7
50	10	0	0	0
50	17	0	0	0
50	80*	0	0.30	4.7

* This test was conducted at room temperature after 7 days of cooling.

Table 5
BFS System (4/12)

Pressure of Gas (psi)	Time (days)	Pressure inside casing (psi)	Flow rate (l/min)	Perm (md)
50	3	0	3.3	233
50	3	1000	3.3	233
50	3	2000	3.3	233
50	3	3000	3.3	233
50	3	4000	4.2	297
50	3	5000	4.3	304
50	3	6000	4.5	318
50	3	7000	4.6	325
50	3	8000	4.6	325
50	3	9000	5.8	410
50	3	10000	6.3	446
50	10	0	2.0	141
50	10	10000	5.5	388
50	17	0	1.4	99
50	80*	0	7.7	543.2

* This test was conducted at room temperature after 7 days of cooling.

Table 6
BFS System (4/0)

Pressure of Gas (psi)	Time (days)	Pressure inside casing (psi)	Flow rate (l/min)	Perm (md)
50	3	0	5.7	403
50	3	1000	8.5	601
50	3	2000	9.0	636
50	3	3000	9.0	636
50	3	4000	9.0	636
50	3	5000	9.0	636
50	3	6000	9.0	636
50	3	7000	9.2	650
50	3	8000	9.2	650
50	3	9000	9.2	650
50	3	10000	9.2	650
50	10	0	7.0	495
50	10	10000	12.5	884
50	17	0	10.75	760
50	80*	0	10.4	735

* This test was conducted at room temperature after 7 days of cooling.

Performance Studies of Mud Converted to Cement (Blast Furnace Slag Cement)

Final Report - DEA-87
December 1994

Joe P. Pavlich,
W. Benton, W. Bodenhamer, H.J. Choi,
T. Edwards, P. Ferrero, J. Jones,
R. Leonard, K. Love, R. Maharidge,
L. Nuebling, F. Sabins, J. Scholten, D. Young

WTCI - 94-120

DEA - 87
"PERFORMANCE STUDIES OF MUD CONVERTED TO CEMENT"

SPONSORS:

The Gas Research Institute
Baker Hughes Inteq
Baroid
Blue Circle Cement
BP Exploration
Chevron
Conoco, Inc.
CTC International
Dowell Schlumberger
Halliburton Energy Services
Kock Minerals
M-I Drilling Fluids
Mobil EPTC
Maersk Oil & Gas
NOWSCO Well Services, Ltd.
Shell Development Co.
Texaco EPTD

Table of Contents

FORWARD

This research project is the "brainchild" of Joe Pavlich, and without his engineering and design this project would not have been successfully conducted. Special credit goes to all the sponsors that provided information during the research project, test parameters, prior research and field data. The Westport technical staff has spent diligent and long hours to achieve the following test results.

The following is a FINAL REPORT, with changes and modifications following the final review meeting held on October 27, 1994, as well as any other input received from Sponsors, and additional data on the long term "creep" test. The deadline for comments was November 17, 1994.

Pursuant to the terms and conditions of the participation agreement, Westport and the Sponsors will keep the Program Results confidential for a period of 12 months from October 27, 1994. Any exceptions to, or waiver of, this strict confidential requirement will require a formal letter request followed by unanimous written consent of all Sponsors. Subject to these provisions, each party shall have the right to freely use any of the Program Results for its own purposes and may only disclose such Program Results and to extend the right to use such information to each of its Affiliates subject to the confidentiality obligation set forth in the participation agreement between Sponsor(s) and Westport.

Following expiration of the confidentiality period, Westport and each Sponsor in the Program may freely use, sell, or license the Program Results developed or acquired by Westport hereunder without accounting to any other party.

WESTPORT MAKES NO REPRESENTATIONS OR WARRANTIES, WHETHER EXPRESS OR IMPLIED, BY OPERATION OF LAW OR OTHERWISE AND SPECIFICALLY PROVIDES PROGRAM RESULTS ON AN "AS IS" BASIS. WESTPORT DISCLAIMS AN IMPLIED WARRANTY OF MERCHANTABILITY OR FITNESS FOR A PARTICULAR PURPOSE. Therefore, all Program Results shall be furnished to Sponsors hereunder without any representation, guaranty, or warranty concerning the accuracy, correctness, soundness, and/or reliability thereof, and the use of such Program Results (including but not limited to, any technique or theory included therein) shall be solely at the risk of the Sponsor or Affiliate receiving and using same. Westport shall not be liable for any damage resulting (i) from inaccuracy, incorrectness, unsoundness, and/or unreliability of Program Results, or (ii) from the use of such Program Results (including by not limited to, any technique or theory included therein). In no event shall Westport's liability include any liability for incidental, indirect, special or consequential damages or loss of use, revenue or profit, even if Westport has been advised of the possibility of such damages.

INTRODUCTION

Executive Summary

The conversion of drilling mud to cement has been discussed in the oil industry for many years, but not until the advent of Shell Oil Company's Blast Furnace Slag Cement (BFS Cement) has a potentially viable system been developed. The effectiveness of using BFS Cement, a combination of blast furnace slag and drilling mud, is the basis of the results reported here. The results are presented as a comparison between BFS Cement and Portland Cement with various additives. These have been generated as agreed upon in the DEA-87 proposal of November 1993 "Performance Studies of Mud Converted to Cement (S-Mix)", hereinafter referred to as BFS. They include analysis of gas migration from a 15' column, simulating a geo-pressured reservoir (Section 1), the thermal and chemical stability of BFS cement under hostile environments including temperature and CO_2 (Section 2), dimensional stability during hydration (Section 3) and testing of mechanical properties of both BFS and Portland cements (Section 4). As BFS cement is a relatively new material these results should be considered as preliminary and, as there is not much of a body of data on which to draw, each section is followed by recommendations for further study. A summation of these recommendations follows this introduction.

Section 1 Gas Migration. A total of nine tests were performed with the gas migration model, but the first five were considered part of the evolutionary process in the design of the model. The last four tests run, two Portland cements (both with fluid loss additives), and two Blast Furnace Slag (BFS) cements (one with partially hydrolyzed poly acrylamide and one with dispersed mud), were considered successful runs. The final four runs showed that gas could enter the cement to one degree or another.

The gas used for gas uptake was dry nitrogen gas at 1.7 psi below the starting hydrostatic cement pressure. In the geometries tested a static gel strength of 90 lbs/100 ft2 was needed before the hydrostatic pressure in the column fell to the gas pressure. This overbalance is indicative of a severe gas flow problem. Both of the slag cements tested lost the initial overbalance pressure in the first several hours and behaved very similar to the Portland cement pressure loss. The total amount of gas that entered the BFS cement systems however was substantially more than the Portland cement systems particularly in the latter stages of the test. This phenomena may indicate differences in the mechanism of gas flow between Portland cements and the BFS cement systems. Also the total amount of gas that entered the Portland cement systems was less than the hydration volume reduction occurring. The total cement volume used was 5057 cc's. The gas flow for both the slag systems was substantially more than the hydration volume reduction (measured at 4 to 6 %). Visual inspection and liquid permeability measured after the tests were completed did not indicate any flow channels to have formed. Analysis of the gas flow data from test two and test four however, did reveal that the bulk permeability to

gas using the steady state linear gas flow equation was 6 millidarcies (md) for the dispersed mud and 15 md for the PHPA system. The set matrix permeability for these two systems was measured at about 5.54 X 10-5 md. Microscopic flow channels were obviously formed during the gas migration tests due to the relatively high bulk permeability. This indicates that at the test conditions studied and the BFS cement systems used that the BFS cement systems were less effective in controlling gas migration than the Portland cement tested. More detailed testing is required to completely describe the applicability of the BFS cement to all gas migration scenarios and slurry compositions.

Section 2.1 Flowloop Tests. This section consists of two sub-sections: Long-Term Flowloop Tests and Galvanic Corrosion Tests of BFS and Portland Cements. The flowloop test determines the long-term thermal and chemical stability under controlled flow conditions of the two cements in simulated oil and gas producing environments. It was found that the flowloop, coupled with Inductively Coupled Plasma Spectroscopy (ICP) measurements, could effectively determine dissolution rates of BFS and Portland Cement under the chosen test conditions; temperature, partial pressure of CO_2 and flow velocity. If the BFS cement systems (40% by weight slag) are normalized for available reactive calcium with Portland cement (72% by weight cement) the conversion rate should be considered the same, as indicated by the data. Below 20 ft/sec dissolution rates of the three samples were insensitive to flow velocity but became flow-dependent at 25 ft/sec. Temperature affected the dissolution to a less degree. However under a nitrogen blanket BFS-dispersed mud dissolved more rapidly than the others. All three test variables (temperature, flow velocity and CO_2) affected the dissolution rates of the cements to a different degree. Among them 200 psi CO_2 was the strongest factor, accelerating dissolution of the three cements, followed by temperature and flow velocity.

The objective of the galvanic test was to investigate the occurrence of accelerated corrosion at the interface between BFS and Portland cements and P-110 carbon steel. Neither the BFS nor Portland cement coatings promoted any unacceptable galvanic corrosion to P-110 carbon steel casing under a stagnant 3.3% NaCl at 150°F and 1 atm CO_2. Corrosion potentials and corrosion rates were measured by an electrochemical technique. These measurements indicated that corrosion of cement coated P-110 was dependent upon the water intake. Of the three coatings, Portland cement promoted the greatest corrosion rate to P-110 carbon steel under the test conditions. This was followed by BFS-PHPA and BFS-dispersed mud.

Section 2.2 Galvanic Corrosion Tests. An electrochemical study was performed to investigate galvanic corrosion between P-110 and BFS (or Portland cement) in a stagnant 3.3% NaCl solution at 150 °F under 1 atm CO_2. BFS (1 & 2) or Portland cement coating did not promote any unacceptable galvanic corrosion to P-110 carbon steel casing at the test condition. Corrosion potential and corrosion rate measured by an electrochemical technique indicated that corrosion of coated P-110 depended upon the water intake and its corrosivity. Among the three coatings, BFS-PHPA, BFS-dispersed mud and Portland cement, all appeared to produce the same low corrosion rate.

Section 3. Dimensional Stability. Based on the BFS compositions used in these tests, both BFS and Portland class G cement mixtures exhibited similar overall hydration volume reductions (HVR) of 4%-6% when in continual contact with water. The magnitude of the HVR's were found to be slightly lower at higher pressure. However, when normalizing the HVR to the volume percentage of slag (26% in the BFS system) and cement (41% in the Portland cement system) in each system, the BFS showed a HVR of approximately 1.5 times that of Portland cement.

Matrix permeability of the two systems were both very low, however, BFS was two orders lower than Portland cement. Attempts to independently measure the bulk and internal volume reductions were frustrated by unidentified interactions between the three chambers of the slurry test vessel.

Section 4. Mechanical Properties Testing. The compressive and tensile strengths of Blast Furnace Slag were compared with Portland Class G cement. For the BFS compositions used in this study, three out of eleven BFS samples showed comparable tensile strengths with Portland. The average tensile strength of Portland cement was 436 psi compared to 290 psi in the three PHPA prepared BFS. However, eight out of the eleven BFS samples failed at lower than 15 psi tensile stress.

The compressive strength of Portland cement was found to be approximately 15% greater than BFS with dispersed mud. The Portland cement also displayed a brittle-ductile transition, while BFS displayed only brittle behavior. The shear strength of Portland cement was slightly greater than BFS. Shear strength increased with increasing confining stress in the Portland cement, but remained constant in the BFS.

Long-term creep tests demonstrated all three systems exhibited axial "creep" phenomena over a 38 day period. Axial strain did not reach equilibration after 38 days. The axial strain rates of all the samples were low, but the BFS rates were approximately 50% lower than the Portland. Total axial strains after this time were between 1% - 1.5%. None of the samples failed as a result of the "creep" response.

Attempts to compare fracture toughness failed because of the inability to extract BFS specimens from their molds. All ten BFS samples broke apart upon removal, while the Portland samples did survive extraction from their molds.

Section 5. Advisory Systems. Unfortunately, the amount of data made available by the members skilled in the 'art' of BFS cements, and having at least a year of field data, has been insufficient to develop a meaningful data set as the basis of an advisory system. As a result, little success was achieved in meeting the objective of developing even the rudiments of an advisory system applicable to BFS cements.

However a few results are reported here using multivariate regression analysis as the basis for deduction. Three parameters were deduced as having relevant relationships to a rudimentary system using multivariate regression analysis. Namely: Mud base density, dilution to base mud (% volume), and the amount of dispersant. This process resulted in relationships among these three parameters and the amount of slag added. However due to the paucity of available data it is advisable not to use these coefficients at the present time due to the confidence interval in the equations being fairly wide (up to 50% of the value of the coefficient for 95% of probability) and a number of important parameters having to be eliminated to reduce the noise to a manageable level.

A more extensive advisory system will have to await sufficient data generation from both laboratory and field to prove its worth.

Section 1 - Gas Migration Analysis

1.1 Summary

A total of nine tests were performed with the gas migration model, but the first five were considered part of the evolutionary process in the design of the model. The last four tests run, two Portland cements (both with fluid loss additives), and two Blast Furnace Slag (BFS) cements (one with partially hydrolyzed poly acrylamide and one with dispersed mud), were considered successful runs. The final four runs showed that gas could enter the cement to one degree or another.

The gas used for gas uptake was dry nitrogen gas at 1.7 psi below the starting hydrostatic cement pressure. In the geometries tested a static gel strength of 90 lbs/100 ft^2 was needed before the hydrostatic pressure in the column fell to the gas pressure. This overbalance is indicative of a severe gas flow problem. Both of the slag cements tested lost the initial overbalance pressure in the first several hours and behaved very similar to the Portland cement pressure loss. The total amount of gas that entered the BFS cement systems however was substantially more than the Portland cement systems particularly in the latter stages of the test. This phenomena may indicate differences in the mechanism of gas flow between Portland cements and the BFS cement systems. Also the total amount of gas that entered the Portland cement systems was less than the hydration volume reduction occurring. The total cement volume used was 5057 cc's. The gas flow for both the slag systems was substantially more than the hydration volume reduction (measured at 4 to 6 %). Visual inspection and liquid permeability measured after the tests were completed did not indicate any flow channels to have formed. Analysis of the gas flow data from test two and test four however, did reveal that the bulk permeability to gas using the steady state linear gas flow equation was 6 millidarcies (md) for the dispersed mud and 15 md for the PHPA system. The set matrix permeability for these two systems was measured at about 5.54 X 10-5 md. Microscopic flow channels were obviously formed during the gas migration tests due to the relatively high bulk permeability. This indicates that at the test conditions studied and the BFS cement systems used that the BFS cement systems were less effective in controlling gas migration than the Portland cement tested. More detailed testing is required to completely describe the applicability of the BFS cement to all gas migration scenarios and slurry compositions.

1.2 Objective

The scope of this experiment is to investigate the effects of Blast Furnace Slag (BFS) cement slurries as compared to Portland Cements when used in geopressured areas. Gas migrating into a cement column following primary cementing can cause channels to occur within the cement column and allow the encroachment of unwanted fluids. This test will investigate the effectiveness of BFS cementing slurries to prevent the migration of gas. A test cell of sufficient length is required in order to measure pressure loss at various points of the cement column. Test results will help to determine if BFS Cement is a viable approach to the mitigation of gas encroachment problems.

1.3 Experimental Procedures

1.3.1 Blast Furnace Slag (BFS) and Portland Cement Formulations

Blast Furnace Slag (BFS) with dispersed mud or partially hydrolyzed poly acrylamide (PHPA) and Portland Class "H" Cements were designed to represent typically field systems. The formulations design was intended for comparison of the effectiveness of their performance properties in geopressured zones for prevention of gas migration. Two Class "H" systems at 16.5 ppg, and two BFS systems utilizing two typical mud systems were tested for physical performance properties following API specifications. The 12.5 ppg mud systems were characterized as a dispersed lignosulfonate clay mud and a Partially Hydrolyzed Poly Acrylamide (PHPA) mud resulting in a mud conversion-to-cement at 15.57 ppg and 15.56 ppg respectively. Table 1 below provides the specific formulation information. These same formulations were used for the tests described in Sections 2, 3 and 4.

TABLE 1 PORTLAND CLASS "H" AND BFS CEMENT GAS MIGRATION MODEL FORMULATIONS

16.5 ppg Portland Cement Class "H"

1 Sack Class H	1 Sack Class H
1.0% D160 (Fluid Loss)	0.6% Halad 344 (Fluid Loss)
2.0% Bentonite (Extender)	2.0% Bentonite (Extender)
0.2% D65 (TIC Dispersant)	0.2% CFR3 (Dispersant)

15.56 ppg Blast Furnace Slag

1 bbl 12.5 ppg Dispersed mud	1 bbl 12.5 ppg PHPA mud
5 ppb Sodium Hydroxide	5 ppb Sodium Hydroxide
10 ppb Sodium Carbonate	10 ppb Sodium Carbonate
0 ppb CLS (Unical)	1 ppb CLS (Unical)
350 ppb Blast Furnace Slag (Blue Circle)	350 ppb Blast Furnace Slag (Blue Circle)

1.3.2 Gas Migration Model

A ten foot scaffold was built (see Figure 1.1 Schematic of Gas Migration Model) to accommodate a ten foot joint of 2" (1.81" I.D.) tubing having strategically located portholes for five pressure transducers and three temperature thermocouples for pressure and temperature acquisition. The prepared slurry was pumped into the 10 foot cell and capped with a five foot water column. Heat tape was used to heat the model and slurries. A gas pressure inlet was attached to the bottom of the cell to allow a differential pressure of 1.7 psi less than the combined hydrostatic pressure of the slurry and water column. If the hydrostatic pressure declines below this gas pressure level, before sufficient gel strength develop, the gas would then encroach into the slurry column. The test cell was monitored and data acquired utilizing LABView programs on a Macintosh computer. Real time data was displayed constantly during the test for immediate analysis and control. Accumulated data was graphed showing pressure and temperature profiles of each slurry.

1.3.3 Gas Migration Model, API and Other Test Procedures

Testing of the BFS and Portland cements was conducted according to "Specification for Materials and Testing for Well Cements; API Specification 10A (Spec 10A), Twenty-First Edition, September 1, 1991" and "API Specification 10 (Spec 10), Fifth Edition, July 1, 1990". These tests include; Thickening Time, Fluid Loss, Rheology, and Free Fluid. Other tests not specifically covered by the API Specification manuals included Ultrasonic Cement Analyzer for Compressive Strengths, 10 second & 10 minute Gel Strengths, and the BPX Settlement test. Testing comprised of laboratory and pilot tests as well as testing of actual slurry mixed and pumped into the Gas Migration Test Cell.

Gas Model Testing consisted of mixing 15 gallons of Portland cement or 11 gallons of BFS, and circulating the slurries through the bottom of the 10 foot Gas Migration test cell and back into the mix tank until uniform flow of returning slurry was observed. The slurry was then trapped in the gas model by valve isolation. A five foot column of water was then imposed on the top of Gas Model and slurry. Hydrostatic pressures were then confirmed by both a Heise pressure transducer (referred to as System Pressure on graphs) and five pressure transducers placed at regular intervals on the Gas test cell. A fluid loss of the slurry was taken from a port just above the gas pressure port at the bottom of the test cell. Nitrogen gas pressure of 1.7 psi less than the total calculated by hydrostatic pressure of combined slurry and water column was applied to the bottom of the test cell. This pressure was then held constant throughout the test. Any pressure change (positive or negative) within this line was monitored by changes in water weight of the pressurized gas setup. All pressures, temperatures, and gas uptake were recorded by Lab View data acquisition. The cell was then heated externally by heat tape and controlled by Athena Temperature Controllers to 150 °F. The test was run and data accumulated for up to 20 hours on some tests.

All slurries tested in the gas migration model were preceded by laboratory pilot tests. The results of the four slurries can be found in Appendix I. The large volume slurries that were mixed and pumped into the gas migration test cell were also laboratory tested. All laboratory test results are shown in Appendix I.

1.3.4 Liquid Permeability Measurements

Permeability measurements on the Portland Cement and the BFS cement were conducted in accordance with Darcy's Law. The samples measuring one inch in diameter and approximately two inches long were mounted in hassler type core holder under 1500 psi confining stress. Deionized water, filtered to 0.45 microns, was used as the flowing medium. A constant inlet pressure of 500 psi was applied and the flow rate was monitored as a function of time. Calculations are based on a linear flow rate and permeability's are reported in millidarcies.

1.4 Results

The design of the gas migration model itself and the testing procedures developed for successful execution of the four successful tests was an evolutionary process. Equipment and test conditions were systematically resolved and the design and procedural problems encountered during this evolutionary process are described in detail in Appendix II. The end result is a gas migration design and test procedure which is reliable and accurate, as well as being more sensitive than originally anticipated.

The results of the four tests are outlined and plotted below. The graphed data shows the gas pressure in green, and is from the in line Heise display. The System pressure is from the line Heise display. The System pressure is from the second Heise pressure gauge which was located at the same level as pressure transducer five just above the gas pressure inlet at the bottom of the model, and is graphed in blue (See Figure 1). The pressure transducers are labeled one through five with one on top of the model, just below the water column, and it is graphed in yellow. Pressure two is graphed in red, pressure three is cyan, and pressure four is maroon. The gas uptake, also graphed in red, is the reading taken from the balance, which is the weight of displaced water in grams. One gram of water is equivalent to one cubic centimeter (cc) of gas. With regard to the graphs, please note that whether or not the balance was zeroed after setting the gas pressure produces differences in the graph scales. Therefore, care must be taken to note gas uptake scale when interpreting graphed results.

Gas Migration Test No.1: Portland cement Class "H" + 1.0% D160 + 2.0% Bentonite + 0.2% D65, Density: 16.5 ppg; Yield: 1.08 cu ft/sk; Water: 4.3 gals/sk

The mixed Portland cement slurry weight was 16.5 ppg which was pumped into the model and hydrostatic pressure showed 11.4 psi. A gas pressure of 9.7 psi was set and maintained throughout the test. Hydrostatic pressure began to decline after 307 minutes and continued to drop through 661 minutes. Hydrostatic pressures remained lower than initial pressure until test completion. Gas Uptake (GU) or gas entry declined gradually through 386 minutes and then increased through 1253 minutes when the test was terminated. The results are plotted in Figure 1.2 for gas pressures and gas uptake against elapsed time. The total uptake of gas in the model during the test time was about 25 cc's. This is only about 0.5% of the volume of the model. The uptake of gas was only due to hydration. No flow up through the model occurred.

Gas Migration Test No.2: 12.5 ppg BFS-dispersed mud + 5 ppb Sodium Hydroxide + 10 ppb Sodium Carbonate + 350 ppb Blast Furnace Slag, Density: 15.57 ppg; Yield: 7.63 cu ft/bbl.

The mixed BFS-dispersed mud slurry weight was 16.1 ppg but resulting hydrostatic pressure showed 13.5 psi, should have been 11.03 for a 16.1 density, and gas pressure was set for 11.8 psi. Hydrostatic pressure began declining rapidly within the first thirty minutes of the test, and reached lowest point after only seventy five minutes. Hydrostatic pressure then rapidly returned to initial pressures within ninety eight minutes. Gas uptake increased slightly after 82 minutes and did not cross above zero until 290 minutes. From this point gas uptake increased constantly for the next three hours until maximum testing limit was reached and the test was terminated. The total uptake of gas in the model during the test time was 6 cc's in the first few hours and 475 cc's in the later stages (6 + hours). This total volume is more than what could be accounted for by hydration volume reduction (about 10% of slurry volume). Using a flow rate of gas from linear part of the gas uptake curve in figure 1.3.1 and with the linear gas flow equation a bulk permeability to gas was calculated at 6 md. This is substantially higher than the matrix permeability of cores taken from the test model (5.54 X 10-5 md). Comparison of the bulk and matrix permeability's indicate a mechanism of gas flow other than matrix flow. This indicates the flow occurred through micro channels.

The pressures and gas uptake against elapsed time are shown in Figure 1.3.1 for the complete test run. Figure 1.3.2 shows the same results but expanded with the elapsed time up to about 80 minutes into the test. It should be noted that the lowest pressure reading from each of the pressure transducers occurs in sequence against time from pressure transducer #4 through pressure transducer #1, #4 occurring earliest. This demonstrates the sensitivity of the gas migration model indicating that pressure influences the hydration process even under hydrostatic conditions. It is also clear that the initiation point for gas uptake occurs as the initial hydration process is taking place, in this case after 68 minutes. Figure 1.3.3 is a plot of the thermocouple activity against elapsed time.

As these thermocouples are placed inside the model within the cement they are reading the change in temperature of cement itself. In this case an endothermic reaction is quite apparent which follows closely the trough of the pressure readings.

Gas Migration Test No.3: Portland cement Class "H" + 0.6% Halad-344 + 2.0% Bentonite +0.2% CFR-3, Density: 16.5 ppg; Yield: 1.07 cu ft/sk; Water: 4.27 gals/sk

The mixed Portland cement slurry weight was 16.1 ppg which was pumped into the model and hydrostatic pressure showed only 10.3 psi. A gas pressure of 8.6 psi was set and maintained throughout the test. Hydrostatic pressure began to decline rapidly after 177 minutes and continued to drop through 334 minutes. The hydrostatic pressures then began to increase throughout the test but never recovered to initial pressure. Gas Uptake (GU) declined gradually through 331 minutes and then increased through 1310 minutes when the test was terminated. The total uptake of gas in the model during the test time was about 60 cc's. This is only about 1.2% of the volume of the model. The uptake of gas was probably due to hydration. No flow up through the model occurred.

Figure 1.4.1 plots the change in pressure from the pressure transducers and the gas uptake against elapsed time. Figure 1.4.2 shows the thermocouple reading for the test and a similar trend is shown as in Test #2 where an endothermic behavior of the cement follows the hydration process as shown by the initial downward trend of the pressures.

Gas Migration Tests No.4: 12.5 ppg BFS-PHPA mud + 5 ppb Sodium Hydroxide + 10 ppb Sodium Carbonate + 4 ppb Unical (chrome lignosulfonate) + 350 ppb Blast Furnace Slag, Density: 15.56 ppg; Yield: 7.67 cu ft/bbl

The mixed BFS-PHPA slurry weight was 15.6 ppg, resulting hydrostatic pressure was 10.6 psi, gas pressure was set for 8.9 psi. Just like the Dispersed BFS slurry, hydrostatic pressure began declining rapidly within the first thirty minutes of the test, and reached lowest point after 160 minutes. All of the pressures then rapidly increased to above initial pressures within 225 minutes, and remained fairly constant until 1251 minutes, at which time they began declining slowly through termination of the test. Because the slurry essentially had not taken on much gas after 20 hours the test was extended for an additional 22 hours. Gas uptake increased slightly after 225 minutes and then remained essentially at zero until 1360 minutes. From this point gas uptake increased rapidly until maximum testing limit was reached and the test was terminated. The pressures and gas uptake are plotted against elapsed time in Figure 1.5. The total uptake of gas in the model during the test time was 40 cc's in the first few hours and 1800 cc's in the later stages (21 + hours). This total volume is more than what could be accounted for by hydration volume reduction (about 35% of slurry volume). Using a flow rate of gas from linear part of the gas uptake curve in figure 1.3.1 and with the linear gas flow equation a bulk permeability to gas was calculated at 15 md. This is substantially higher than the matrix permeability of cores taken from the test model (5.54×10^{-5} md). Comparison of these and bulk and matrix permeability's indicate a mechanism of gas flow other than matrix flow. This indicates the flow occurred through micro channels.

The graphs illustrate some dissimilar trends for BFS cement slurries compared to the Portland cement slurries. Both the BFS-PHPA and BFS-dispersed mud slurries showed early rapid decline in hydrostatic pressure with gas uptake remaining low and below the fluids hydrostatic pressure until late in the test. Whereas the cements gas uptake increased immediately through the cements decline in hydrostatic pressure and followed the cements subsequent rise in pressure.

1.4.1 Liquid Permeability Measurements

One inch diameter by two inch long cores were cut from similar sections of the column for Test No.s' 3 and 4 after the experiments had been completed. Test No.3 was a Portland cement and Test No.4 was a BFS-PHPA cement. The Portland cement had a liquid permeability of 3.8×10^{-3} md and the BFS-PHPA cement an order of magnitude lower at 5.54×10^{-5} md.

1.5 Recommendations

The Westport Gas Migration Model has evolved into a sensitive system for the measurement of gas migration and it is recommended, based on the results presented here to extend the tests to include:

a) Tests with no gas present to provide a baseline for further gas migration tests.

b) Tests with various overbalance pressure applied to alter the degree of the gas flow problem.

c) Vary the composition of BFS cements.

d) Extend experimental time to define gas flow behavior during the latter stages of hydration.

1.6 Appendix I: Physical Properties of Cement Formulations

Gas Model Test #	1	3	Gas Model Test #	2	4
Date	9/22/94	9/27/94	Date	9/25/94	9/30/94
Material	1.0% D160	0.6% H344	Material		
	2.0% Gel	2.0% Gel	Mud	Dispersed	PHPA
	0.2% D65	0.2% CFR2	Int. mud wt	12.5	12.5
			Final mud wt	12.5	12.5
			ppb:		
			NaOH	5	5
			Na2CO3	10	10
			CLS	0	4
			BFS	350	350
Density-ppg	16.5	16.5	Density-ppg	15.57	15.56
Yield-cuft/sk	1.08	1.07	Yield-cuft/bbl	7.63	7.67
Water-gals/sk	4.3	4.27			
Results:			Results:		
Thicken. Time	1:50	1:45	Thicken. Time	1:46	4:58
Fluid Loss	48	34	Fluid Loss	127	88
UCA Strengths			UCA Strengths		
50 psi	3:29	3:04	50 psi	2:29	3:42
500 psi	4:37	4:14	500 psi	2:49	3:54
24:00 hours	3000	2563	24:00 hours	1783	1802
Rheology-rpm	80°F/110°F	80°F/110°F	Rheology-rpm	80°F/110°F	80°F/100°F
300	300+/300+	300+/284	300	264/241	189/161
200	299/236	238/207	200	223/204	129/110
100	161/134	139/124	100	174/161	73/64
6	20/16	19/17	6	116/108	12/10
3	14/11	11/11	3	113/104	9/8
600	300+/300+	300+/300+	600	300+/300+	300+/300+
Gel St-rpm			Gel St-rpm		
10"	16/49	12/13	10"	102/102	16/12
10'	13/44	21/22	10'	111/119	49/43
mls FW @45°	0	0	mls FW @45°	0	0
Settlement:			Settlement:		
Depth TFC	2/32"	8/32"	Depth TFC	0"	3/32"
Stability %	1	1.5	Stability %	2.2	0.5

1.7 Appendix II: Design and Procedural Evolution of the Gas Migration Model

The original objective was to run four gas migration tests with nitrogen gas pressure being set at 1.7 psi less than the combined hydrostatic pressure of the slurry and water column. It required nine tests to accomplish this goal. The chronological sequence of the first five tests are as follows: Test one had a 1/8" nylon nitrogen gas pressure line which filled several feet with slurry and physically blocked the gas inlet. Also a six inch void space at the top of the cement column was discovered upon disassembly. Unanticipated problems with settlement ultimately resulted in the necessity to switch from Class G to Class H and to increase slurry density.

Test two had a 1/8" stainless steel tube with slots cut into it placed inside the gas model to which the 1/8" nylon gas line was connected. This also became blocked early in the test when the gas pressure was reduced below the combined slurry and water hydrostatic pressure. Additionally the desired 150°F temperature was never obtained because two of the three ground fault circuit interrupt safety switches tripped. This problem was not identified until after the test was completed. Light displays were installed for visual means of confirming electrical continuity of heating circuit for all subsequent tests.

For test three the 1/8 " nylon as line was replaced with 1/4" copper tubing, which was coiled around the model in an attempt to heat the inlet gas. Following the test this line was discovered to be filled with hardened cement of approximately two feet. To overcome the gas line being filled and blocked by cement the gas pressure was set equivalent to the combined cement and water hydrostatic pressure on the following two tests (tests four and five). This actually resulted in the slurry and inlet gas pressure being balanced to each other. Naturally as soon as the slurry and water hydrostatic pressure began to decline through its transition zone, it resulted in immediate gas flow into the model. Also the data acquisition system had not been programmed to record the gas inlet pressure. This was corrected by installing another Heise pressure gauge that would communicate with the computer and that data acquisition sequence was added to the LabView monitoring program. The gas line being filled and blocked by slurry was resolved by placing a 10 micron polypropylene filter paper between two 325 mesh screens which was placed in the gas inlet valve.

To ensure the gas inlet line was free of solids for each of the remaining tests, a bubble test was employed immediately after pumping the slurry into the model. The bubble test was simply increasing the gas inlet pressure very slowly until a bubble was detected by the pressure transducers moving up the column of slurry and displacing a small amount of water out of the water column. The volume of gas to accomplish this was very small, in the range of two to five cc's of gas. The water column was refilled before setting the gas pressure. Gas inlet pressure was then set to the desired 1.7 psi less than combined fluids hydrostatic, this set pressure is labeled "Gas pressure" and plotted in green on the graphs.

Formulations for all tests run:

Gas Migration Test #1: Class "G" + 1.0% D160, Density: 15.56 ppg; Yield; 1.19 cu ft/sk; Water: 5.27 gals/sk

Gas Migration Test #2: Class "H" + 1.0% D160, Density: 16 ppg; Yield: 1.12 cu ft/sk; Water: 4.76 gals/sk

Gas Migration Test #3: Class "H" + 1.0% D160 + 2.0% Bentonite + 0.2% D65 Density: 16.5 ppg; Yield: 1.08 cu ft/sk; Water: 4.3 gals/sk

Gas Migration Test #4: Class "H" + 0.6% Halad-344 + 2.0% Bentonite +0.2% CFR-3, Density: 16.5 ppg; Yield: 1.07 cu ft/sk; Water: 4.27 gals/sk

Gas Migration Test #5: 12.5 ppg PHPA mud + 5 ppb Sodium Hydroxide + 10 ppb Sodium Carbonate + 4 ppb Unical (chrome lignosulfonate) + 350 ppb Blast Furnace Slag Density: 15.56 ppg; Yield: 7.67 cu ft/bbl

Gas Migration Test #6: Class "H" + 1.0% D160 + 2.0% Bentonite + 0.2% D65, Density: 16.5 ppg; Yield: 1.08 cu ft/sk; Water: 4.3 gals/sk

Gas Migration Test #7: 12.5 ppg Dispersed mud + 5 ppb Sodium Hydroxide + 10 ppb Sodium Carbonate + 350 ppb Blast Furnace Slag Density: 15.57 ppg; Yield: 7.63 cu ft/bbl

Gas Migration Test #8: Class "H" + 0.6% Halad-344 + 2.0% Bentonite +0.2% CFR-3, Density: 16.5 ppg; Yield: 1.07 cu ft/sk; Water: 4.27 gals/sk

Gas Migration Test #9: 12.5 ppg PHPA mud + 5 ppb Sodium Hydroxide + 10 ppb Sodium Carbonate + 4 ppb Unical (chrome lignosulfonate) + 350 ppb Blast Furnace Slag Density: 15.56 ppg; Yield: 7.67 cu ft/bbl

Figure 1.1

GAS MIGRATION MODEL

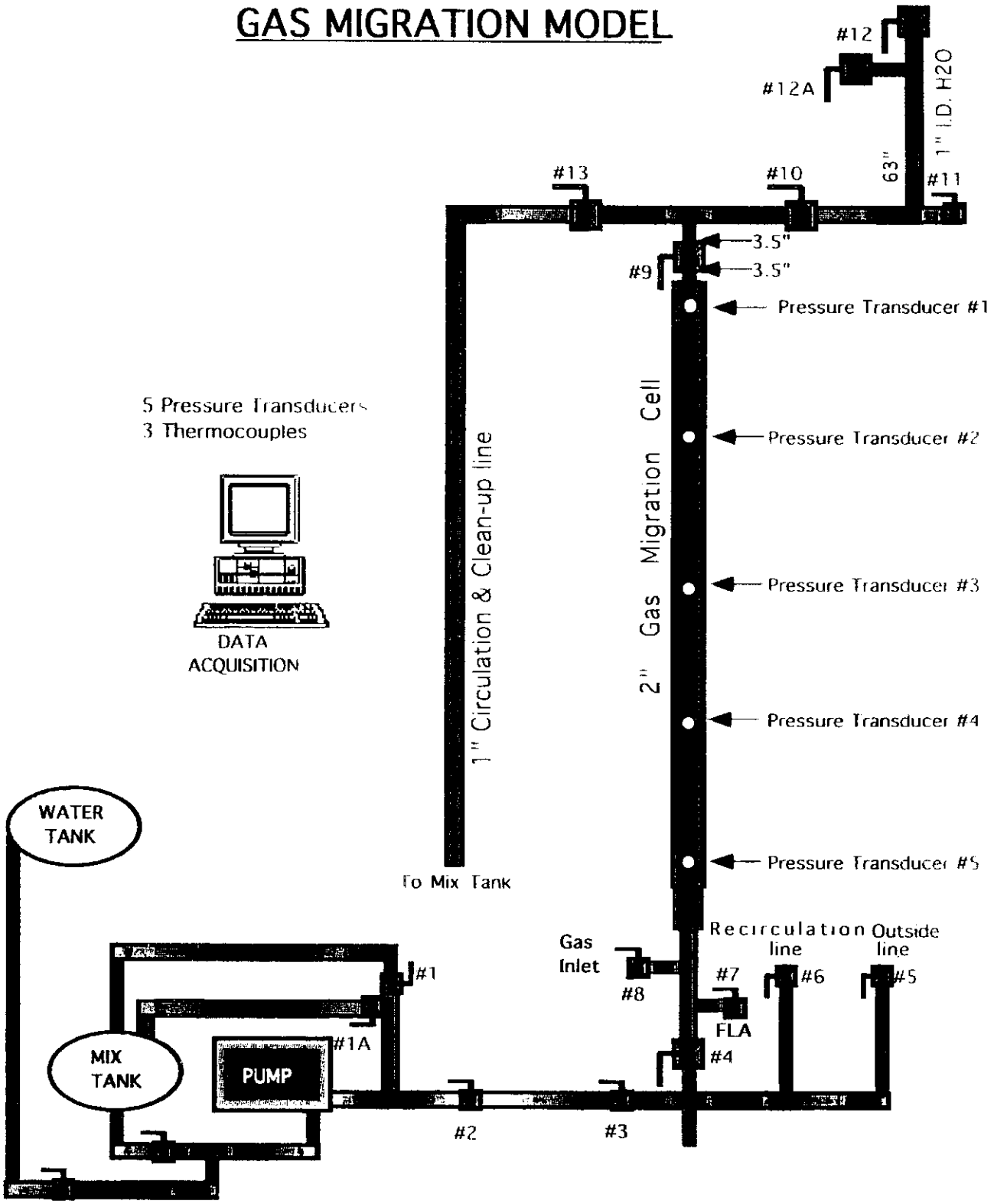

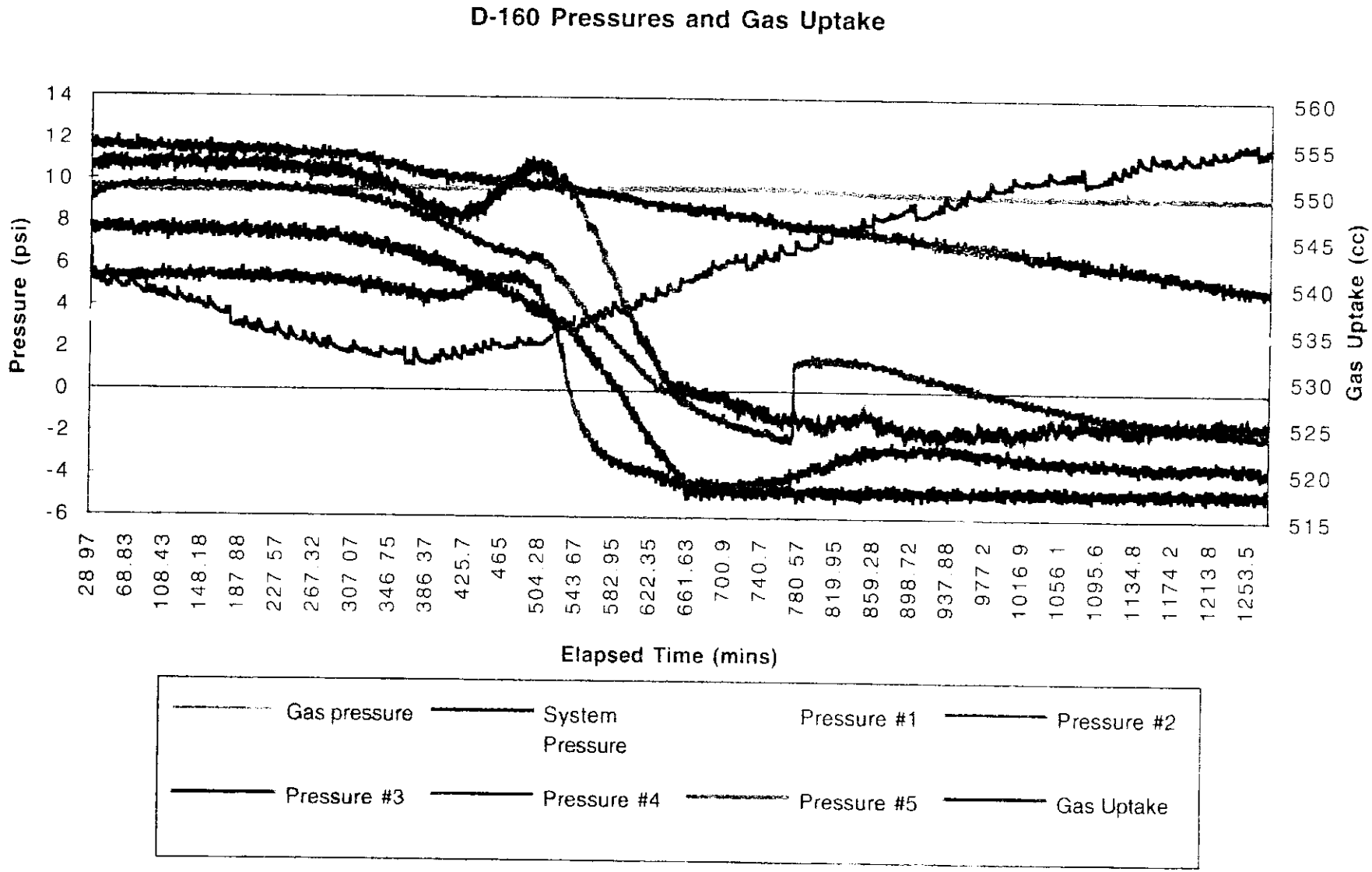
D-160 Pressures and Gas Uptake
Pressure (psi)
14
12
10
8
6
4
2
0
-2
-4
-6
Gas Uptake (cc)
560
555
550
545
540
535
530
525
520
515
28 97
68.83
108.43
148.18
187 88
227 57
267.32
307 07
346 75
386 37
425.7
465
504 28
543 67
582 95
622.35
661.63
700.9
740.7
780 57
819 95
859.28
898 72
937.88
977 2
1016 9
1056 1
1095.6
1134.8
1174 2
1213 8
1253.5
Elapsed Time (mins)
Gas pressure
System Pressure
Pressure #1
Pressure #2
Pressure #3
Pressure #4
Pressure #5
Gas Uptake

Figure 1.2

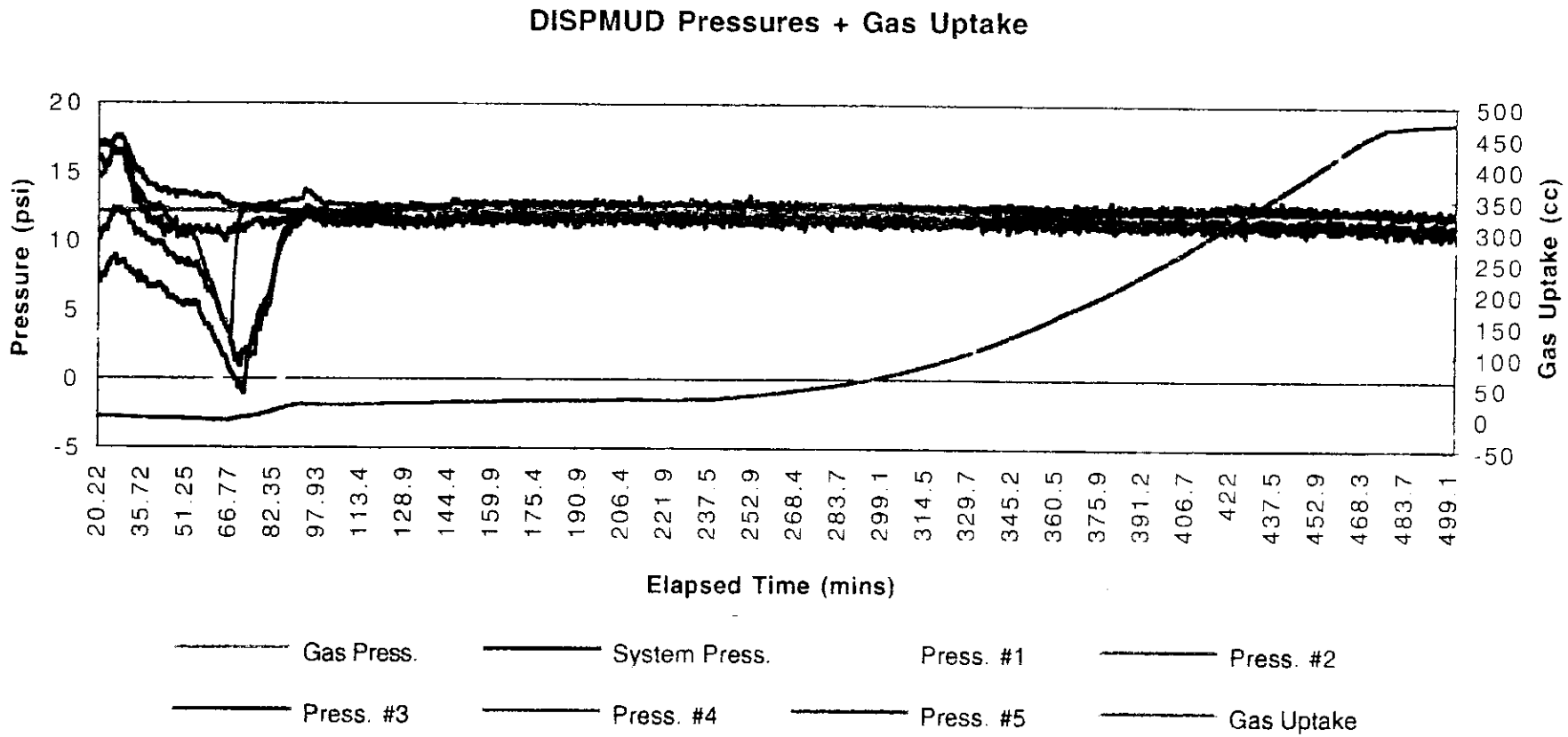
DISPMUD Pressures + Gas Uptake
Pressure (psi)
20
15
10
5
0
-5
Gas Uptake (cc)
500
450
400
350
300
250
200
150
100
50
0
-50
20.22
35.72
51.25
66.77
82.35
97.93
113.4
128.9
144.4
159.9
175.4
190.9
206.4
221.9
237.5
252.9
268.4
283.7
299.1
314.5
329.7
345.2
360.5
375.9
391.2
406.7
422
437.5
452.9
468.3
483.7
499.1
Elapsed Time (mins)
Gas Press.
System Press.
Press. #1
Press. #2
Press. #3
Press. #4
Press. #5
Gas Uptake

Figure 1.3.1

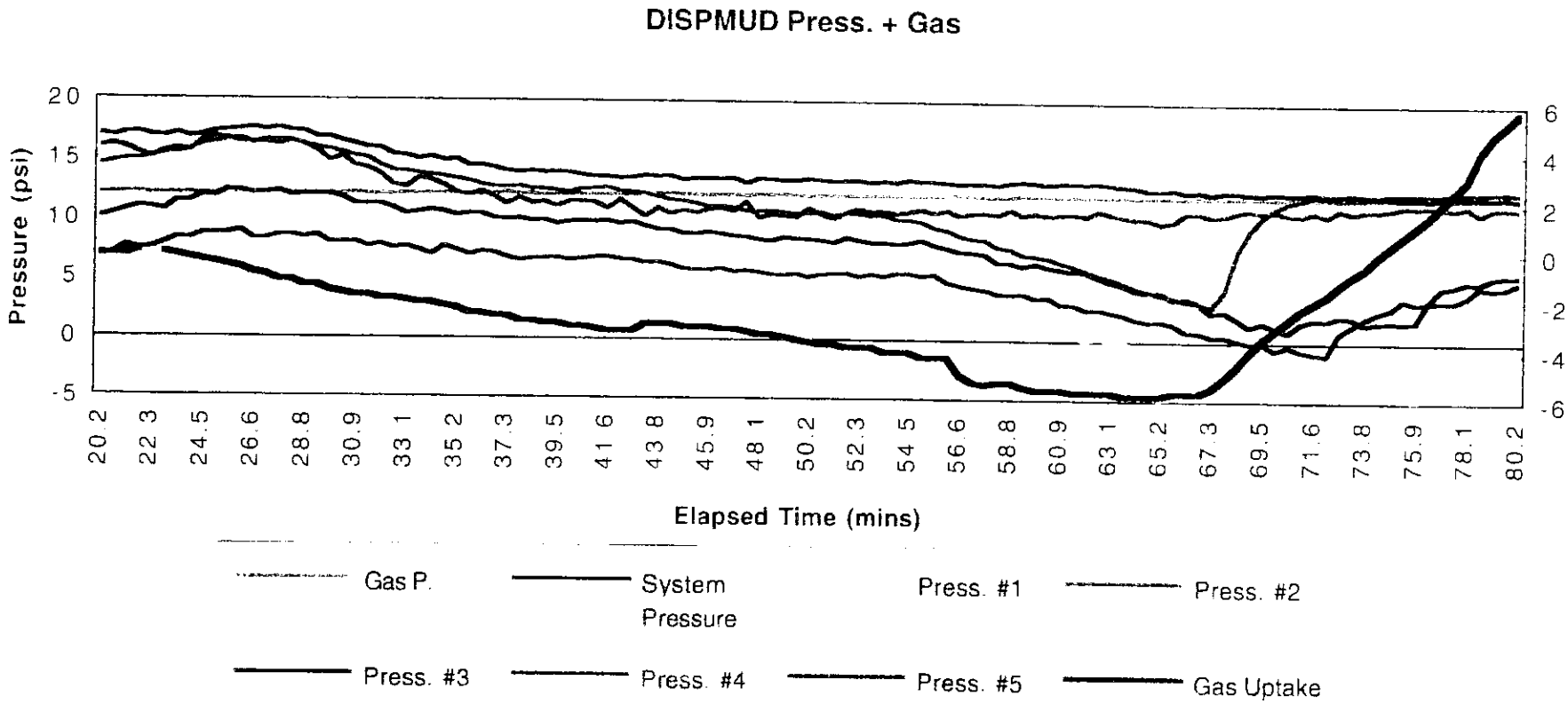
DISPMUD Press. + Gas
Pressure (psi)
20
15
10
5
0
-5
6
4
2
0
-2
-4
-6
20.2
22.3
24.5
26.6
28.8
30.9
33.1
35.2
37.3
39.5
41.6
43.8
45.9
48.1
50.2
52.3
54.5
56.6
58.8
60.9
63.1
65.2
67.3
69.5
71.6
73.8
75.9
78.1
80.2
Elapsed Time (mins)
Gas P.
System Pressure
Press. #1
Press. #2
Press. #3
Press. #4
Press. #5
Gas Uptake

Figure 1.3.2

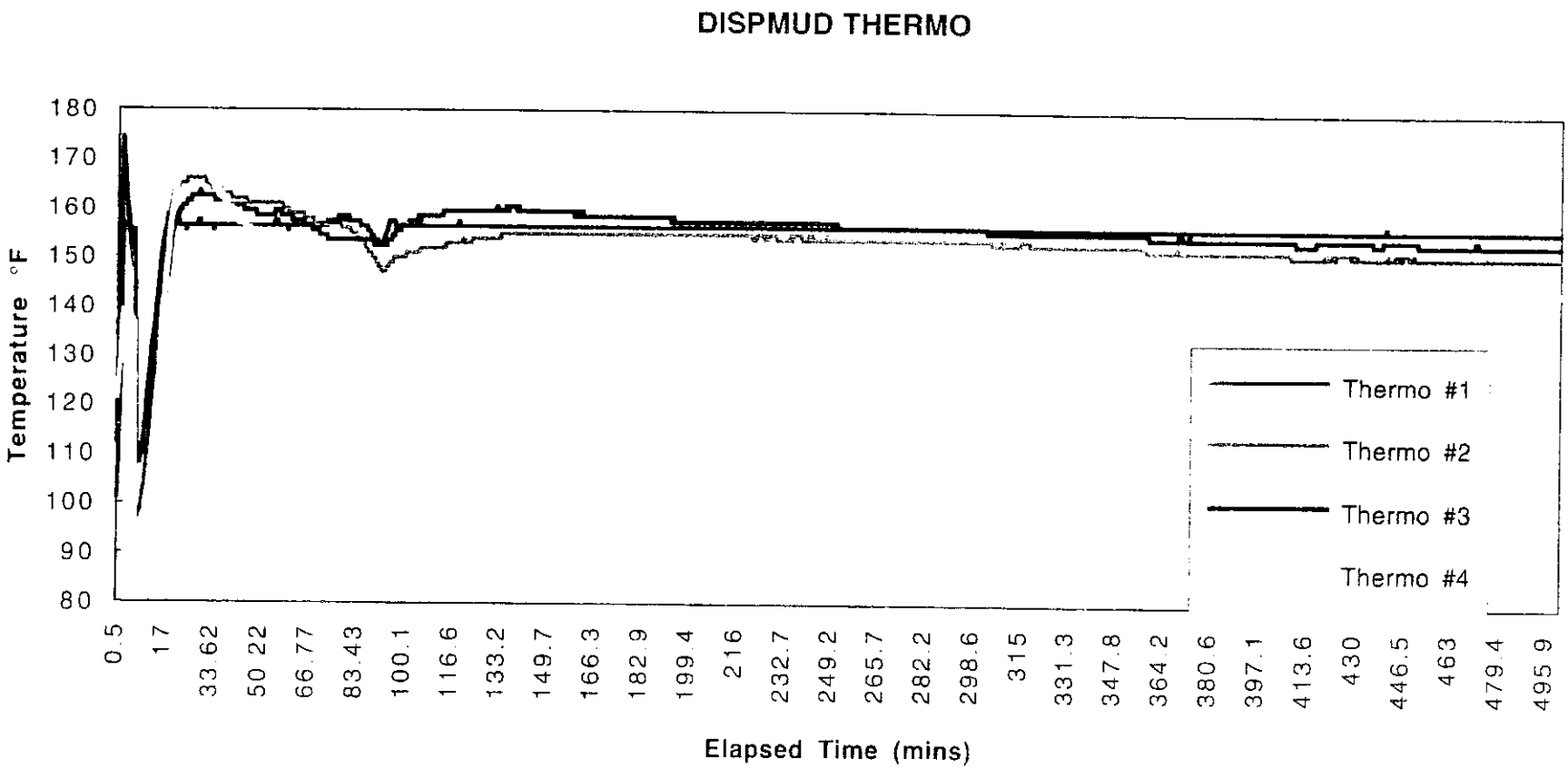
DISPMUD THERMO
Temperature °F
180
170
160
150
140
130
120
110
100
90
80
0.5
17
33.62
50.22
66.77
83.43
100.1
116.6
133.2
149.7
166.3
182.9
199.4
216
232.7
249.2
265.7
282.2
298.6
315
331.3
347.8
364.2
380.6
397.1
413.6
430
446.5
463
479.4
495.9
Elapsed Time (mins)
Thermo #1
Thermo #2
Thermo #3
Thermo #4

Figure 1.3.3.

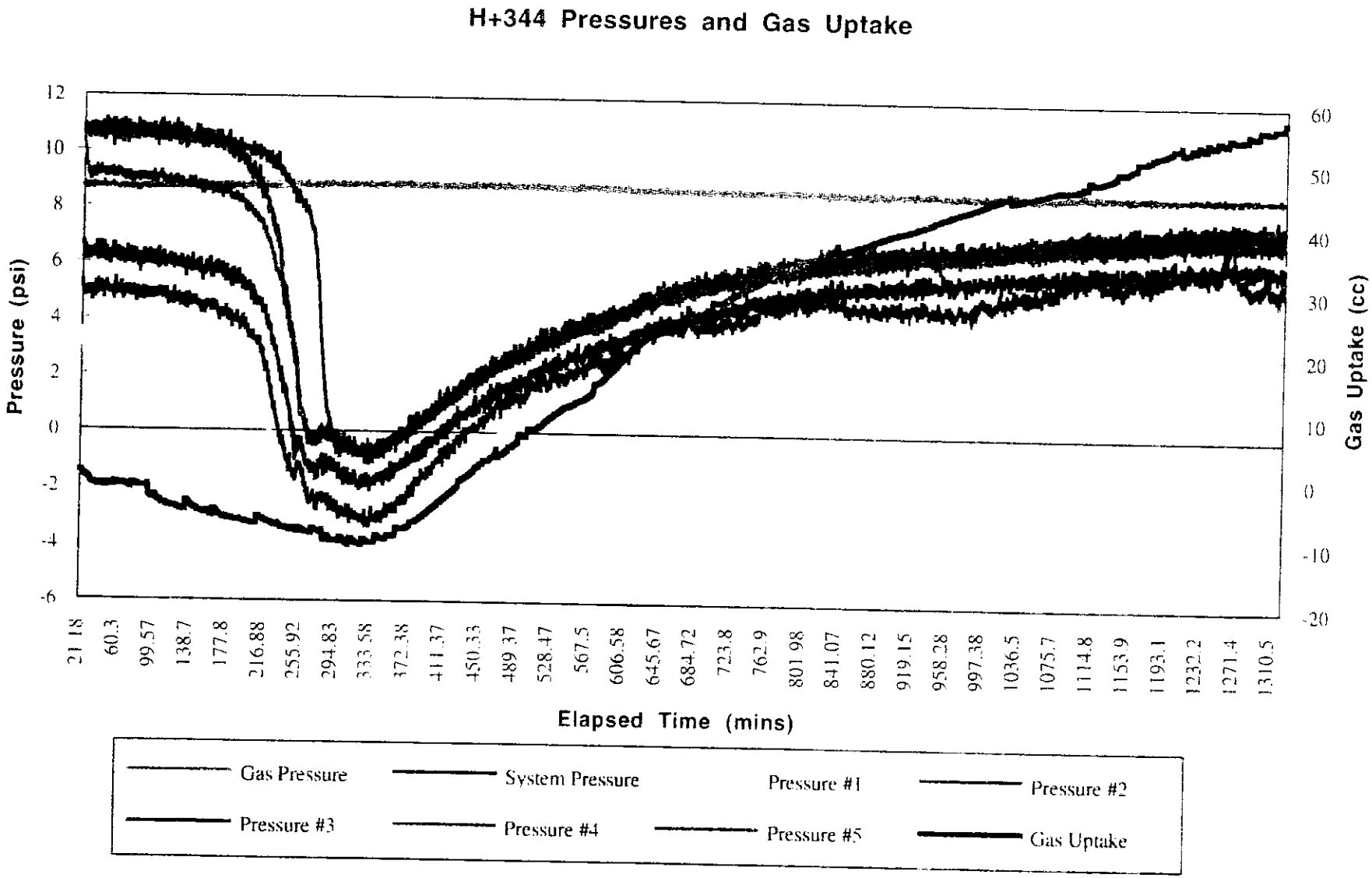
H+344 Pressures and Gas Uptake
Pressure (psi)
12
10
8
6
4
2
0
-2
-4
-6
Gas Uptake (cc)
60
50
40
30
20
10
0
-10
-20
21.18
60.3
99.57
138.7
177.8
216.88
255.92
294.83
333.58
372.38
411.37
450.33
489.37
528.47
567.5
606.58
645.67
684.72
723.8
762.9
801.98
841.07
880.12
919.15
958.28
997.38
1036.5
1075.7
1114.8
1153.9
1193.1
1232.2
1271.4
1310.5
Elapsed Time (mins)
Gas Pressure
System Pressure
Pressure #1
Pressure #2
Pressure #3
Pressure #4
Pressure #5
Gas Uptake

Figure 1 4.1

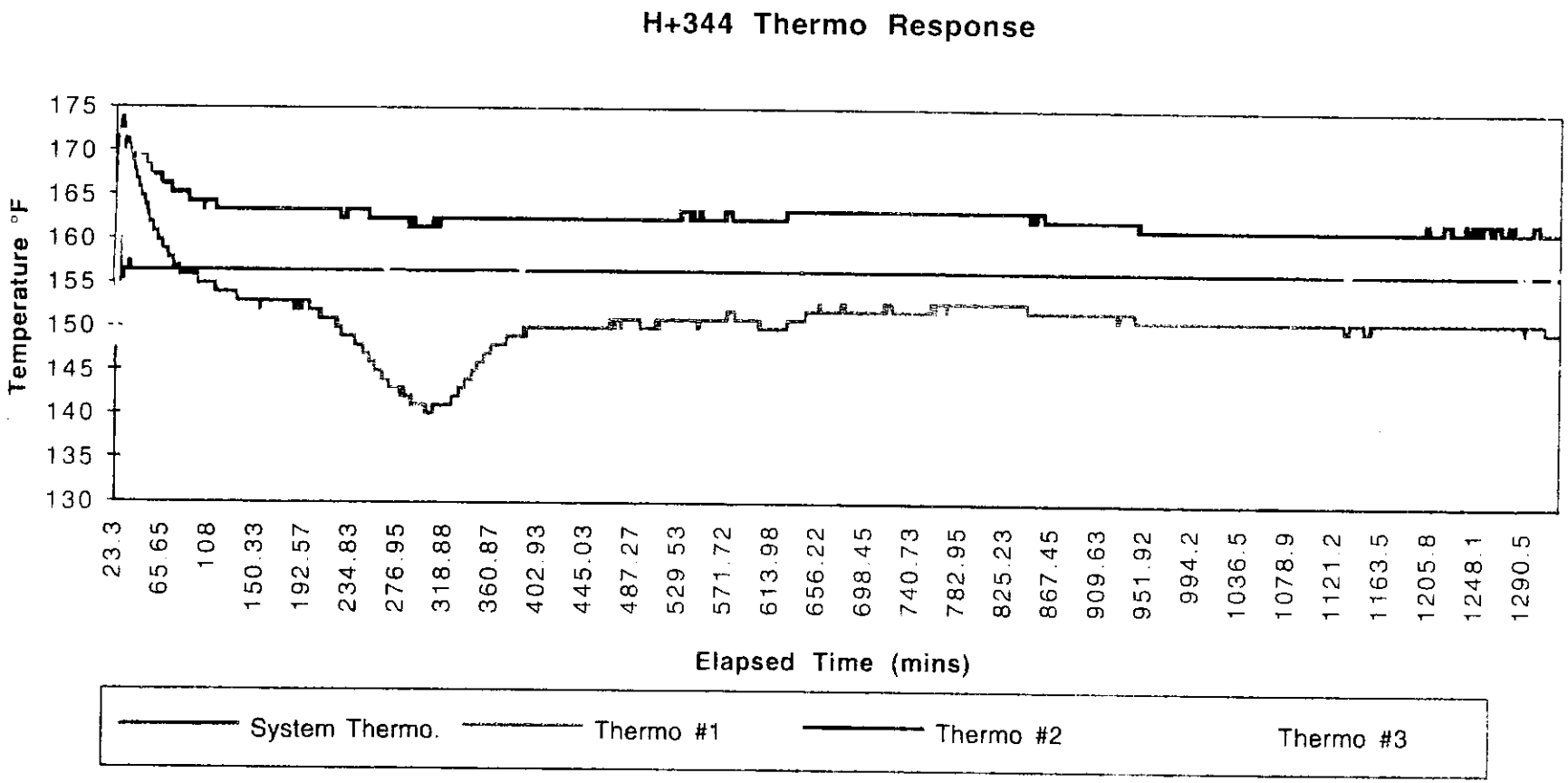
H+344 Thermo Response
Temperature °F
175
170
165
160
155
150
145
140
135
130
23.3
65.65
108
150.33
192.57
234.83
276.95
318.88
360.87
402.93
445.03
487.27
529.53
571.72
613.98
656.22
698.45
740.73
782.95
825.23
867.45
909.63
951.92
994.2
1036.5
1078.9
1121.2
1163.5
1205.8
1248.1
1290.5
Elapsed Time (mins)
System Thermo.
Thermo #1
Thermo #2
Thermo #3

Figure 1.4.2.

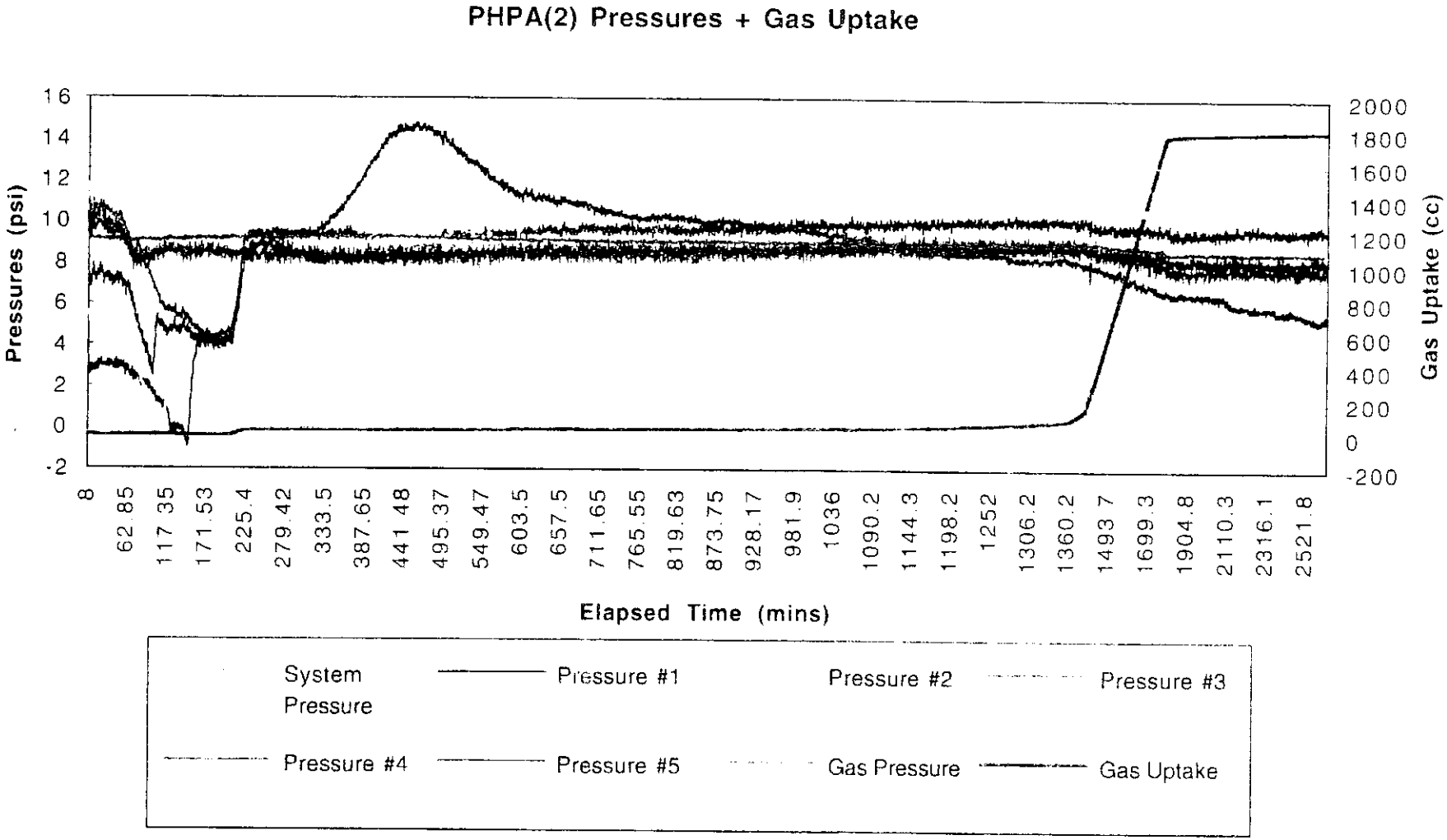
PHPA(2) Pressures + Gas Uptake
Pressures (psi)
16
14
12
10
8
6
4
2
0
-2
Gas Uptake (cc)
2000
1800
1600
1400
1200
1000
800
600
400
200
0
-200
8
62.85
117.35
171.53
225.4
279.42
333.5
387.65
441.48
495.37
549.47
603.5
657.5
711.65
765.55
819.63
873.75
928.17
981.9
1036
1090.2
1144.3
1198.2
1252
1306.2
1360.2
1493.7
1699.3
1904.8
2110.3
2316.1
2521.8
Elapsed Time (mins)
System Pressure
Pressure #1
Pressure #2
Pressure #3
Pressure #4
Pressure #5
Gas Pressure
Gas Uptake

Figure 1.5.1.

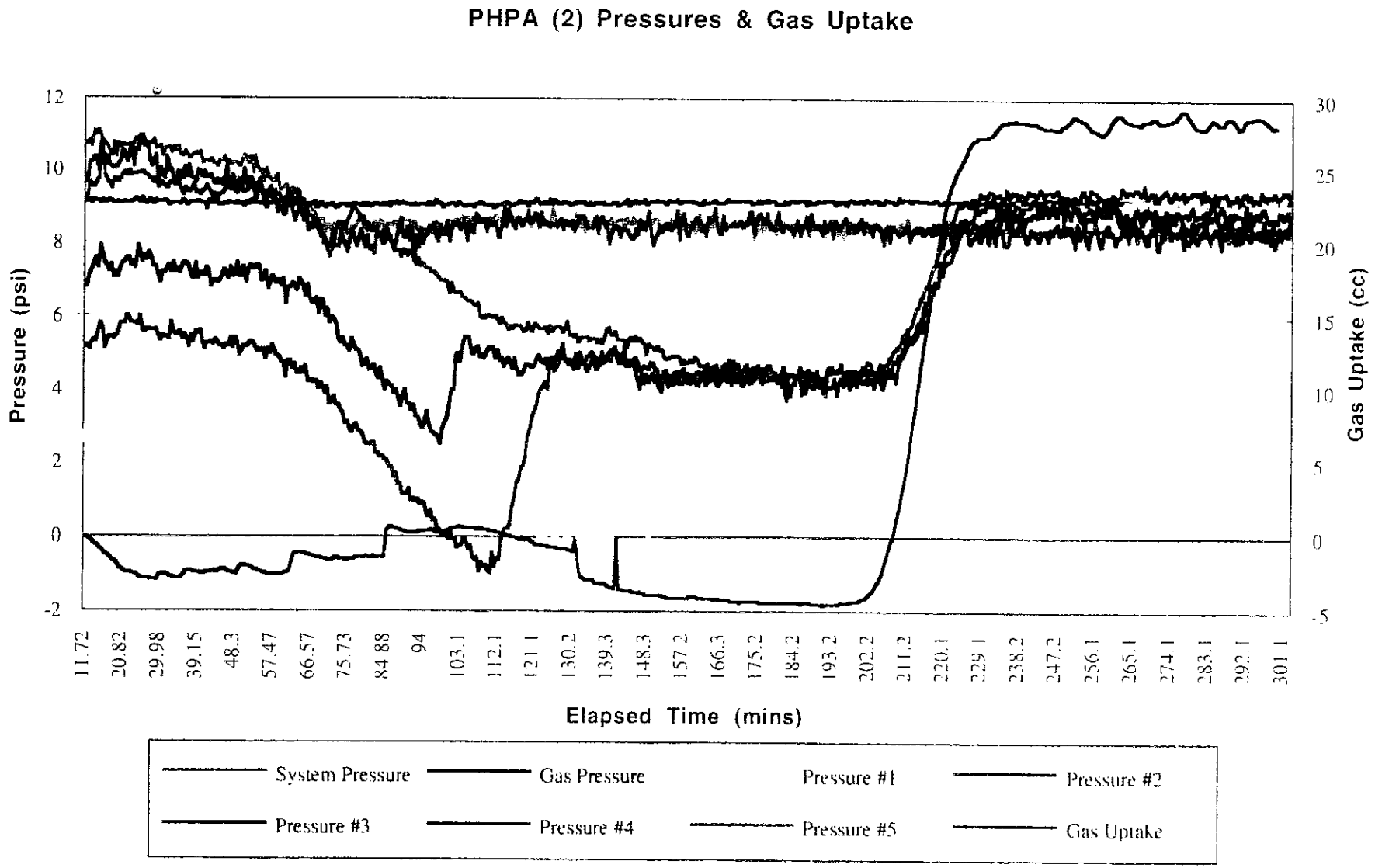
PHPA (2) Pressures & Gas Uptake
Pressure (psi)
Gas Uptake (cc)
Elapsed Time (mins)
12
10
8
6
4
2
0
-2
30
25
20
15
10
5
0
-5
11.72
20.82
29.98
39.15
48.3
57.47
66.57
75.73
84.88
94
103.1
112.1
121.1
130.2
139.3
148.3
157.2
166.3
175.2
184.2
193.2
202.2
211.2
220.1
229.1
238.2
247.2
256.1
265.1
274.1
283.1
292.1
301.1
System Pressure
Gas Pressure
Pressure #1
Pressure #2
Pressure #3
Pressure #4
Pressure #5
Gas Uptake

Figure 1.5.2.

Section 2 - Thermal and Chemical Stability

2.0.1 Summary

This section consists of two sub-sections: Long-Term Flowloop Tests and Galvanic Corrosion Tests of BFS and Portland Cements. The flowloop test determines the long-term thermal and chemical stability under controlled flow conditions of the two cements in simulated oil and gas producing environments. It was found that the flowloop, coupled with Inductively Coupled Plasma Spectroscopy (ICP) measurements, could effectively determine dissolution rates of BFS and Portland Cement under the chosen test conditions; temperature, partial pressure of CO_2 and flow velocity. If the BFS cement systems (40% by weight slag) are normalized for available reactive calcium with Portland cement (72% by weight cement) the conversion rate should be considered the same, as indicated by the data. Below 20 ft/sec dissolution rates of the three samples were insensitive to flow velocity but became flow-dependent at 25 ft/sec. Temperature affected the dissolution to a less degree. However under a nitrogen blanket BFS-dispersed mud dissolved more rapidly than the others. All three test variables (temperature, flow velocity and CO_2) affected the dissolution rates of the cements to a different degree. Among them 200 psi CO_2 was the strongest factor, accelerating dissolution of the three cements, followed by temperature and flow velocity.

The objective of the galvanic test was to investigate the occurrence of accelerated corrosion at the interface between BFS and Portland cements and P-110 carbon steel. Neither the BFS nor Portland cement coatings promoted any unacceptable galvanic corrosion to P-110 carbon steel casing under a stagnant 3.3% NaCl at 150°F and 1 atm CO_2. Corrosion potentials and corrosion rates were measured by an electrochemical technique. These measurements indicated that corrosion of cement coated P-110 was dependent upon the water intake. Of the three coatings, Portland cement promoted the greatest corrosion rate to P-110 carbon steel under the test conditions. This was followed by BFS-PHPA and BFS-dispersed mud.

2.0.2 Objective

This series of tests were designed to determine the long-term thermal and chemical stability of BFS and Portland cements in oil and gas producing environments under controlled flow conditions. Long-term integrity of BFS cement is essential for its use as a well cementing material. However, the effect of temperature and produced fluids on these properties has never been analyzed. If BFS is not stable, the down hole results could be serious enough to cause catastrophic contamination of aquifers and even total loss of the well. Testing was conducted utilizing Westport's Hastalloy C-276 high-temperature/high-pressure flowloops, C-276 static autoclaves and electrochemical galvanic corrosion systems employing a DC potentiostat coupled with a frequency response analyzer.

2.1 Long-Term Flowloop Test of Blast Furnace Slag and Portland Cements

2.1.1 Summary

The purpose of these experiments was to determine the long-term thermal and chemical stability of two blast furnace slag (BSF) cements (PHPA mud and dispersed mud) and Portland Class "G" cement in brine under controlled flow conditions. It was found that the flowloop test, coupled with ICP measurements, could effectively monitor dissolution rates of BFS and Portland cements under controlled conditions of temperature, partial pressure of CO_2 and flow velocity. All three test variables (temperature, flow velocity and CO_2) affected dissolution rates of the three cements to a different degree. CO_2 accelerated dissolution in all three samples. Under aqueous carbon dioxide (CO_2) environment the calcium oxide (CaO) in both slag and Portland cements can convert to calcium carbonate (CaCO2) and then to calcium bicarbonate Ca(CO2)2. The calcium bicarbonate is water soluble and can be measured by the calcium ions in solution. If the BFS cement systems (40% by weight slag) are normalized for available reactive calcium with Portland cement (72% by weight cement) the conversion rate should be considered the same, as indicated by the data. Below 20 ft/sec dissolution rates of the three samples were insensitive to flow velocity but became flow-dependent at 25 ft/sec. Temperature affected the dissolution to a less degree.

Under exposure to hydrochloric acid all three cement samples lost similar weight in the absence of CO2. Whereas under 200 psi CO2 the Portland cement sample tested at 225 °F lost more weight than the tested BFS samples. This test however, only tests surface reactivity and is dependent on the sample permeability. Based on the results, the effects of H2S and sulfate on dissolution of BFS cements under a simulated downhole condition is recommended to be investigated.

2.1.2 Objective

The objective of this project was to determine the long-term thermal and chemical stability of two BFS cements and Portland Class "G" cement in brine under controlled flowing conditions.

2.1.3 Experimental Details

2.1.3.1 Specimen Preparation

A cement slurry was poured into a Teflon specimen mold that had a diameter of 1/2" by 2" in length. An excess of the slurry was released through a pinhole at the top of the mold. This design allowed a specimen to retain the intended dimension after curing. Figure 2.1.1 (a) shows the Teflon mold and a typical cylindrical specimen after curing. At the center of the specimen an 1/8" threaded rod was imbedded. This configuration made it possible to mount the specimen on a specimen holder. After being poured into the Teflon mold, the assembled mold was placed in a 150°F water bath. For the first half of the runs, specimens were cured for one week in the 150°F water bath. Later the curing time was reduced to three days. A cured specimen was released from the mold by using a press and was then immediately weighed. Specimens were kept wet before and after tests to prevent dehydration of sample. The BFS-PHPA and dispersed mud systems and the Portland class "G" cement were tested. Slight dryness promoted hairline cracks in BFS specimens but most of the specimens remained intact during the test. Chemical compositions of the three samples tested are listed in Table 2.1.1.

Figure 2.1.1 (b) is a SEM micrograph of blast furnace slag. Its chemical components are mainly Ca- and Si- oxides as shown in Figure 2.1.1 (c). Reproducibility of the slurries from test to test was attained by having all formulations prepared by Timothy Edwards. Teflon washers (1/8"-thickness and 1/2"-diameter) were placed at both ends of the specimen. This provided a uniform flow around the specimen and kept specimens intact while on the specimen holder.

2.1.3.2 Test Solution

A 3.3% NaCl solution was selected as a test fluid. Besides Na and Cl other impurities were not detected by ICP (Inductively Coupled Plasma Spectroscopy).

Table 2.1.1 Chemical compositions of BFS-PHPA and dispersed mud and Class "G" Portland cement

Portland Cement	API Portland Class "G" Cement	
BFS-PHPA	PHPA mud	525.21 gm
	NaOH	5 gm
	Na_2CO_3	10 gm
	Blast furnace slag	350 gm
BFS-Dispersed Mud	Dispersed mud	525.21 gm
	NaOH	5 gm
	Na_2CO_3	10 gm
	Blast furnace slag	350 gm

2.1.3.3 Flowloop

Figure 2.1.2 (a) shows a schematic of a high-temperature high-pressure (HT/HP) flowloop. The flowloop consisted of a HT/HP centrifugal pump, 1-gallon Hastalloy C-276 autoclave, and a turbine flow meter. All the wetted areas of the components were made of AISI Type 316 stainless steel which exhibited an excellent resistance to flow-accelerated sweet corrosion. Figure 2.1.2 (b) is a schematic of a specimen chamber that was designed to maintain hydrodynamically controlled flow around a test specimen. The flowloop could promote a flow velocity of 25 ft/sec.

2.1.3.4 Test Conditions

Test variables were selected as follows:

Temperature	150, 225 °F
Flow velocity	5, 20, 25 ft/sec
Gas	1 atm nitrogen, 200 psig CO_2
Test duration	One week or three days

2.1.3.5 Test Procedure

1) 4.3-liters of 3.3% NaCl were deaerated for 16 hours prior to being charged into the flowloop.

2) The flowloop containing 4.3-liters of deaerated 3.3% NaCl was heated to a desired test temperature. During this heating period the test solution circulated through the by-pass.

3) A cured cylindrical specimen removed from the Teflon mold was mounted to the specimen holder. The specimen was wet during this assembly.

4) The assembled specimen holder was placed in the specimen chamber which was sparged with a nitrogen gas for 5 minutes. After 5-minute deaeration, the prepared solution was allowed to flow through the specimen chamber with a desired flow velocity.

5) At every 24 hours 30-ml of test solution was sampled and diluted with nitric acid for ICP elemental analysis.

6) After one week (or three days), the power was turned off and the specimen chamber was isolated to cool below 100°F.

7) Below 100°F the flowloop was depressurized and the specimen holder removed from the specimen chamber for weight loss measurement and visual examination.

2.1.3.6 Data Analysis

Samples of test solution were analyzed daily by ICP. Fourteen different elements were measured: Al, Ba, Ca, Cr, Fe, Mg, Mn, Mo, Na, Ni, P, Pb, Si, and Zn. Of these, five elements (Ba, Ca, Fe, Mg, Si) were considered for determining dissolution rate of the cementitious systems. Although weight loss measurements were also conducted, they did not reveal completely the dissolution rate of test specimen. This is because specimens should be wet before and after the run for maintaining dimensional integrity. It was thus difficult to measure an accurate weight loss. Finally, test specimens were dipped in 20% HCl for one minute to determine the effect of acidization. This acidization test only indicates the surface reactivity of the samples, not the total carbonate conversion.

2.1.4 Results and Discussion

Cylindrical test specimens retained their dimensional integrity during the flowloop tests. Periodic ICP measurements successfully determined the dissolution rate of the samples under the test conditions. LF means 5 ft/sec. HF means 20 ft/sec and HHF means 25 ft/sec.

Figure 2.1.3 plots dissolved concentrations of five elements (Ca, Si, Ba, Mg, and Fe) vs. time curves of BFS-PHPA (S1), BFS-dispersed mud (S2) and Portland cement (C) specimens tested in 3.3% NaCl under various conditions. Among the five elements tested, Ca showed the greatest dissolution rate. Regardless of test conditions, the dissolved concentration of Si was next to Ca under a nitrogen blanket. However, under 200 psi CO_2, Fe concentration of all three materials was next to Ca at 150°F, whereas Si dissolved more than Fe for the Portland and BFS-PHPA cements at 225 °F. Dissolved concentrations of the five elements are summarized in Table 2.1.2.

Fe appeared to have come from the flowloop because only BFS-dispersed mud contained any Fe. In short, dissolution rates of Ca and Si were used for comparison of the thermo-chemical stability of the three cements.

2.1.4.1 Effect of CO_2

The presence of CO_2 provided the most significant effect on the dissolution of cement among the three variables including; temperature, flow velocity and CO_2. Figure 2.1.4 shows the dissolution rate of various elements. Pressurizing the flowloop with 200 psi CO_2 accelerated dissolution of most of the elements in all three cements. Exceptions were observed: The Si dissolution of BFS-dispersed mud at 225°F (Figure 2.1.4 (d)) and the Fe dissolution of BFS-dispersed mud at 150°F (Figure 2.1.4 (g)).

Table 2.1.2 Summary of dissolved elements of BFS-PHPA and Dispersed Mud and Portland cement tested in 3.3% NaCl at various test conditions.

Portland Cement	N_2	225°F	HF	Ca> Si> Ba/Fe>Mg
		150°F	HF	Ca> Si> Ba
	CO_2	225 °F	HHF	Ca> Si> Fe> Ba> Mg
		225°F	HF	Ca> Si/Fe> Mg Ba
		225°F	LF	Ca> Si> Fe> Mg> Ba
		150°F	HF	Ca> Fe> Si> Mg> Ba
		150°F	LF	Ca> Fe> Si> Mg> Ba
BFS-PHPA	N_2	225°F	HF	Ca> Si> Ba> Mg> Fe
		150°F	HF	Ca> Si/Ba> Mg> Fe
	CO_2	225°F	HHF	Ca> Si> Fe Mg> Ba
		225°F	HF	Ca> Si> Fe> Mg> Ba
		225°F	LF	Ca> Si> Fe> Mg/Ba
		150°F	HF	Ca> Fe> Mg/Si> Ba
		150°F	LF	Ca> Fe> Mg> Si> Ba
BFS-Dispersed Mud	N_2	225°F	HF	Ca/Si> Ba> Fe> Mg
		150°F	HF	Ca> Si/Ba> Fe> Mg
	CO_2	225°F	HHF	Ca> Si> Fe> Ba/Mg/
		225°F	HF	Ca> Fe> Si> Ba/Mg
		225°F	LF	Ca> Fe> Si> Mg/Ba
		150°F	HF	Ca> Fe> Si> Mg/Ba
		150°F	LF	Ca> Fe> Mg> Si> Ba

2.1.4.2 Effect of Temperature

Figure 2.1.5 shows the effect of temperature on dissolution rate of various elements of the three cements. Increasing the test temperature increased dissolution rates for most of the elements. The only exception was for the Ca dissolution rate of BFS-PHPA tested under 200 psi CO_2.

2.1.4.3 Effect of Flow Velocity

Figure 2.1.6 shows concentration vs. time curves of Ca and Si with 200 psi CO_2. Flow dependency was evident for the Ca and Si dissolution of all of three samples under 200 psi CO_2 at flow velocities greater than 25 ft/sec. Below 20 ft/sec the dissolution rate was insensitive to flow rate. The effect of flow velocity on dissolution rate of the elements was not as strong as that of CO_2. Ca dissolution of Portland cement and BFS-PHPA tested at 150°F was marginally increased by increasing flow velocity from 5 ft/sec to 20 ft/sec.

Figures 2.1.7 and 2.1.8 compare Ca and Si, respectively the dissolution of the three tested cements. Portland cement showed the greatest susceptibility to dissolution under 200 psi CO_2. If the weight percent of reactive slag (40%) and cement (72%) are normalized, then the dissolution per unit weight of reactive species will be about the same. Under a nitrogen blanket, BFS-dispersed mud cement dissolved more rapidly than either BFS-PHPA or Portland cement. Dissolution rate of total dissolved species, except species such as Fe, Cr, Mo, Ni and Na, was computed and plotted in Figure 2.1.9.

Figure 2.1.10 shows photographs of specimens before being tested in 3.3% NaCl under various test conditions. Both BFS cements had a greenish color (the photographs do not reveal the real color because no correction filter was available to correct for fluorescent light in the laboratory). A drastic appearance change took place with the Portland cement samples tested with 200 psi CO_2. They had dark-reddish color. After each run test samples were kept in distilled water. Portland cement samples tested under a nitrogen blanket produced calcium carbonates even when stored at room temperature, whereas when tested under 200 psi CO_2 they produced only a small amount of calcium carbonate. Both BFS cements did not show any visible calcium carbonate after having been stored in distilled water more than one month. Figure 2.1.10 (l) shows a BFS-PHPA specimen tested at 225 °F under 200 psi CO_2. The specimen disintegrated because the specimen was prematurely removed from the specimen chamber while it was hotter than 200 °F. When test specimens were properly handled, such experimental artifact did not occur. Figure 2.1.11 shows the result of X-ray elemental analysis on black deposits of Figure 2.1.10 (g).

2.1.4.4 Effect of Acidization

After each test, a cylindrical specimen was dipped in 20% HCl for one minute. Weight change was measured and listed in Table 2.1.3. Figure 2.1.12 compares the weight change after acidization for three samples. In the absence of CO_2 all of three samples exhibited similar weight change, whereas under 200 psi CO_2 Portland cement sample tested at 225 °F lost weight much more than BFS cements did, regardless of flow velocity. This difference however, is probably due to the test only measuring the surface reactivity of the sample. In this case the permeability of the sample probably influenced the test. If the BFS systems (40% by weight slag) and the Portland cement system (72% by weight cement) are normalized the reactivity and subsequent conversion per unit of active slag or cement is about the same.

Table 2.1.3 Weight loss measurements of three cement samples tested in 3.3% NaCl under various test conditions before and after acidization

Sample	Test Condition			Weight Loss	
	Temp (°F)	Flow Rate (ft/sec)	CO2 (psi)	Wt. Loss Before Acidization (gm/day)	Wt. Change After Acidization (gm)
Portland Cement	150	20	0	0.0032	0.3348
	150	5	200	0.2523	0.1039
	150	20	200	0.1958	0.0665
	225	20	0	w.g.	0.2938
	225	5	200	0.4943	2.0438
	225	20	200	0.2220	2.0438
	225	25	200	0.4549	2.6988
BFS-PHPA	150	20	0	0.0721	0.3008
	150	5	200	0.0076	0.006
	150	20	200	0.1019	0.0011
	225	20	0	na	na
	225	5	200	0.1784	0.006
	225	20	200	na	na
	225	25	200	0.0836	0.0168
BFS-Dispersed	150	20	0	0.0792	0.5410
	150	5	200	na	na
	150	20	200	na	na
	225	20	0.	0.1458	0.2868
	225	5	200	0.1033	0.0641
	225	20	200	0.3075	0.0523
	225	25	200	na	na

Where,
w.g. means weight gain
na means that the specimen was broken after test

2.1.5 Conclusions

Flowloop test coupled with ICP measurements was an effective tool for determining the thermo-chemical stability of the three cement systems under a simulated reservoir condition. All three test variables (temperature, flow velocity and CO_2) affected dissolution rates of the three cements to a different degree. CO_2 accelerated dissolution in all three samples. Below 20 ft/sec dissolution rates of the three samples were insensitive to flow velocity but became flow-dependent at 25 ft/sec. Temperature affected the dissolution to a less degree.

2.1.6 Recommendations

Since partial pressure of CO_2 and temperature strongly influence dissolution rates of BFS and Portland cements, the following controlling parameters are recommended to be investigated as future work:

° Determine the stability of BFS and Portland cements in brine under various gas mixtures of H_2S and CO_2 at elevated temperatures.

° Investigate the effect of sulfate on dissolution of BFS and Portland cements under a simulated downhole condition.

Figure 2.1.1 (a) A Teflon specimen mold
(b) A cylindrical specimen

(a)

(b)

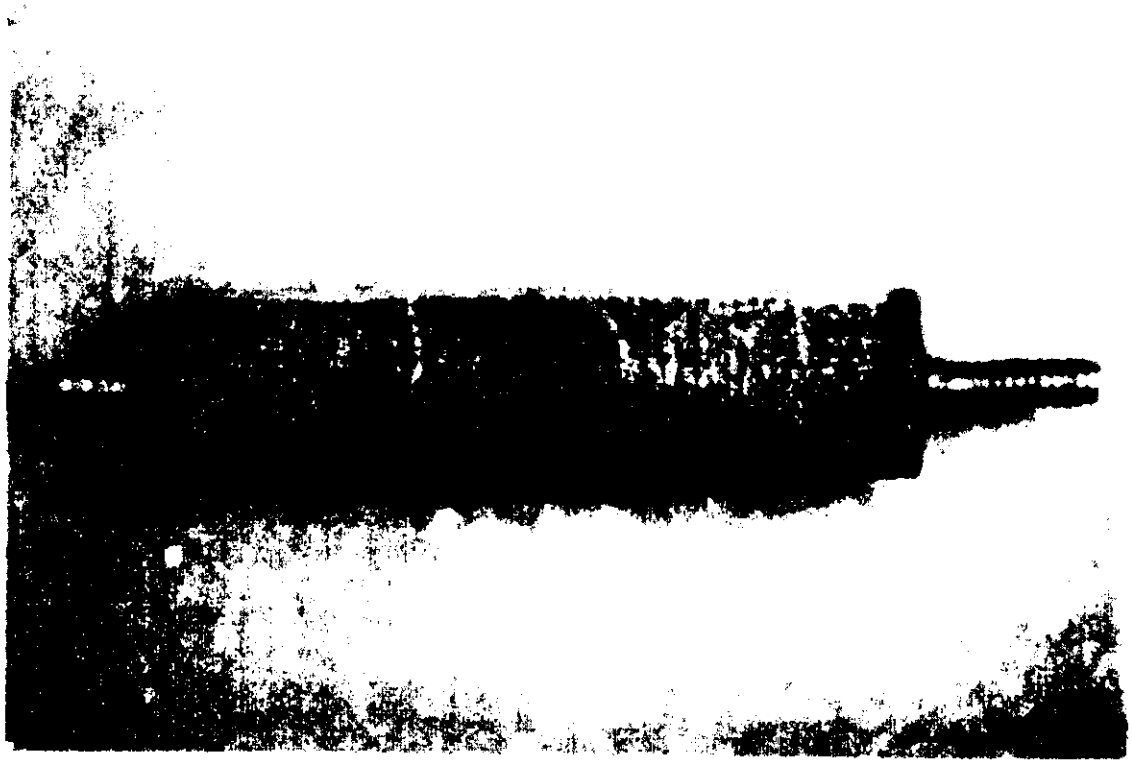

Figure 2.1.1 (c) SEM micrographs of the blast furnace slag (BFS) used in this work

(c1) Low magnification (x1000)
(c2) High magnification (x2000)

(c1)

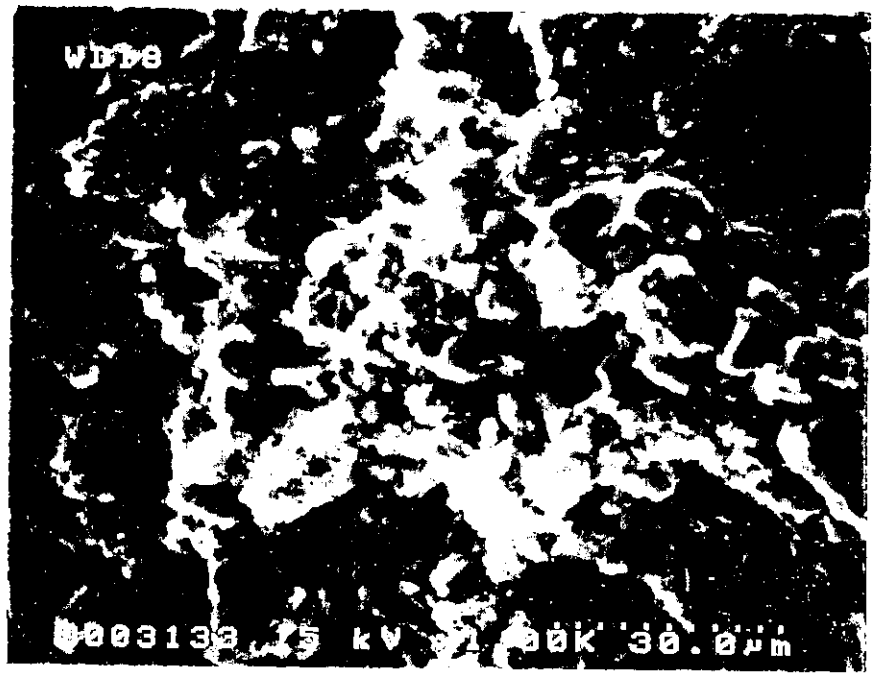

(c2)

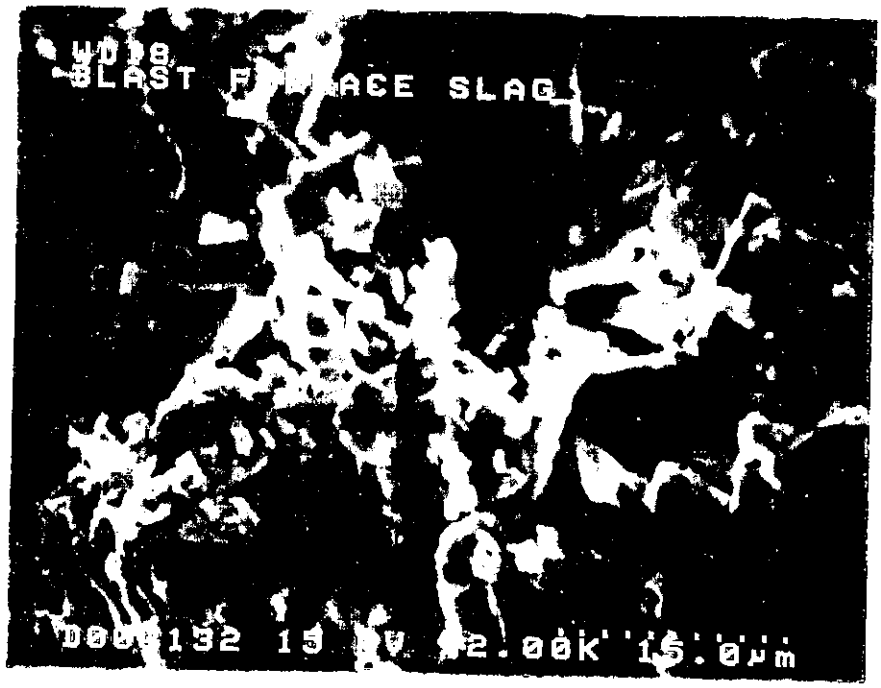

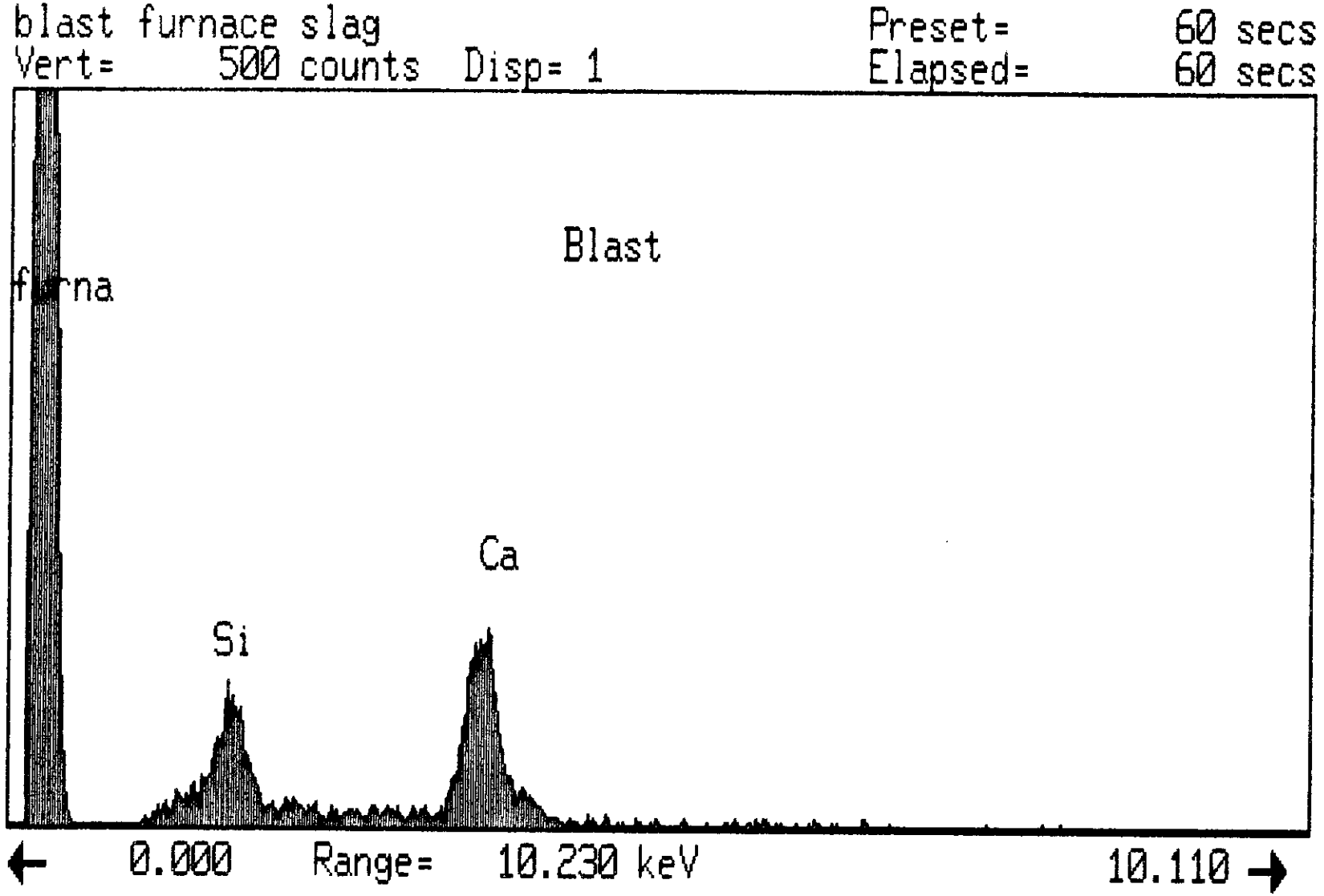

Figure 2.1.1 (d) X-ray elemental anaysis of blast furnace slag

Figure 2.1.2 (a) A schematic of a high-temperature high-pressure flowloop

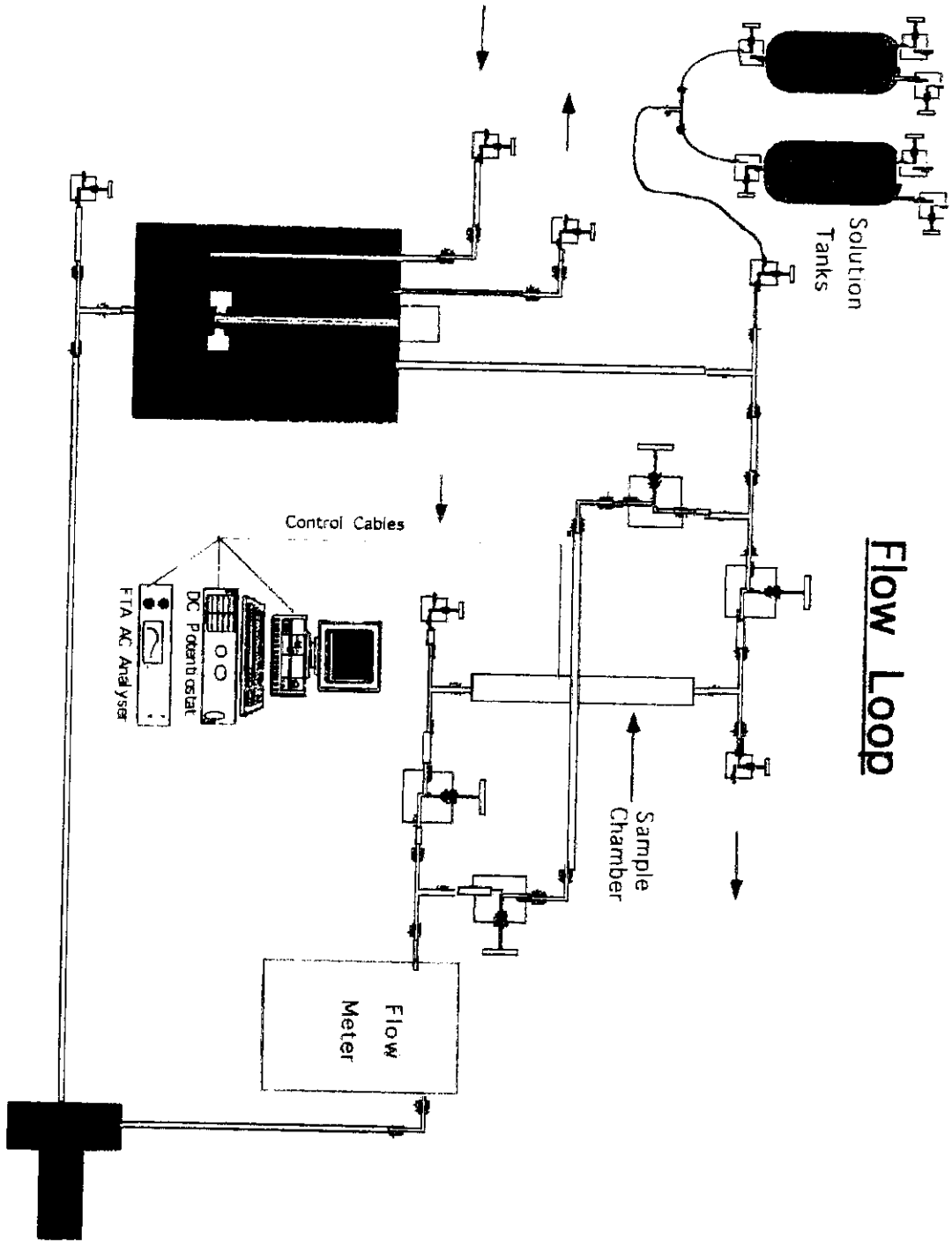

Figure 2.1.2 (b) A schematic of a specimen chamber

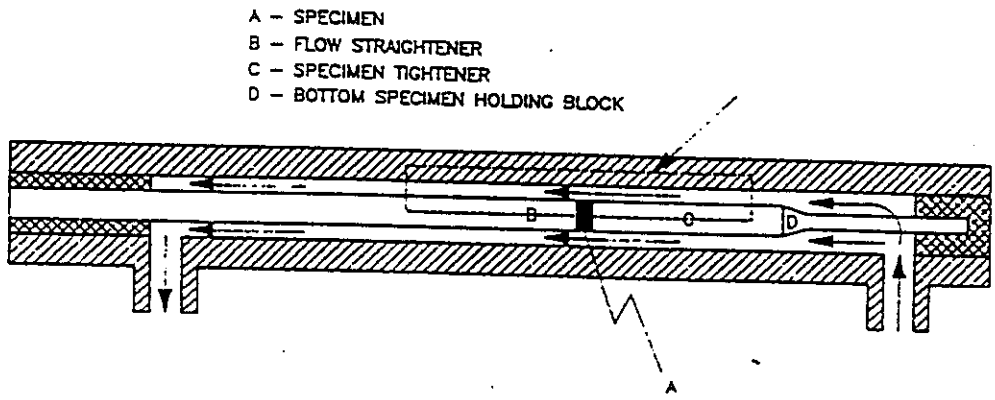

Figure 2.1.3 Dissolution of five elements of BFS-PHPA, BFS-dispersed mud and Portland cement tested in 3.3% NaCl under various test conditions

(a) Portland cement, 1 atm N_2, 150 °F, 20 ft/sec

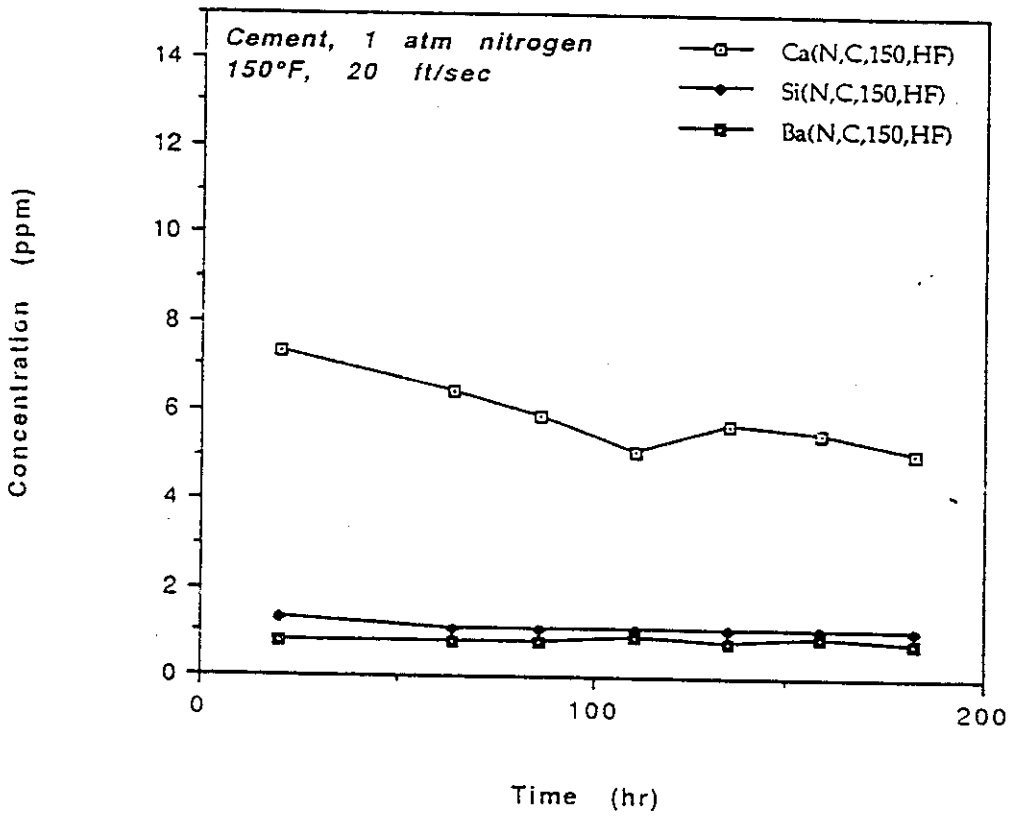

Figure 2.1.3 Dissolution of five elements of BFS-PHPA, BFS-dispersed mud and Portland cement tested in 3.3% NaCl under various test conditions

(b) Portland cement, N_2, 225 °F, 20 ft/sec

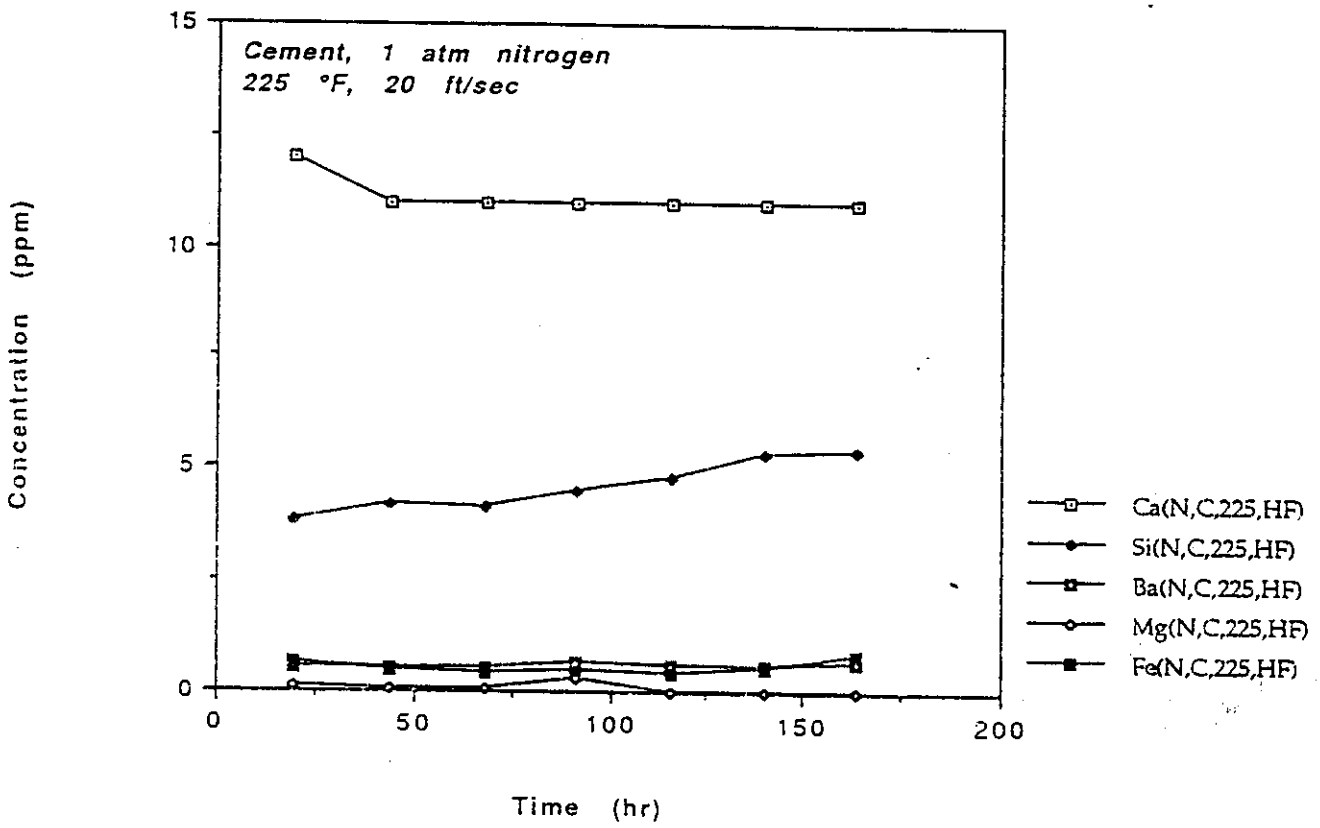

Figure 2.1.3 Dissolution of five elements of BFS-PHPA, BFS-dispersed mud and Portland cement tested in 3.3% NaCl under various test conditions

(c) Portland cement, 200 psi CO_2, 150 °F, 5 ft/sec

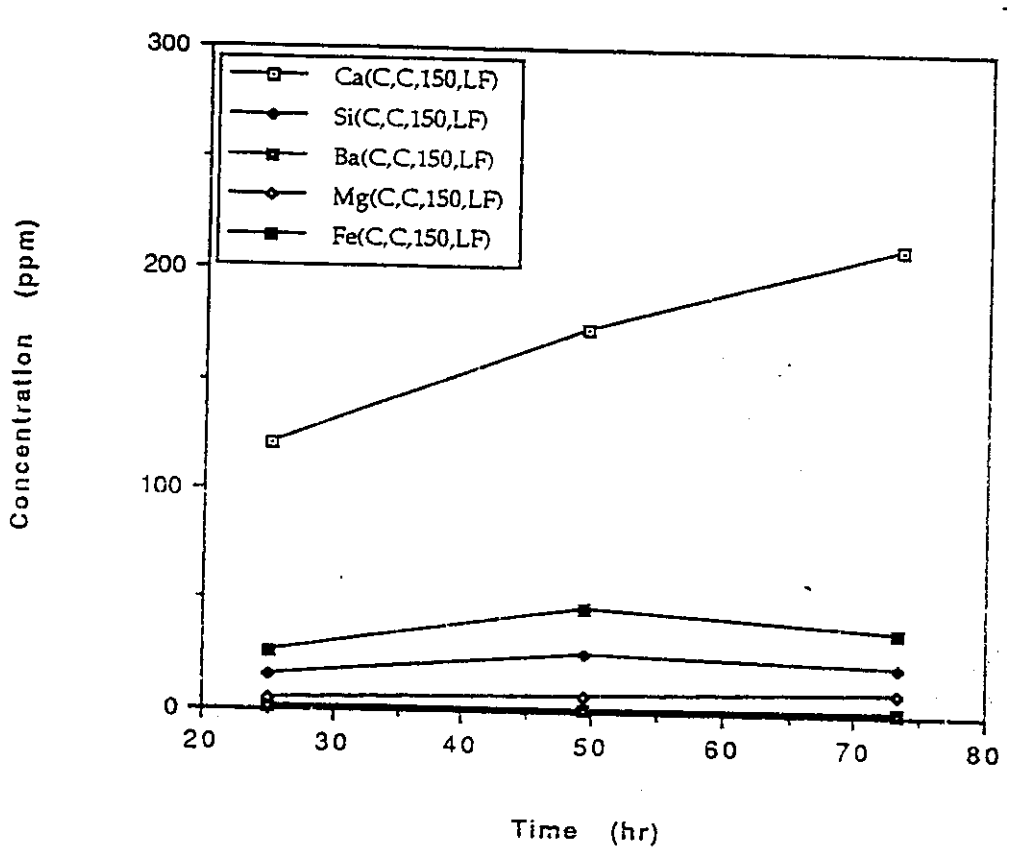

Figure 2.1.3 Dissolution of five elements of BFS-PHPA, BFS-dispersed mud and Portland cement tested in 3.3% NaCl under various test conditions

(d) Portland cement, 200 psi CO_2, 150 °F, 20 ft/sec

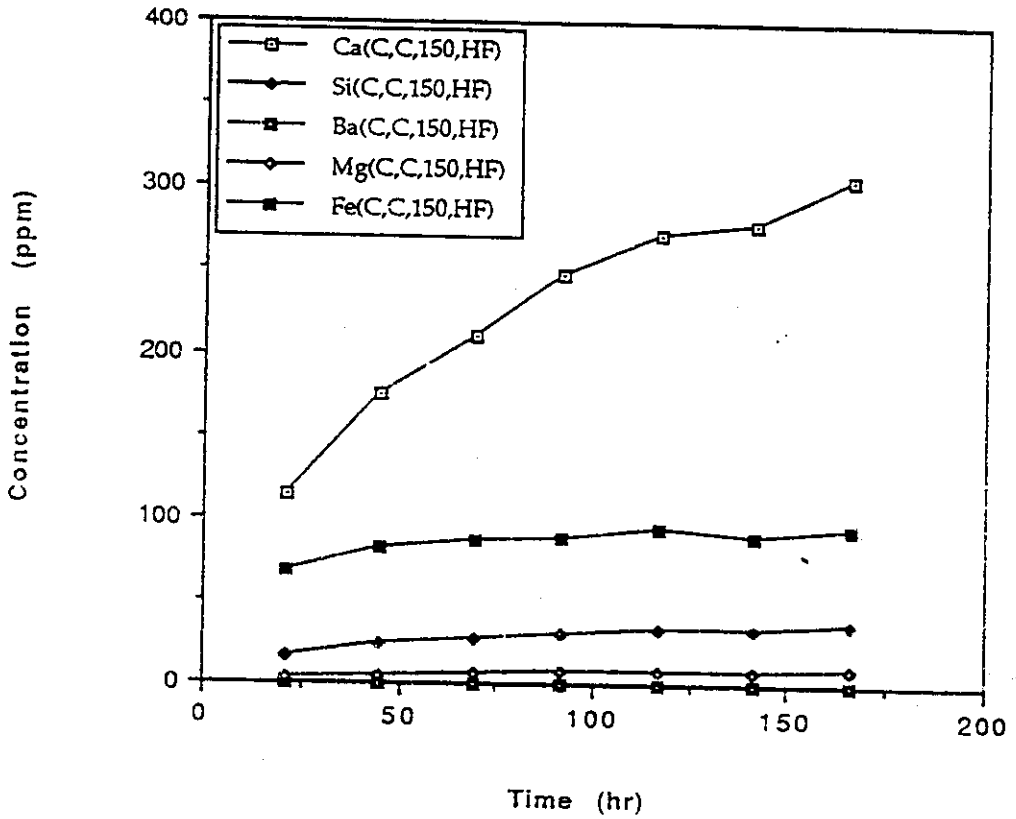

Figure 2.1.3 Dissolution rates of five elements of BFS-PHPA, BFS-dispersed mud and Portland cement tested in 3.3% NaCl under various test conditions

(e) Portland cement, 200 psi CO_2, 225 °F, 5 ft/sec

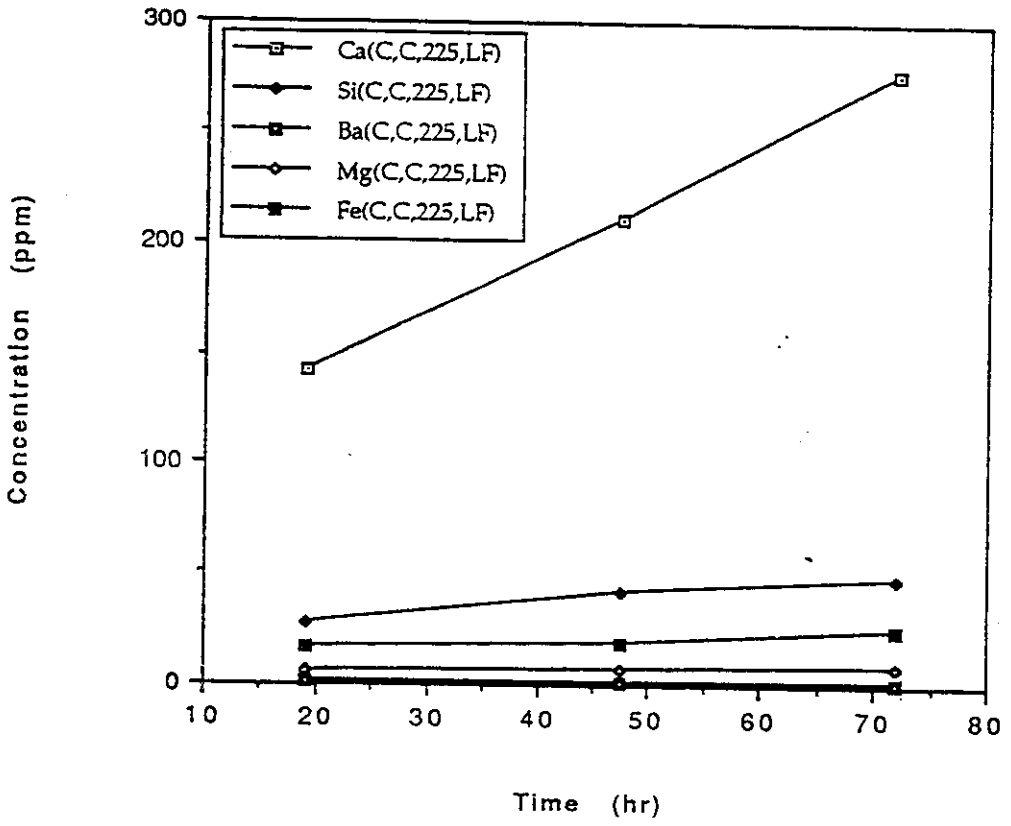

Figure 2.1.3 Dissolution of five elements of BFS-PHPA, BFS-dispersed mud and Portland cement tested in 3.3% NaCl under various test conditions

(f) Portland cement, 200 psi CO_2, 225 °F, 20 ft/sec

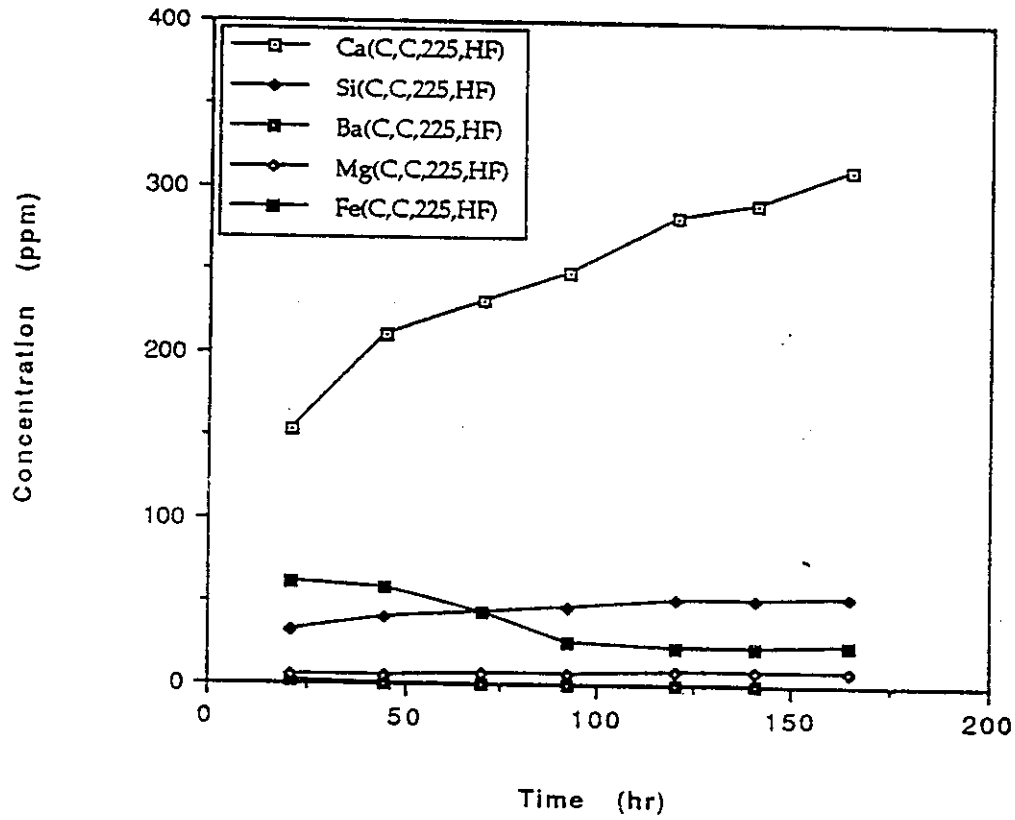

Figure 2.1.3 Dissolution of five elements of BFS-PHPA, BFS-dispersed mud and Portland cement tested in 3.3% NaCl under various test conditions

(g) BFS-PHPA, N_2, 150 °F, 20 ft/sec

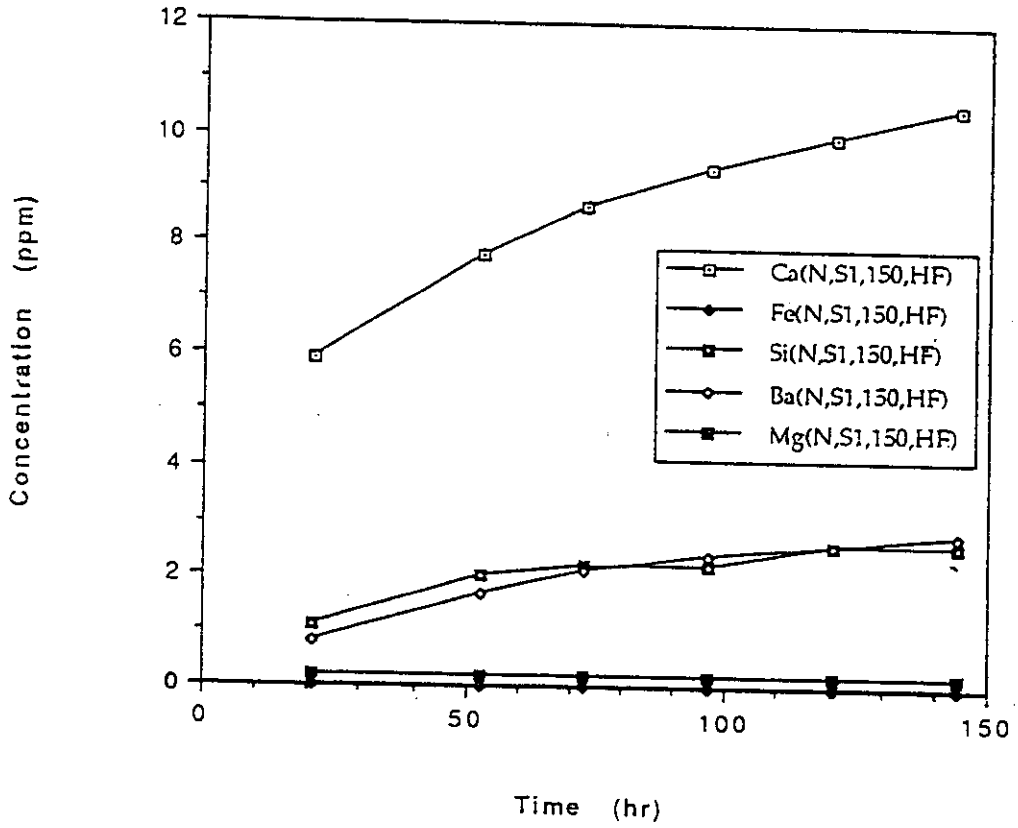

Figure 2.1.3 Dissolution of five elements of BFS-PHPA, BFS-dispersed mud and Portland cement tested in 3.3% NaCl under various test conditions

(h) BFS-PHPA, N_2, 225 °F, 20 ft/sec

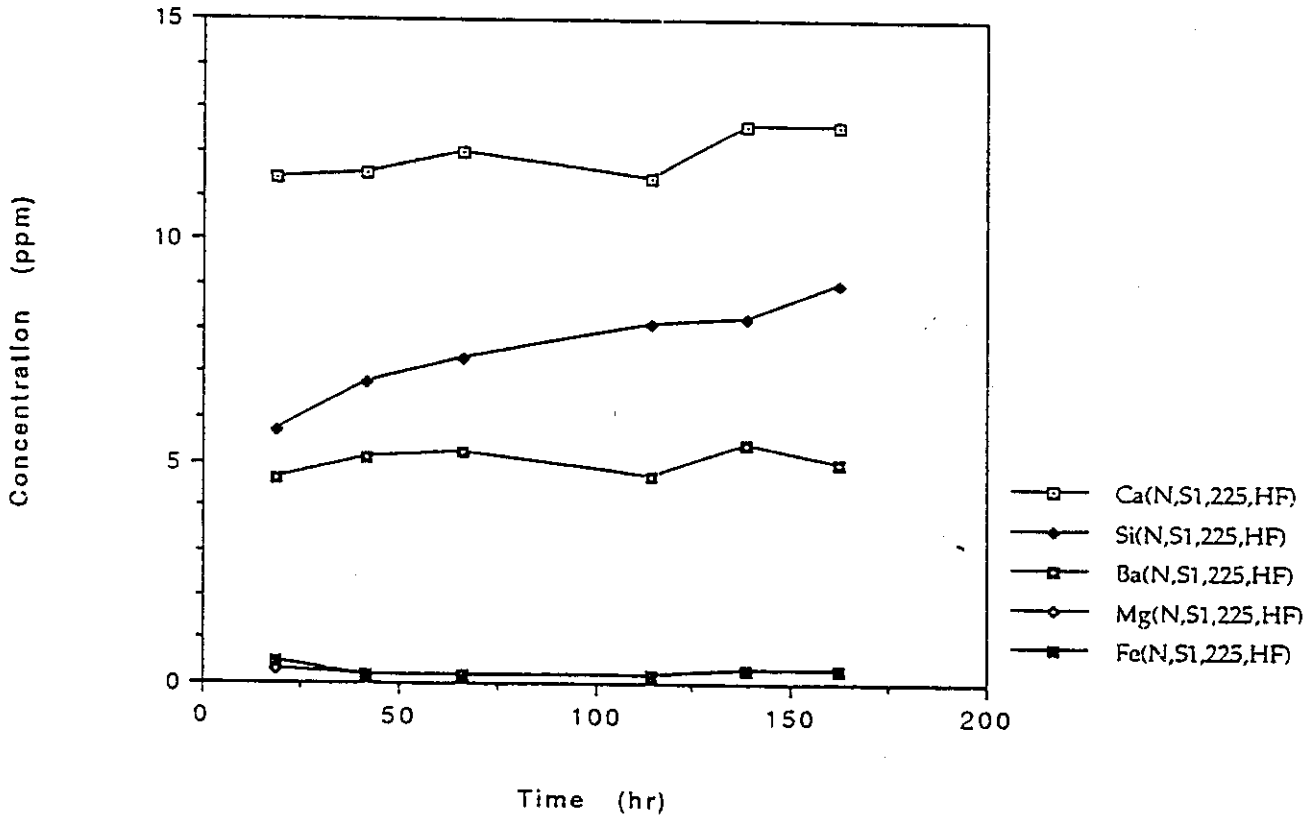

Figure 2.1.3 Dissolution of five elements of BFS-PHPA, BFS-dispersed mud and Portland cement tested in 3.3% NaCl under various test conditions

(i) BFS-PHPA, 200 psi CO_2, 150 °F, 5 ft/sec

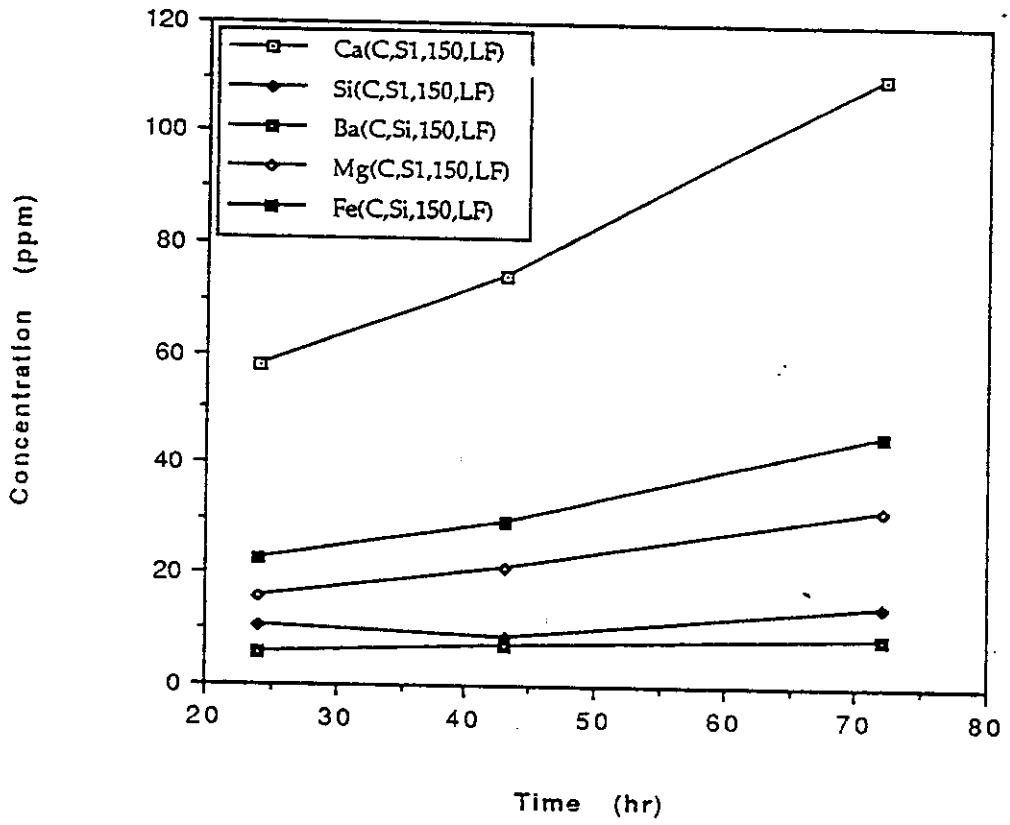

Figure 2.1.3 Dissolution of five elements of BFS-PHPA, BFS-dispersed mud and Portland cement tested in 3.3% NaCl under various test conditions

(j) BFS-PHPA, 200 psi CO_2, 150 °F, 20 ft/sec

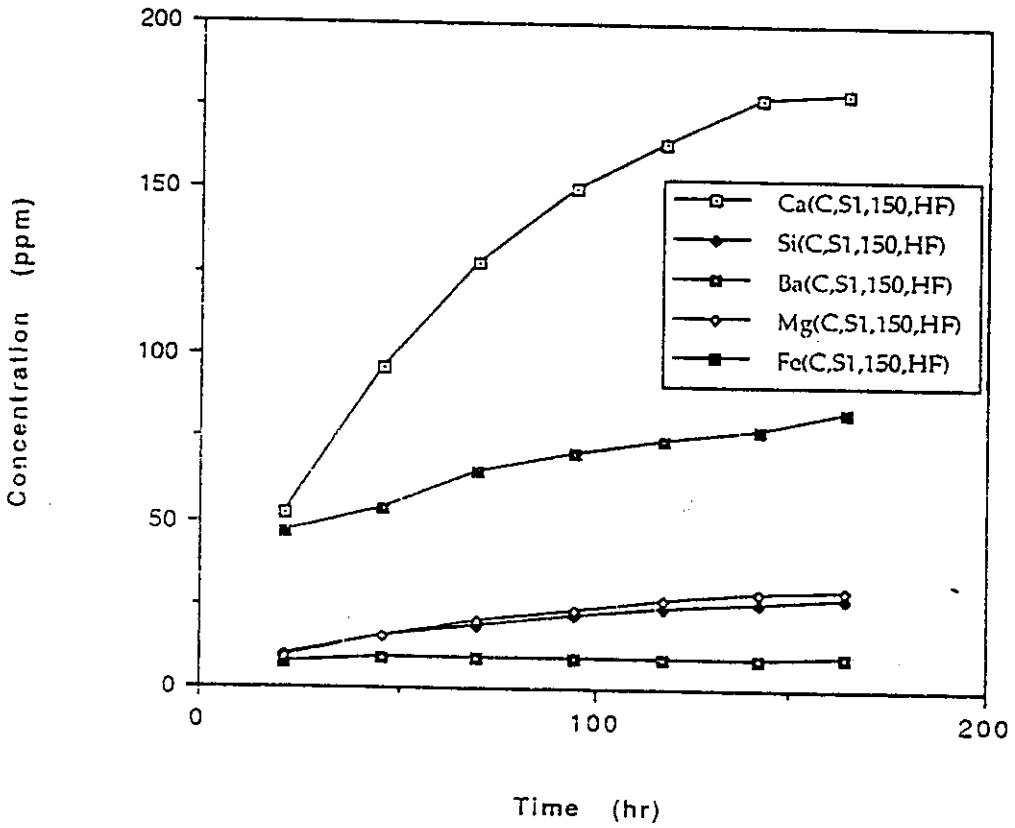

Figure 2.1.3 Dissolution of five elements of BFS-PHPA, BFS-dispersed mud and Portland cement tested in 3.3% NaCl under various test conditions

(k) BFS-PHPA, 200 psi CO_2, 225 °F, 5 ft/sec

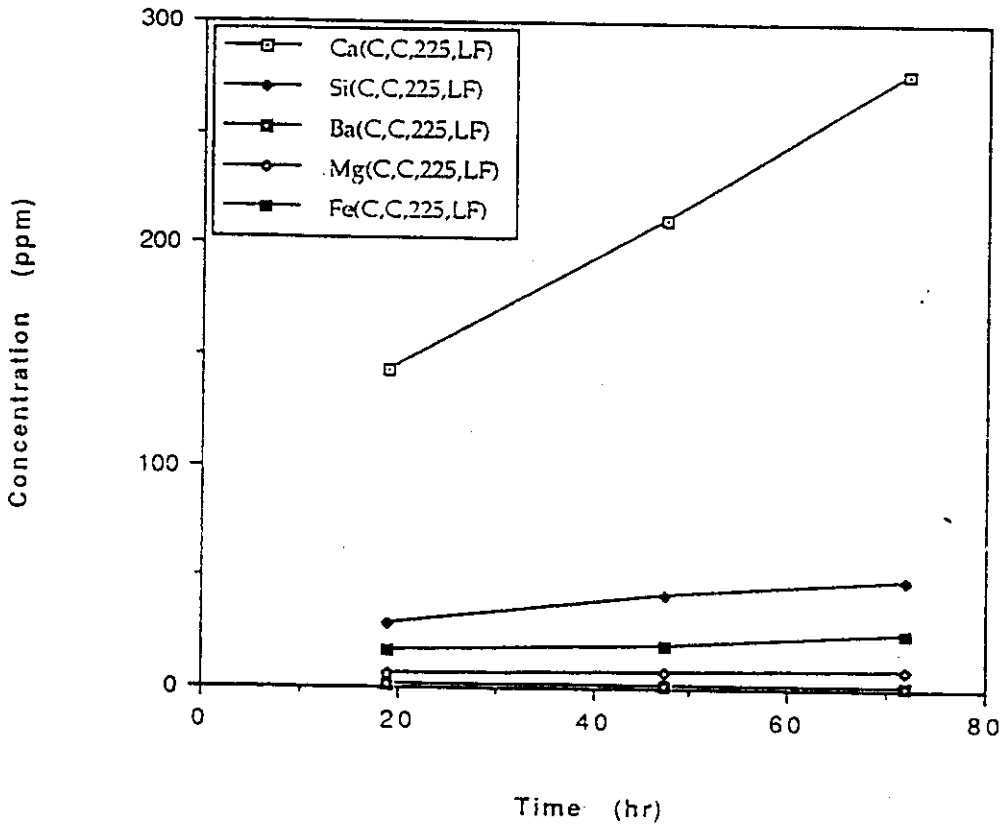

Figure 2.1.3 Dissolution of five elements of BFS-PHPA, BFS-dispersed mud and Portland cement tested in 3.3% NaCl under various test conditions

(I) BFS-PHPA, 200 psi CO_2, 225 °F, 20 ft/sec

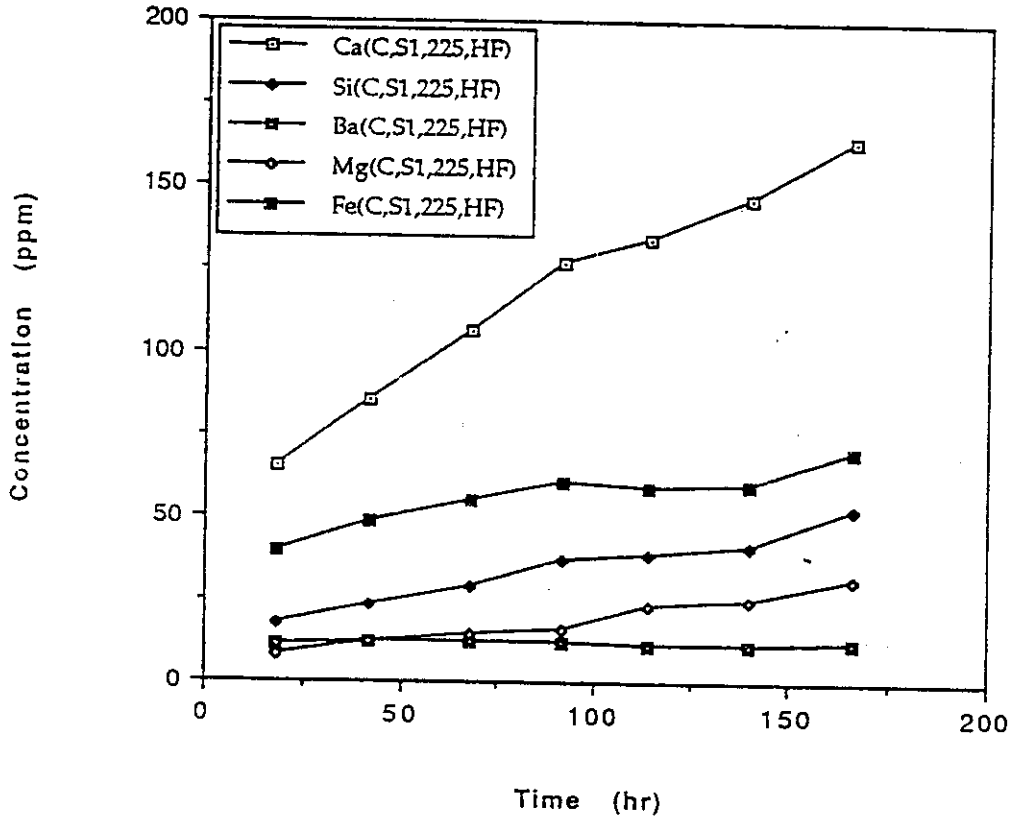

Figure 2.1.3 Dissolution of five elements of BFS-PHPA, BFS-dispersed mud and Portland cement tested in 3.3% NaCl under various test conditions

(m) BFS-dispersed mud, N_2, 150 °F, 20 ft/sec

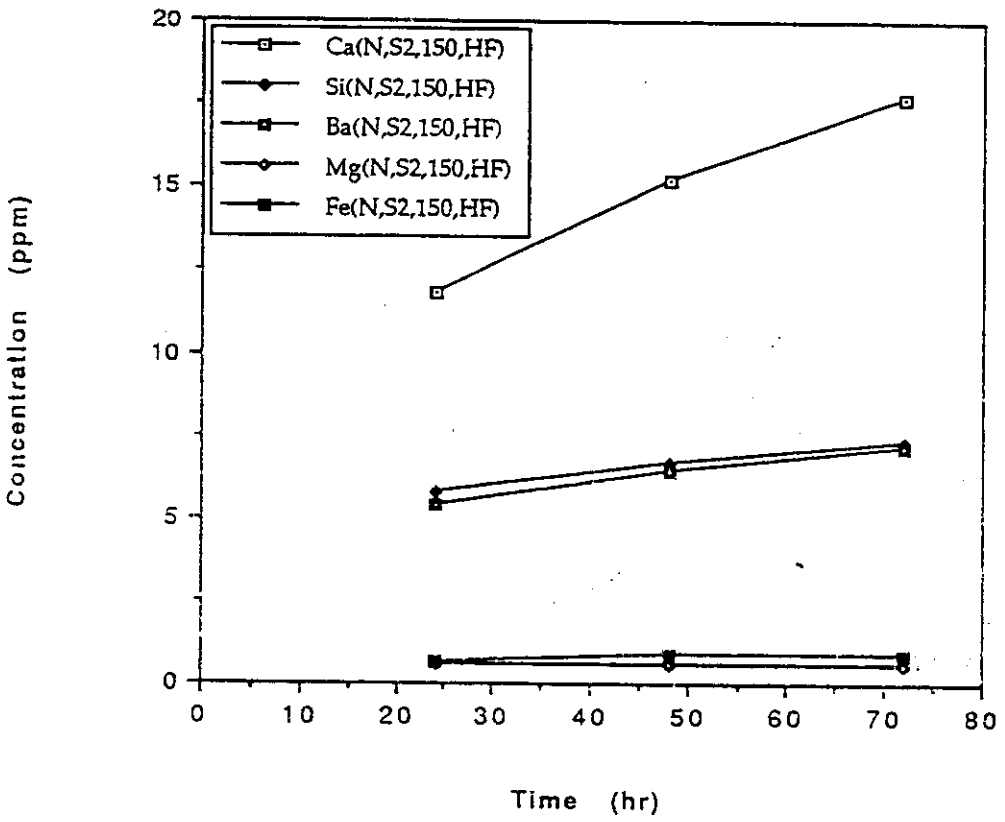

Figure 2.1.3 Dissolution of five elements of BFS-PHPA, BFS-dispersed mud and Portland cement tested in 3.3% NaCl under various test conditions

(n) BFS-dispersed mud, N_2, 225 °F, 20 ft/sec

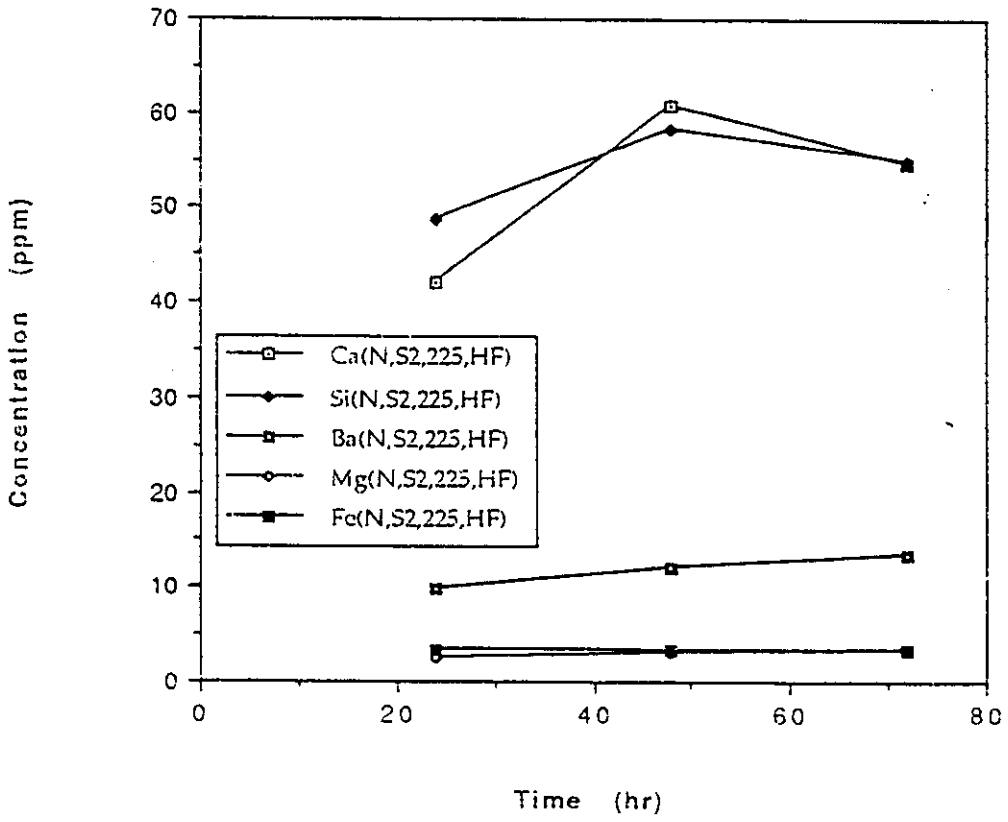

Figure 2.1.3 Dissolution of five elements of BFS-PHPA, BFS-dispersed mud and Portland cement tested in 3.3% NaCl under various test conditions

(o) BFS-dispersed mud, 200 psi CO_2, 150 °F, 5 ft/sec

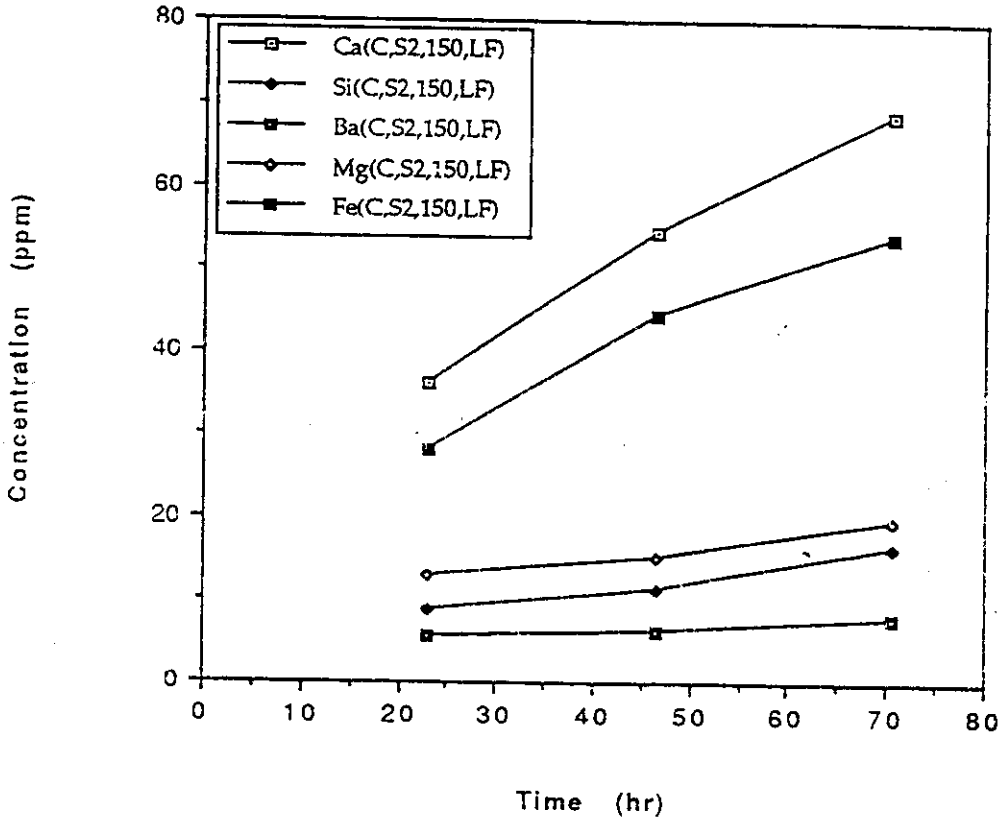

Figure 2.1.3 Dissolution of five elements of BFS-PHPA, BFS-dispersed mud and Portland cement tested in 3.3% NaCl under various test conditions

(p) BFS-dispersed mud, 200 psi CO2, 150 °F, 20 ft/sec

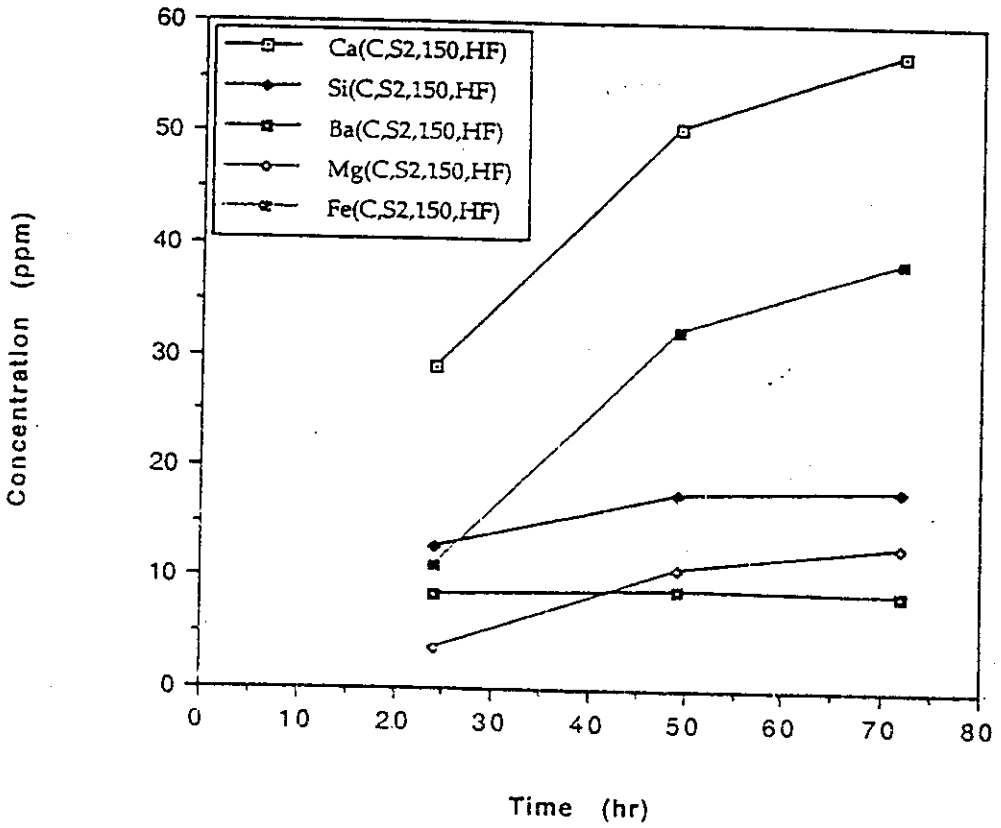

Figure 2.1.3 Dissolution of five elements of BFS-PHPA, BFS-dispersed mud and Portland cement tested in 3.3% NaCl under various test conditions

(q) BFS-dispersed mud, 200 psi CO_2, 225 °F, 5 ft/sec

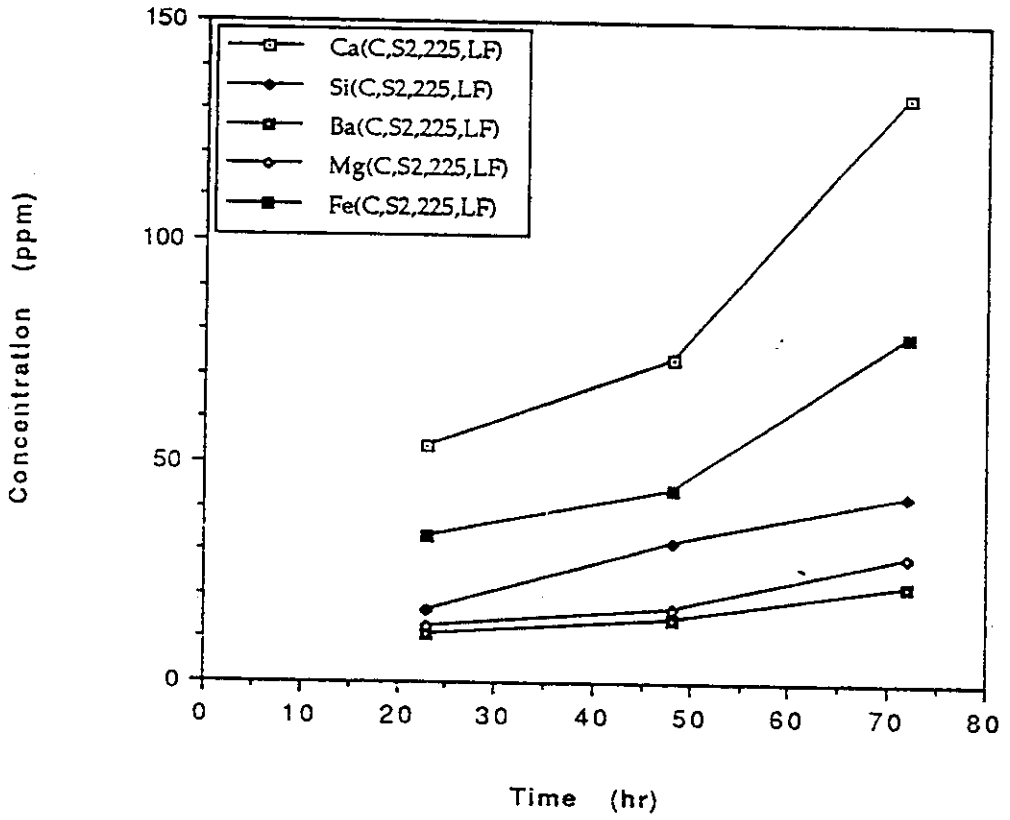

Figure 2.1.3 Dissolution of five elements of BFS-PHPA, BFS-dispersed mud and Portland cement tested in 3.3% NaCl under various test conditions

(r) BFS-dispersed mud, 200 psi CO_2, 225 °F, 20 ft/sec

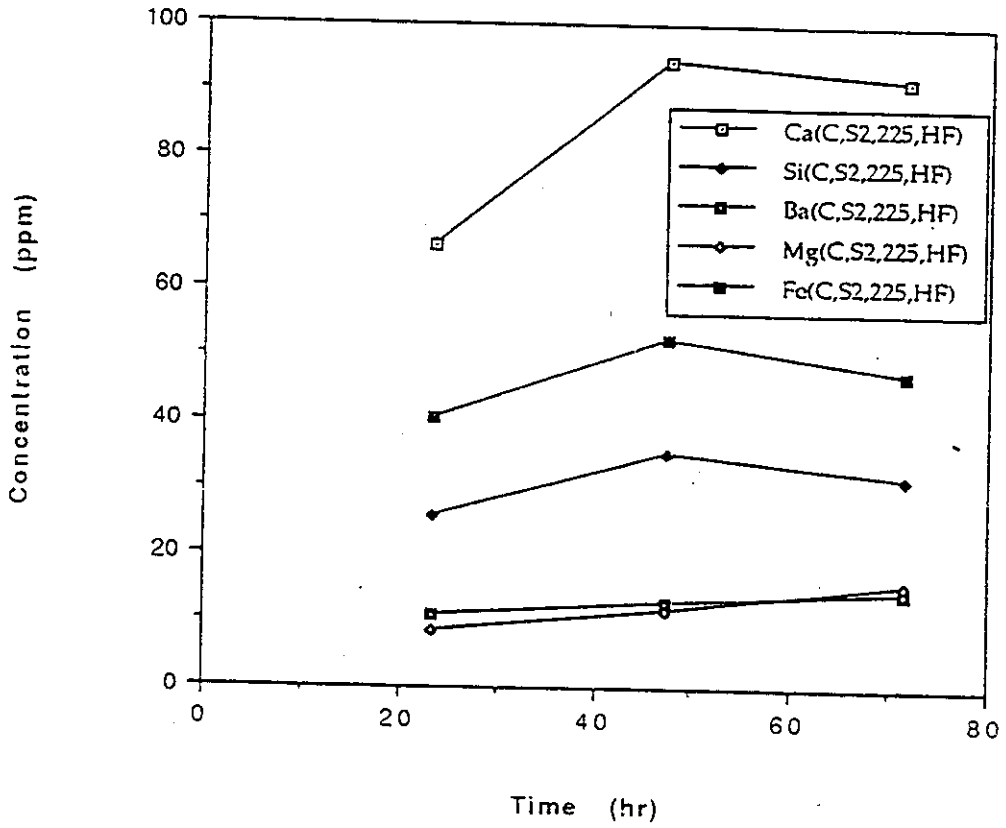

Figure 2.1.3 Dissolution of five elements of BFS-PHPA, BFS-dispersed mud and Portland cement tested in 3.3% NaCl under various test conditions

(s) Portland cement, 200 psi CO_2, 225 °F, 25 ft/sec

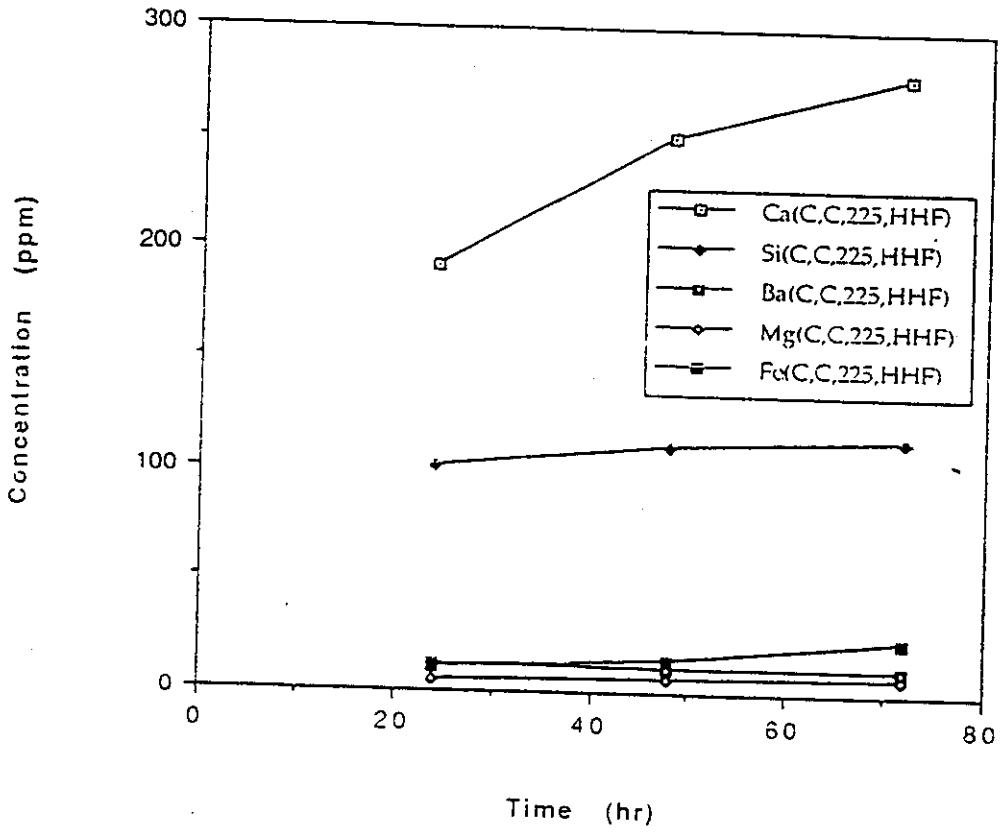

Figure 2.1.3 Dissolution of five elements of BFS-PHPA, BFS-dispersed mud and Portland cement tested in 3.3% NaCl under various test conditions

(t) BFS-PHPA, 200 psi CO_2, 225 °F, 25 ft/sec

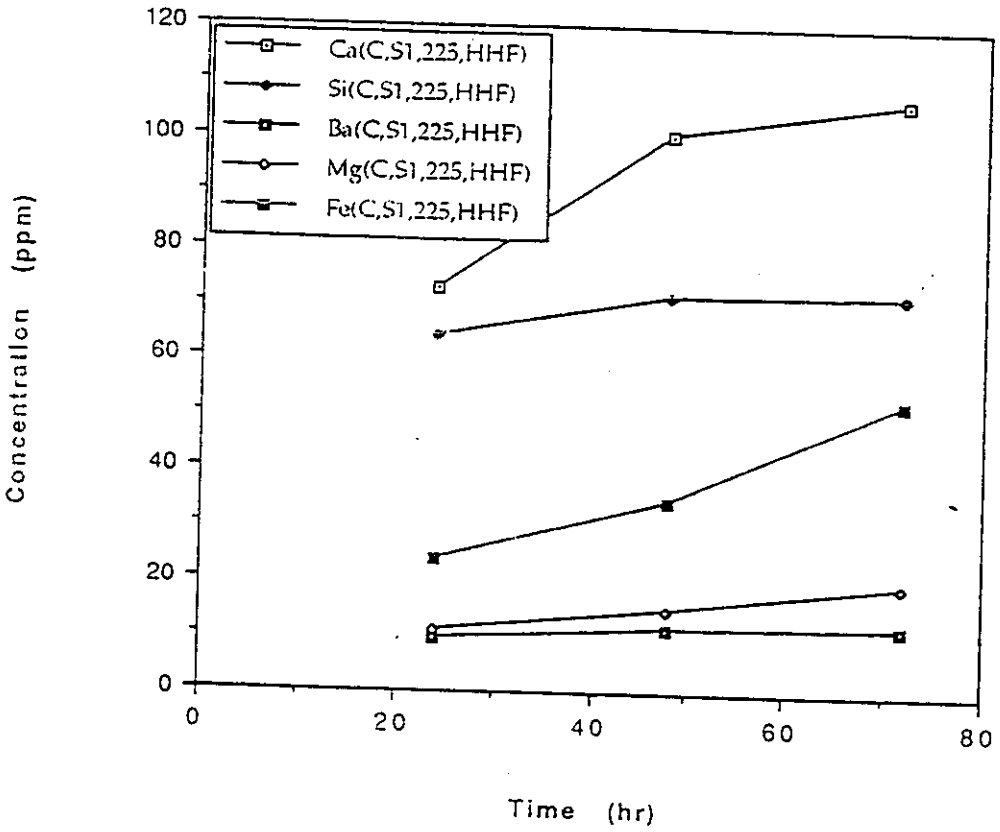

Figure 2.1.3 Dissolution of five elements of BFS-PHPA, BFS-dispersed mud and Portland cement tested in 3.3% NaCl under various test conditions

(u) BFS-dispersed mud, 200 psi CO_2, 225 °F, 25 ft/sec

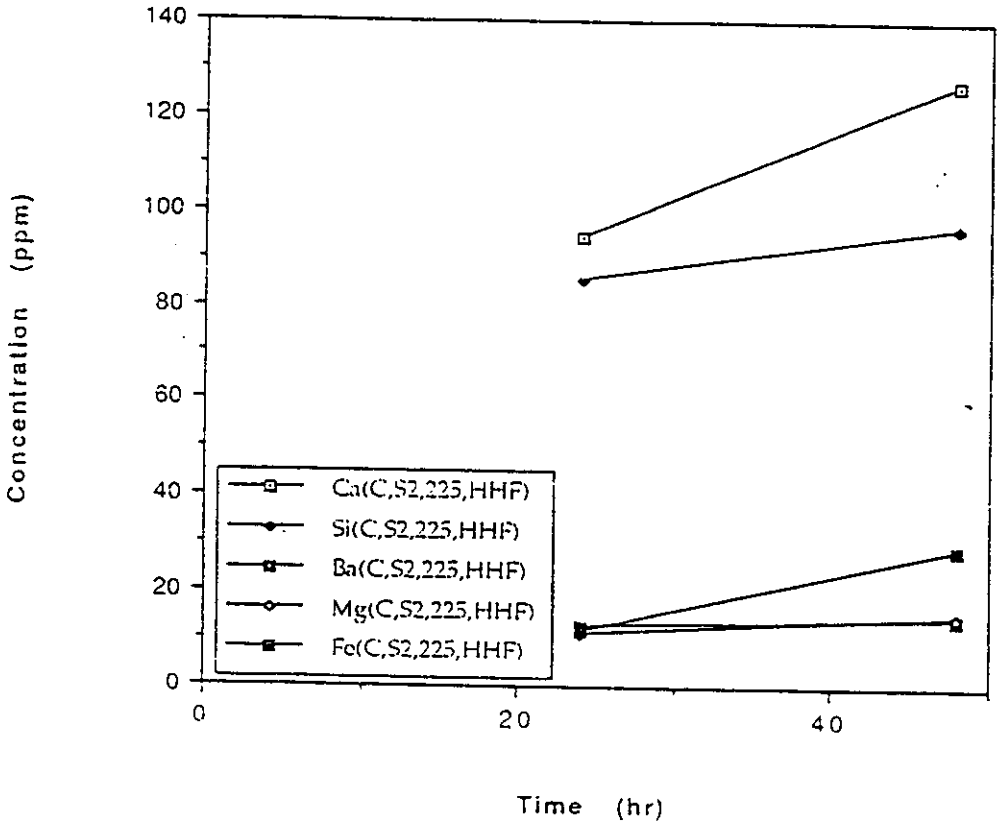

Figure 2.1.4 Effect of CO_2 on dissolution of five elements of BFS-PHPA, BFS-dispersed mud and Portland cement in 3.3% NaCl under various test conditions

(a) Ca, 150 °F, 20 ft/sec

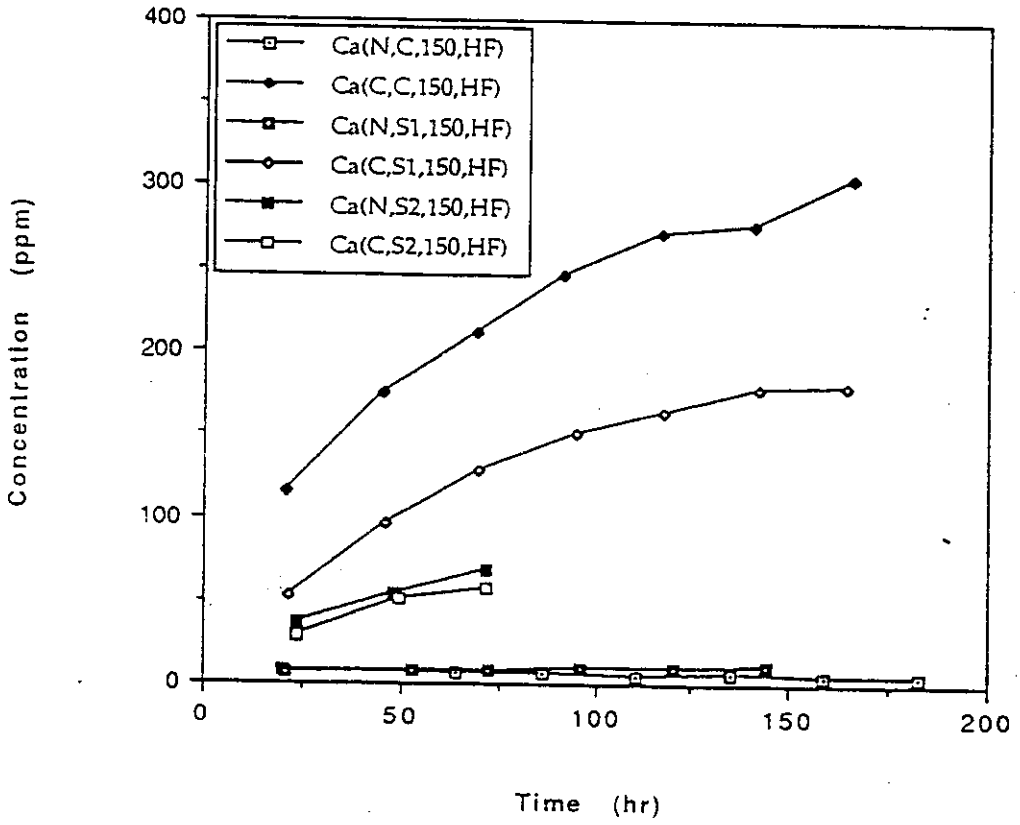

Figure 2.1.4 Effect of CO_2 on dissolution of five elements of BFS-PHPA, BFS-dispersed mud and Portland cement in 3.3% NaCl under various test conditions

(b) Ca, 225 °F, 20 ft/sec

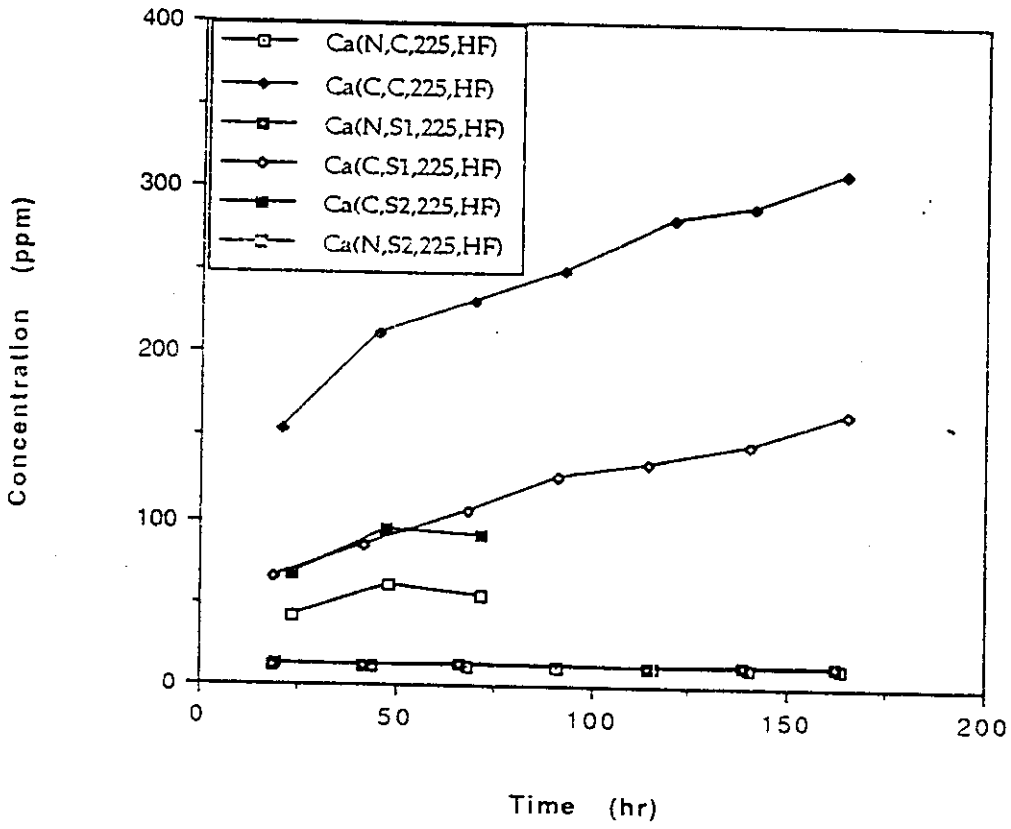

Figure 2.1.4 Effect of CO_2 on dissolution of five elements of BFS-PHPA, BFS-dispersed mud and Portland cement in 3.3% NaCl under various test conditions

(c) Si, 150 °F, 20 ft/sec

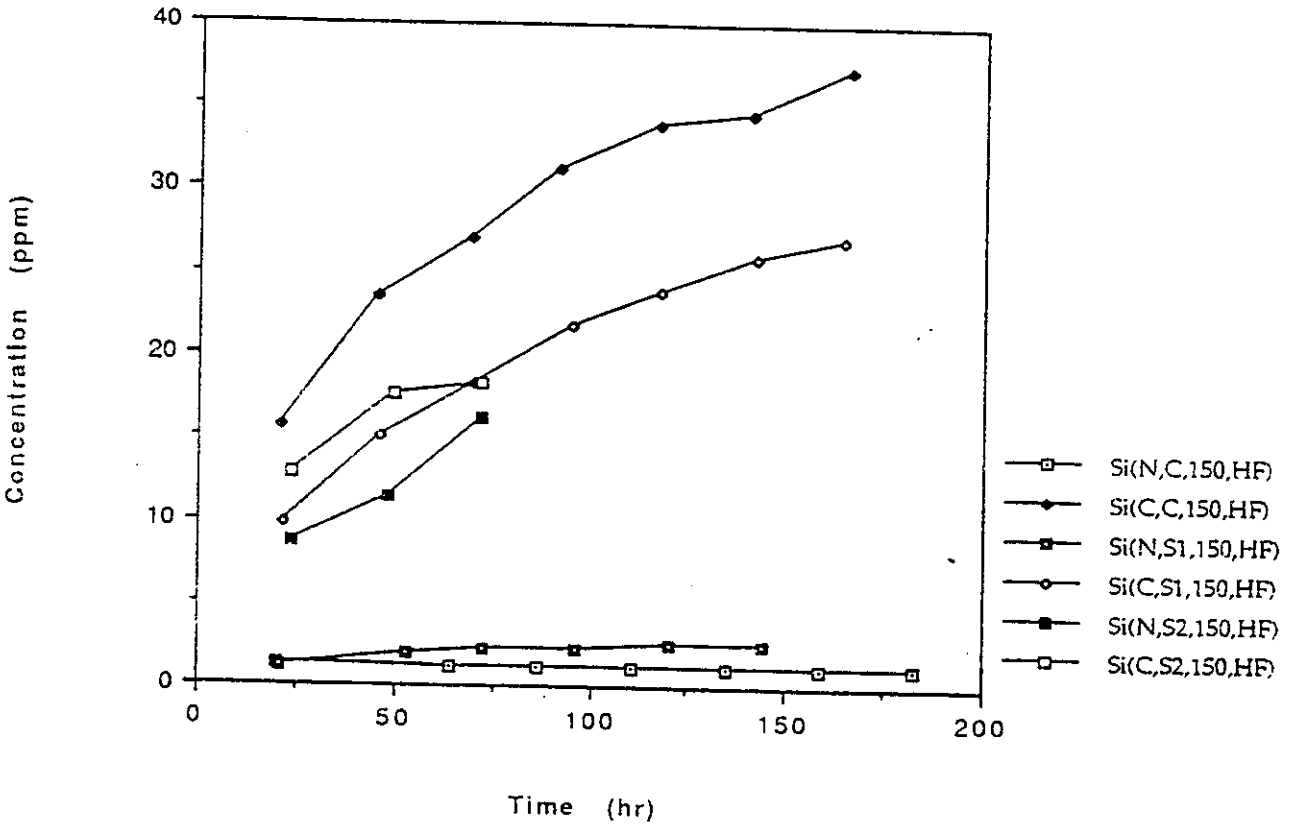

Figure 2.1.4 Effect of CO_2 on dissolution of five elements of BFS-PHPA, BFS-dispersed mud and Portland cement in 3.3% NaCl under various test conditions

(d) Si, 225 °F, 20 ft/sec

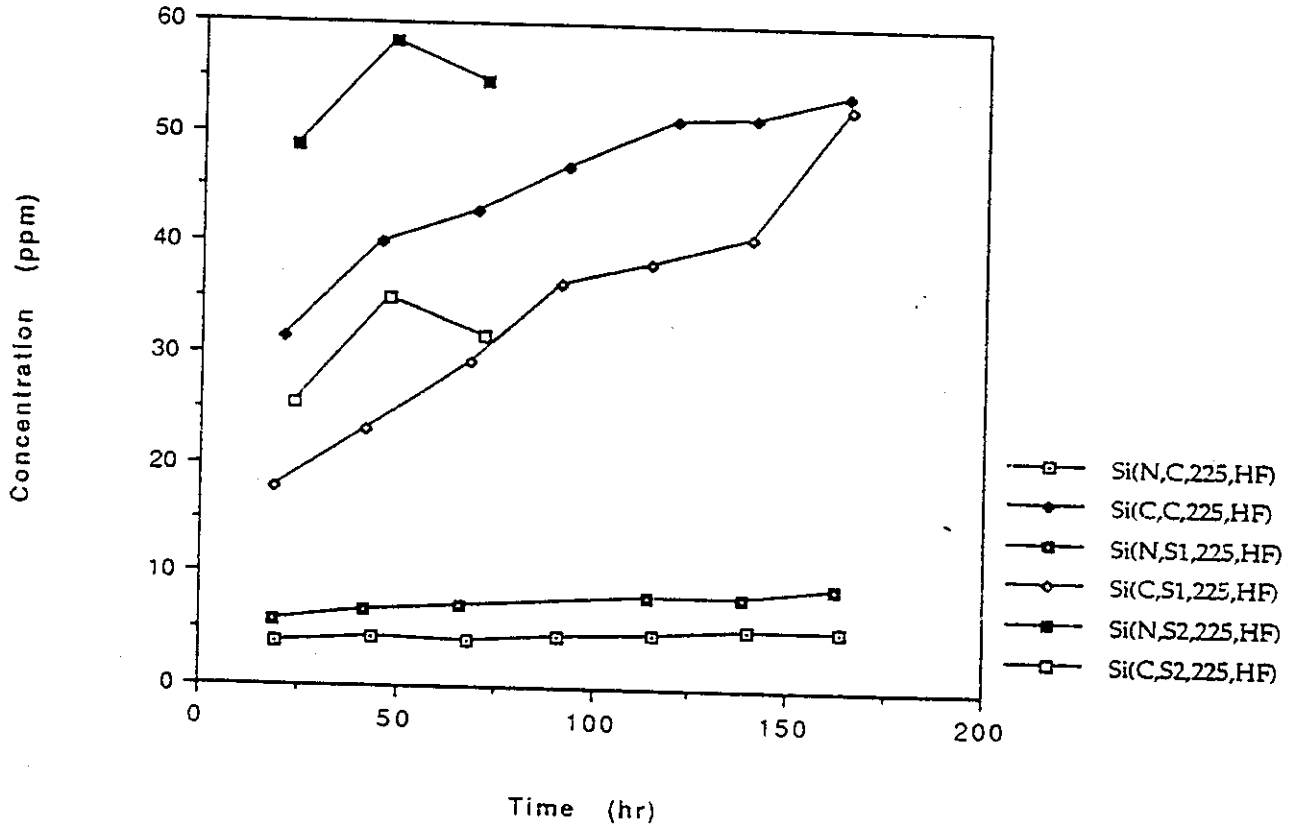

Figure 2.1.4 Effect of CO_2 on dissolution of five elements of BFS-PHPA, BFS-dispersed mud and Portland cement in 3.3% NaCl under various test conditions

(e) Ba, 150 °F, 20 ft/sec

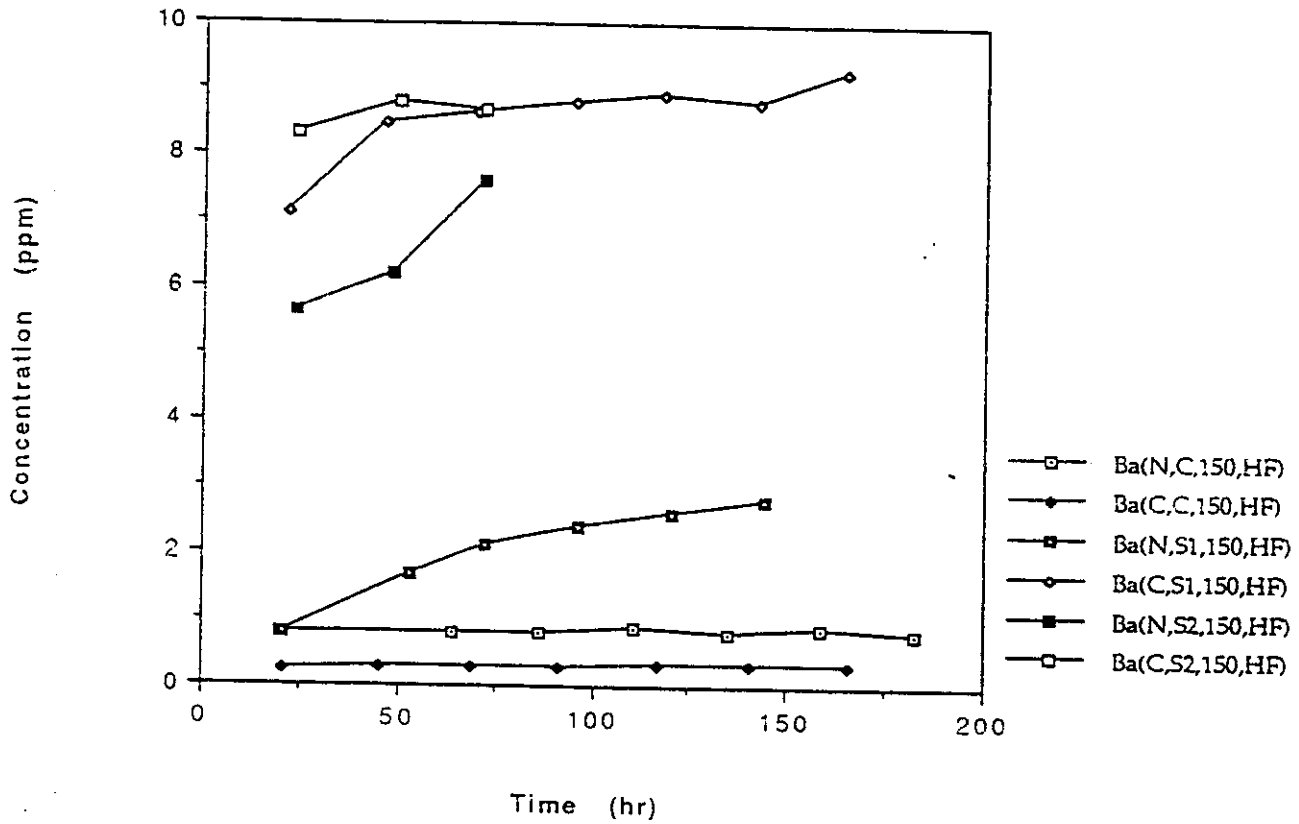

Figure 2.1.4 Effect of CO_2 on dissolution of five elements of BFS-PHPA, BFS-dispersed mud and Portland cement in 3.3% NaCl under various test conditions

(f) Ba, 225 °F, 20 ft/sec

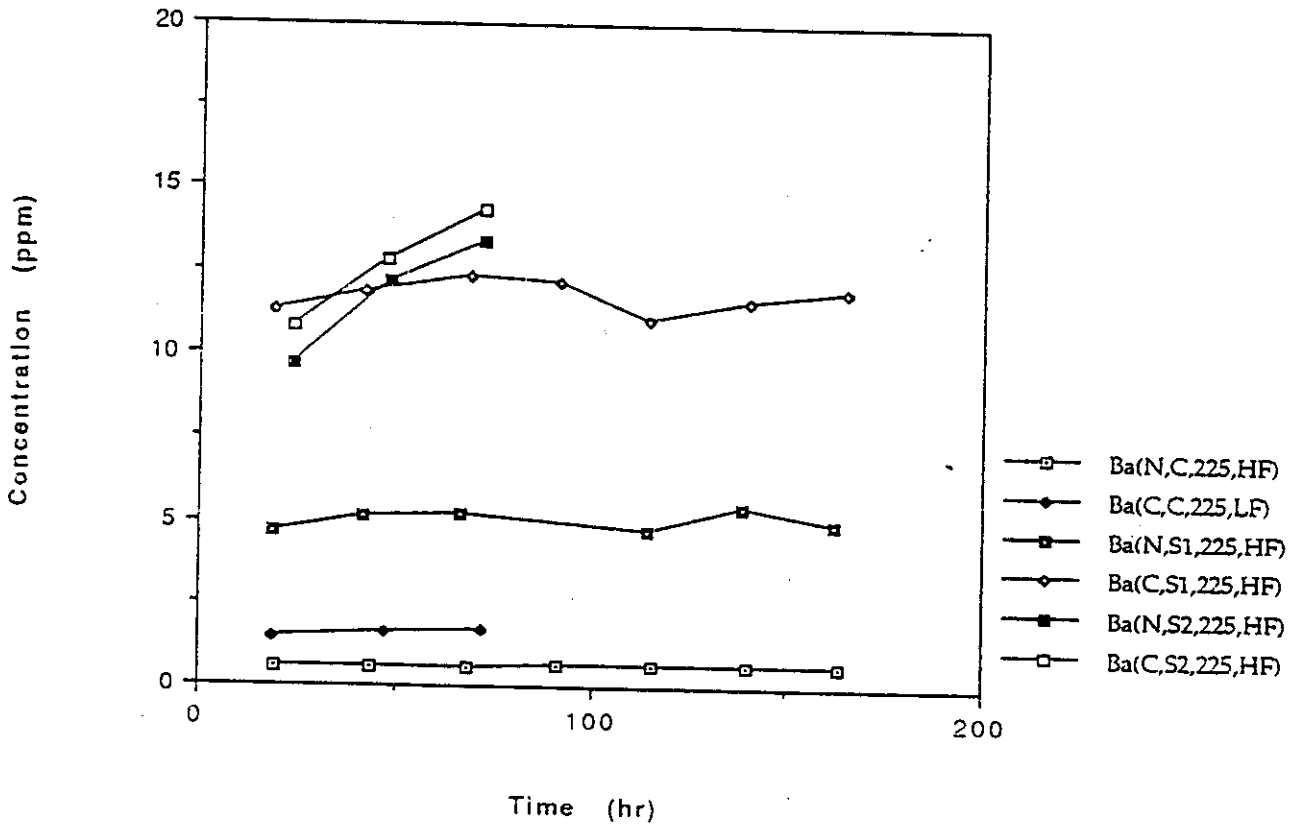

Figure 2.1.4 Effect of CO_2 on dissolution of five elements of BFS-PHPA, BFS-dispersed mud and Portland cement in 3.3% NaCl under various test conditions

(g) Fe, 150 °F, 20 ft/sec

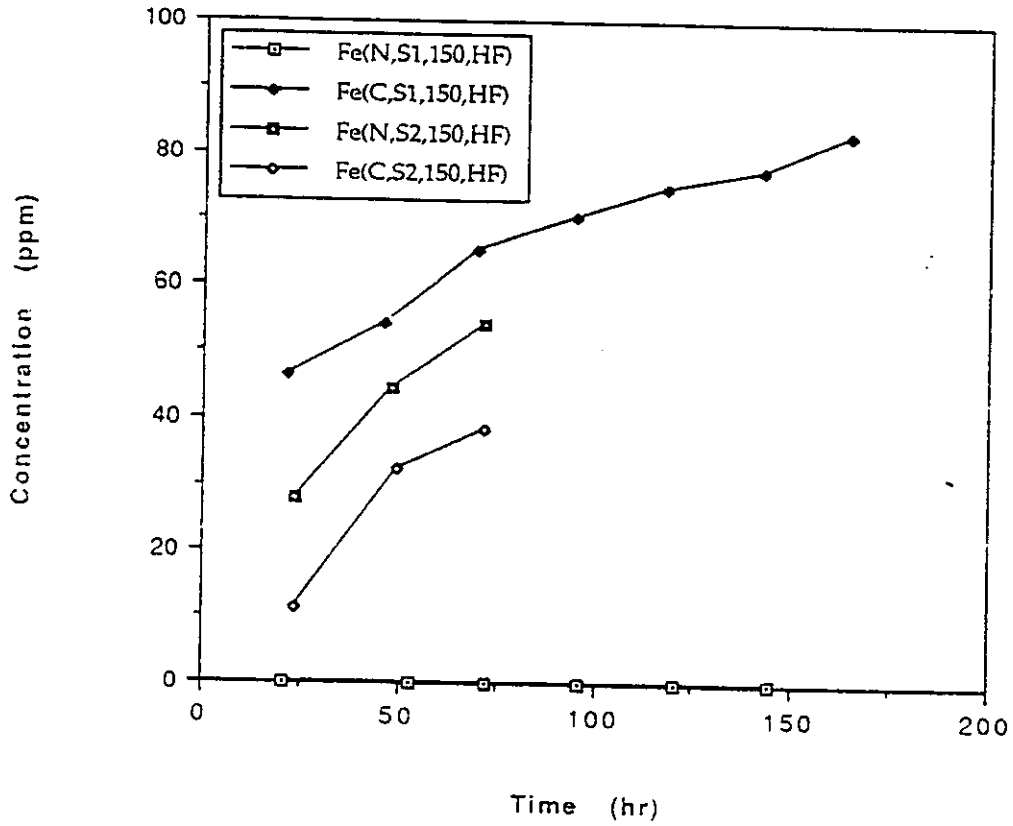

Figure 2.1.4 Effect of CO_2 on dissolution of five elements of BFS-PHPA, BFS-dispersed mud and Portland cement in 3.3% NaCl under various test conditions

(i) Mg, 225 °F, 20 ft/sec

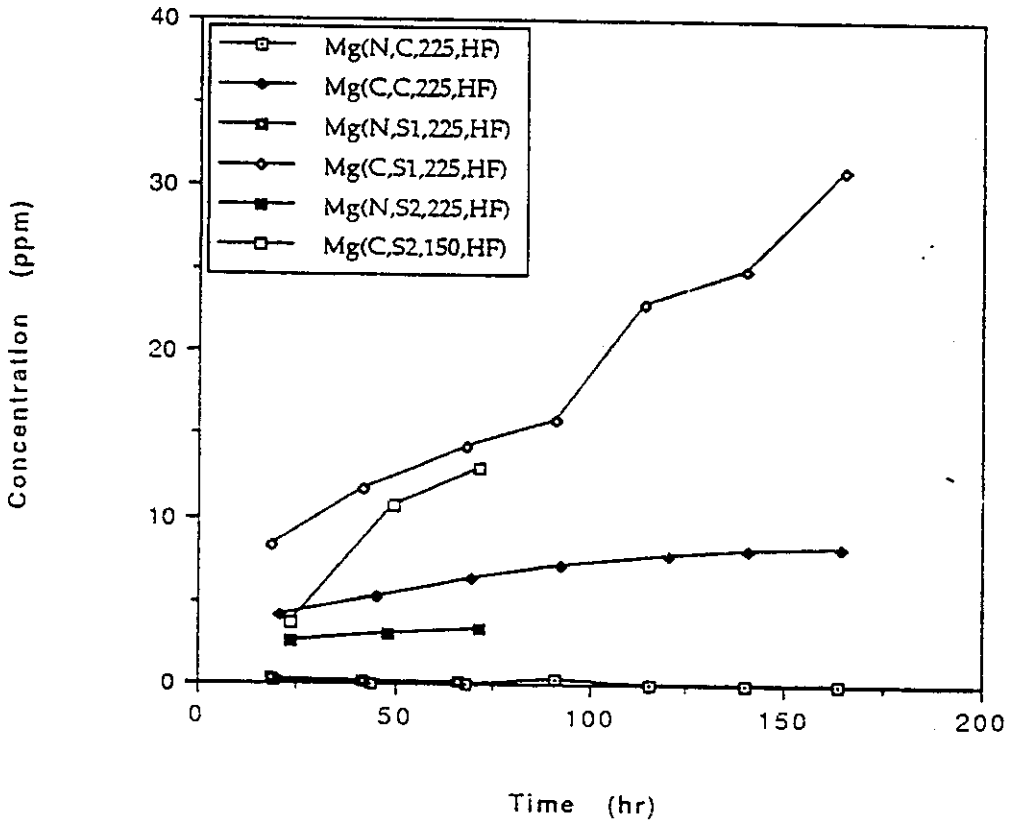

Figure 2.1.5 Effect of temperature on dissolution of Ca, Si, Ba of BFS-PHPA, BFS-dispersed mud and Portland cement in 3.3% NaCl under various test condition

(a) Ca, Portland cement

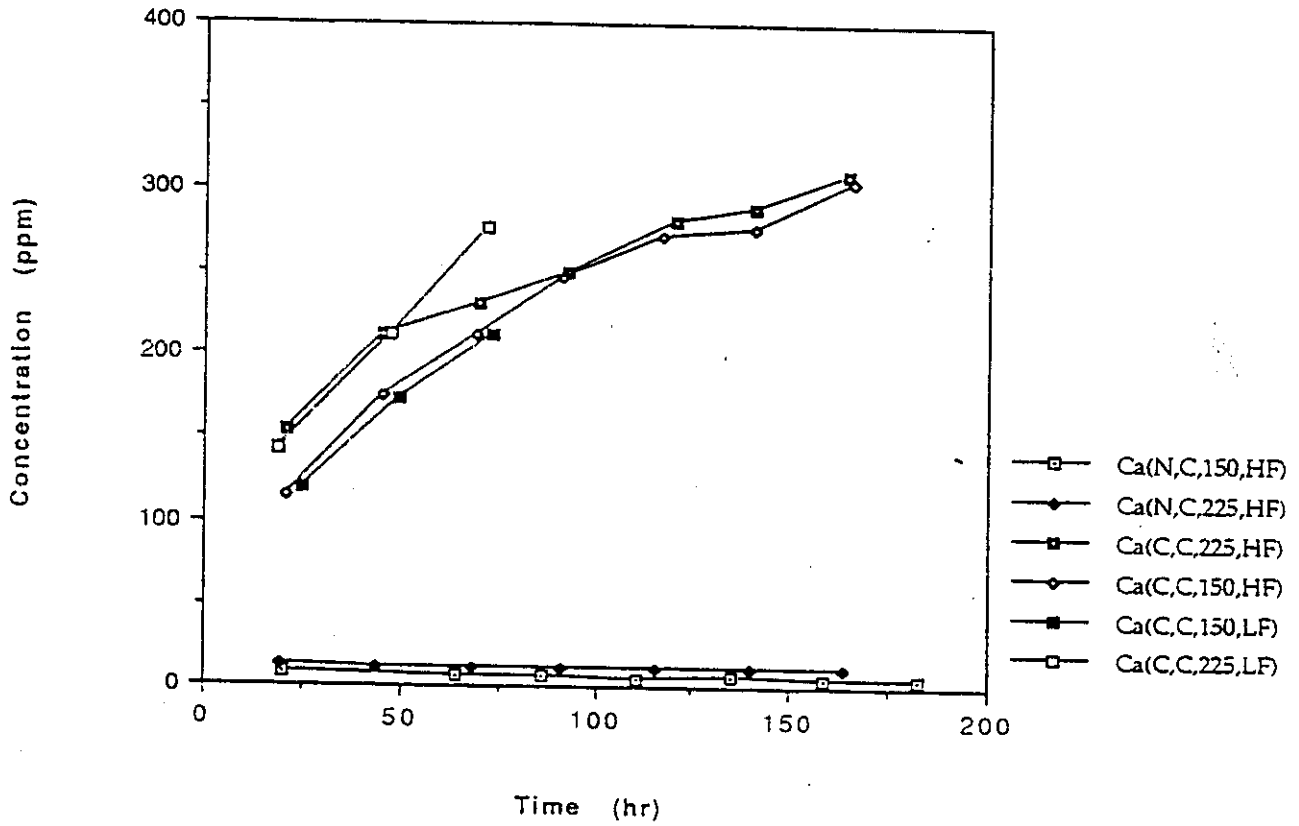

Figure 2.1.5 Effect of temperature on dissolution of Ca, Si, Ba of BFS-PHPA, BFS-dispersed mud and Portland cement in 3.3% NaCl under various test condition

(b) Ca, BFS-PHPA

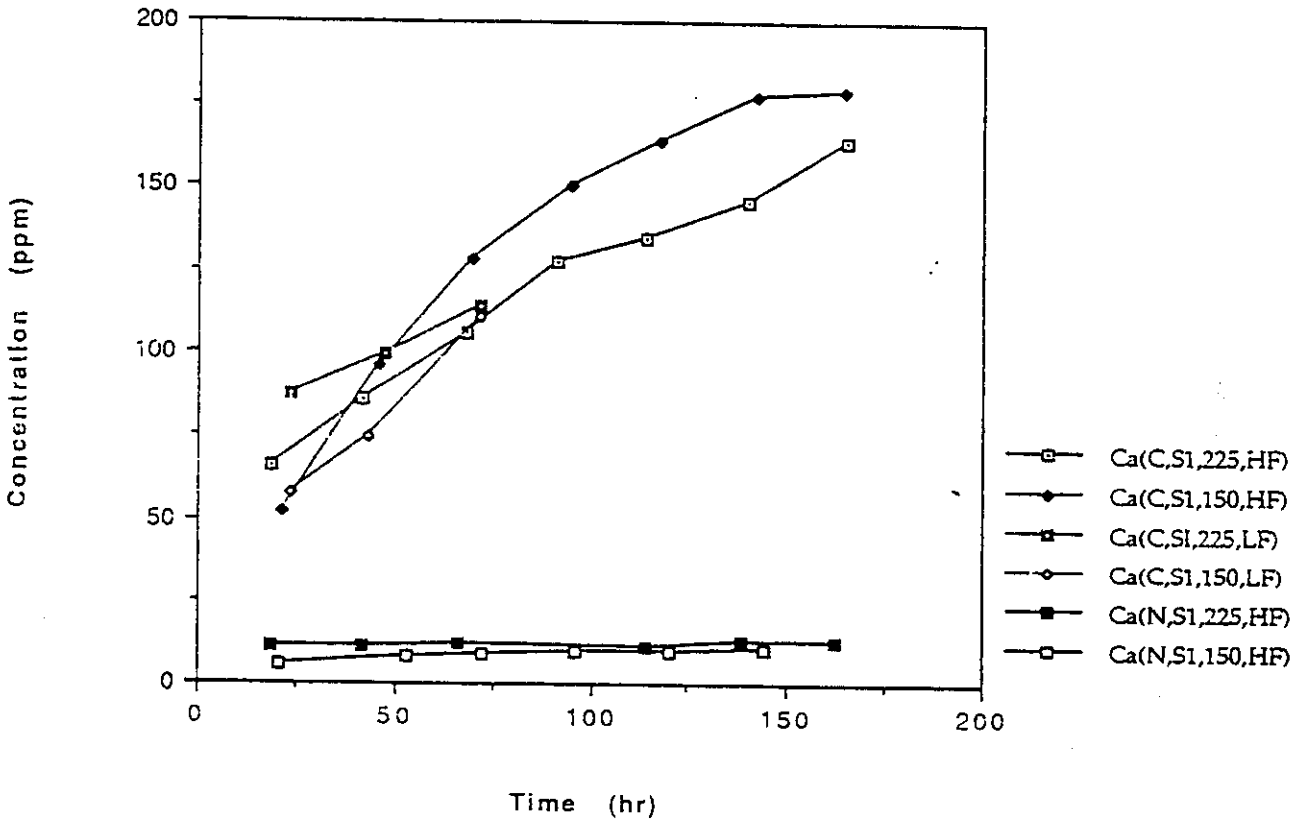

Figure 2.1.5 Effect of temperature on dissolution of Ca, Si, Ba of BFS-PHPA, BFS-dispersed mud and Portland cement in 3.3% NaCl under various test condition

(c) Ca, BFS-dispersed mud

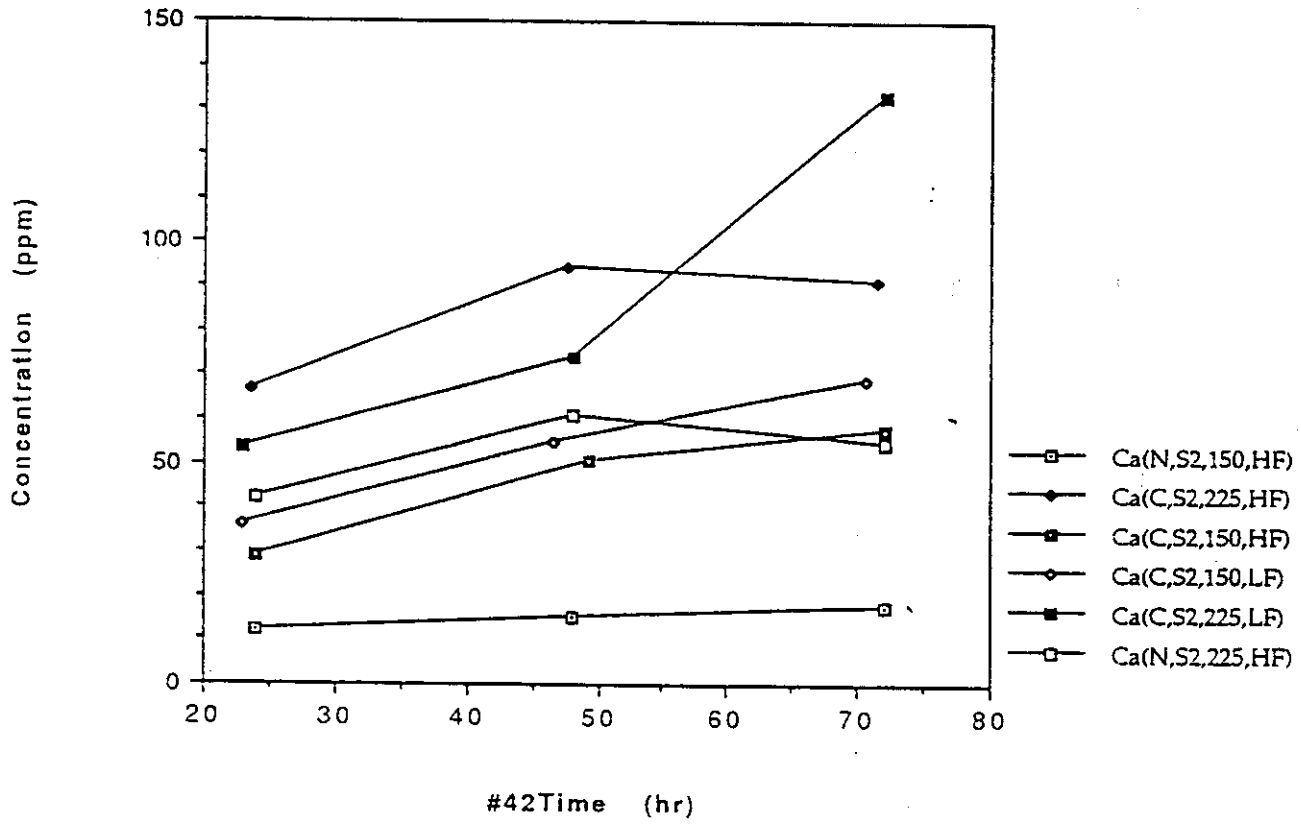

Figure 2.1.5 Effect of temperature on dissolution of Ca, Si, Ba of BFS-PHPA, BFS-dispersed mud and Portland cement in 3.3% NaCl under various test condition

(d) Si, Portland cement

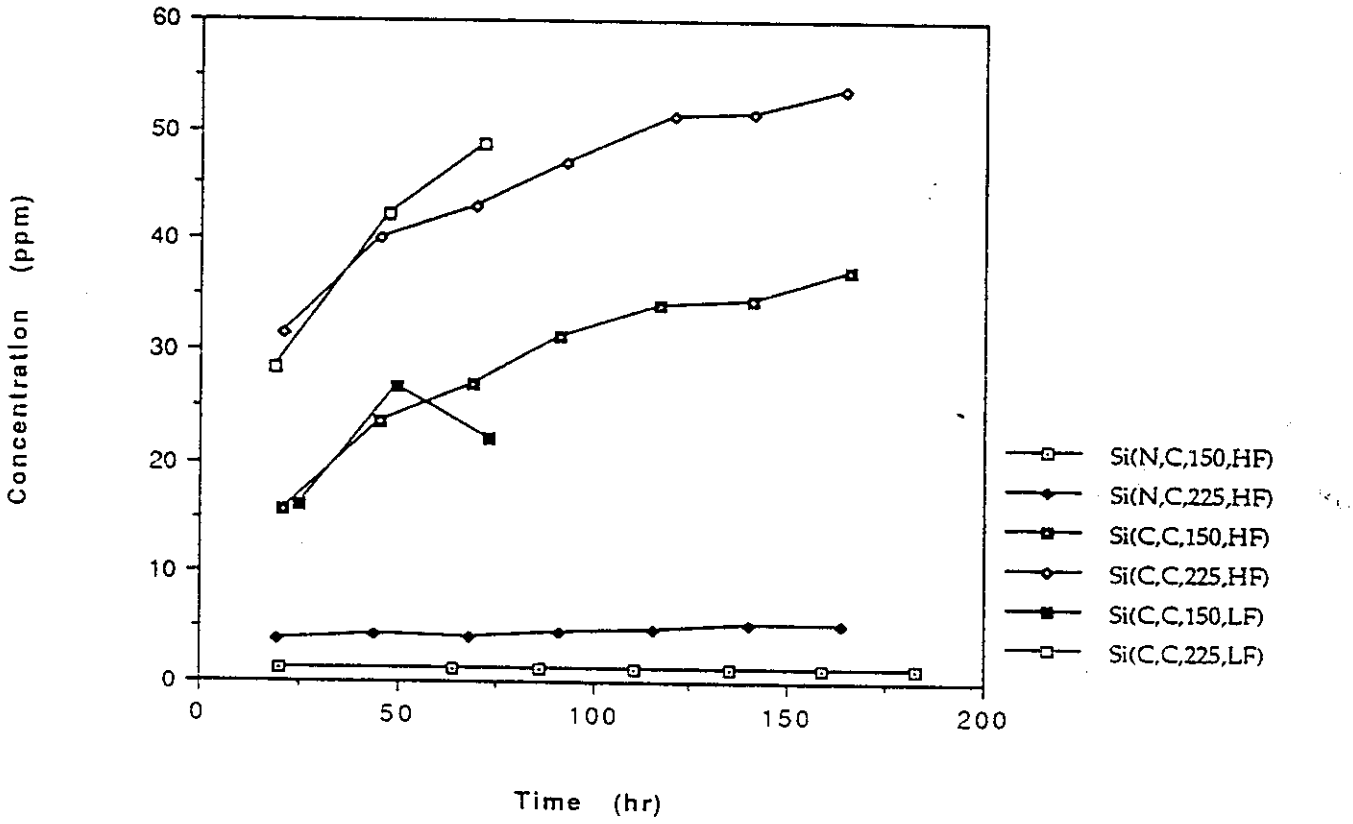

Figure 2.1.5 Effect of temperature on dissolution of Ca, Si, Ba of BFS-PHPA, BFS-dispersed mud and Portland cement in 3.3% NaCl under various test condition

(e) Si, BFS-PHPA

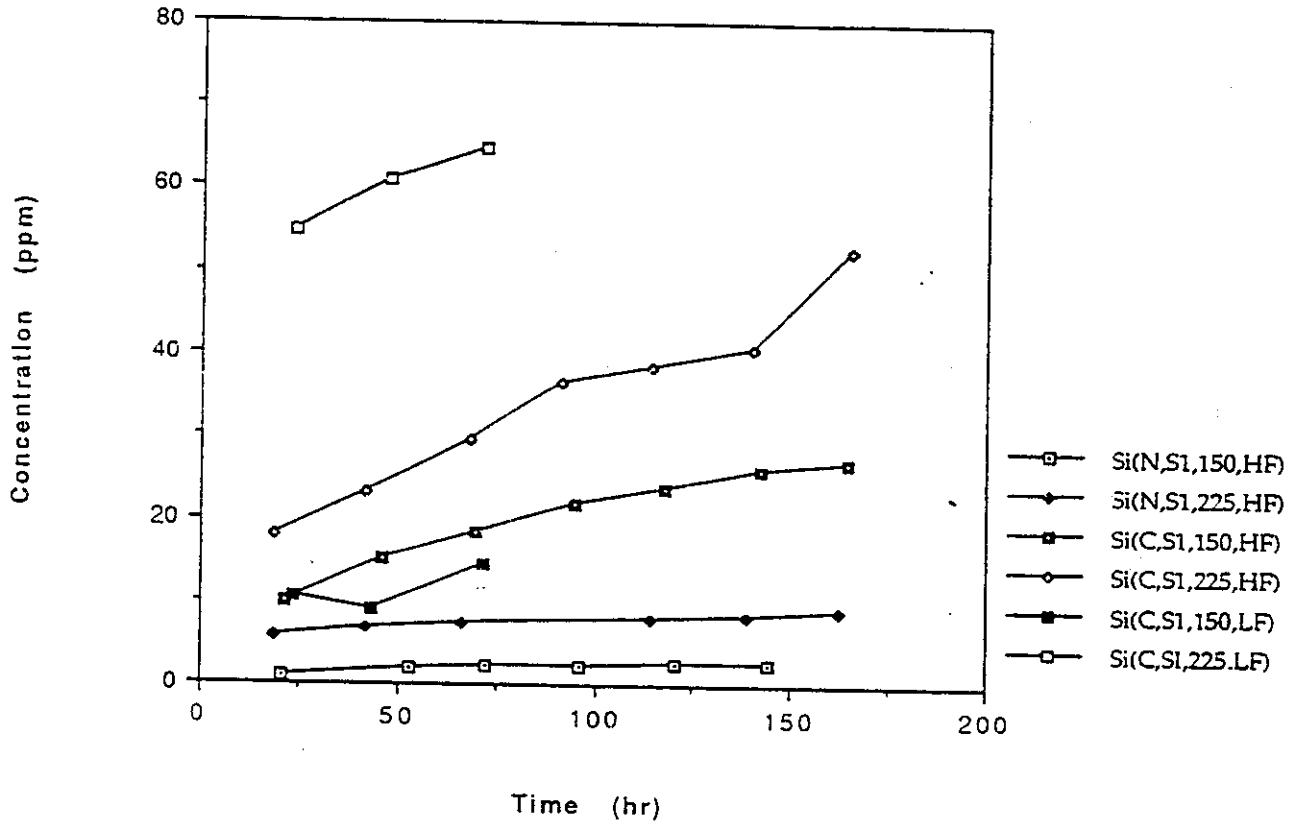

Figure 2.1.5 Effect of temperature on dissolution of Ca, Si, Ba of BFS-PHPA, BFS-dispersed mud and Portland cementt in 3.3% NaCl under various test condition

(f) Si, BFS-dispersed mud

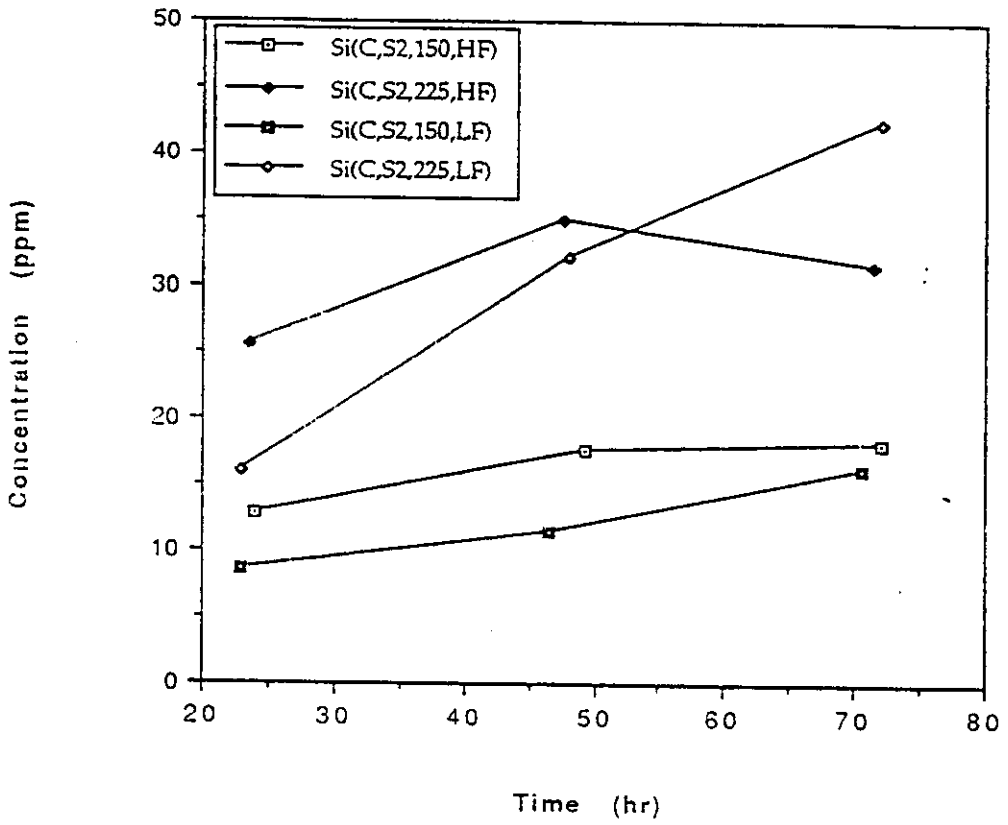

Figure 2.1.5 Effect of temperature on dissolution of Ca, Si, Ba of BFS-PHPA, BFS-dispersed mud and Portland cement in 3.3% NaCl under various test condition

(g) Ba, BFS-PHPA

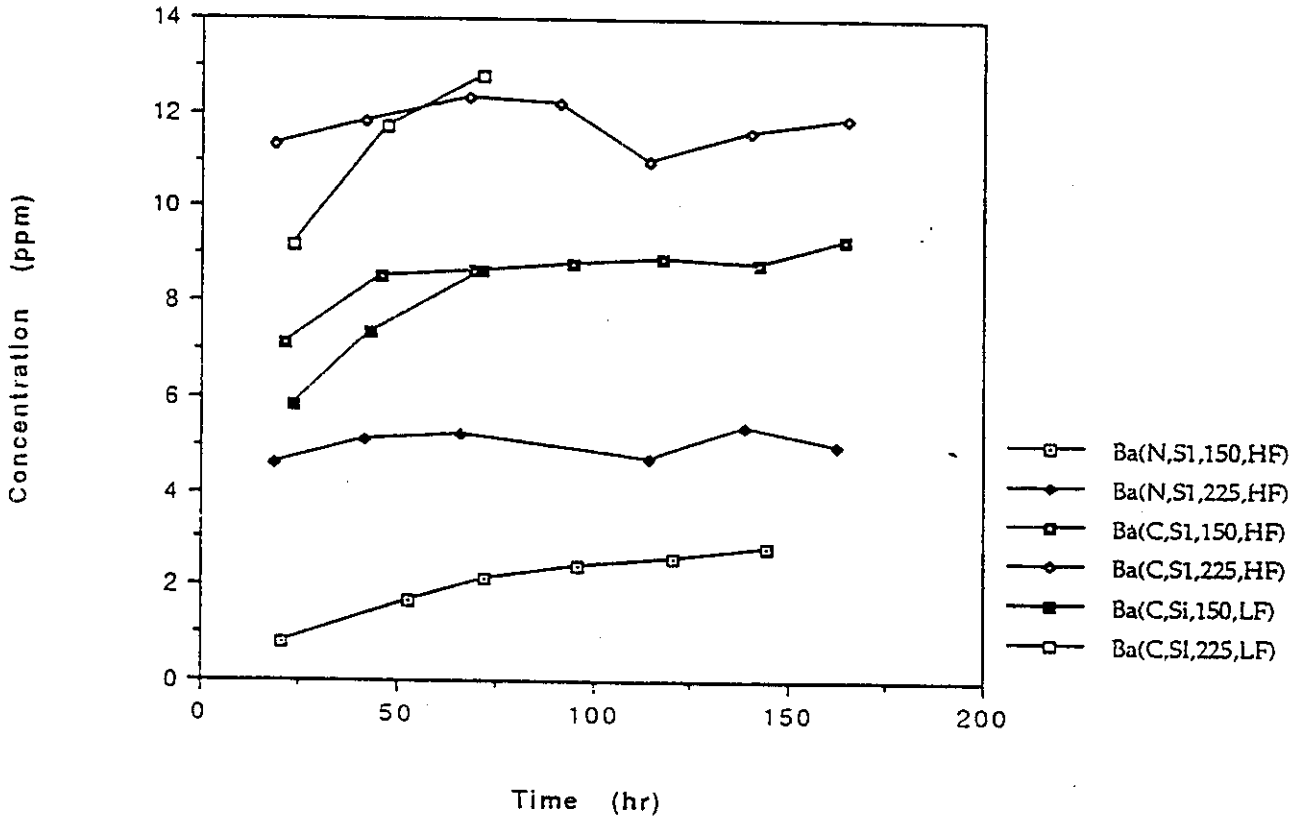

Figure 2.1.6 Effect of flow velocity on Ca and Si of BFS-PHPA, BFS-dispersed mud and Portland cement in 3.3% NaCl under various conditions

(a) Ca, 200 psi CO_2, 225 °F

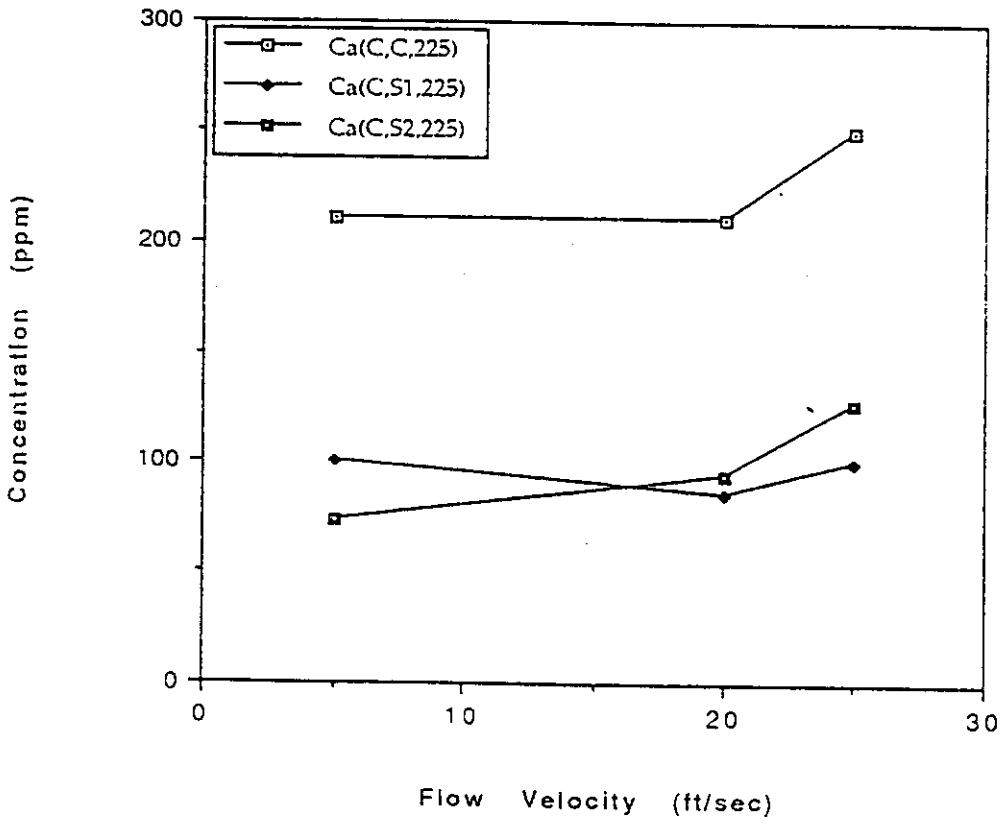

Figure 2.1.6 Effect of flow velocity on Ca and Si of BFS-PHPA, BFS-dispersed mud and Portland cement in 3.3% NaCl under various conditions

(b) Si, 200 psi CO_2, 225 °F

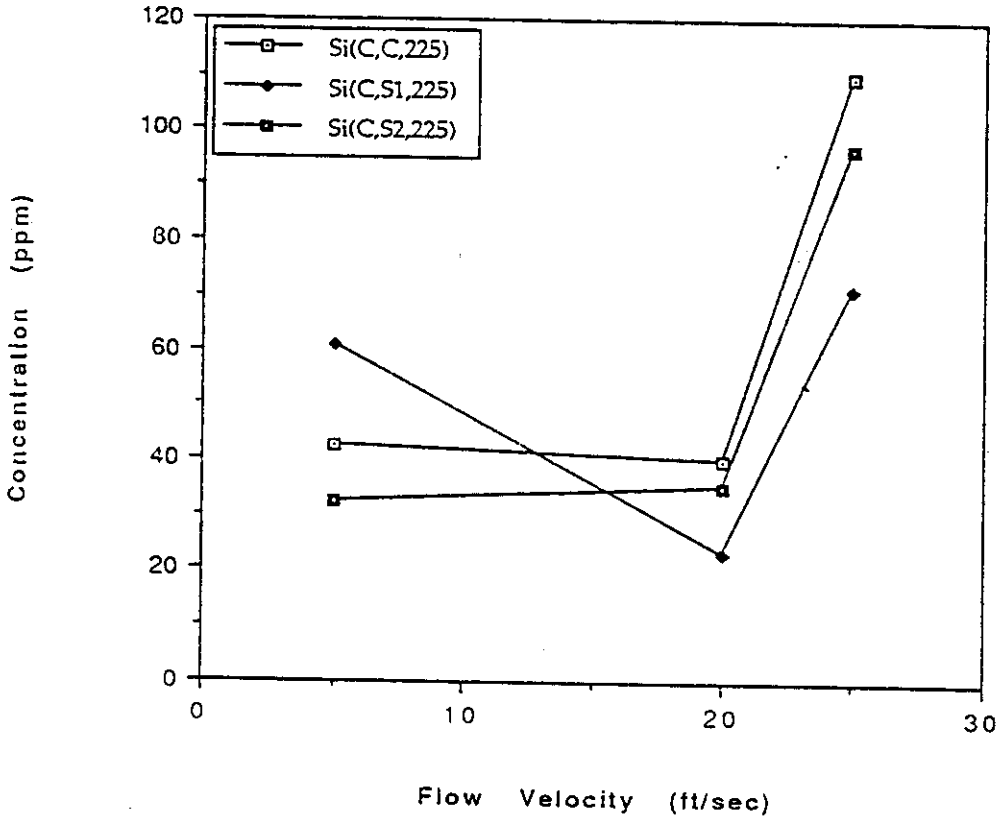

Figure 2.1.6 Effect of flow velocity on Ca and Si of BFS-PHPA, BFS-dispersed mud and Portland cement in 3.3% NaCl under various conditions

(c) Ca, 200 psi CO_2, 150 °F

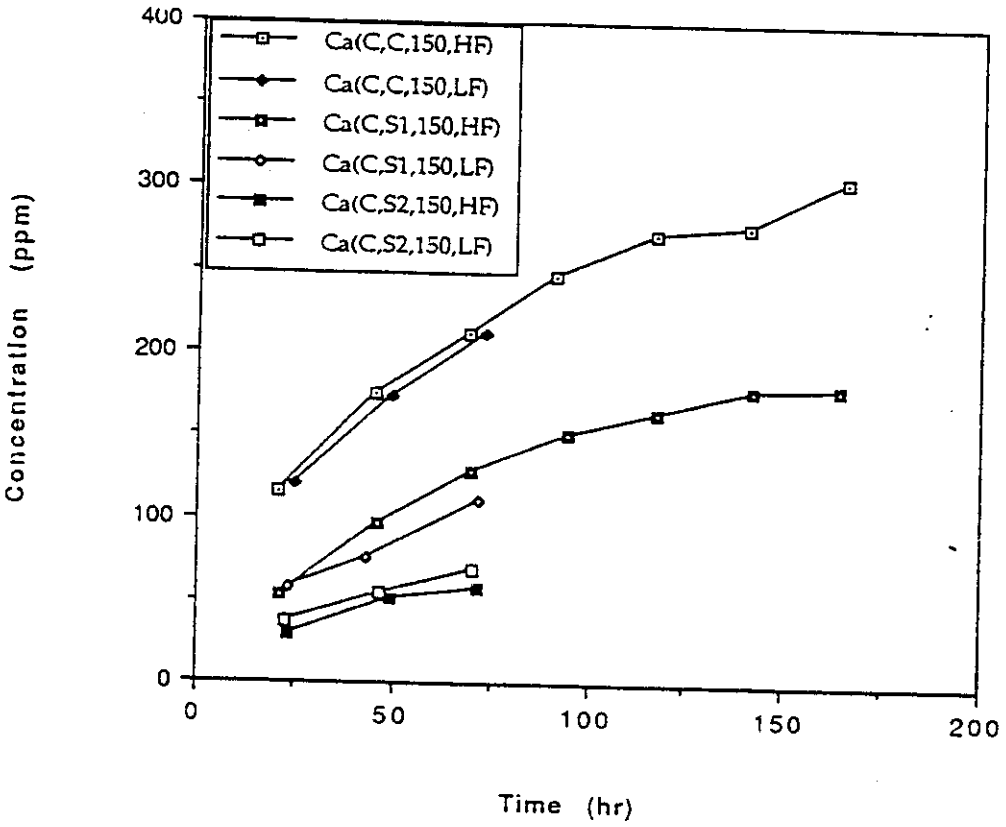

Figure 2.1.7 Comparison of Ca dissolution of BFS-PHPA, BFS-dispersed mud and Portland cement in 3.3% NaCl under various test conditions

(a) 200 psi CO_2, 225 °F, 20 ft/sec

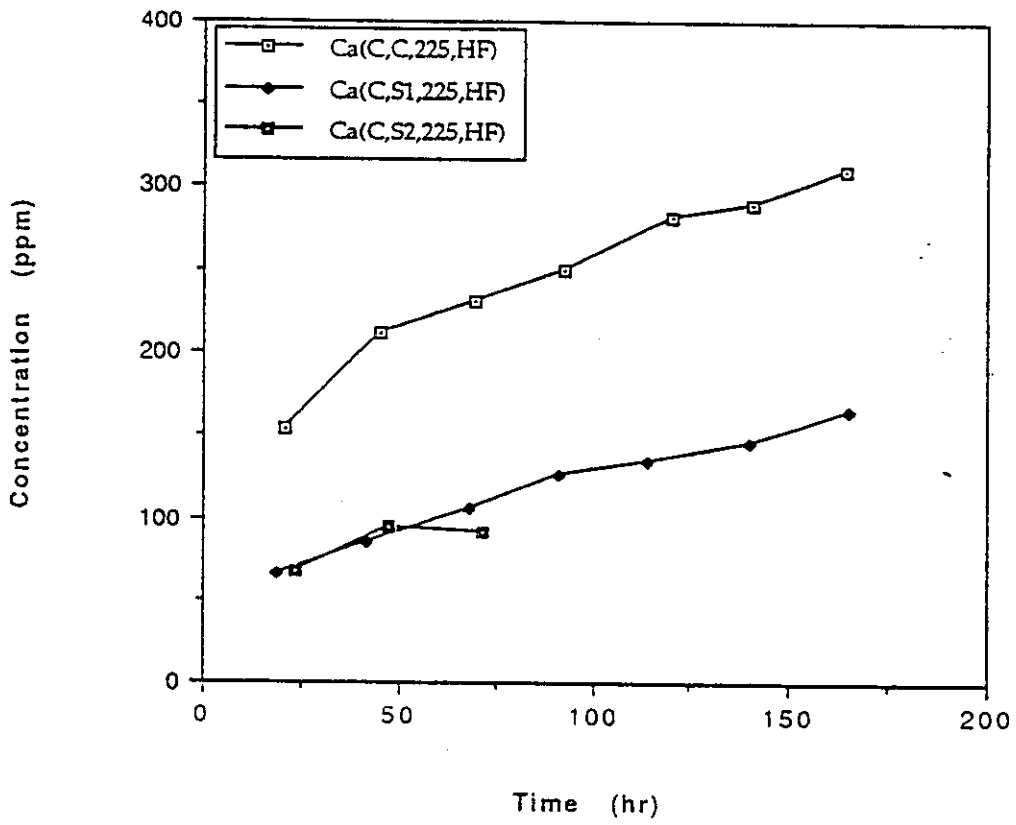

Figure 2.1.7 Comparison of Ca dissolution of BFS-PHPA, BFS-dispersed mud and Portland cement in 3.3% NaCl under various test conditions

(b) 200 psi CO_2, 225 °F, 5 ft/sec

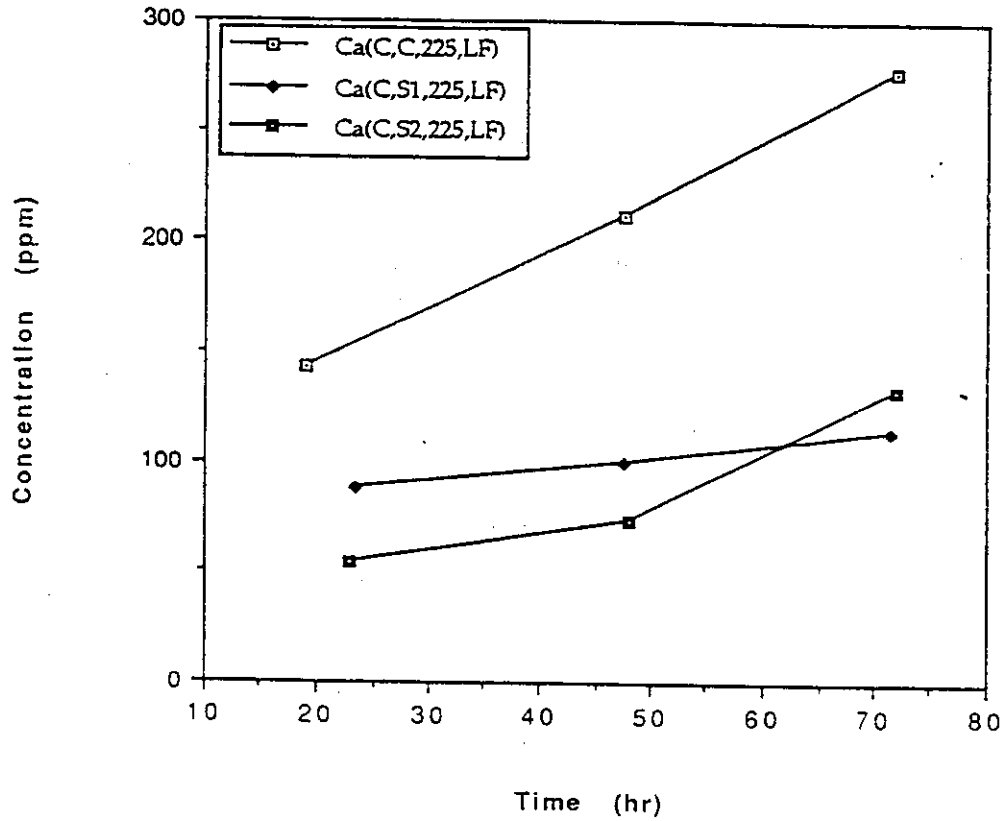

Figure 2.1.7 Comparison of Ca dissolution of BFS-PHPA, BFS-dispersed mud and Portland cement in 3.3% NaCl under various test conditions

(c) 200 psi CO_2, 150 °F, 20 ft/sec

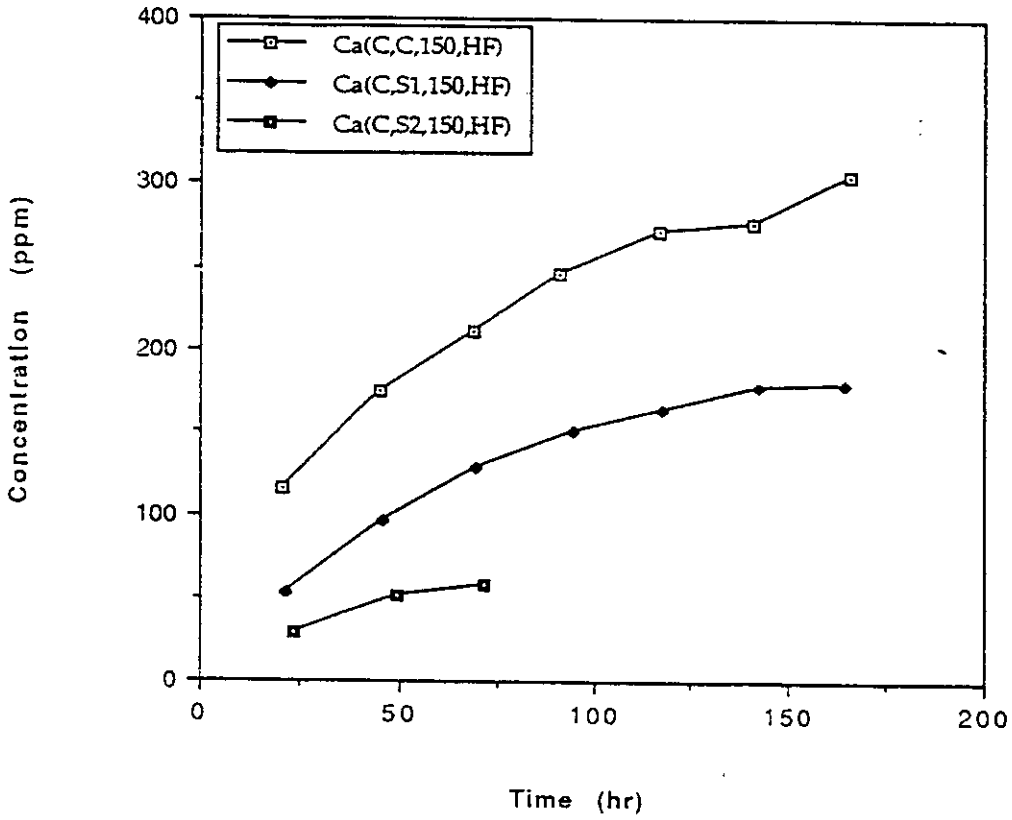

Figure 2.1.7 Comparison of Ca dissolution of BFS-PHPA, BFS-dispersed mud and Portland cement in 3.3% NaCl under various test conditions

(d) 200 psi CO_2, 150 °F, 5 ft/sec

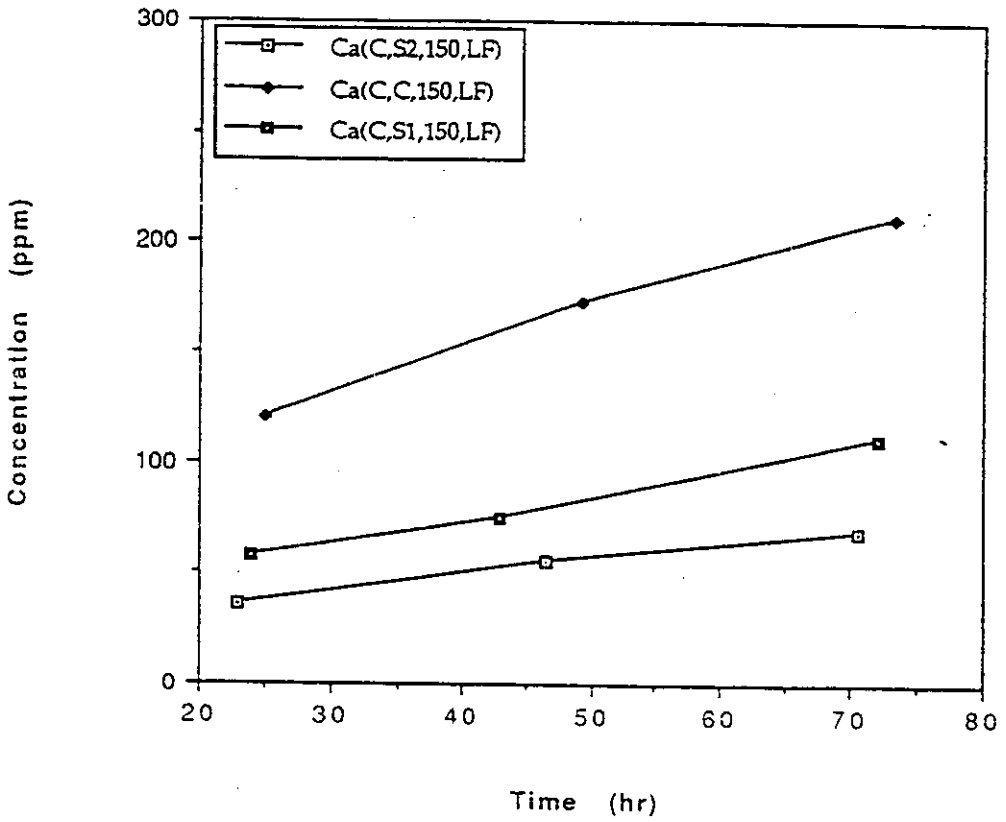

Figure 2.1.7 Comparison of Ca dissolution of BFS-PHPA, BFS-dispersed mud and Portland cement in 3.3% NaCl under various test conditions

(e) N_2, 225 °F, 20 ft/sec

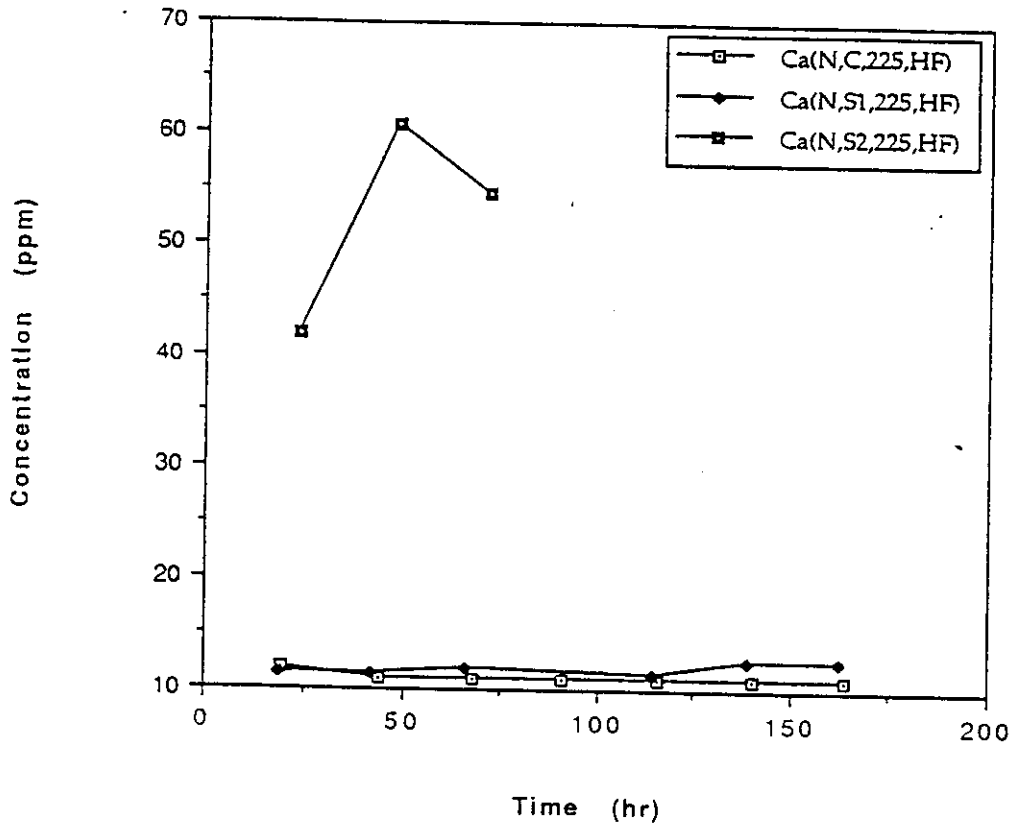

Figure 2.1.7 Comparison of Ca dissolution of BFS-PHPA, BFS-dispersed mud and Portland cement in 3.3% NaCl under various test conditions

(f) N_2, 150 °F, 20 ft/sec

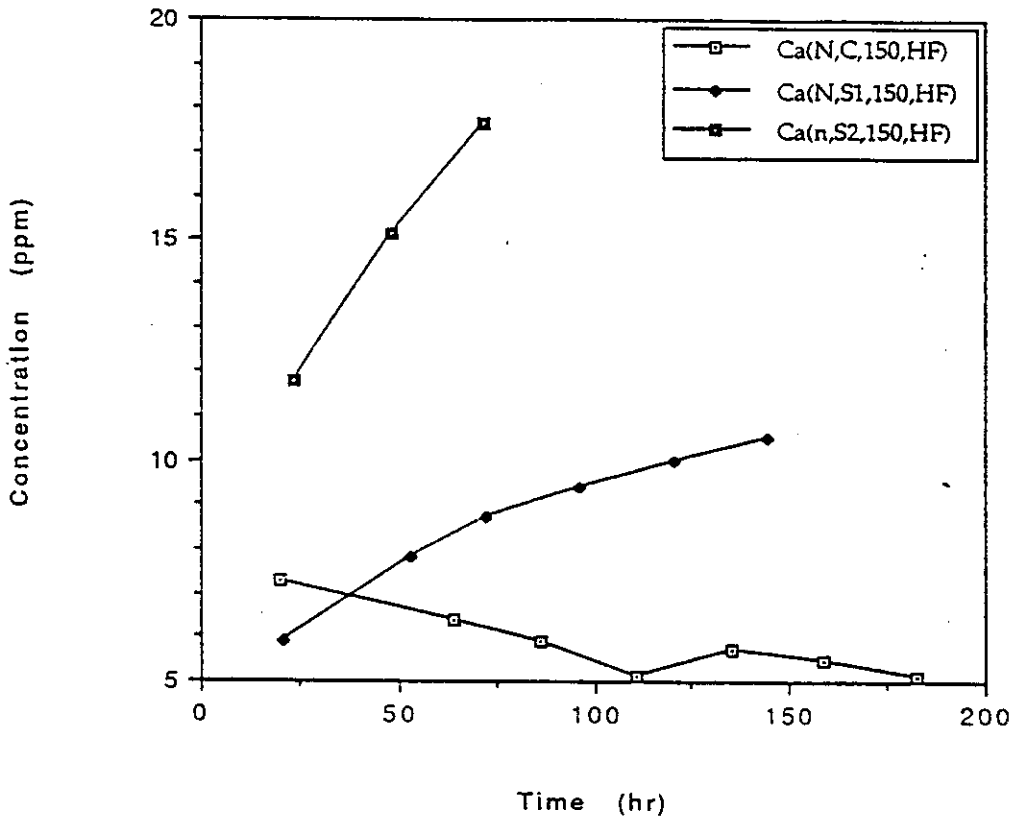

Figure 2.1.8 Comparison of Si dissolution of BFS-PHPA, and BFS-Dispersed mud and Portland cement in 3.3% NaCl under various test condition

(a) 200 psi CO_2, 225 °F, 20 ft/sec

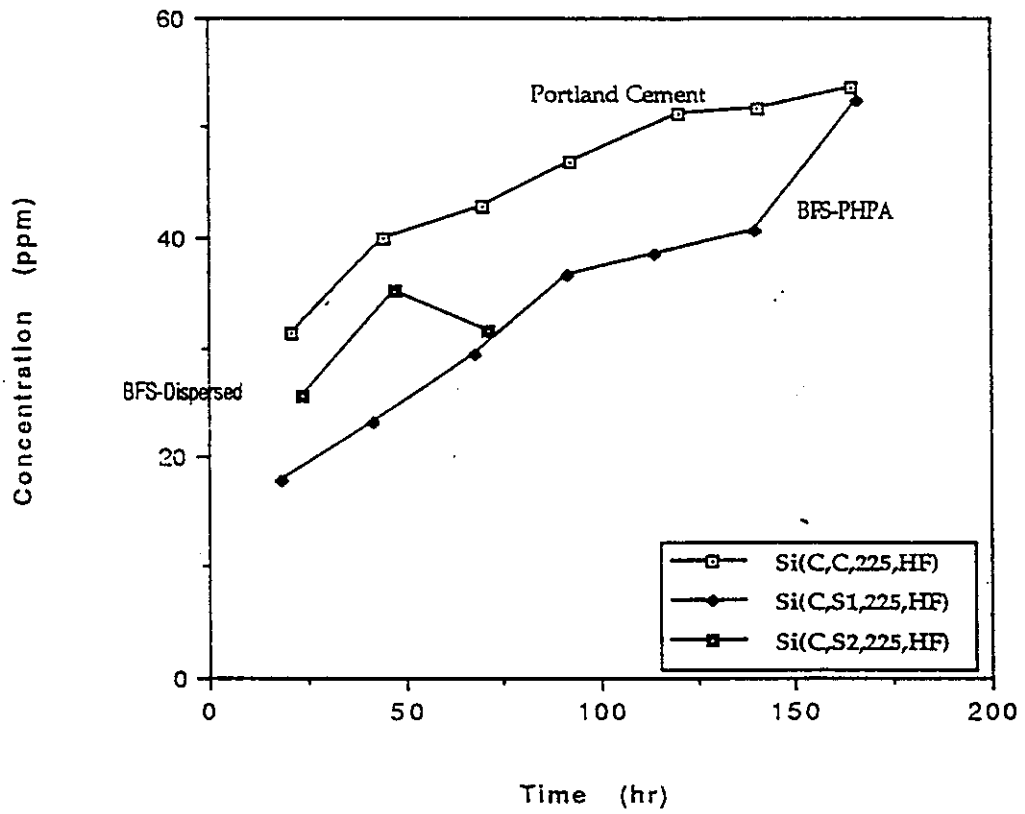

Figure 2.1.8 Comparison of Si dissolution of BFS-PHPA, and BFS-Dispersed mud and Portland cement in 3.3% NaCl under various test conditions

(b) 200 psi CO_2, 150 °F, 20 ft/sec

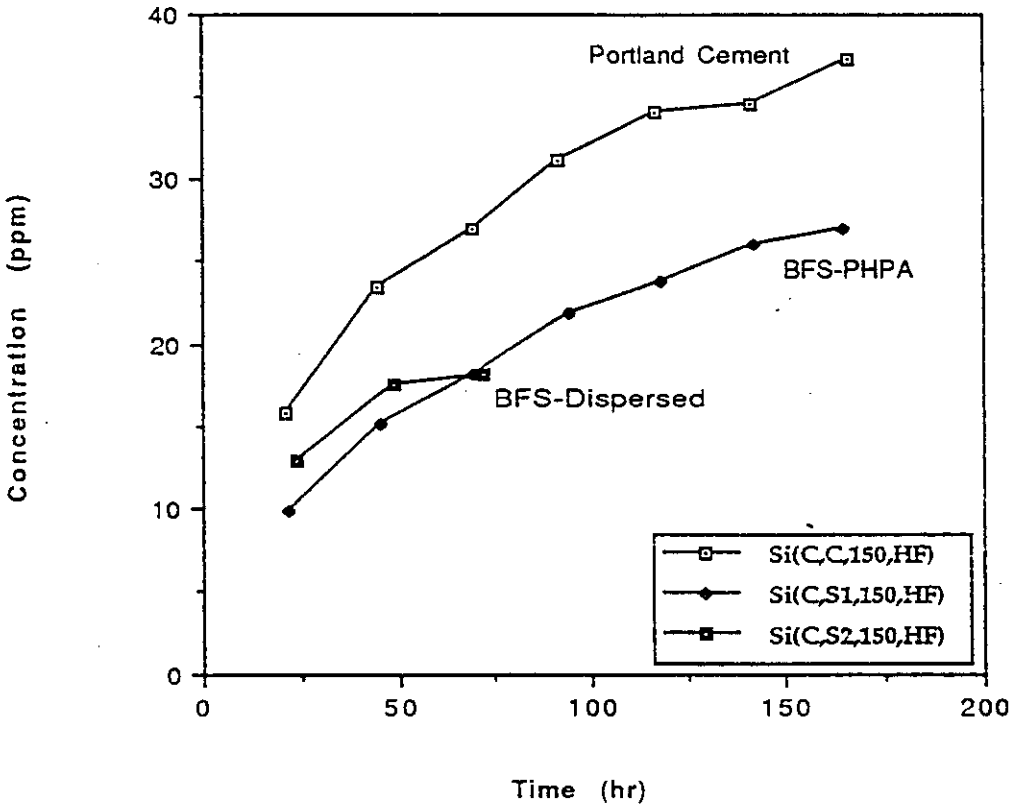

Figure 2.1.9 Comparison of dissolution rate of total dissolved species of BFS-PHPA, BFS-Dispersed and Portland cements in 3.3% NaCl under various test conditions

(a) 150°F, 200 psi CO_2, LF (5 ft/sec), HF (20 ft/sec), HHF (25ft/sec)

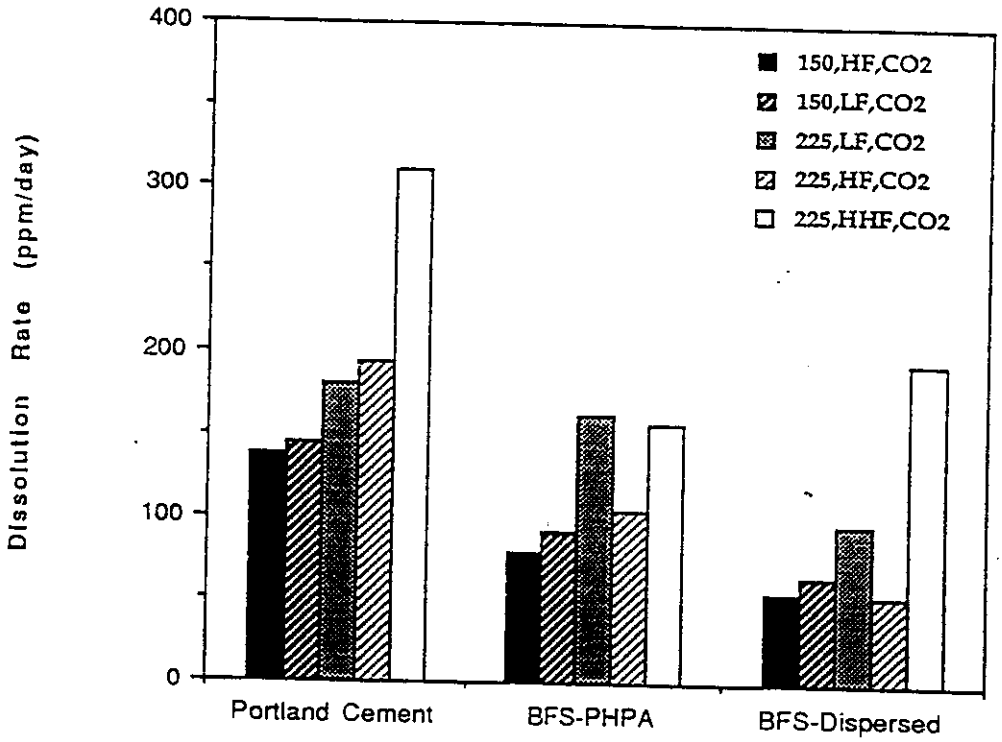

Figure 2.1.9 Comparison of dissolution rate of total dissolved species of BFS-PHPA, BFS-Dispersed and Portland cements in 3.3% NaCl under various test conditions

(b) 150°F, Nitrogen, HF (20 ft/sec),

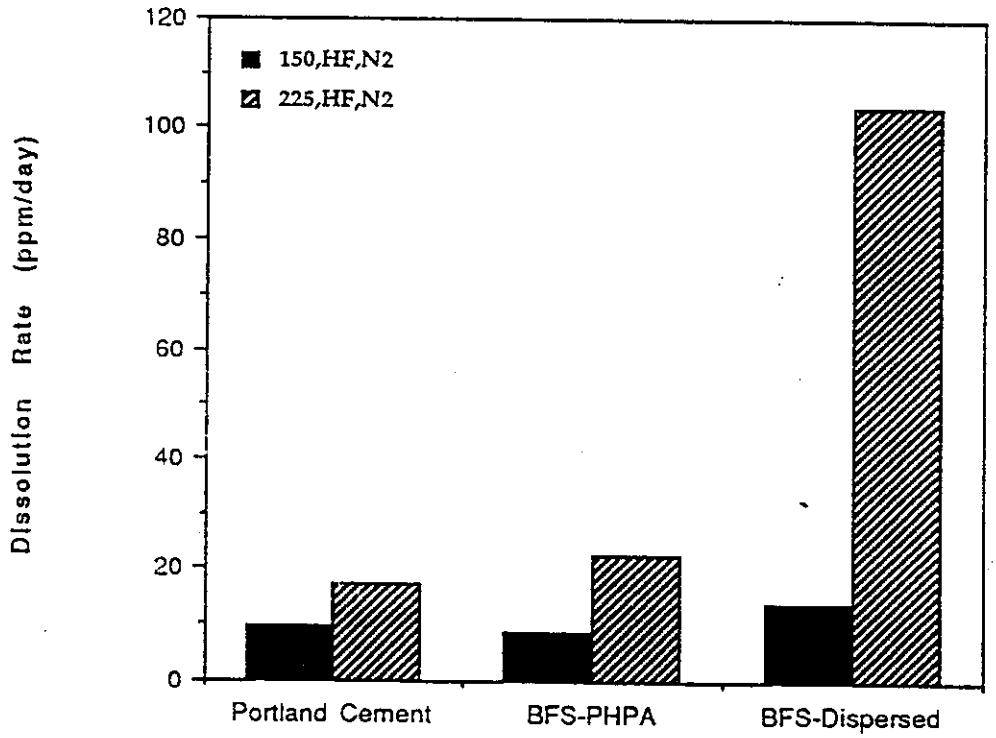

Figure 2.1.10 As-tested appearances of cylindrical specimens of BFS-PHPA, BFS-dispersed mud and Portland cement tested in 3.3% NaCl under various conditions

(a) Portland cement, N_2, 150 °F, 20 ft/sec
(b) Portland cement, N_2, 225 °F, 20 ft/sec

(a)

(b)

Figure 2.1.10 As-tested appearances of cylindrical specimens of BFS-PHPA, BFS-dispersed mud and Portland cement tested in 3.3% NaCl under various conditions

(c) Portland cement, 200 psi CO_2, 150 °F, 5 ft/sec
(d) Portland cement, 200 psi CO_2, 150 °F, 20 ft/sec

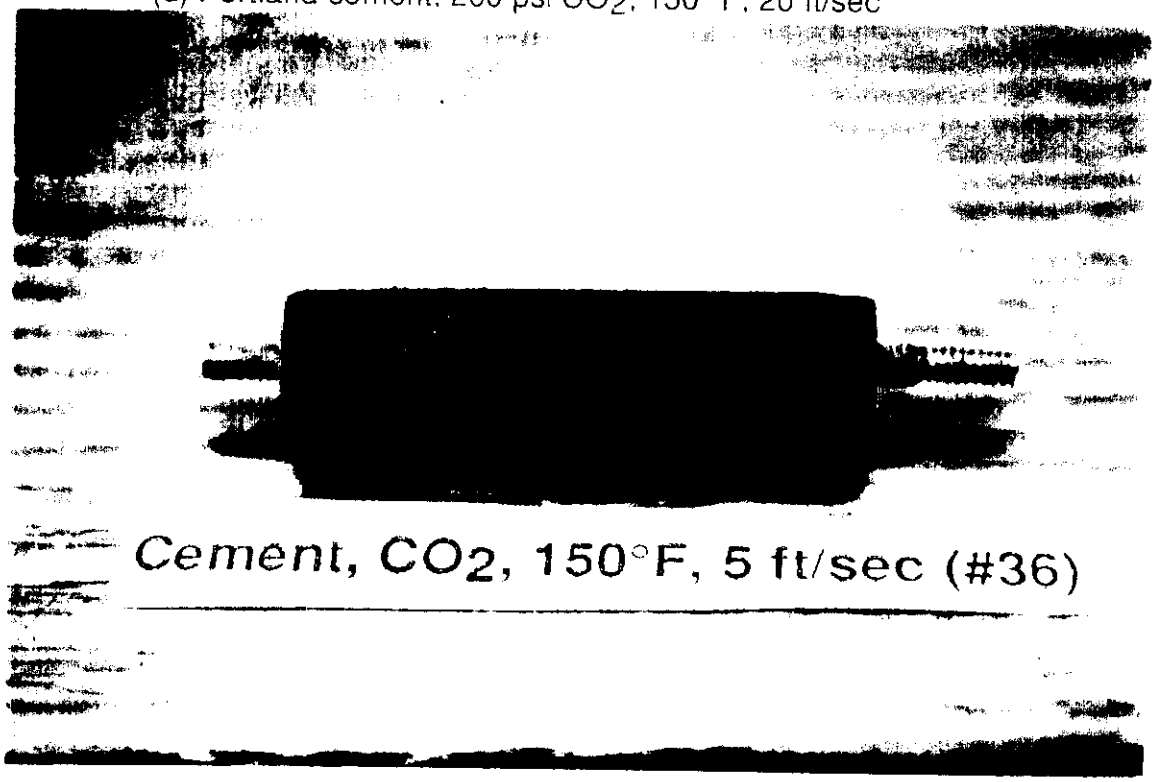

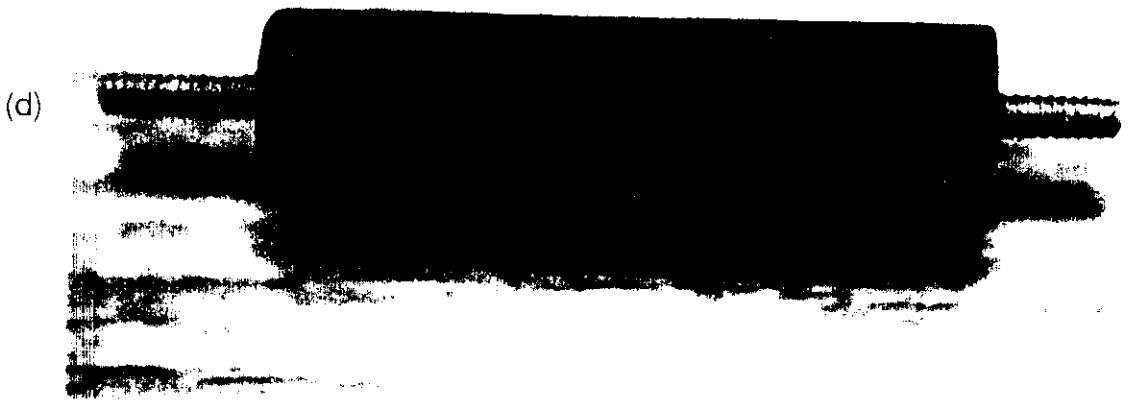

Figure 2.1.10 As-tested appearances of cylindrical specimens of BFS-PHPA, BFS-dispersed mud and Portland cement tested in 3.3% NaCl under various conditions

(e) Portland cement, 200 psi CO_2, 225 °F, 5 ft/sec
(f) Portland cement, 200 psi CO_2, 225 °F, 20 ft/sec

(e)

ment, CO_2, 225 F, 5 ft/sec (f

(f)

ment, CO_2, 225°F, 20 ft/sec

Figure 2.1.10 As-tested appearances of cylindrical specimens of BFS-PHPA, BFS-dispersed mud and Portland cement tested in 3.3% NaCl under various conditions

(g) BFS-PHPA, N_2, 150 °F, 20 ft/sec
(h) BFS-PHPA, N_2, 225 °F, 20 ft/sec

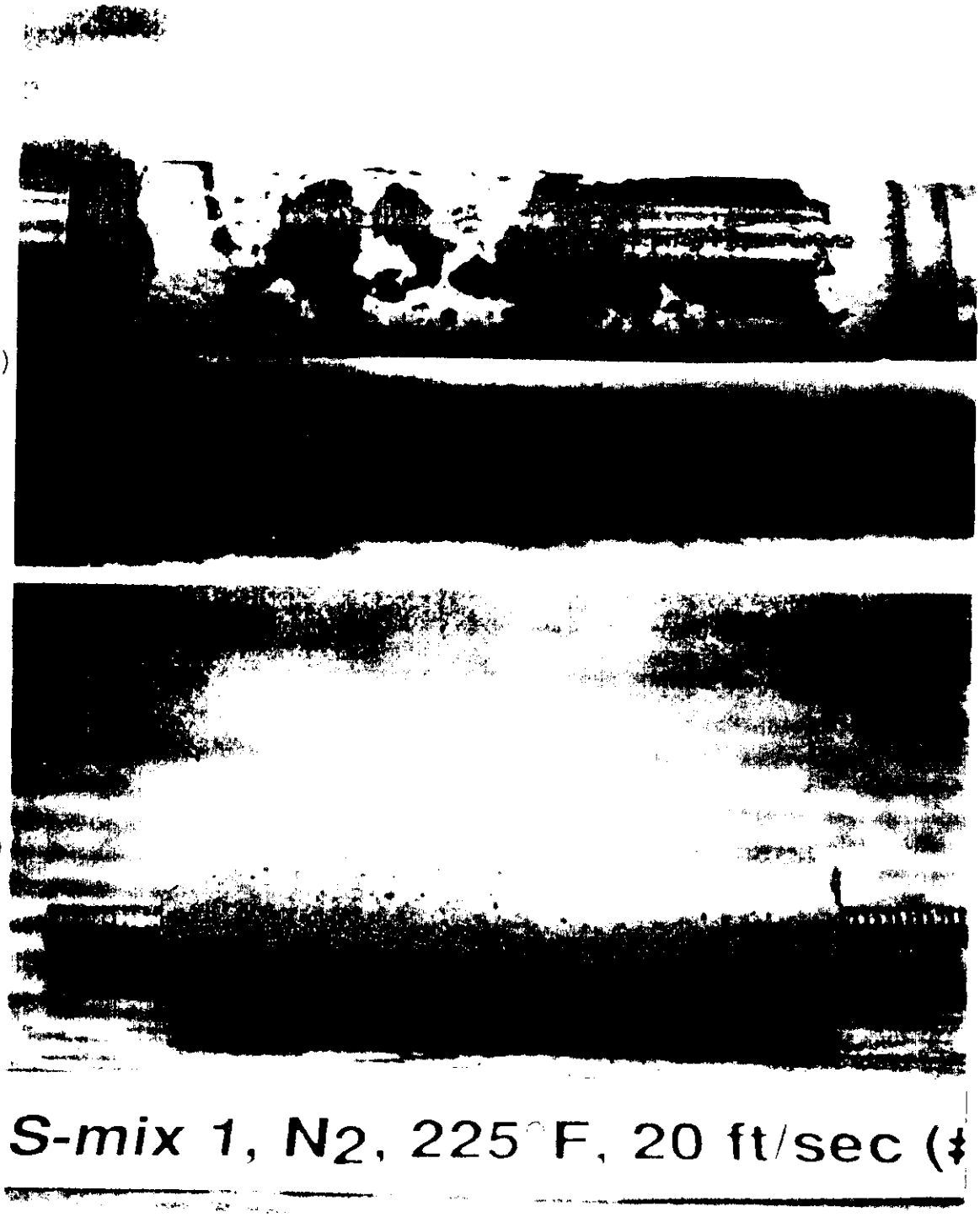

Figure 2.1.10 As-tested appearances of cylindrical specimens of BFS-PHPA, BFS-dispersed mud and Portland cement tested in 3.3% NaCl under various conditions

(i) BFS-PHPA, 200 psi CO_2, 150 °F, 5 ft/sec
(j) BFS-PHPA, 200 psi CO_2, 150 °F, 20 ft/sec

(i)

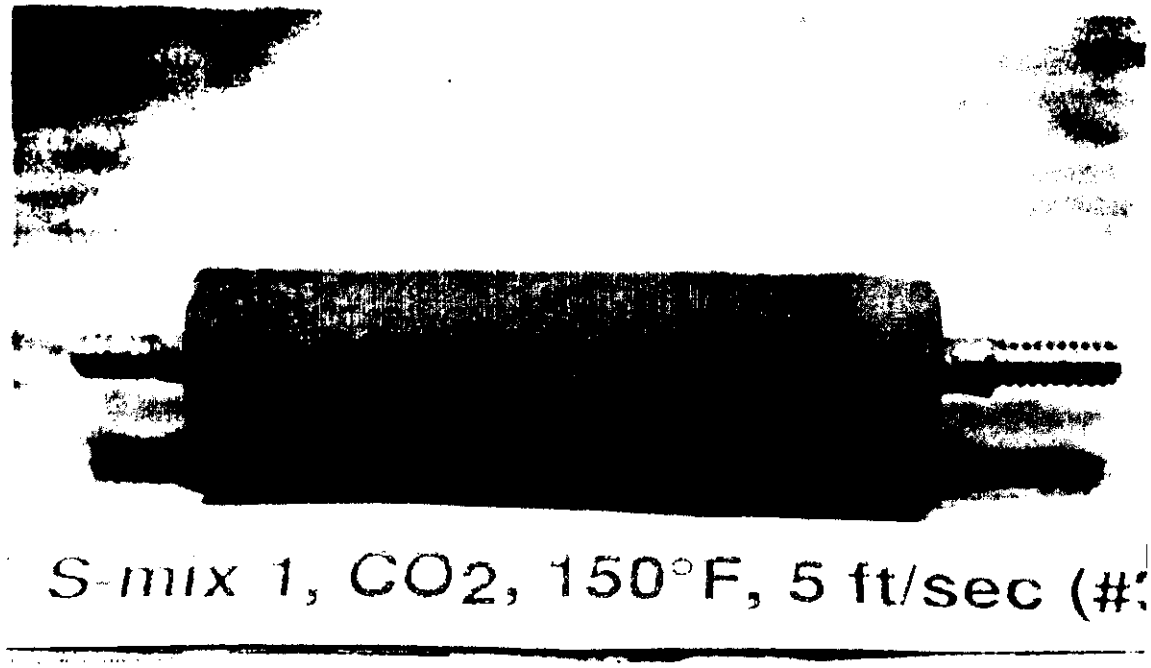

(j)

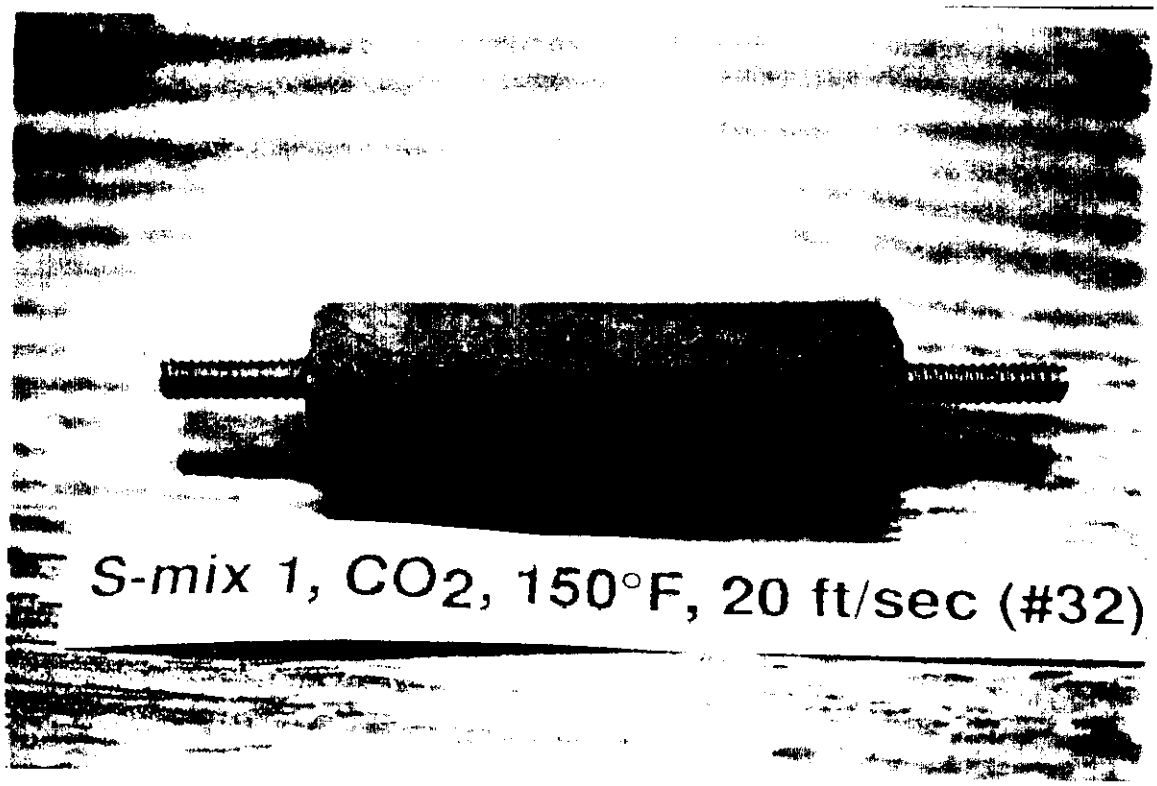

Figure 2.1.10 As-tested appearances of cylindrical specimens of BFS-PHPA, BFS-dispersed mud and Portland cement tested in 3.3% NaCl under various conditions

(k) BFS-PHPA, 200 psi CO_2, 225 °F, 5 ft/sec
(l) BFS-PHPA, 200 psi CO_2, 225 °F, 20 ft/sec (The specimen disintegrated because it was prematurely removed at ~200 °F)

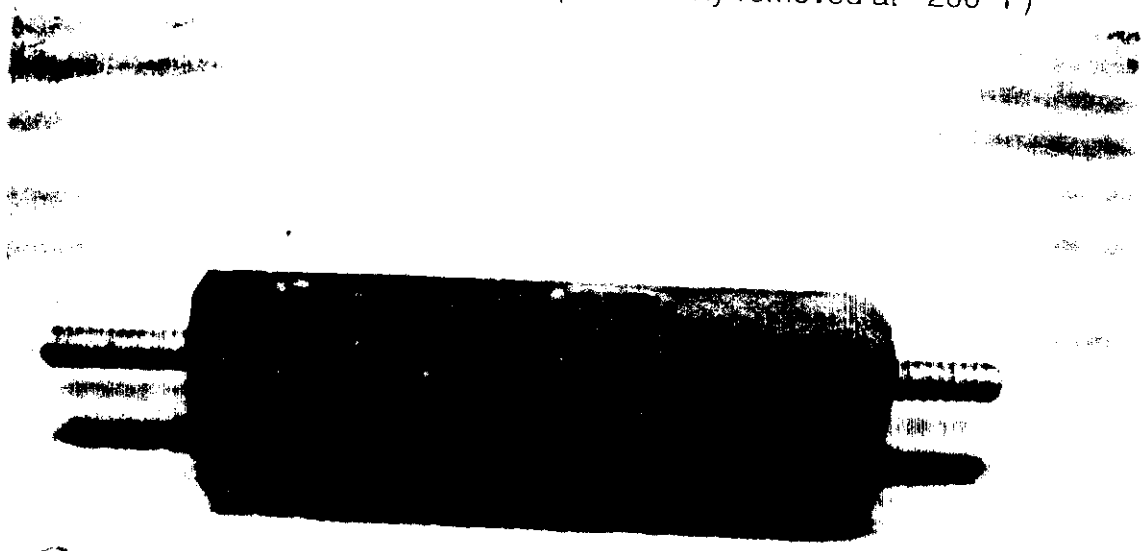

(k)

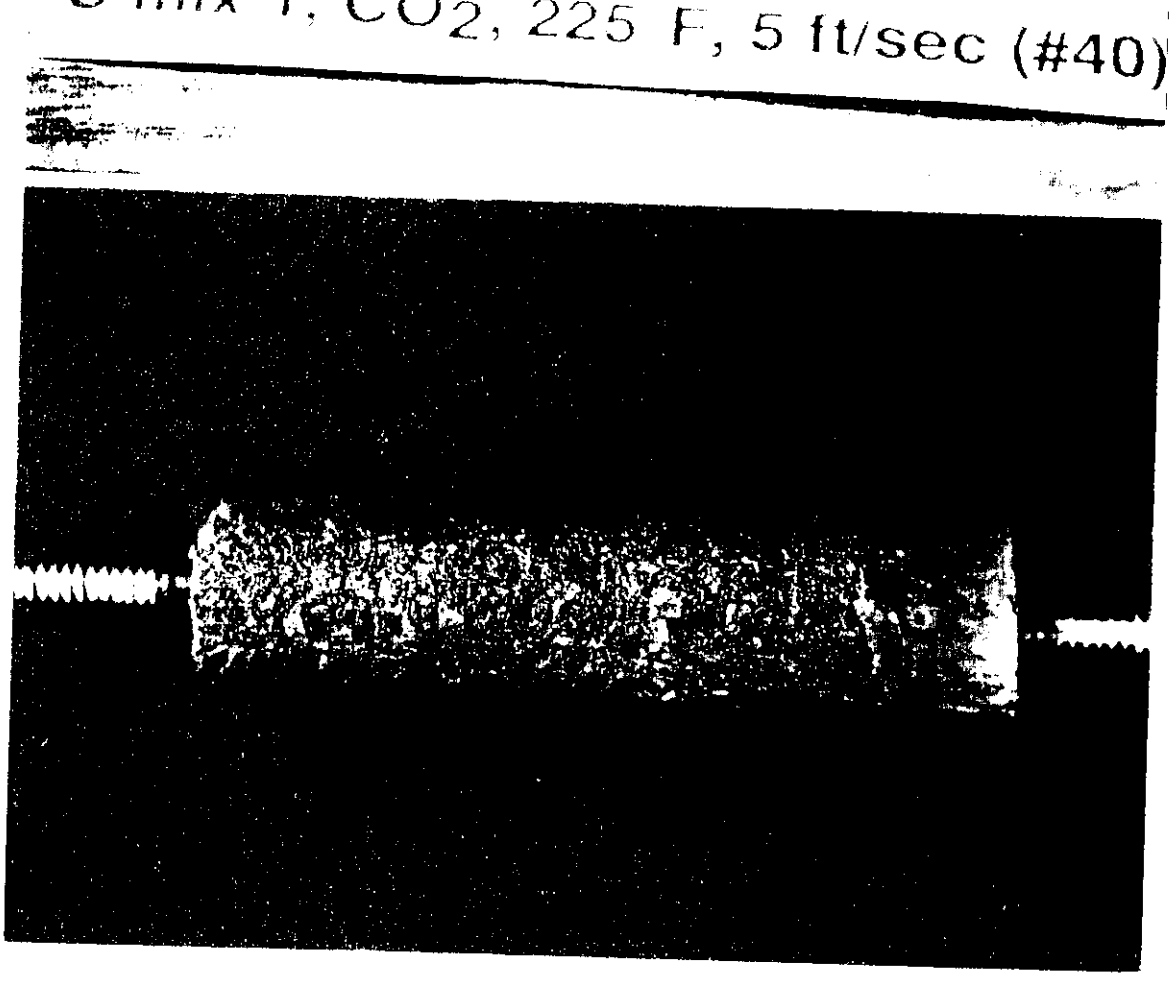

(l)

Figure 2.1.10 As-tested appearances of cylindrical specimens of BFS-PHPA, BFS-dispersed mud and Portland cement tested in 3.3% NaCl under various conditions

(m) BFS-dispersed mud, N_2, 150 °F, 20 ft/sec
(n) BFS-dispersed mud, N_2, 225 °F, 20 ft/sec

(m)

mix 2, N2, 150 F, 20 ft/sec (

(n)

-mix 2, N2, 225 F, 20 ft/sec (

Figure 2.1.10 As-tested appearances of cylindrical specimens of BFS-PHPA, BFS-dispersed mud and Portland cement tested in 3.3% NaCl under various conditions

(o) BFS-dispersed mud, 200 psi CO_2, 150 °F, 5 ft/sec
(p) BFS-dispersed mud, 200 psi CO_2, 150 °F, 20 ft/sec

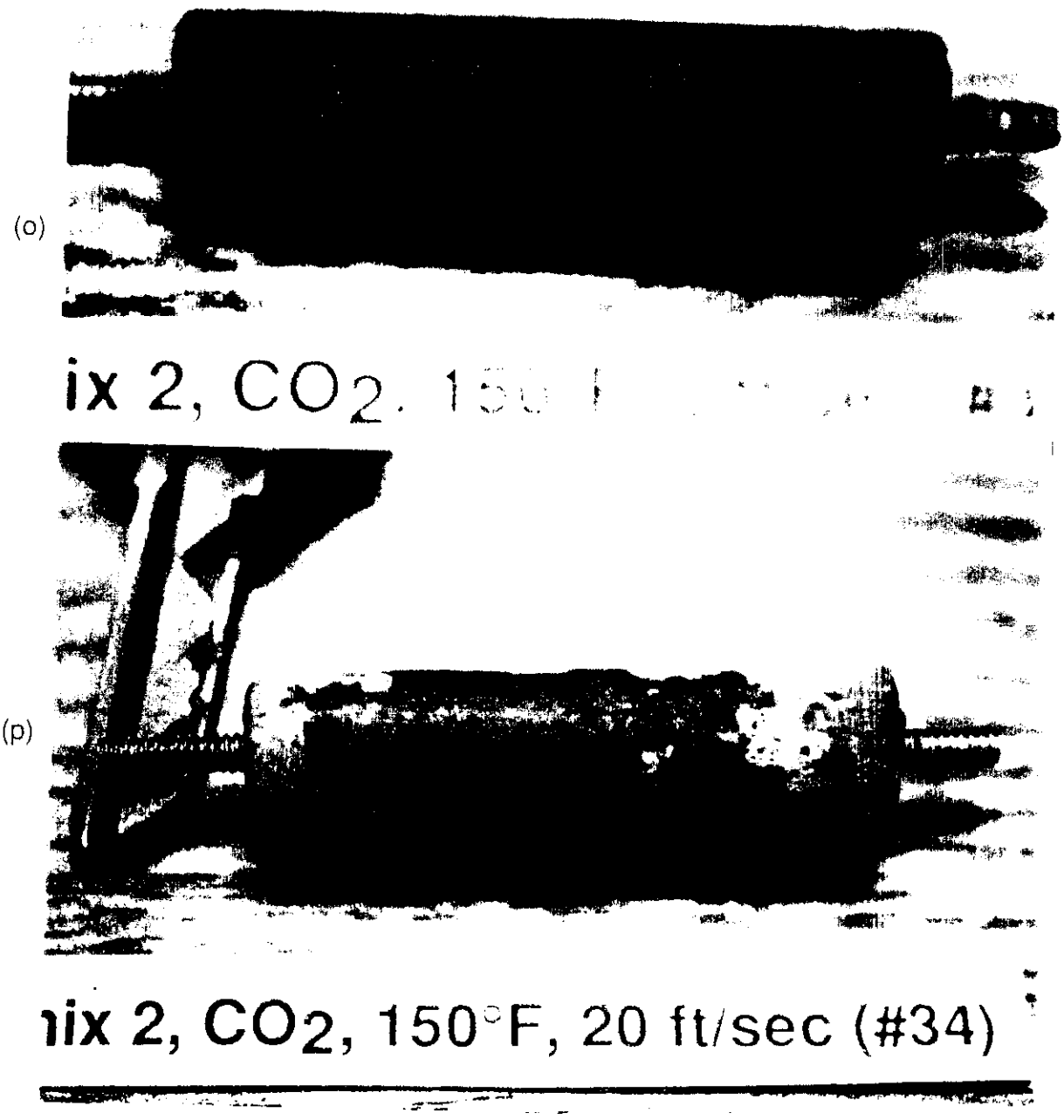

Figure 2.1.10 As-tested appearances of cylindrical specimens of BFS-PHPA, BFS-dispersed mud and Portland cement tested in 3.3% NaCl under various conditions

(q) BFS-dispersed mud, 200 psi CO_2, 225 °F, 5 ft/sec
(r) BFS-dispersed mud, 200 psi CO_2, 225 °F, 20 ft/sec

(q)

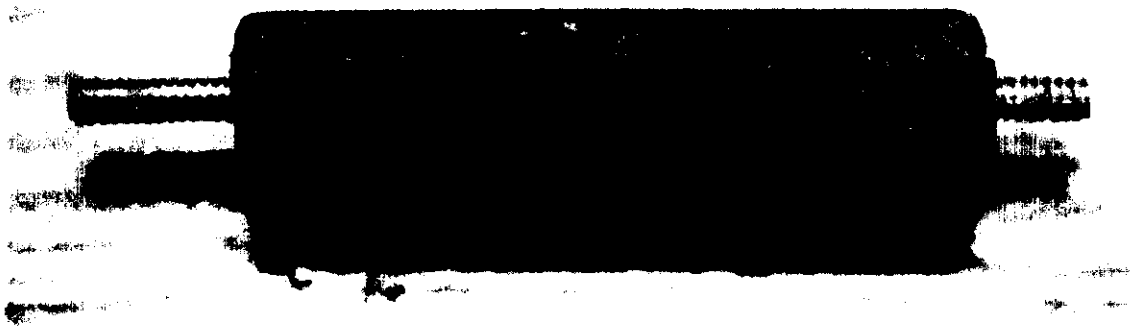

mix 2, CO_2, 225 F, 5 ft sec (#38)

(r)

2, CO_2, 225°F, 20 ft/sec (#3

Figure 2.1.10 As-tested appearances of cylindrical specimens of BFS-PHPA, BFS-dispersed mud and Portland cement tested in 3.3% NaCl under various conditions

(s) BFS-PHPA mud, 200 psi CO_2, 225 °F, 25 ft/sec
(t) BFS-dispersed mud, 200 psi CO_2, 225 °F, 25 ft/sec

(s)

CO_2, 225 °F, 25 ft/sec (#43)

(t)

nix 2, CO_2, 225 F, 25 ft/sec (

Figure 2.1.10 As-tested appearances of cylindrical specimens of BFS-PHPA, BFS-dispersed mud and Portland cement tested in 3.3% NaCl under various conditions

(u) Portland cement, 200 psi CO_2, 225 °F, 25 ft/sec

ment, CO_2 225°F, 25 ft/sec (#

Figure 2.1.11 X-ray elemental analysis of black deposits of Figure 2.1.8 (g)

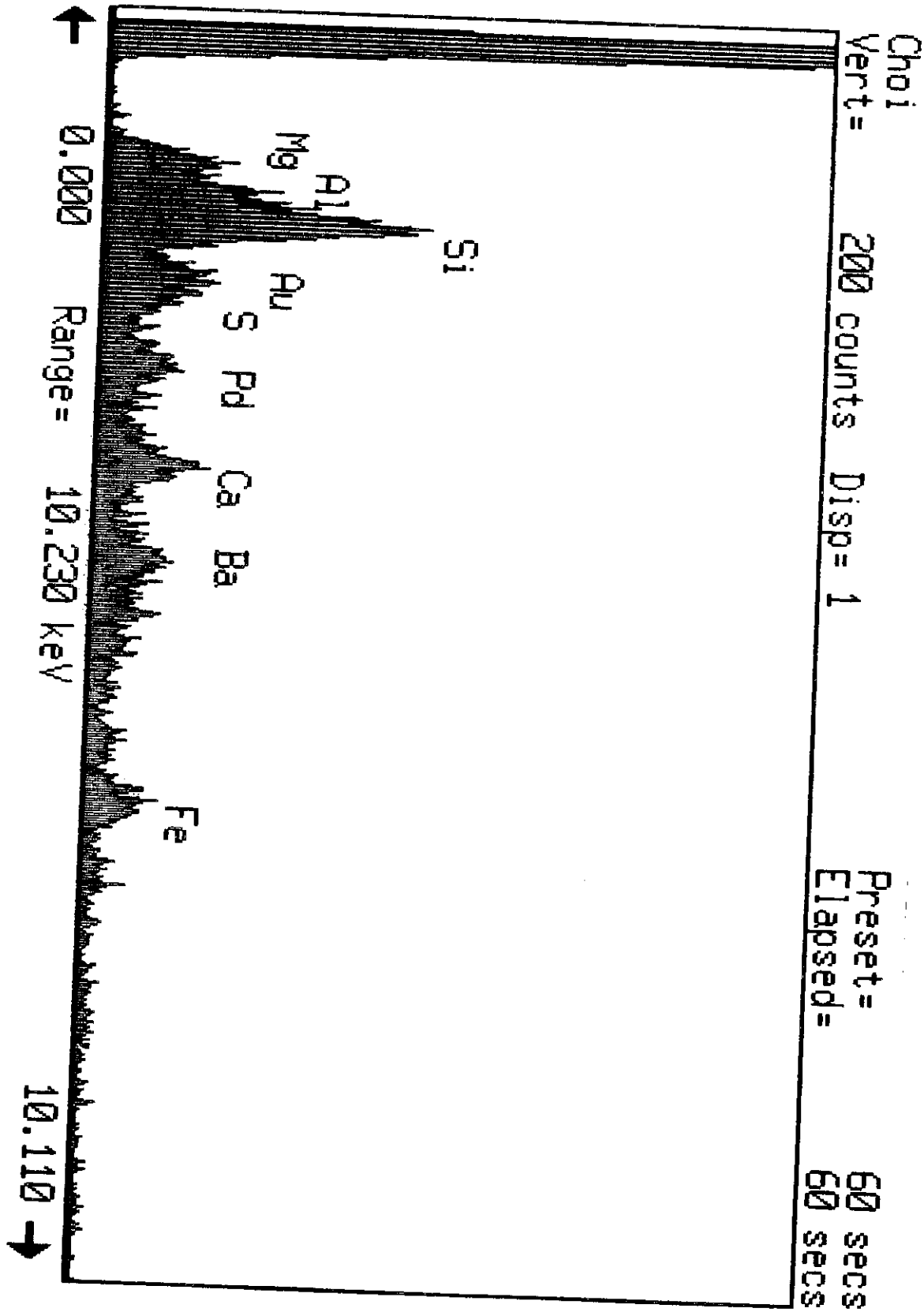

Figure 2.1.12 Effect of acidization on weight change of three cement samples

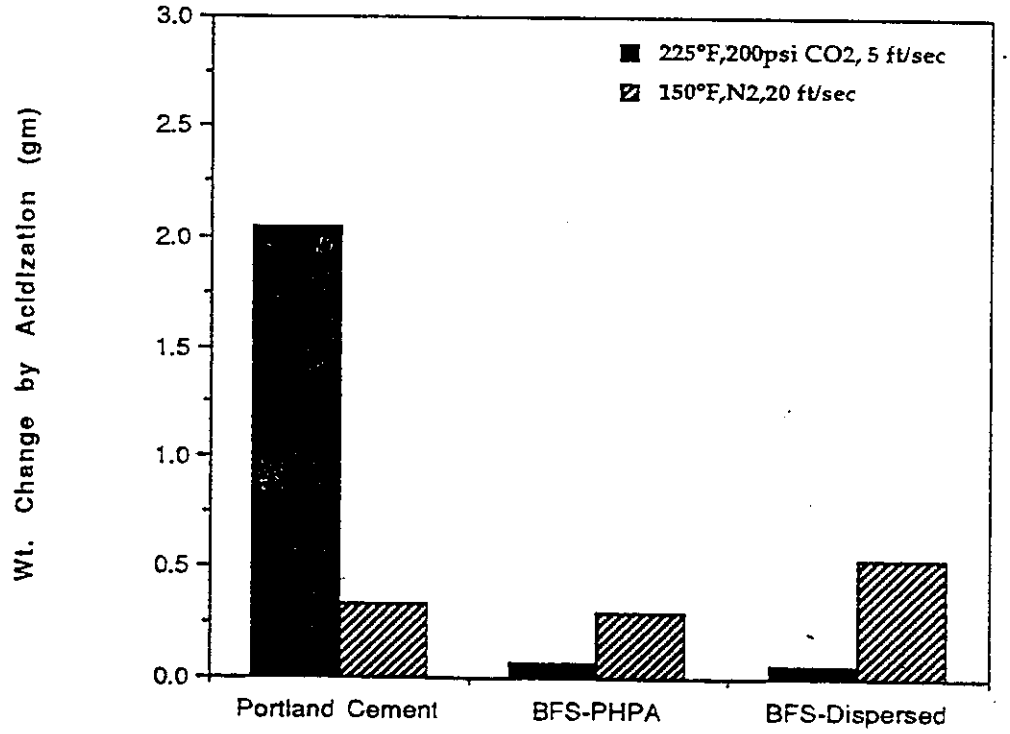

2.2 Galvanic Corrosion Between P-110 and BFS and Portland Cements

2.2.1 Summary

An electrochemical study was performed to investigate galvanic corrosion between P-110 and BFS (or Portland cement) in a stagnant 3.3% NaCl solution at 150 °F under 1 atm CO_2. BFS (1 & 2) or Portland cement coating did not promote any unacceptable galvanic corrosion to P-110 carbon steel casing at the test condition. Corrosion potential and corrosion rate measured by an electrochemical technique indicated that corrosion of coated P-110 depended upon the water intake and its corrosivity. Among the three coatings, BFS-PHPA, BFS-dispersed mud and Portland cement, all appeared to produce the same low corrosion rate.

2.2.2 Objective

The objective of this sub-project was to investigate any galvanic corrosion reactions between P-110 carbon steel casing and BFS or Portland cement under a simulated downhole condition by using an electrochemical method.

2.2.3 Experimental Procedure

2.2.3.1 Specimen Preparation

Chemical compositions of BFS-PHPA and BFS-dispersed mud are tabulated in Table 2.1.1. A disc with 5/8"-diameter and 1/8"-thickness was machined from P-110 casing. A depression with 1/2"-diameter and 1/16"-depth was made on one side. Figure 2.2.1 shows a schematic of a disc specimen for electrochemical measurements. After machining a disc was degreased with acetone, and rinsed with distilled water and dried in air. BFS or Portland cement slurry was poured into the depression and the slurry-filled side was pressed against a glass slide by using a paper clip. This assembly was placed in a heating bath at 150 °F for 1 week. Four different specimens were tested: BFS-PHPA, BFS-dispersed mud, Portland cement, and bare metal.

2.2.3.2 Test Solution

As recommended at the kick-off meeting, a 3.3% NaCl solution was selected as a test fluid. Besides Na and Cl other impurities were not detected by ICP (Inductively Coupled Plasma Spectroscopy).

2.2.3.3 Test Cell

An electrochemical glass corrosion cell with three electrodes was employed for the measurements. Figure 2.2.1 is a schematic of a galvanic corrosion monitoring cell. The cell was made of nylon to isolate the specimen from the assembly. The depression filled with BFS or Portland cement was exposed to the test solution. Corrosion rate and corrosion potential of coated P-110 were periodically monitored by an EG&G PAR 273 and AC-impedance analyzer which is driven by an IBM personal computer. The test assembly was exposed to 3.3% NaCl for more than 168 hours. During this period, CO_2 gas was gently sparged. Test temperature was 150 °F.

2.2.3.4 Test Procedure

1. A disc specimen was inserted into a nylon specimen holder which was placed in a glass electrochemical cell with 150 ml of 3.3% NaCl.

2. The glass cell was placed in a constant heating bath at 150 °F.

3. For 30 minutes the test solution was de-aerated with CO_2. CO_2 was sparged gently during a run.

4. After a run, a disc specimen was removed from a specimen holder and was photographed while in a wet state. Both Portland cement and BFS showed a strong tendency to crack if they were dried.

2.2.3.5 Data Analysis

Corrosion potential and corrosion rate (or polarization resistance) were monitored for determining the interfacial corrosion between the steel and the cements. The corrosion rate was computed by the linear polarization technique. After a run, the cross-section of a disc specimen was metallographically examined. Additionally, scanning electron microscopic examination was followed.

2.2.4 Results and Discussion

Figure 2.2.2 (a) compares corrosion potentials of P-110 discs coated with BFS-PHPA, BFS-dispersed mud or Portland cement to those of bare P-110 metal. Corrosion potential (mVs.c.e.) of the bare metal quickly reached a steady state value, -750 mVs.c.e., within one hour. In contrast, P-110 specimens coated with BFS and Portland cements took many hours to reach the steady state value of the bare metal. And it was also observed that specimens coated with BFS and Portland cement initially decreased and later approached that of the bare metal. A disc coated with BFS-PHPA showed a slower decrease in corrosion potential than BFS-dispersed mud. The Portland cement sample showed a rapid decrease in corrosion potential as low as -935 mVs.c.e. with 24 hours and then the corrosion potential rose to reach -750 mVs.c.e. after one week.

Figure 2.2.2 (b) plots corrosion rates of four samples. As expected, corrosion rate of the bare metal reached 240 mpy after 48 hours. Corrosion rates of the coated samples were much lower than that of the bare metal but increased with time.

Before being exposed to the test solution, the BFS-PHPA sample in Figure 2.2.2 (a) inadvertently experienced a slight dryness for a few minutes which promoted cracking. In order to examine the pre-cracking of the coating, another sample was prepared which was wet and free from cracking. Figure 2.2.2 (c) plots corrosion potential vs. time curves of the two samples. The corrosion potential of a sample with cracks initially decreased faster than that without cracks. Corrosion rates of the two samples were compared to that of bare P-110 in Figure 2.2.2 (d). Pre-cracking promoted a faster water intake which in turn increased the interfacial corrosion rate of P-110. But again the corrosion rate of coated P-110 with and without pre-cracks was far less than that of bare metal. Figure 2.2.3 shows photos of bare metal and coated samples before and after runs.

In short, the initial decrease in corrosion potential is attributed to the water intake through the coating. As water molecules permeated the coating, neutralization took place at the P-110 surface by the influx of dissolved carbonic acid. The steel showed relatively high pH initially but the interfacial pH decreased with time to the bulk pH, ~5.5. One important observation is that all the three coatings did not promote any unusual accelerated corrosion at the steel surface.

2.2.5 Recommendations

As this electrochemical test successfully examined the interfacial galvanic corrosion between P-110 and the three cement specimens, the following project is recommended to be continued:

° Investigate the effect of H_2S on galvanic corrosion between P-110 casing material and the three cements by an electrochemical DC and/or AC-impedance technique.

Figure 2.2.2(a) Corrosion potentials of P-110 steel coated with BFS-PHPA, BFS-dispersed mud and Portland cements compared to those of the bare metal tested in 3.3% NaCl at 150 °F under 1 atm CO_2

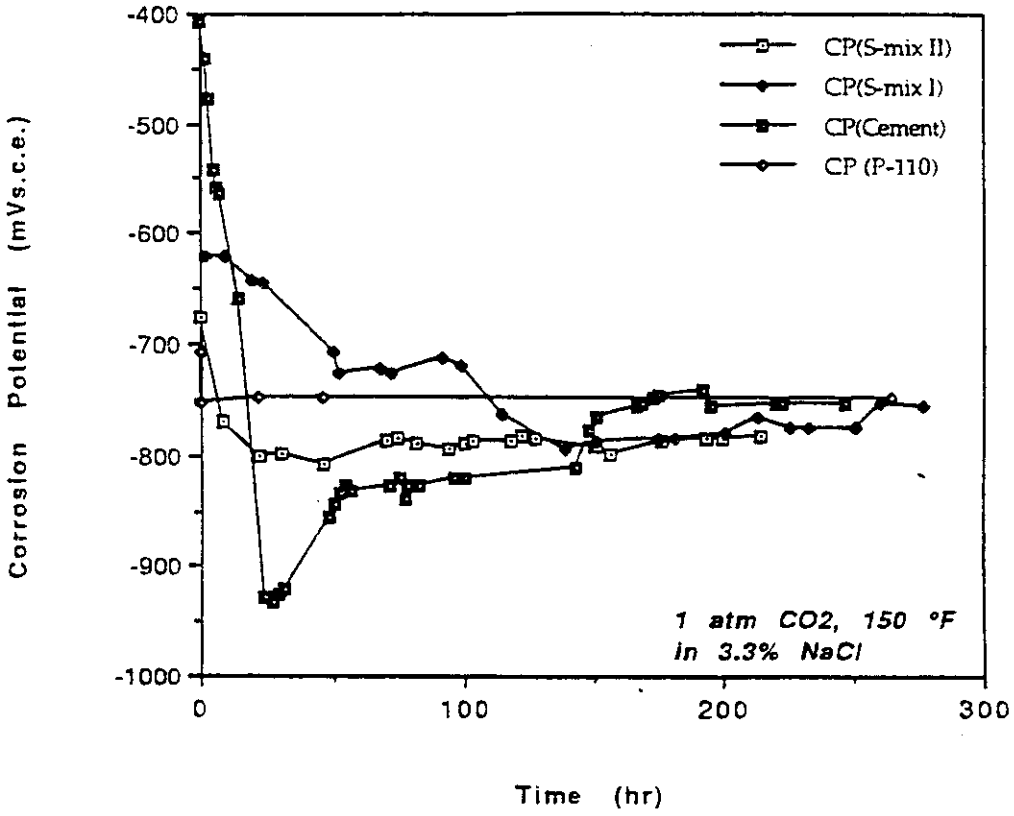

Figure 2.2.1 Schematic of an electrochemical cell

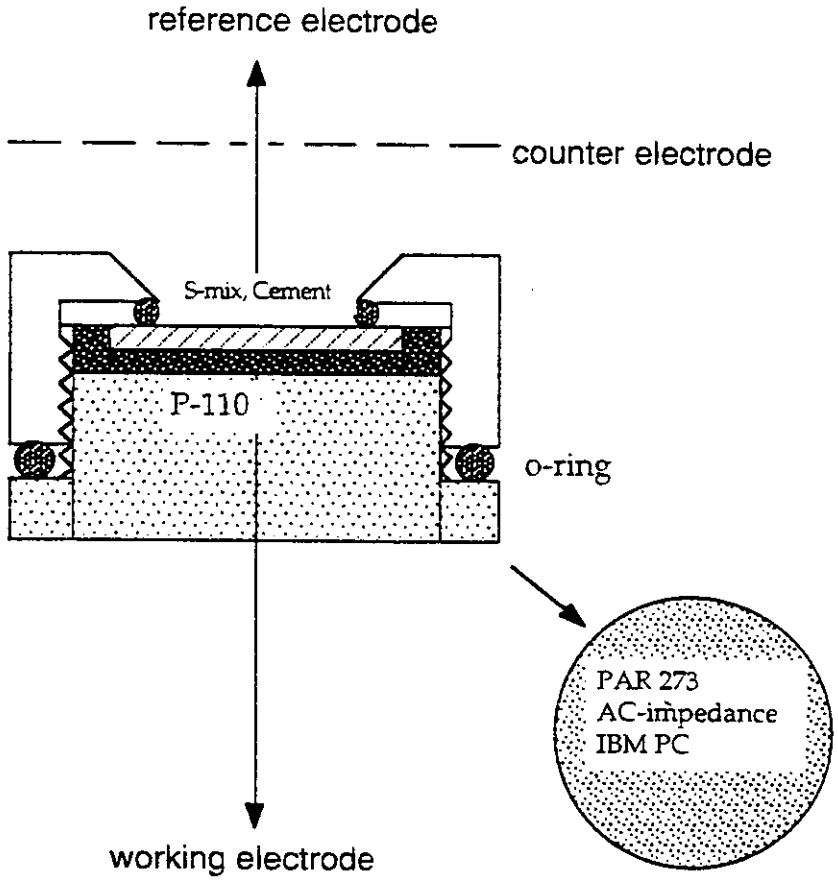

Figure 2.2.2(a) Corrosion potentials of P-110 steel coated with BFS-PHPA, BFS-dispersed mud and Portland cements compared to those of the bare metal tested in 3.3% NaCl at 150 °F under 1 atm CO_2

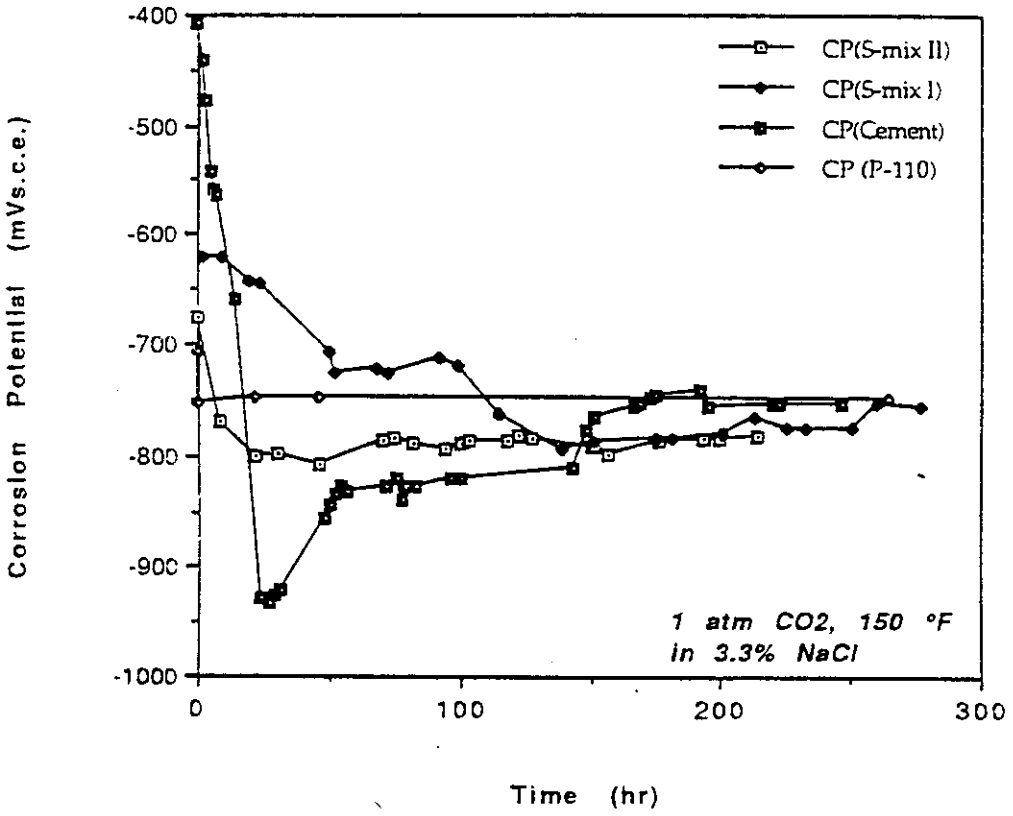

Figure 2.2.2(b) Corrosion rates of P-110 steel coated with BFS-PHPA, BFS-dispersed mud and Portland cements compared to those of the bare metal tested in 3.3% NaCl at 150 °F under 1 atm CO_2

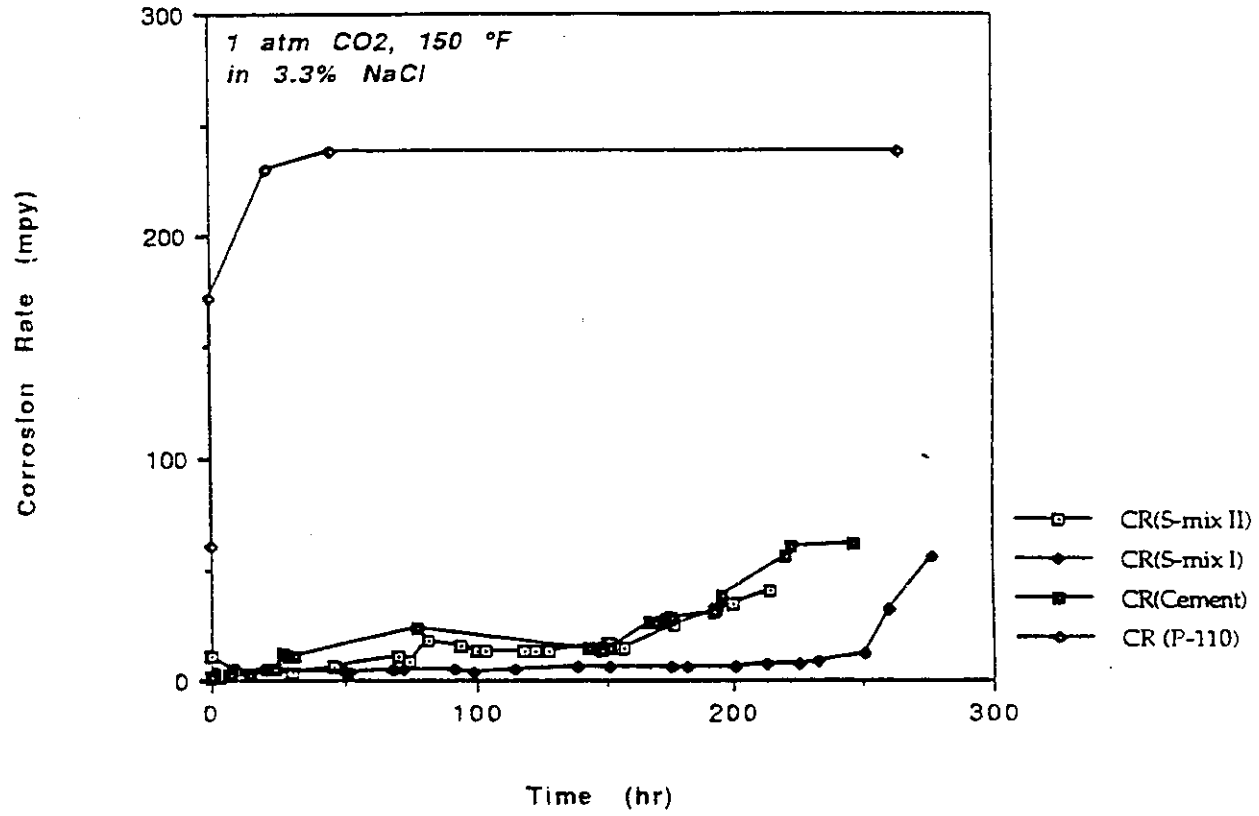

Figure 2.2.2(c) Corrosion potential of P-110 coated with BFS-PHPA that did/did not crack before having been tested in 3.3% NaCl at 150 °F

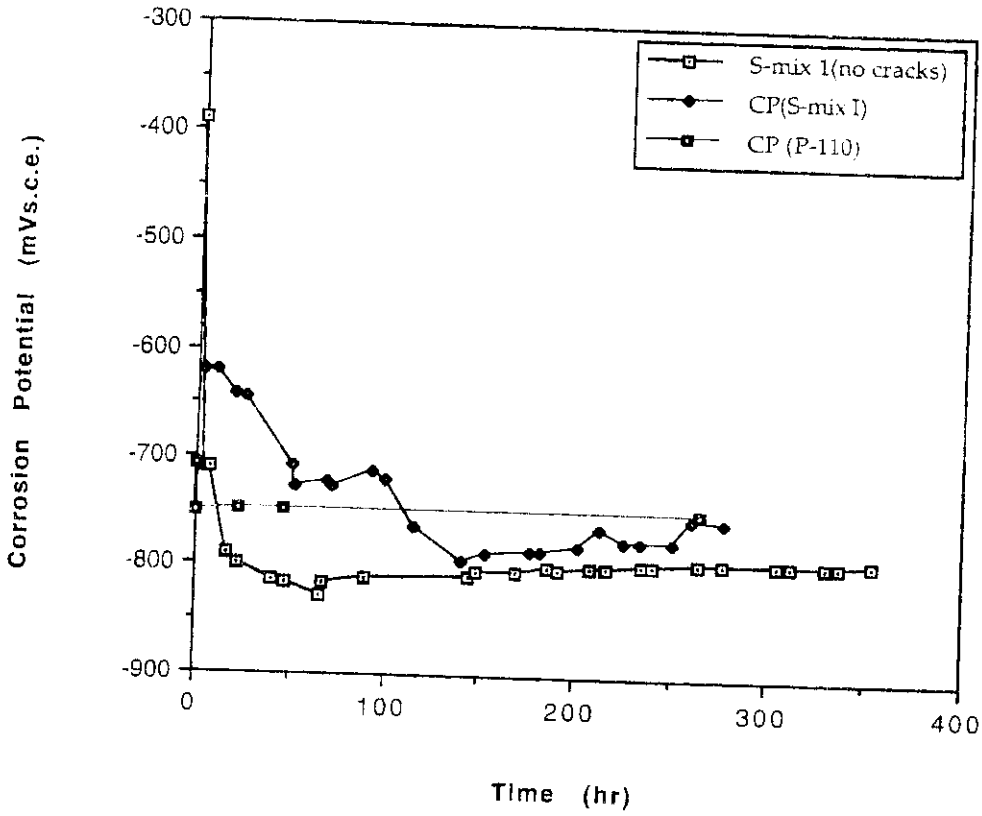

Figure 2.2.2(d) Corrosion rate of P-110 coated with BFS-PHPA that did/did not crack before having been tested in 3.3% NaCl at 150 °F under 1 atm CO2

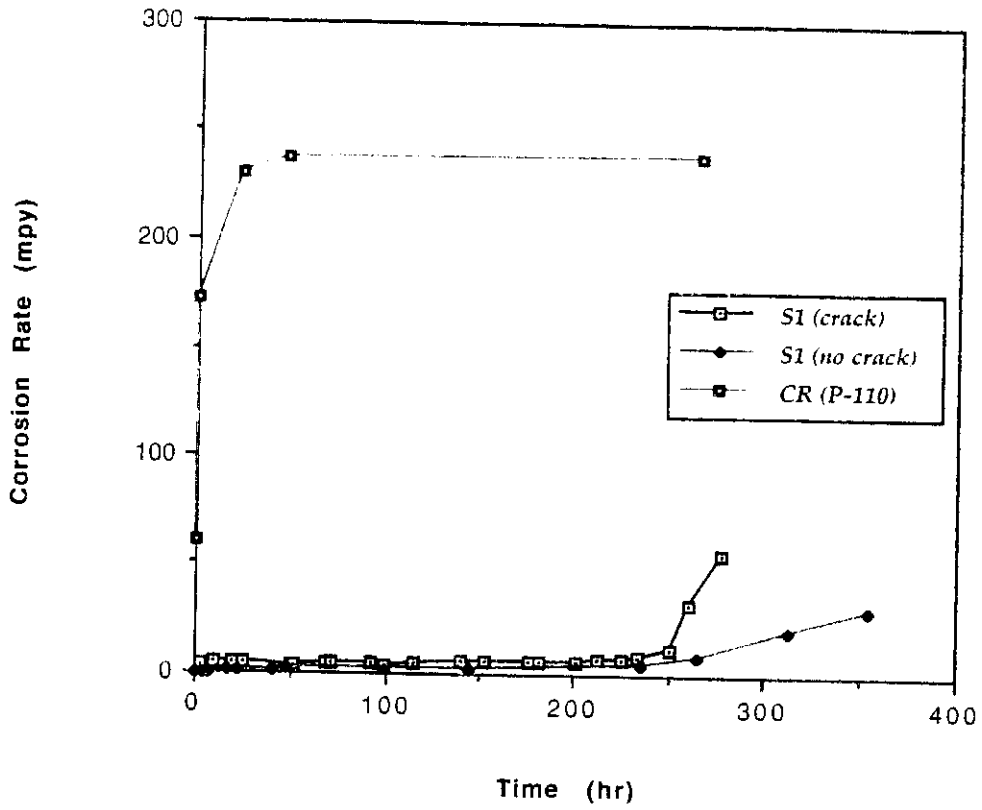

Figure 2 2.3 Disc specimens before and after test in 3.3% NaCl at 150 °F under 1 atm CO_2

(a) P-110 metal after test
(b) Portland cement coated sample before test

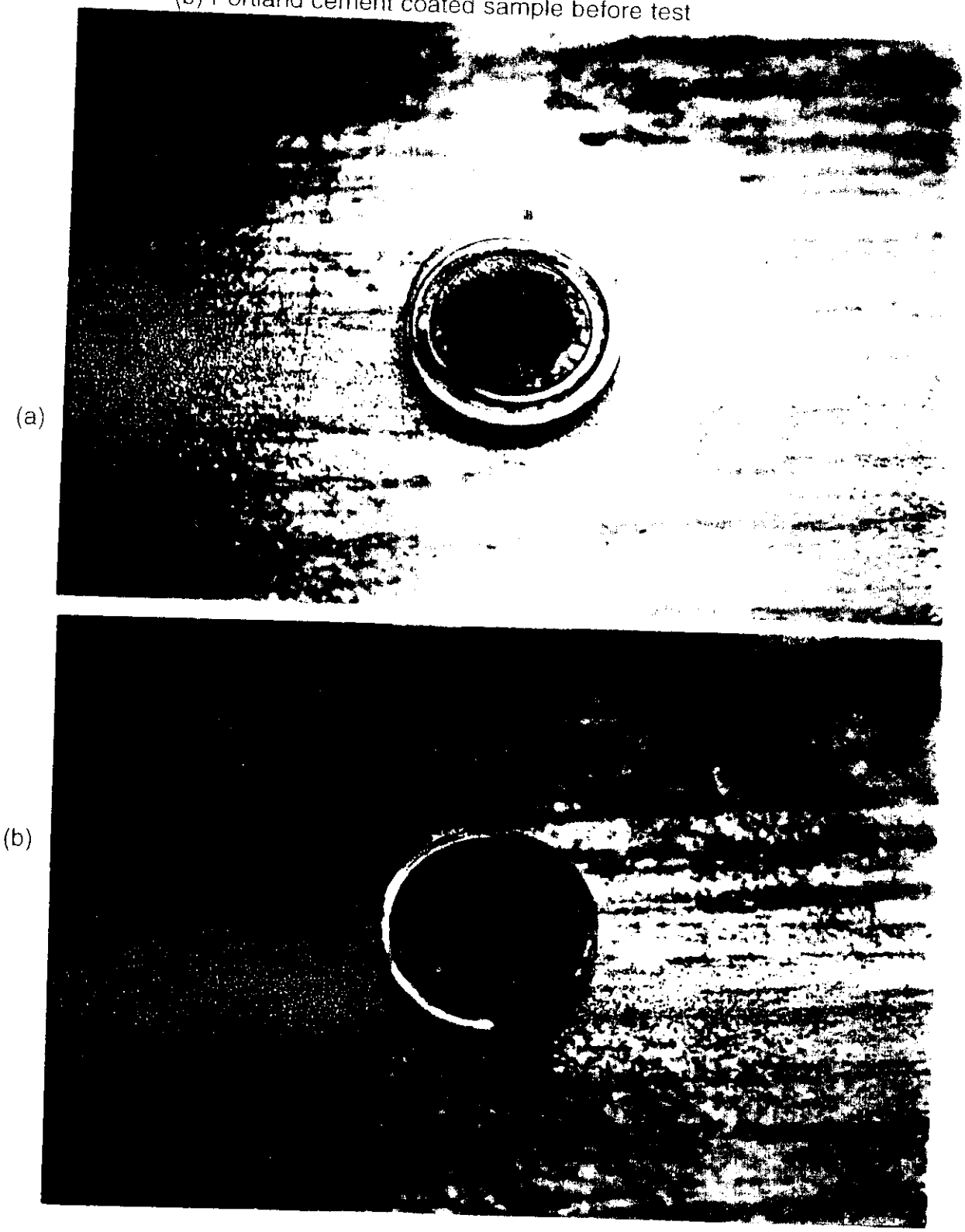

Figure 2.2.3 (Continued)

(c) Portland cement coated sample right after test
(d) Portland cement coated sample after drying (exhibiting fine cracks)

(c)

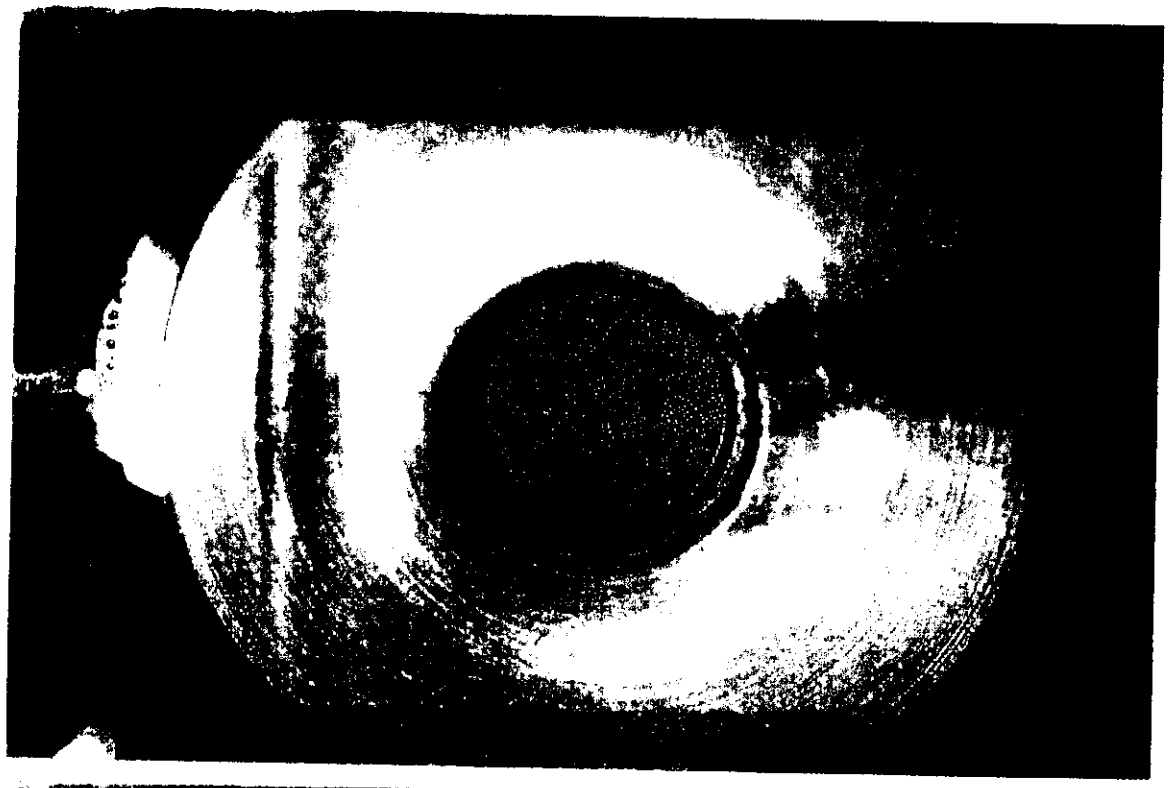

(d)

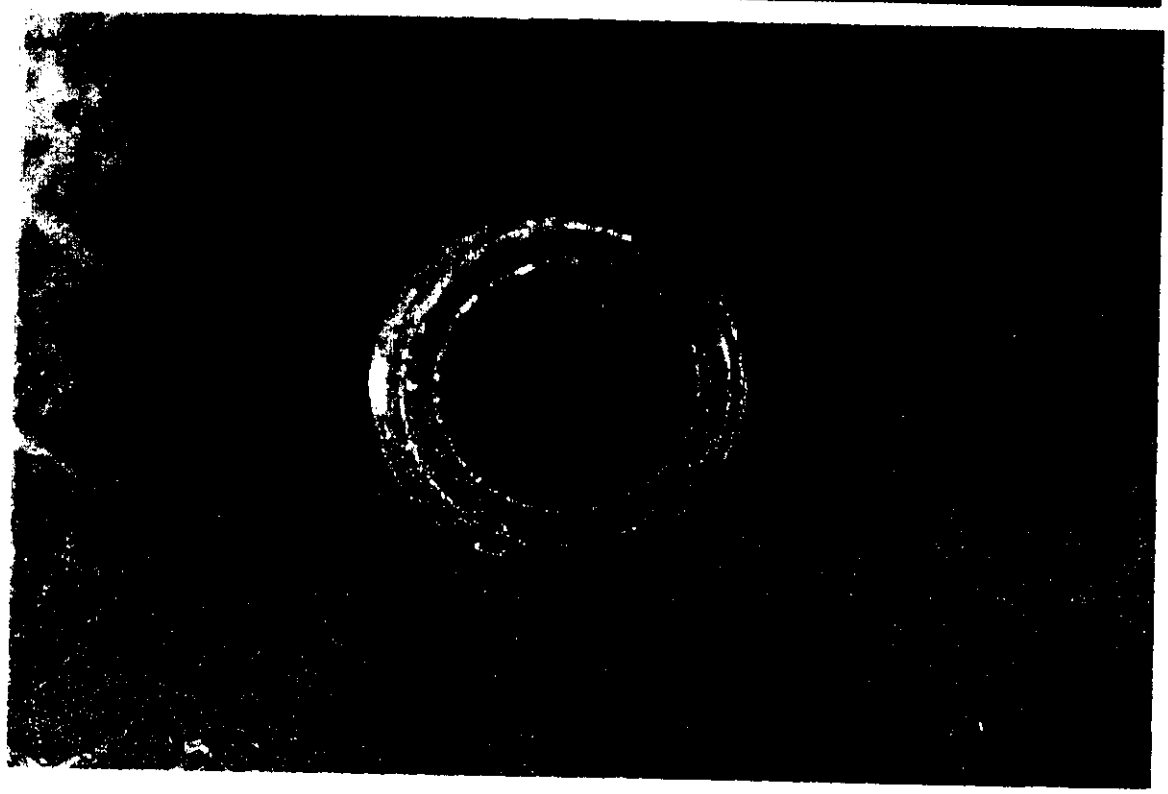

Figure 2.2.3 (Continued)

(e) BFS-PHPA coated sample (with cracks before test) before test
(f) BFS-PHPA coated sample (with cracks before test) after test

(e)

(f)

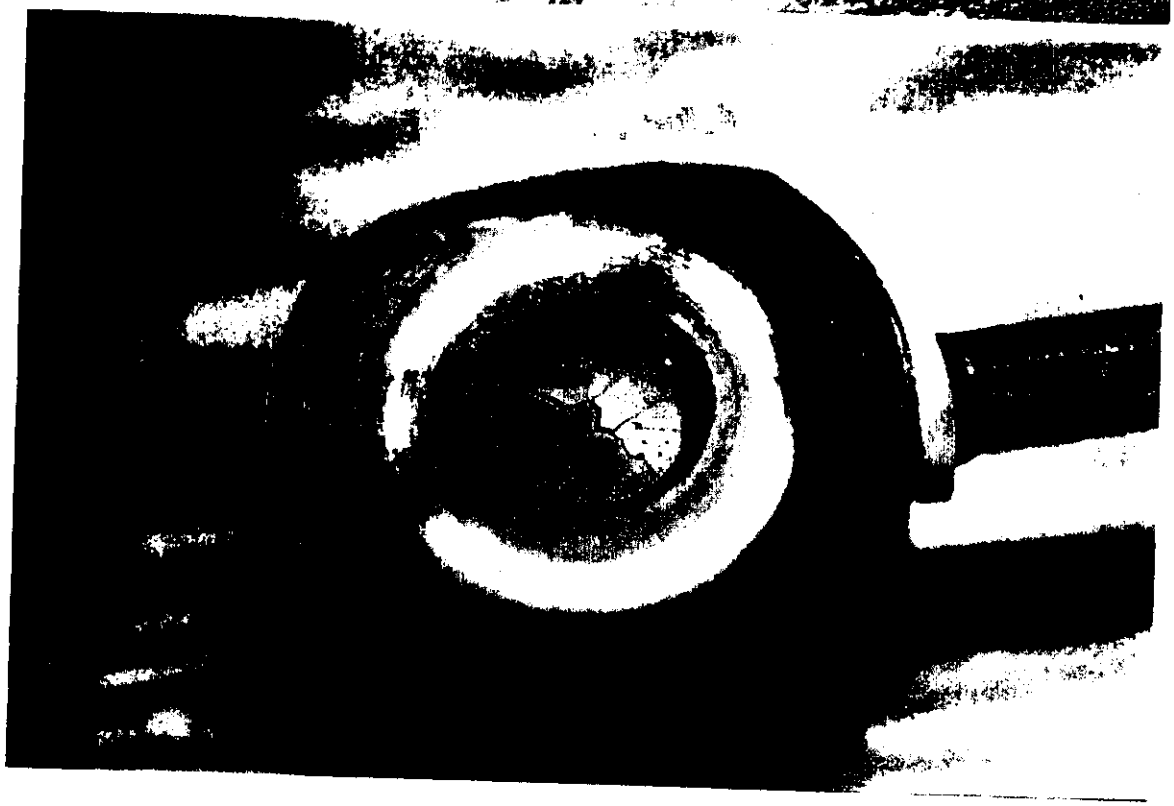

Figure 2.2.3 (Continued)

(g) BFS-PHPA coated sample (no crack before test) before test
(h) BFS-PHPA coated sample (no crack before test) after test

(g)

(h)

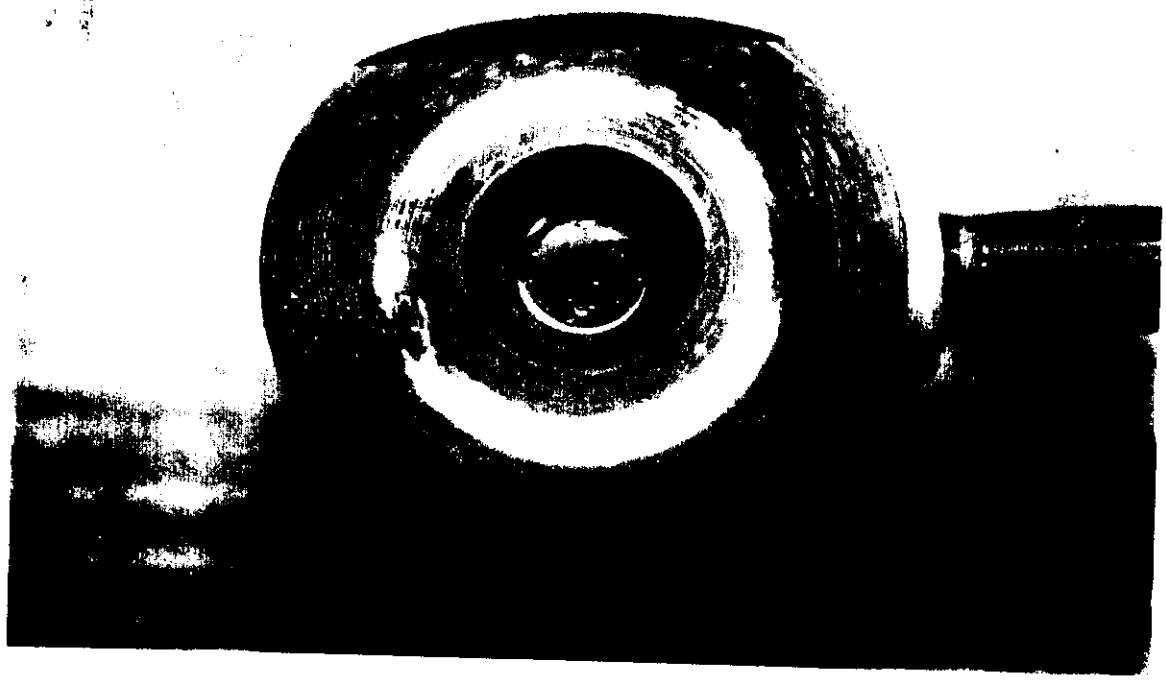

Figure 2.2.3 (Continued)

(i) BFS-dispersed mud coated sample before test
(j) BFS-dispersed mud coated sample after test

(i)

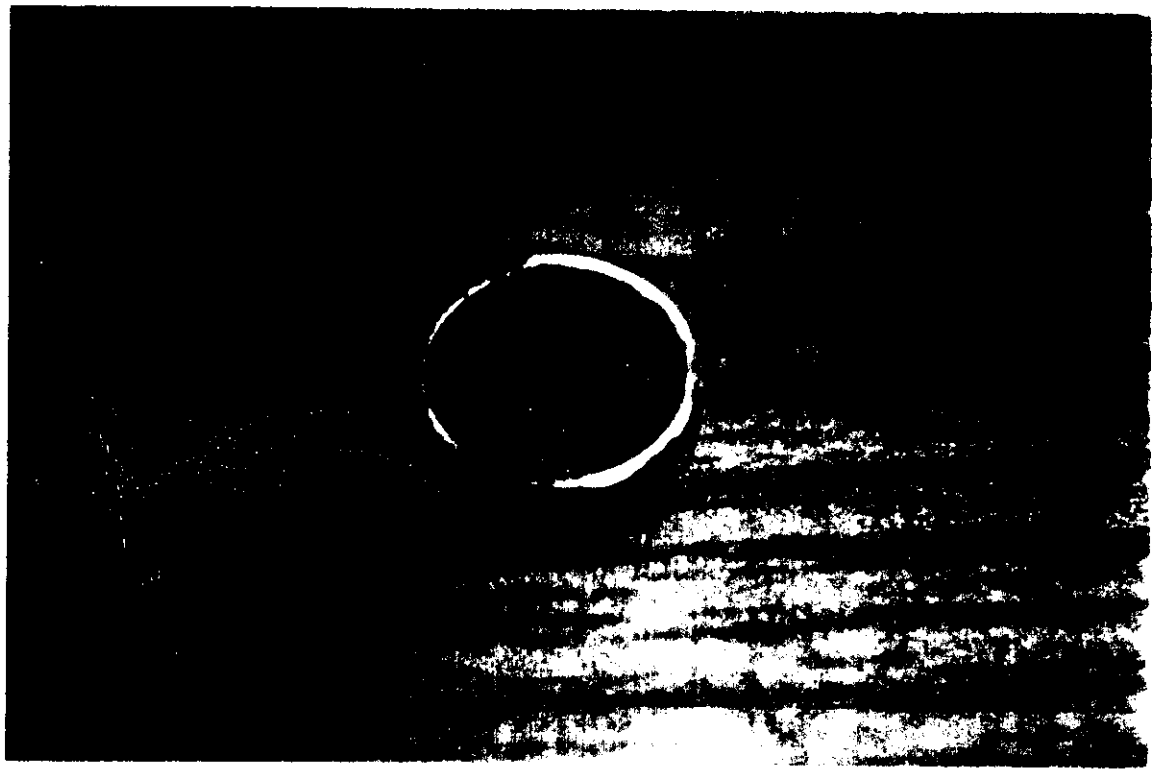

(j)

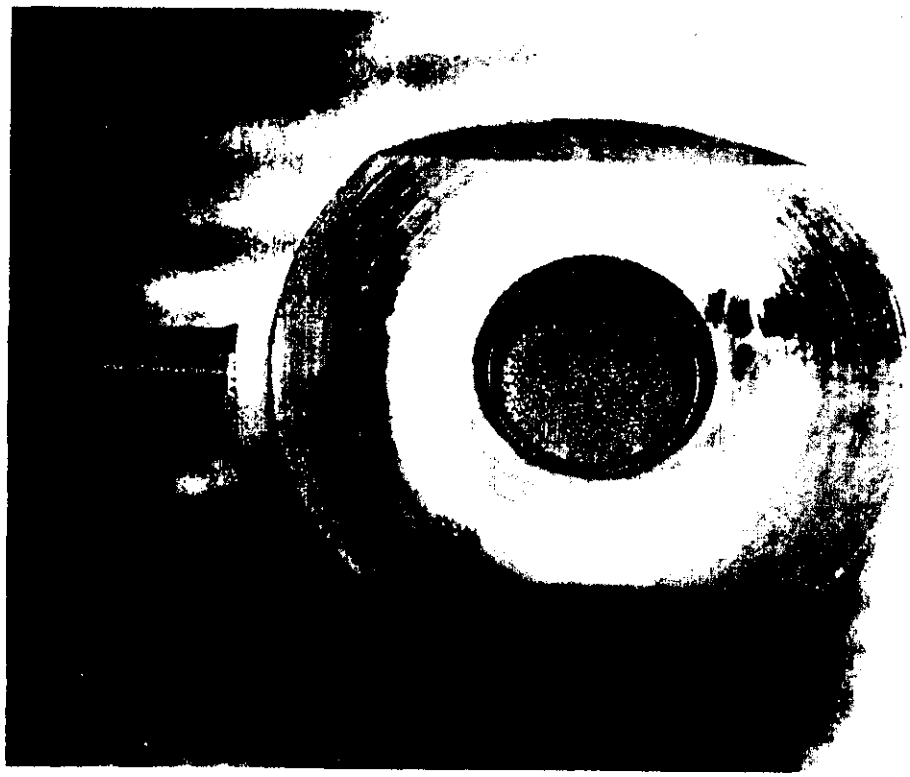

Figure 2.2 4 SEM micrographs of cross-sections of BFS-PHPA and BFS-dispersed mud coatings on P-110 steel disc tested in 3.3% NaCl at 150 °F under 1 atm CO2

(a) BFS-PHPA (x100)
(b) BFS-PHPA (x900)

(a)

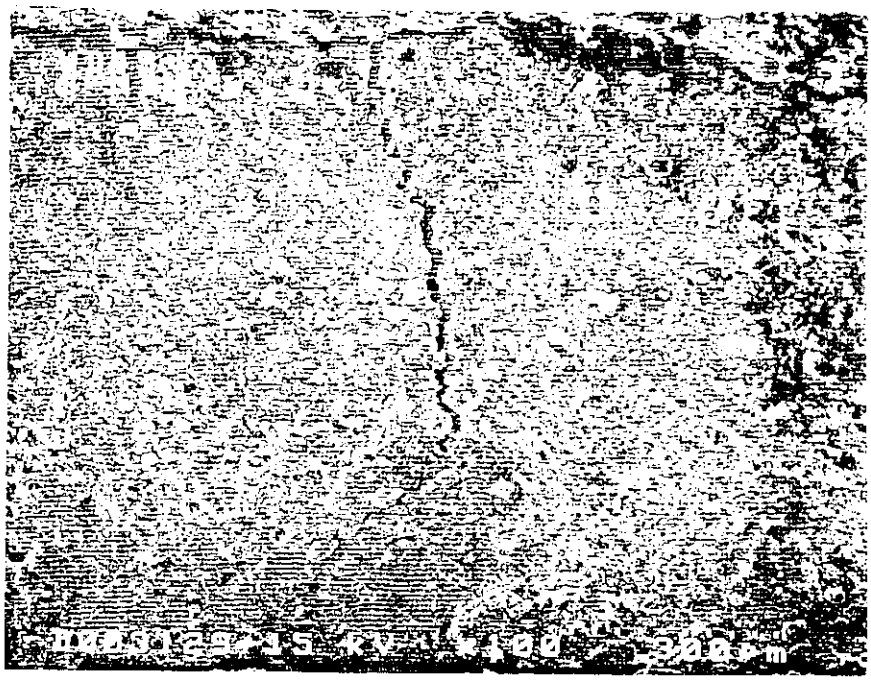

(b)

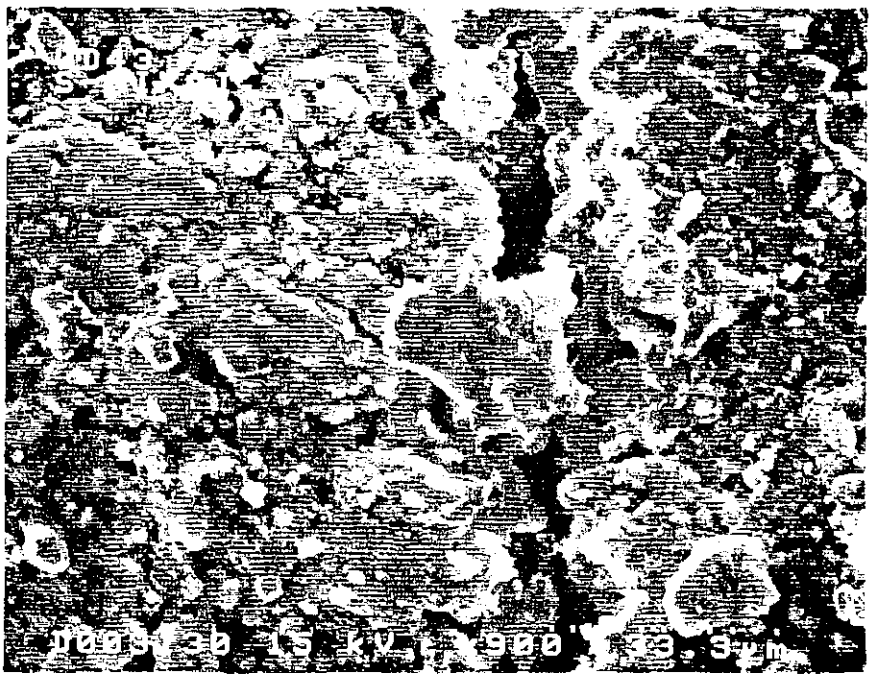

Figure 2.2.4 (Continued)

(c) BFS-dispersed mud (x100)
(d) BFS-dispersed mud (x900)

(c)

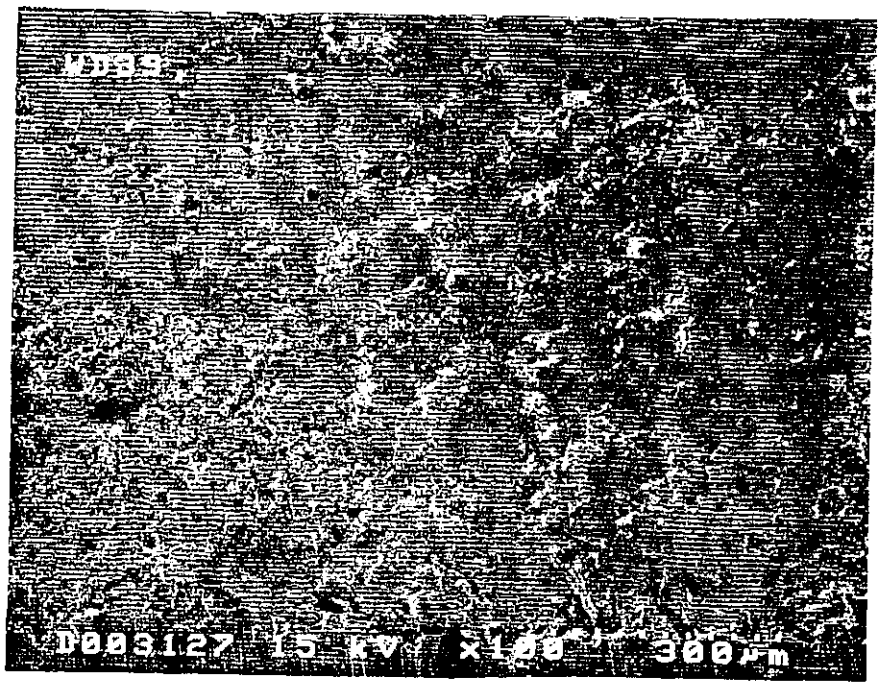

(d)

Section 3 - Dimensional Stability

3.1 Summary

Based on the BFS compositions used in these tests, both BFS and Portland class G cement mixtures exhibited similar overall hydration volume reductions (HVR) of 4%-6% when in continual contact with water. The magnitude of the HVR's were found to be slightly lower at higher pressure. However, when normalizing the HVR to the volume percentage of slag (26% in the BFS system) and cement (41% in the Portland cement system) in each system, the BFS showed a HVR of approximately 1.5 times that of Portland cement.

Matrix permeability of the two systems were both very low, however, BFS was two orders lower than Portland cement. Attempts to independently measure the bulk and internal volume reductions were frustrated by unidentified interactions between the three chambers of the slurry test vessel.

3.2 Objectives

The dimensional stability of Blast Furnace Slag (BFS) as compared with Portland cement is investigated in this part of the study. Of interest is whether the BFS can establish a barrier to gas migration before final set. These tests complement the helium migration tests by attempting to measure the bulk and internal volume reductions independently.

The objectives of these tests are:

(a) measure the bulk and internal volume reductions of two BFS mixtures and Portland cement at reservoir temperature;
(b) determine the residual porosity and permeability;
(c) measure the hydration volume reduction under conditions of "free" water uptake.

3.3 Experimental Procedures

3.3.1 Cement and BFS Formulations

Three cement systems were tested: (1) Portland cement; (2) BFS with dispersed mud; (3) BFS with PHPA mud. These systems were prepared by Timothy Edwards for all of the tests. The procedures and recipes for these cement systems are discussed in Section 1.3.1.

3.3.2 "Free" Water Uptake Tests / Hydration Volume Reduction

The overall hydration volume change of each cement mixture was investigated by measuring the change in volume of an Isco pump reservoir operated in a constant pressure mode. Water remained in direct contact with the slurry through out hydration and final set phases. The change in pump volume represents the combined effects of the slurry bulk and internal volume changes, water uptake, and water expulsion.

The change in volume of the slurry is equal to the change in volume of the pump minus apparent changes in volume due to temperature changes. The change in slurry volume can be expressed as:

$$\Delta V_S = \Delta V_p - \alpha \Delta T \qquad (1)$$

where Vs is the slurry bulk volume, Vp is the volume of the pump reservoir, T is temperature, and α is an isobaric thermal expansion coefficient of water. α was determined experimentally by heating the water in the confinement chamber while maintaining constant pressure. The change in pump reservoir volume with change in temperature was recorded. This test exhibited linear behavior and the slope represents the α coefficient. The data for this calibration is located in the Appendix. The negative sign in equation. (1) compensates for the apparent increase in volume, ΔVp, due to increasing temperature. This calibration was necessary because in all these tests the slurries had been prepared at room temperature and then heated to 160 °F. Also, the water was heated slightly during hydration of the slurry. Approximately two hours were needed to raise each slurry to test temperature.

The apparatus for these tests is illustrated in Figure 3.1. The apparatus is comprised of a stainless steel container for the slurries with a test tube mounted in the slurry, a containment vessel for applying pressure to the slurry, two temperature probes, and Isco flow pump.

The function of the Isco pump was maintenance of constant hydrostatic pressure within the containment vessel while monitoring the reservoir volume. The pump was programmed to operate in constant pressure mode. As the slurry contracts or expands, it causes the pump pressure to drop or increase. In response, the pump pushes or withdraws fluid as necessary to maintain constant pressure. The pump was tested early on to verify that a given volume of fluid removed from the vessel was compensated by an equal volume of fluid added by the pump. Results of these tests showed that the pump responded to changes in volume on the order of 0.01 cc.

Each test was performed by the following sequence of steps:

a) 143 cc of slurry were poured into a stainless steel container; air bubbles were removed by gently stirring;
b) a test tube and thermocouple were placed into the slurry;
c) the container was placed into the pre-heated containment vessel;
d) the containment vessel was filled with water and pre-heated;
e) the top of the containment vessel was bolted shut and connected to the Isco pump; pressure was set to 30 or 3000 psi;
f) this system was heated to 160 °F while maintaining constant pressure;
g) pressure, temperature (two probes), and pump volume were recorded during the course of the test; data was recorded every 30 seconds;
h) data acquisition was automated by computer using National Instrument's LabView software.

Tests lasted 20 - 30 hours.

Calibrations

The thermocouples used in these tests had to be calibrated to the same temperature. This was accomplished by comparing them to a thermometer reading. All three devices were placed into a water bath and heated. Thermocouple temperature vs. thermometer value were plotted. A linear regression of the data was used to correct the thermocouples to thermometer temperature. This data is presented in the Appendix.

3.3.3 Bulk and Internal Volume Reduction Tests

Theory of Operation

A tri-chamber slurry cell was designed and constructed to independently measure the bulk and internal volume reductions and / or expansions. Figure 3.2 illustrates the components of the cell and test apparatus. The apparatus could be operated as shown in the figure or inverted with the lower chamber containing the helium. In most of the tests the lower chamber contained helium and was separated from the middle chamber by a porous metal plate. Filter paper was placed between the slurry and the porous plate. The middle chamber contained the test slurry, and the upper chamber contained water. The middle and upper chambers were separated by an elastic nonporous latex membrane. Ports in all three chambers allowed for pressure and temperature to be independently recorded. The water chamber was connected to the Isco pump that applied pressure to the slurry. In these tests, the slurries were isolated from water uptake.

The Isco pump volume was used to measure the bulk volume change. The theory of operation is identical to that discussed in the previous section. Equation (1) was used to calculate the bulk volume change of the slurry.

The internal volume change was determined by measuring the pressure drop in the helium. Helium was used because it is an inert gas that should closely exhibit ideal gas behavior. A porous metal plate and filter paper, separating the lower and middle chambers, acted as a semi-permeable barrier that allowed helium to enter the slurry, but kept the slurry from entering the lower chamber. Internal volume changes were calculated from the ideal gas law:

$$PV = nRT \qquad (2)$$

where P is absolute pressure, V is volume, n is the number of moles of gas, T is temperature in degrees K, and R is the gas constant. It was assumed that the expansion of helium into the slurry would occur slow enough to be considered an isothermal process. This is not strictly true since external factors caused the temperature in the helium to vary through out the tests. Thus, a pseudo-isothermal expression was derived which compensated for temperature. The internal volume reduction of the slurry was inferred from the change in helium pressure alone.

As connected void space is created, helium is free to fill the space. This "free" expansion results in a pressure drop measured in the helium chamber. Given that $P_iV_i = P_fV_f$, the fractional change in volume of the slurry can be calculated:

$$\Delta V/V_i = -\Delta P/P_f = -(P'_f - P_o)/P'_f \qquad (3)$$

where subscripts "i" and "f" refer to the initial and final values, respectively. P'_f is the pressure of the helium after correction for temperature changes. The change in helium volume was calculated by multiplying Equation (3) by the initial helium volume, V_i, which was the volume of the helium chamber (271 cc). The change in helium volume was equated to the change in the internal volume of the slurry. The percent change in slurry internal volume was calculated by dividing the internal volume change by slurry volume (530 cc).

Helium pressure was maintained at equal or slightly below the water pressure. This was done to keep the helium pressure from interacting with the Isco pump. The method used to correct the measured helium pressure for temperature changes is discussed in the next section.

Calibrations

A series of calibrations had to be performed to compensate for temperature changes. The isobaric volume expansion of the upper water chamber was determined first. The volume-temperature curve (see Appendix) was fit to a second-order polynomial.

$$V_a = a_1 + a_2T + a_3T^2 \quad (4)$$

$$\Delta V_a = a_2(T_f - T_i) + a_3(T_f^2 - T_i^2) \quad (5)$$

where ΔV_a is the change in pump volume required to maintain constant pressure. This correction was subtracted from the measured change in pump volume, ΔV_p, during the course of a test.

$$\Delta V_{net} = \Delta V_p - \Delta V_a \quad (6)$$

The second calibration measured the change in helium pressure with temperature at constant volume. The sources of temperature change were the oven temperature and the heat liberated during hydration of the slurry. A thermocouple probe was mounted inside the helium chamber to measure helium temperature. Helium pressure, P_g, vs. temperature was measured and a linear regression performed on the data.

$$P_g = a_1 + a_2T \quad (7)$$

or

$$\Delta P_g = a_2\Delta T \quad (8)$$

Equation (8) was used to correct the measured helium pressure, P_m, at temperature, T, back to the pressure that the helium would have had (P_g') at some arbitrary initial temperature, T_o.

$$P_f' = P_m(T) - a_2(T - T_o) \quad (9)$$

The fractional change in volume in Equation (3) is then calculated using P_f'. This resulted in the expression:

$$\Delta V/V_o = P_o/P_f' - 1 \quad (10)$$

The choice of initial temperature and pressure is arbitrary, but it was chosen at a point where the temperatures of the helium, water, and slurry were close to the test temperature and before the start of the heat of hydration phase.

Procedures

The slurries were prepared with a retarder that postponed the chemical reactions for approximately three hours. This allowed sufficient time to transfer the slurry to the chamber, assemble the tri-chamber cell, and heat it to test temperature (150 °F). These tests were performed at one of two pressures: 30 psi; 1000 psi. The pressures in the helium and slurry were stepped up together.

It should be noted that most of the tests were conducted with the apparatus inverted with respect to the diagram in Figure 3.2, so that the upper chamber was filled with water and the lower chamber filled with helium. This was done to eliminate the contribution of the weight of the slurry on the water pressure.

While heating to test temperature, the helium was constantly "bled" from the chamber in order to keep the pressure slightly lower than the water pressure in the upper chamber. This was necessary to ensure that the Isco pump reacted only to bulk changes in slurry volume, and not to pressure generated by the helium. Once the temperature in the helium reached within 10 °C of the test temperature, it was isolated (held at constant molarity) and the pressure recorded. The choice of initial conditions for calculating the change in internal volume were taken after the chamber was isolated. Temperatures and pressures in all three chambers were recorded to an EXCEL file every 30 seconds. Because of technical difficulties, the helium temperature did not get recorded until the last test #13. The water bath temperature was used to correct for temperature effects in the helium chamber, since it was found that the temperatures in these two chambers closely followed each other.

The tests were allowed to proceed for up to thirty hours or more. Afterwards, the tri-cell was disassembled. A CT scan of slurry chamber was performed. One inch diameter plugs were drilled from the cement and porosity and water permeability measured.

3.4 RESULTS

3.4.1 "Free" Water Uptake Tests / Hydration Volume Reduction

Below are the narratives of each test.

Test #1:

Portland class G cement with 1% D160 additive. Water bath pressure equaled 30 psi. Test ambient temperature equaled 70 °C or 158 °F. The slurry and water bath temperatures, and % change in pump volume are shown in Figure 3.3. Test lasted approximately 45 hours. Twenty minutes elapsed between sample preparation and the start of data recording. Overall reduction in volume was 6.4%.

Test #2:

Portland class G cement with D160 additive. Water bath pressure equaled 3000 psi. Test ambient temperature equaled 70 °C or 158 °F. The slurry and water bath temperatures, and % change in pump volume are shown in Figure 3.4. The test lasted approimately 25 hours. Twenty-five minutes elapsed between sample preparation and the start of data recording. Overall reduction in volume was 4%.

Test #3:

Portland class G cement with D160 additive. Water bath pressure equaled 30 psi. Slurry was de-aerated for 2 minutes. Ambient test temperature equaled 70.5 °C or 159 °F. Slurry and water bath temperatures, and % change in pump volume are shown in Figure 3.5. The test lasted approximately 41 hours. Sixteen minutes elapsed between sample preparation and the start of data recording. Overall reduction in volume was 5%.

Test #4:

BFS with dispersed mud. Water bath pressure equaled 30 psi. Ambient test temperature equaled 71 °C or 160 °F. Figure 3.6 shows the slurry and water bath temperatures, and % change in pump volume over the course of the test. The test lasted 90 hours. Overall reduction in volume was 5.6%

Test #5:

BFS with dispersed mud. Water bath pressure equaled 3000 psi. Ambient test temperature equaled 71 °C or 160 °F. The slurry and water temperatures, and % change in pump volume are shown in Figure 3.7. The test lasted approximately 27 hours. Overall reduction in volume was 5%.

Test #6:

BFS with dispersed mud. Water bath pressure equaled 30 psi. Ambient test temperature equaled approximately 159 °F. Figure 3.8 shows the slurry and water temperatures, and % change in volume vs. time. The test lasted approximately 90 hours. Overall reduction in volume was 6%.

Test #7:

BFS with PHPA mud. Water bath pressure equaled 30 psi. Ambient test temperature equaled 71 °C or 160 °F. Water and slurry temperatures, and % change in volume vs. time are shown in Figure 3.9. Test lasted approximately 48 hours. Overall reduction in volume was 4.4%.

Test #8:

BFS with PHPA mud. Water bath pressure equaled 3000 psi. Ambient test temperature equaled 71 °C or 160 °F. Figure 3.10 shows the water and slurry temperatures, and % change in volume vs. time. Test lasted approximately 45 hours. Overall reduction in volume was 2.8%.

Discussion

Casual inspection of the results from the above tests seem to suggest that the hydration volume reductions in BFS and Portland cement closely agree. However, consideration of the volume percentage of the active components in BFS (the slag) and Portland (the cement) reveals that BFS actually exhibits nearly 1.5 times the HVR compared to Portland cement.

In tests using the BFS, 119.9 cc of slag was added to 350 cc (one lab barrel) of mud. The volume percent of slag for this mixture was 26%. In tests using Portland Class G cement, 3.6 gallons (1 sack) of cement were added to 5.27 gallons of water resulting in a cement volume percentage of 41%. This argument shows that the HVR per unit volume of active component is nearly 1.5 times greater in the BFS mixtures than in the Portland cement. The total hydration volume reduction of the slurry systems will depend on the cement and slag concentration.

3.4.2 Bulk Volume and Internal Volume Stability

Test #9:

BFS with PHPA. Initial pressures in the helium, slurry, and water chambers was 30 psi. Data recording began 20 minutes after sample preparation. This was the only test where the water chamber was below the slurry chamber. Pump volume had backed-off completely after 540 minutes into the test. Pressures in all chambers increased during this time. Upon disassembly, it was noticed that no water had leaked into slurry chamber.

Results of this test is shown in Figures 3.11 and 3.12. Figure 3.11 displays the complete time record for the temperatures, pressures, and volumes. Figure 3.11a is an expanded time record for the temperatures and volumes during the heat of hydration phase. On this figure, the start, peak, and final points of the heat of hydration are designated with "A", "B", and "C", respectively. Figure 3.12 displays the time record for changes in pump and helium volumes.

This test may have been driven by the creation of gas within the slurry chamber, possibly H_2. The evidence for this is the continual increase in pump, slurry, and helium pressures throughout the test. This apparent pressure build-up caused the Isco pump to back-off until it was completely full (at t = 500 min.). After the apparatus was disassembled, it was noticed that a few small areas on the flanges that connect the upper and middle chambers showed signs of oxidation. This suggested that the slurry may have reacted at these sites. After this test, all the chambers' internal and external surfaces were coated with Teflon. This was found effective in eliminating the reaction of the slurries in the remaining tests.

Test #10:

BFS with PHPA. Initial water chamber pressure was 30 psi. Data recording began 20 minutes after sample preparation. Water chamber was positioned over slurry chamber with helium chamber at the bottom. Filter paper is placed between porous metal disk and slurry. During initial heating, the helium pressure bled to maintain a constant 30 psi pressure. Once the system reached test temperature, the helium chamber was isolated and the pressure allowed to vary.

At completion of test, approximately 100 cc of an unidentified fluid was discovered in the helium chamber. A fluid specimen was saved. The upper chamber was found not to be leaking. The cement sample slid easily from the chamber. The sample was CT scanned. The liquid permeability of a 1.7" long, 1" diameter plug equaled 2.9×10^{-6} md.

Results of this test is shown in Figures 3.13 and 3.14. Figure 3.13 displays the complete time record for the temperatures, pressures, and volumes. Figure 3.13a is an expanded time record for the temperatures and volumes during the heat of hydration phase. On this figure, the start, peak, and final points of the heat of hydration are designated with "A", "B", and "C", respectively. Figure 3.14 displays the time record for changes in pump and helium volumes.

The pump, again, backed-off completely within 120-150 minutes of the test. Once the pump is completely full, it can no longer maintain a constant pressure on the slurry and follow the change in slurry bulk volume. Unlike the previous test, the cement and gas pressures went through increasing and decreasing cycles and tracked each other throughout the test. At t= 600 minutes the pump began adding fluid because the pump pressure dropped to 30 psi. Most of the dynamic behavior observed in the helium and slurry pressures occurred during the time when the temperature was constant, thus eliminating temperature as the cause for these effects. This test suggests that internal void space may have been created in the slurry until approximately t = 1600 minutes. Afterwards, the void space seemed to have been filled as the helium pressure continuously increased to its initial value.

Test #11:

Portland Class G cement. Data collection began 20 minutes after sample preparation. Pump pressure was set to 30 psi. Water chamber was located above the slurry chamber. The test was conducted similar to test #10.

At the conclusion of the test, 3 cc of unidentified liquid was discovered in the helium chamber. All the fluid was recovered and saved. The cement adhered to the chamber surface. The sample was CT scanned. A 1" diameter by 1.7" long plug from the cement was drilled using water and tested for liquid permeability. The liquid permeability equaled 9×10^{-4} md.

Results of this test is shown in Figures 3.15 and 3.16. Figure 3.15 displays the complete time record for the temperatures, pressures, and volumes. Figure 3.15a is an expanded time record for the temperatures and volumes during the heat of hydration phase. On this figure, the start, peak, and final points of the heat of hydration are designated with "A", "B", and "C", respectively. Figure 3.16 displays the time record for changes in pump and helium volumes.

For a short time, early in the test, the pump had completely backed-off. At t=250 minutes, the pump begins to add water in response to the decrease in slurry pressure. The behavior of the bulk and internal volumes were similar, but less dynamic, compared to the previous test. The helium and slurry pressures tracked each other through out the test. The apparent equilibration of the bulk volume at t = 2000 minutes is due to the fact that the pump volume was full. From the slow but continual increase in slurry pressure from t= 2000 minutes to the end of the test, it appears that the bulk volume may have gone through a slight expansion. Overall, there seems to have been a small increase in both the bulk and internal volumes.

Test #12:

BFS with dispersed mud. Pump pressure was set to 30 psi. Data collection began 20 minutes after sample preparation. The water chamber was located above the slurry chamber. This test developed a leak past the slurry pressure transducer at t=1800 minutes.

At the conclusion of the test, 2 cc of unidentified fluid was recovered in the lower helium chamber. The sample adhered to the chamber wall. It was CT scanned. The liquid permeability of a 1" diameter, 1.55" long plug drilled from the sample equaled 2.8×10^{-6} md.

Results of this test is shown in Figures 3.17 and 3.18. Figure 3.17 displays the complete time record for the temperatures, pressures, and volumes. Figure 3.17a is an expanded time record for the temperatures and volumes during the heat of hydration phase. On this figure, the start, peak, and final points of the heat of hydration are designated with "A", "B", and "C", respectively. Figure 3.18 displays the time record for changes in pump and helium volumes.

This was one test where the Isco pump was able to control the pressure throughout the test. A very small overall reduction in bulk volume was detected. Helium pressure dramatically declined at the conclusion of the heat of hydration phase, followed by a steady, but slower, decline. It is not known whether these sudden changes in helium pressure were the result of the leak. However, at t=1700 minutes, a leak did develop in the slurry pressure transducer port. This led to dramatic decreases in helium and slurry pressure. When the leak was discovered, the test was aborted.

Test #13:

BFS with PHPA. The test was conducted at a pressure of 1000 psi. The water chamber was located above the slurry chamber. Data acquisition began 45 minutes after sample preparation. The "floating" nylon piston was used in place of the elastic membrane. Helium and water pressures were incrementally increased (Δp = 50 psi) until 1000 psi was reached. The data from the helium pressure transducer contained a large noise component. This data was smoothed by using a ten-point averaging window. The slurry transducer appeared to be out of calibration. The pump was able to maintain a constant pressure throughout the test.

At the conclusion of the test, a dark, unidentified fluid was recovered from the helium chamber. A significant amount of gas was dissolved in the fluid. The sample was CT scanned.

Results of this test is shown in Figures 3.19 and 3.20. Figure 3.19 displays the complete time record for the temperatures, pressures, and volumes. Figure 3.19a is an expanded time record for the temperatures and volumes during the heat of hydration phase. On this figure, the start, peak, and final points of the heat of hydration are designated with "A", "B", and "C", respectively. Figure 3.20 displays the time record for changes in pump and helium volumes.

The dynamic behavior of the helium and slurry pressures observed in previous tests is absent in this test. This may be partly due to the higher test pressure. The bulk volume reduced 2% during initial heating. There appears to have been a very small decrease (0.1%) during heat of hydration. Afterwards, the bulk volume slowly and steadily increased by 0.4%. The internal volume appears to have gone through a gradual decline. It is not clear where an internal volume reduction had actually occurred since there was never an initial creation of void space in the first place.

3.5 Recommendations

1. Improve the reliability and functionality of the apparatus.
   a) Reduce noise in pressure transducers.
   b) Add p-wave velocity monitoring.
   c) Reduce the heat transfer from the slurry chamber to the helium and water chambers.
   d) Conduct "real-time" CT scanning of slurry during test.

2. Complete enough additional tests on both the Portland and BFS cements to infer statistically significant results.

3. Identify the fluids that were generated during the course of the tests.

3.6 Appendix I - Calibration Curves

This section presents the calibration curves that were used to correct apparent changes in volume due to temperature variations. This section includes corrections for both water and helium. The list of figures are as follows:

Figure 3.21
"Open" system Volume - Temperature curve for water. This curve allows correction for the apparent increase in slurry volume resulting from only a temperature increase in the water bath. The source of water temperature variations are; (1) the initial heating to bring the system from room temperature to operating temperature (150 °F); heat of hydration from the slurry; (3) fluctuations in oven temperature.

Figure 3.22
Thermocouple calibration curves. The thermocouples were placed together in a water bath along with a Mercury thermometer and heated from room temperature to 170 °F. The figure displays the curves and linear regressions that converts thermocouple readings to the thermometer reading.

Figure 3.23
Tri-chamber volume-temperature curves for water. This curve was produced for the same reason as explained above in Figure 3.21. A unique calibration curve for this cell is needed because the water bath volume is different and the water in the tri-chamber cell is isolated from direct contact with the slurry. It was found that the data was best fit to a second-order polynomial function.

Figure 3.24
Tri-chamber pressure-temperature curve for helium. Temperature changes in the helium cause pressure changes. These changes lead to an incorrect calculation of volume change when using an expression that assumes isothermal expansion of the helium. To account for this, a pressure-temperature curve was derived by measuring the helium pressure at constant volume under controlled temperature conditions. The regression curves that results from this data set were averaged and used to remove the effect of temperature changes on helium volume calculations.

Figure 3.1
Apparatus for Exapnsion/Contraction of Slurry Mixtures
"Open" to Water Uptake

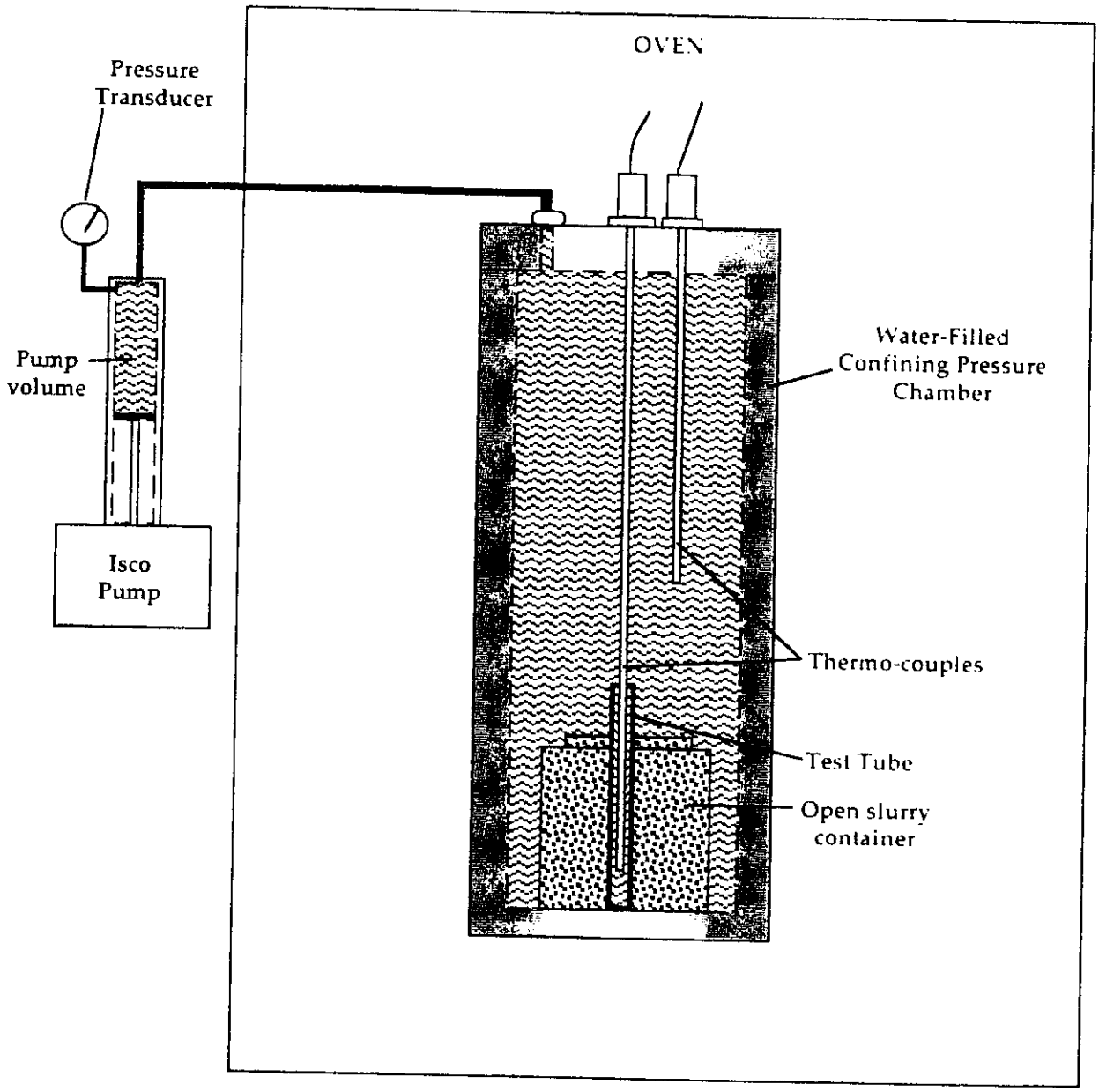

Figure 3.2
Tri-Chamber Expansion/Contraction Cell
IITRI-Westport Technology Center

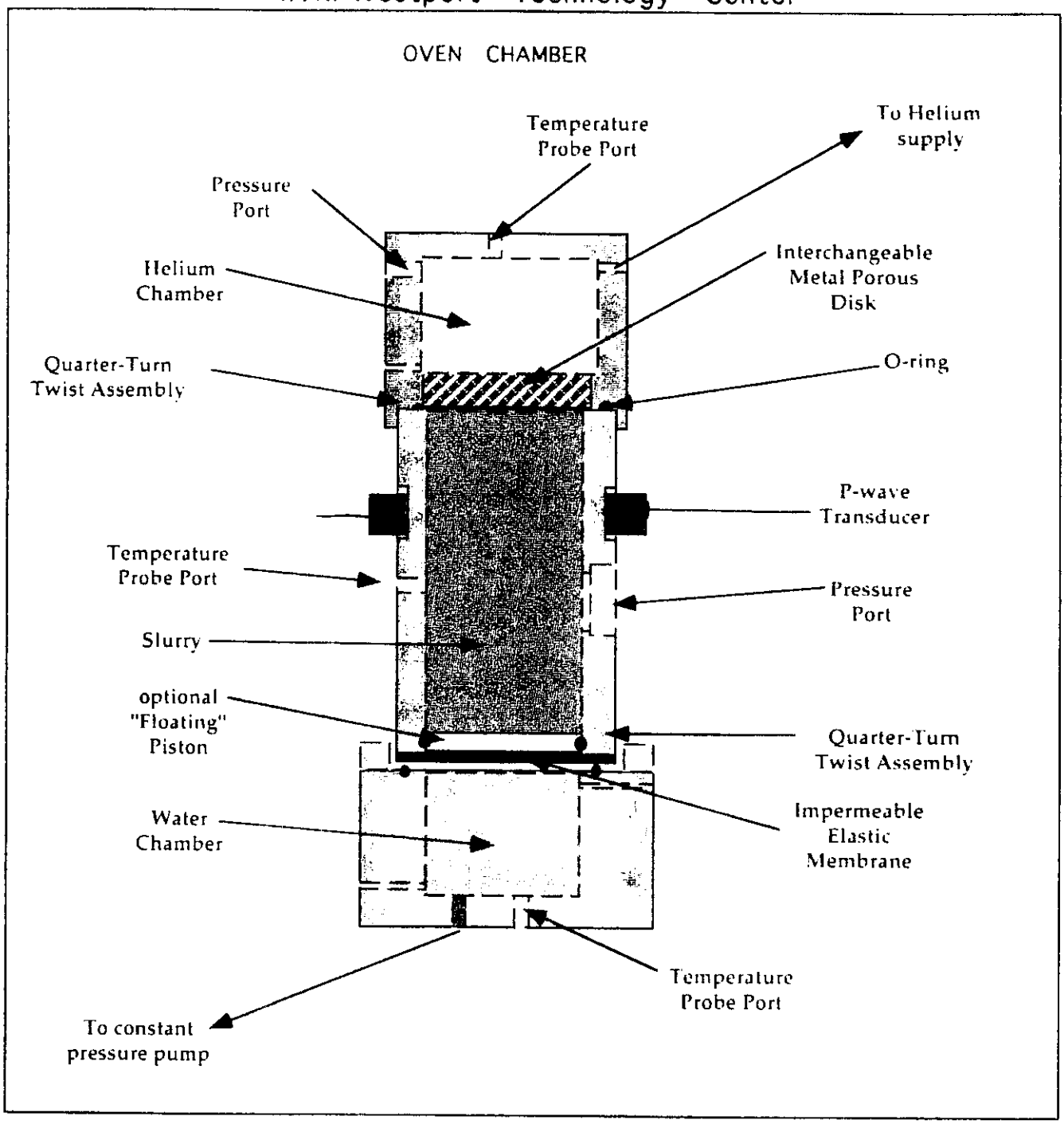

Figure 3.3
Portland Class G Cement Test #1.
Open to water uptake. 30 psi pressure

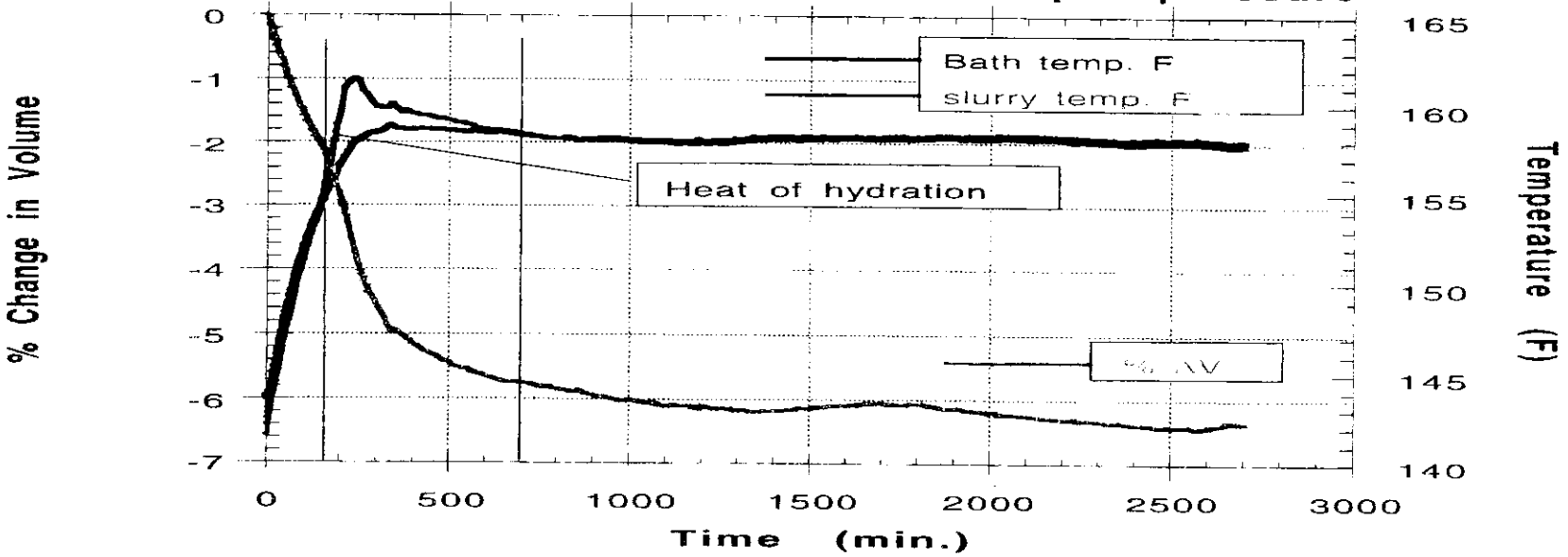

Portland Class G Cement Test #1.
(Expanded time scale)

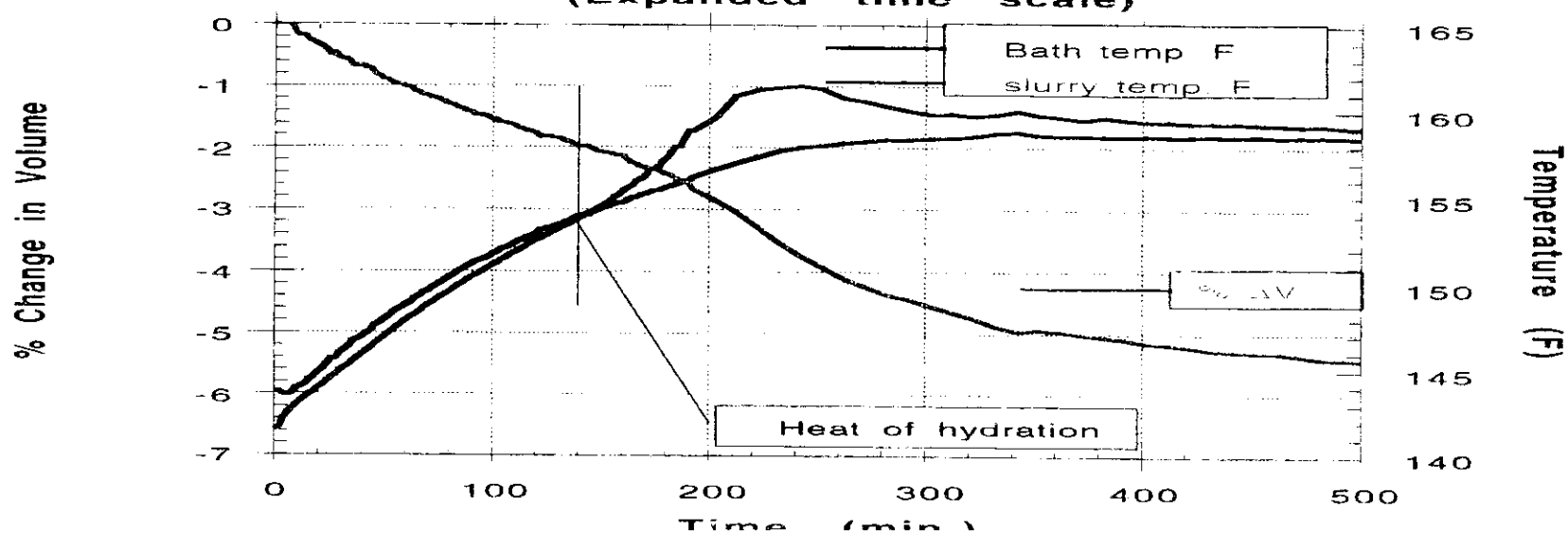

Figure 3.4
Portland Class G Cement Test 2.
Open to water uptake. 3000 psi.

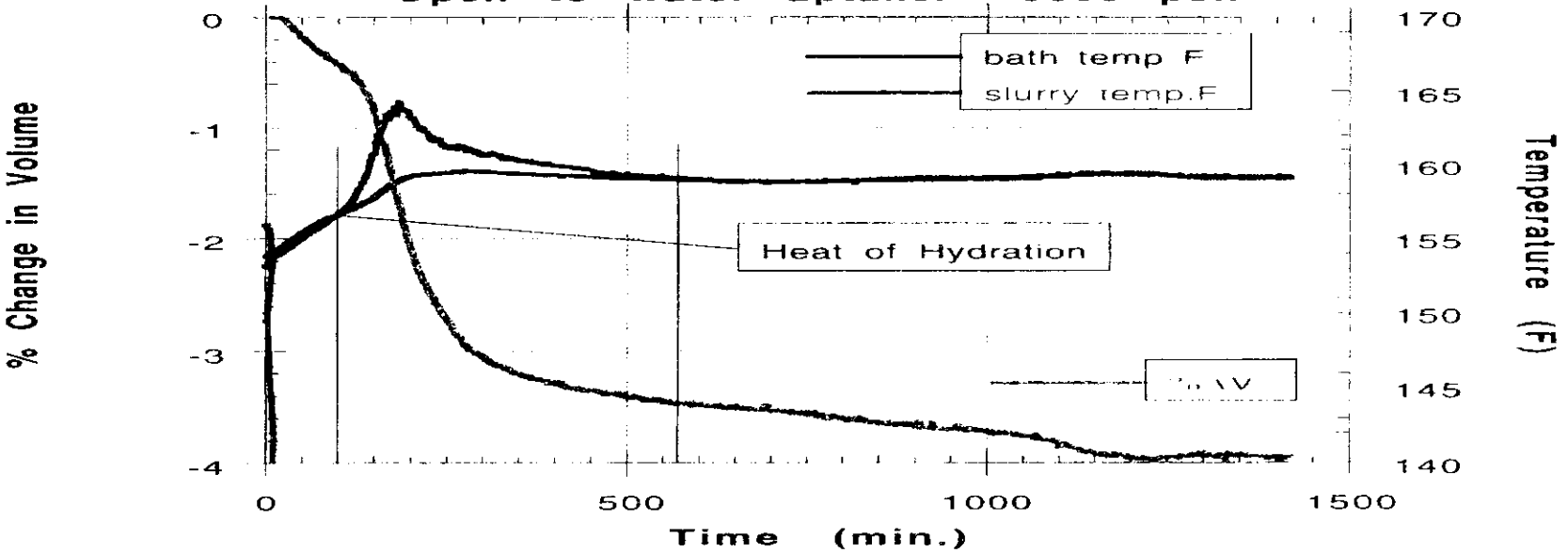

Portland Class G Cement Test 2.
(Expanded time scale)

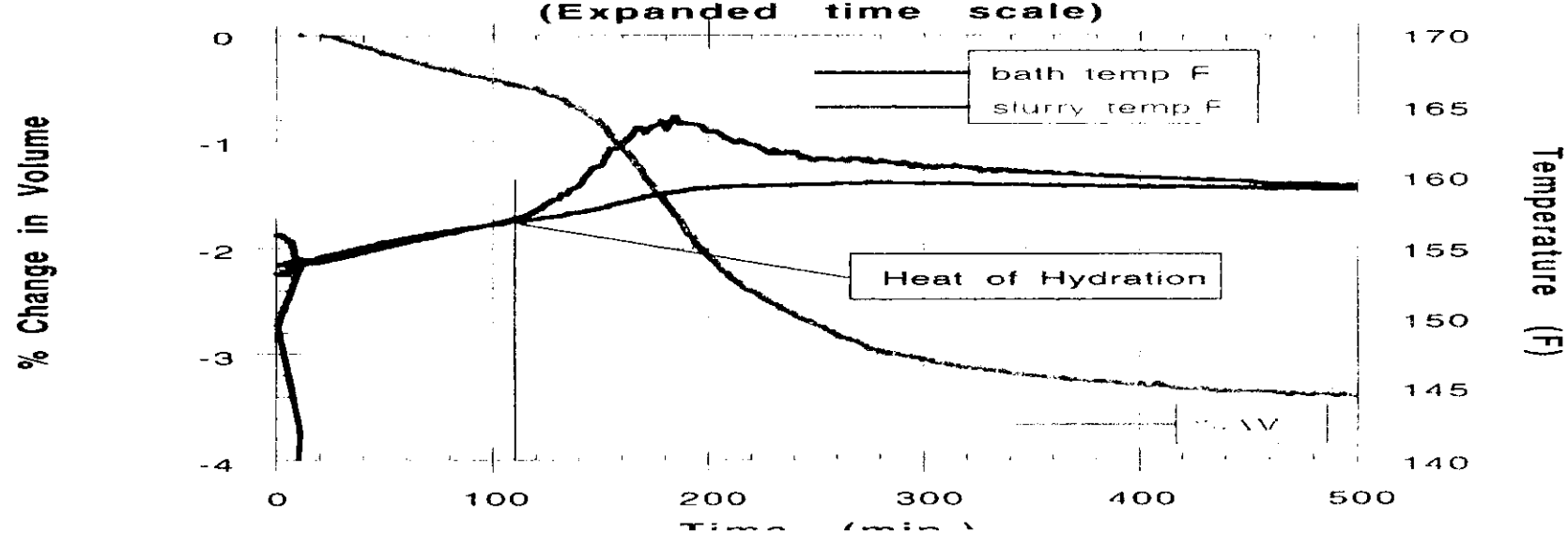

Figure 3.5
Portland Class G Cement Test 3.
Open to water uptake. 30 psi.

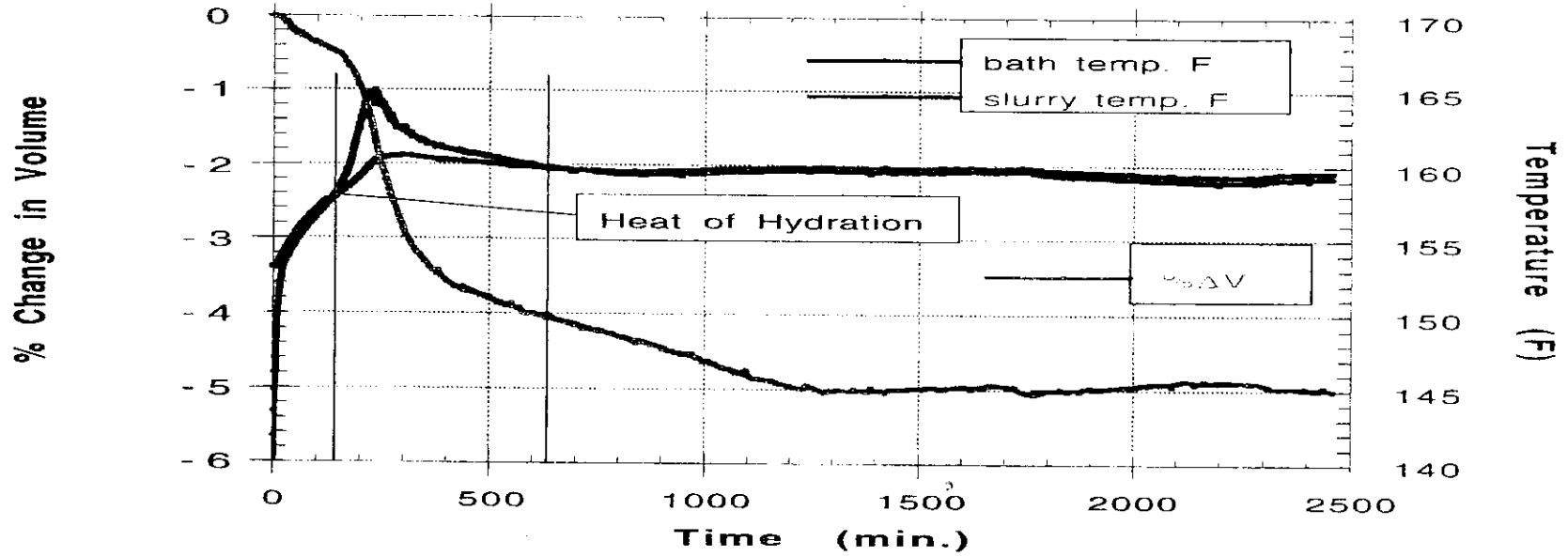

Portland Class G Cement Test 3.
(Expanded time scale)

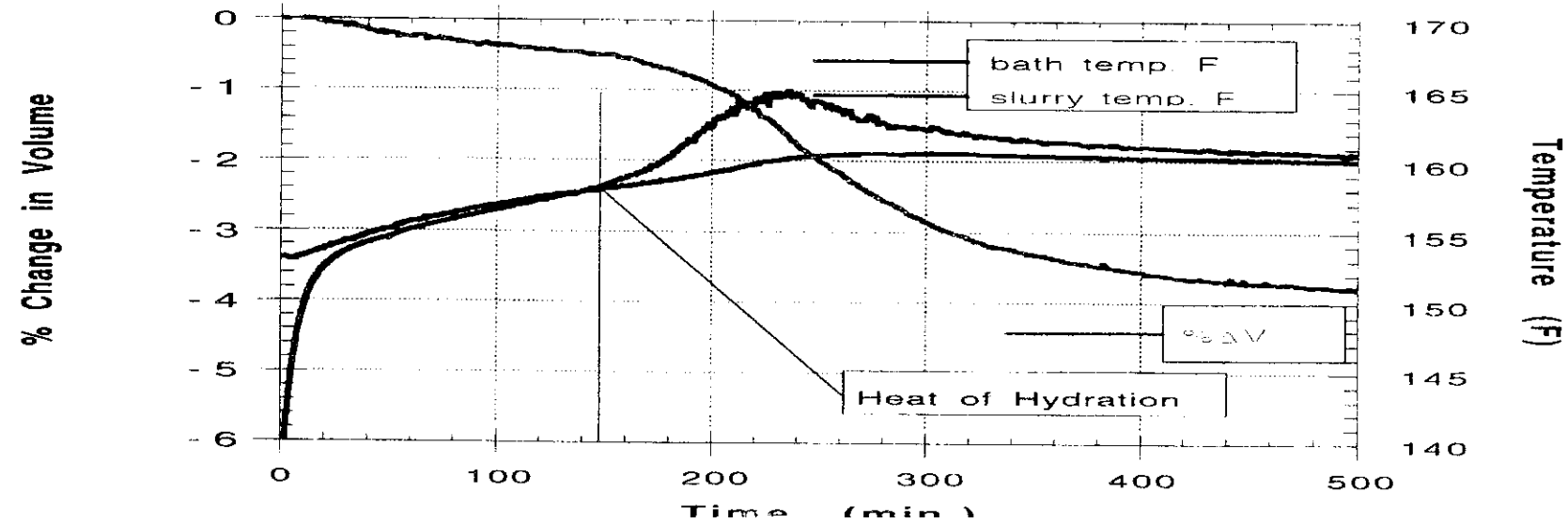

Figure 3.6
BFS with Dispersed Mud Test 4.
Open to water uptake. 30 psi.

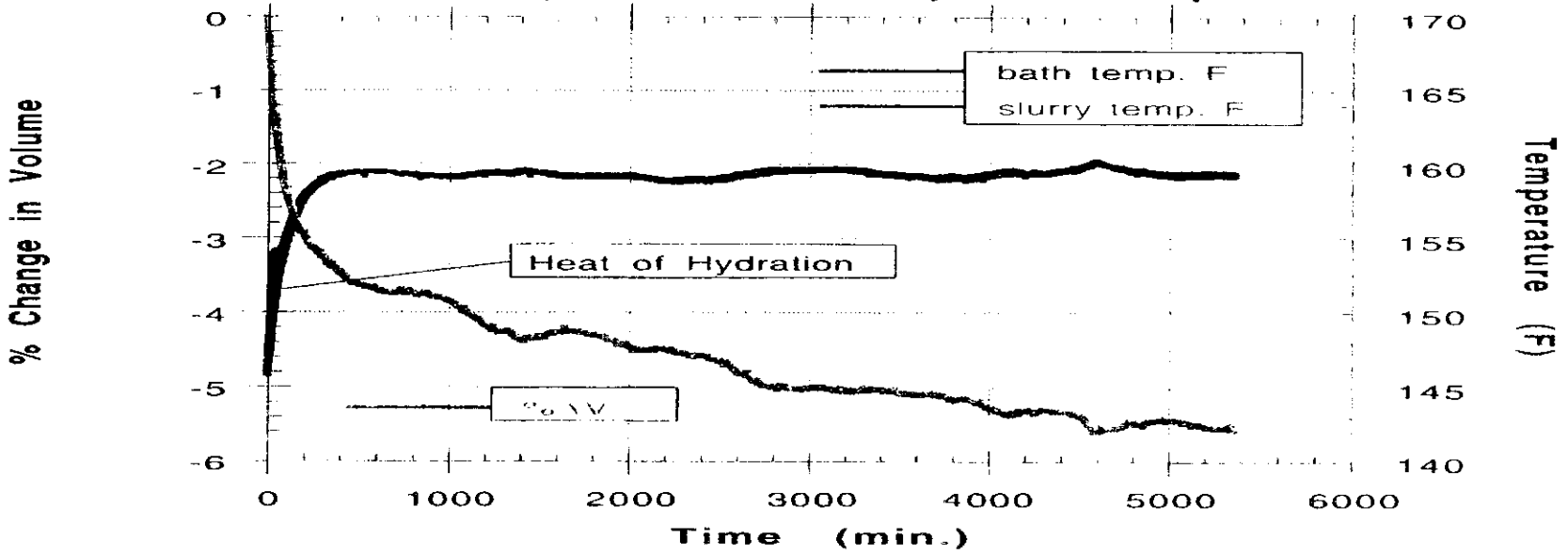

BFS with Dispersed Mud Test 4.
(Expanded time scale)

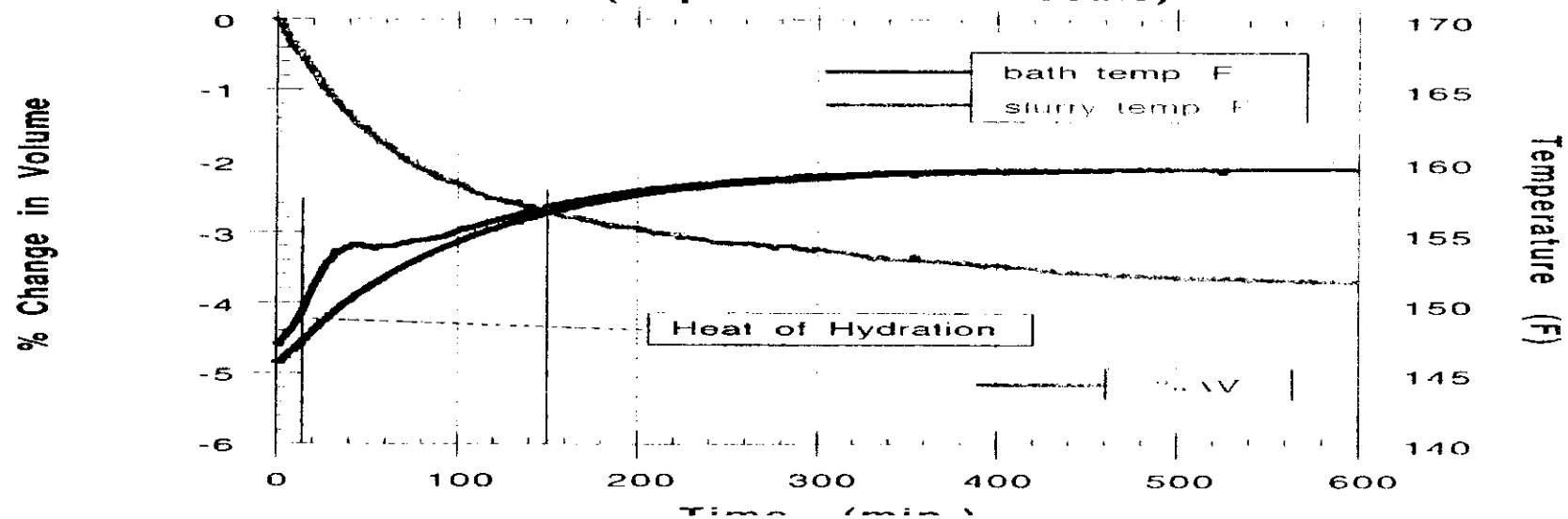

Figure 3.7
BFS with Dispersed Mud Test 5.
Open to water uptake. 3000 psi.

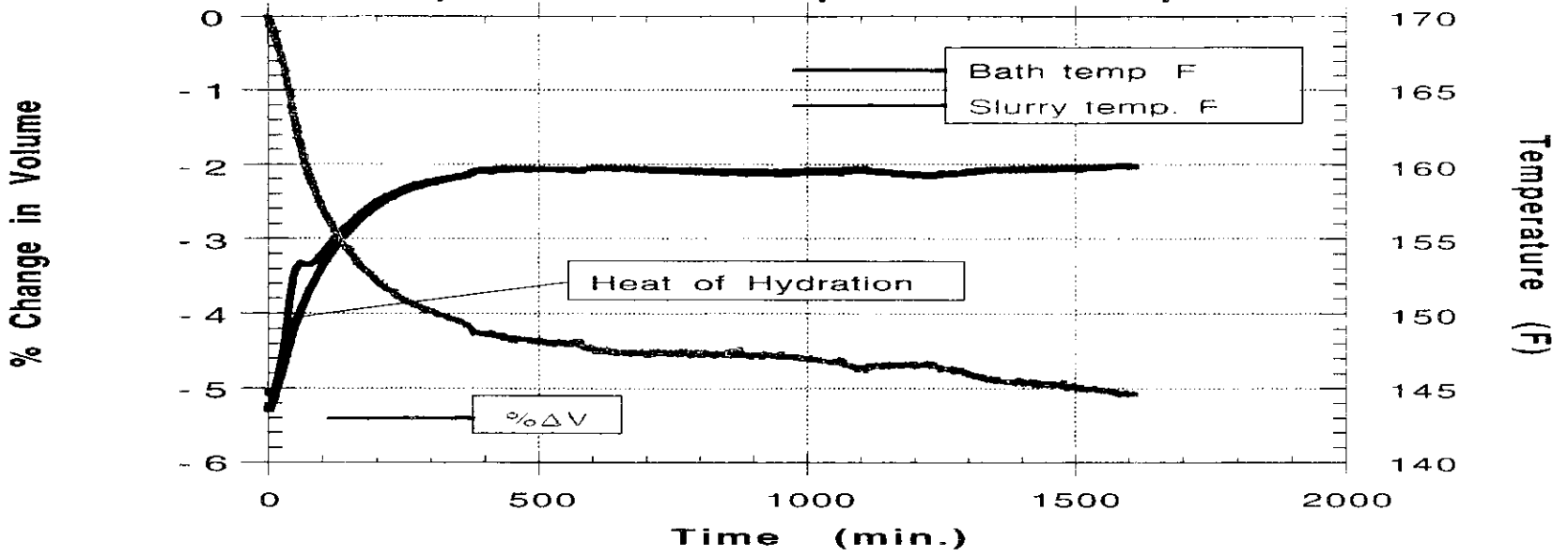

BFS with Dispersed Mud Test 5.
(Expanded time scale)

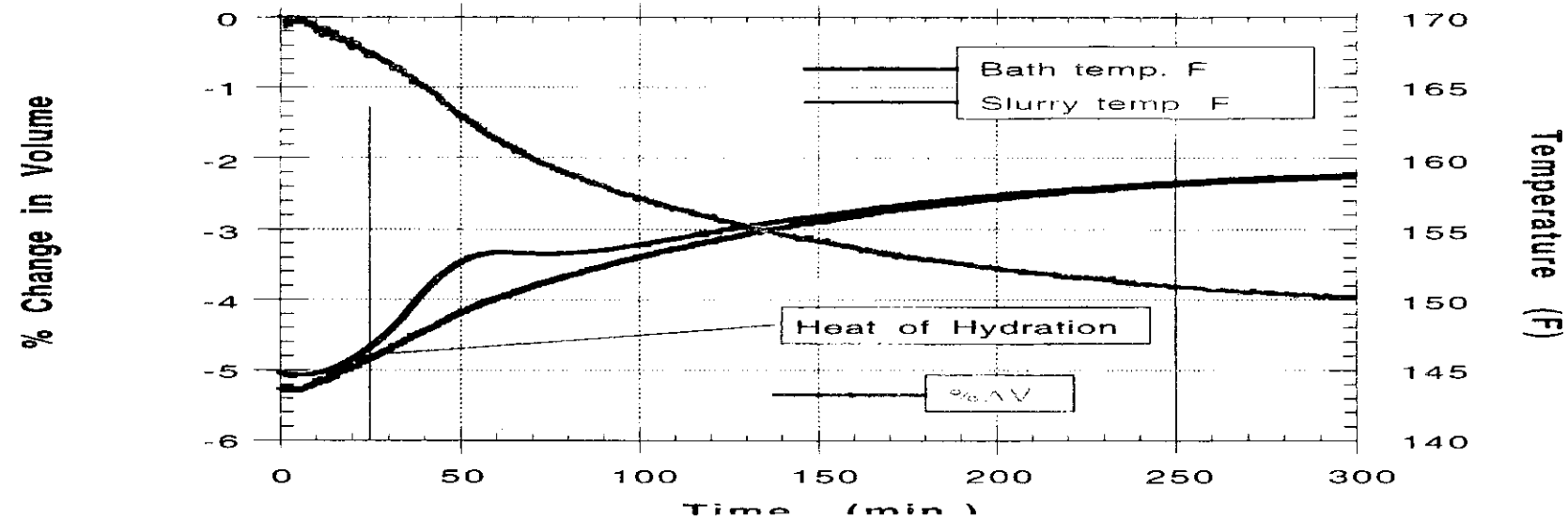

Figure 3.8
BFS with Dispersed Mud Test 6.
Open to water uptake. 30 psi.

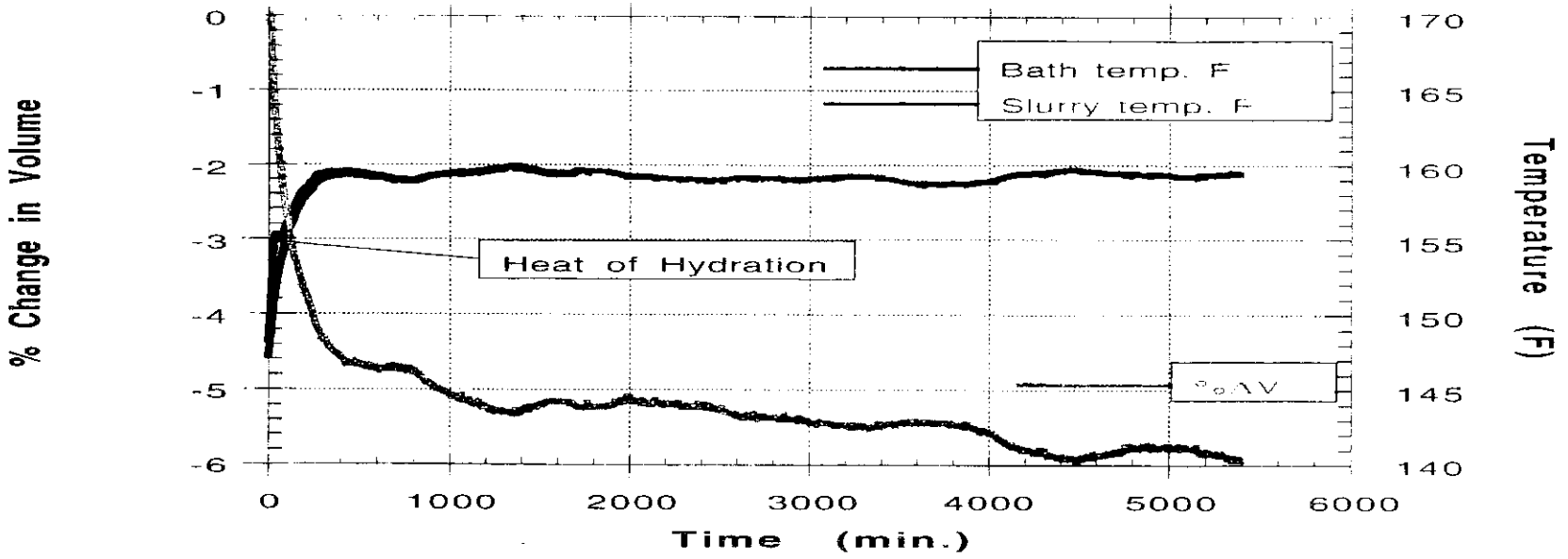

BFS with Dispersed Mud Test 6.
(Expanded time scale)

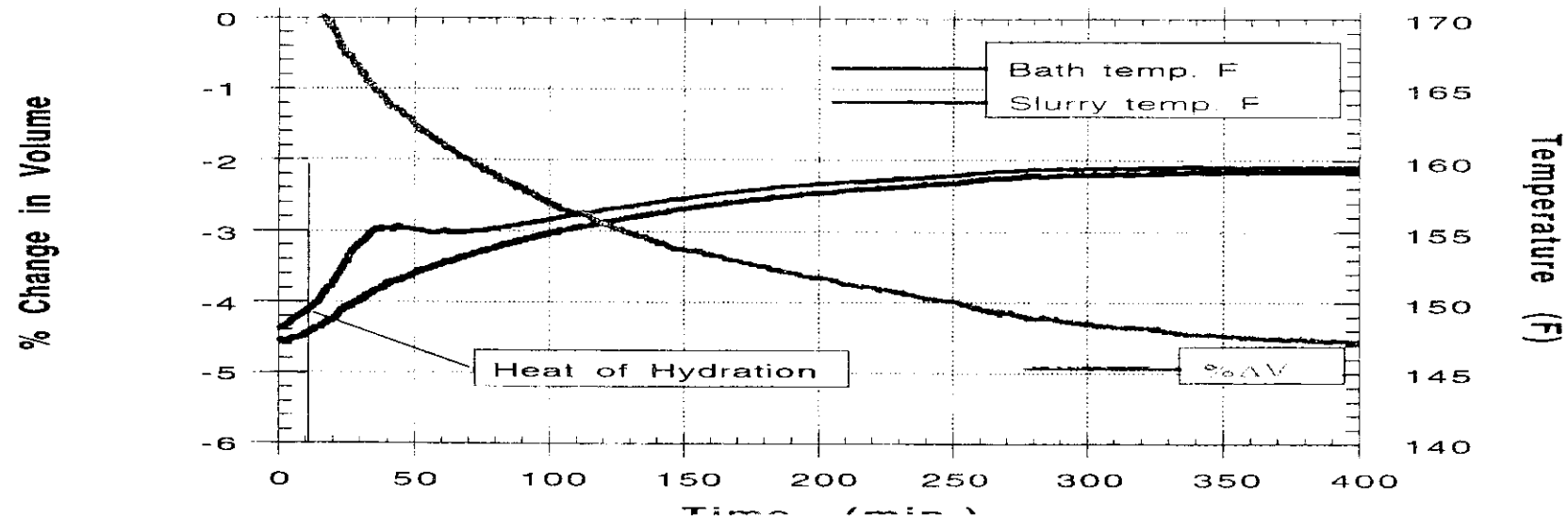

Figure 3.9
BFS with PHPA Test 7.
Open to water uptake. 30 psi.

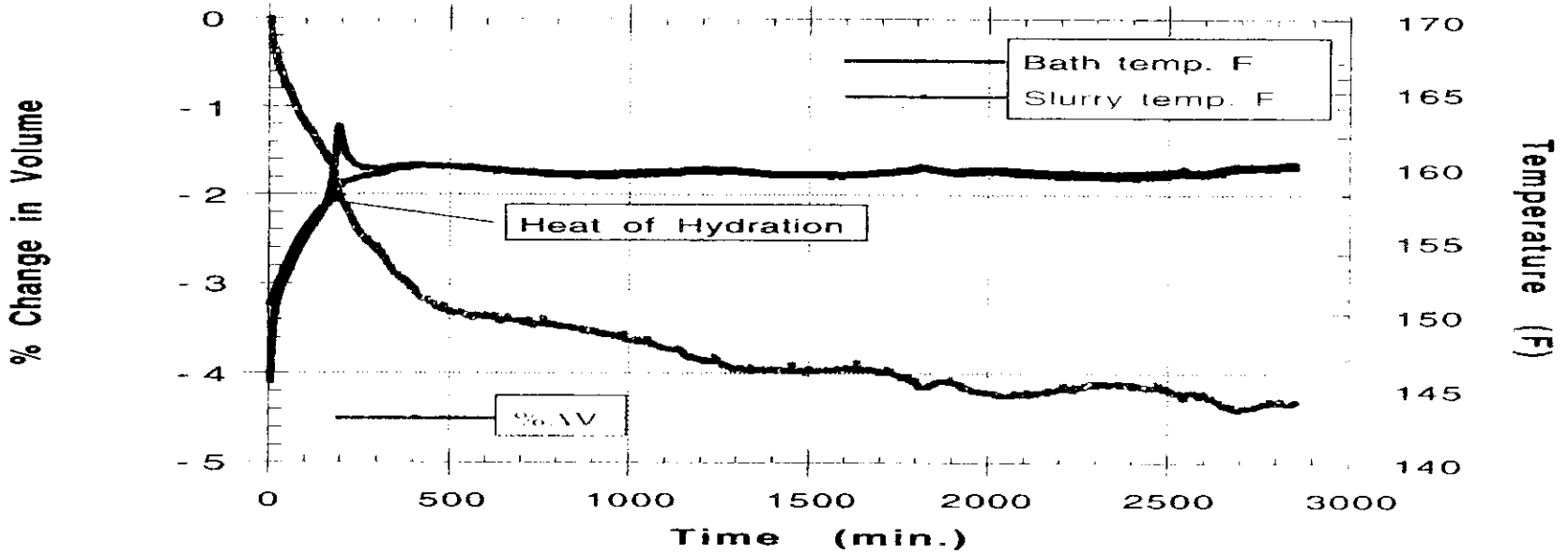

BFS with PHPA Test 7.
(Expanded time scale)

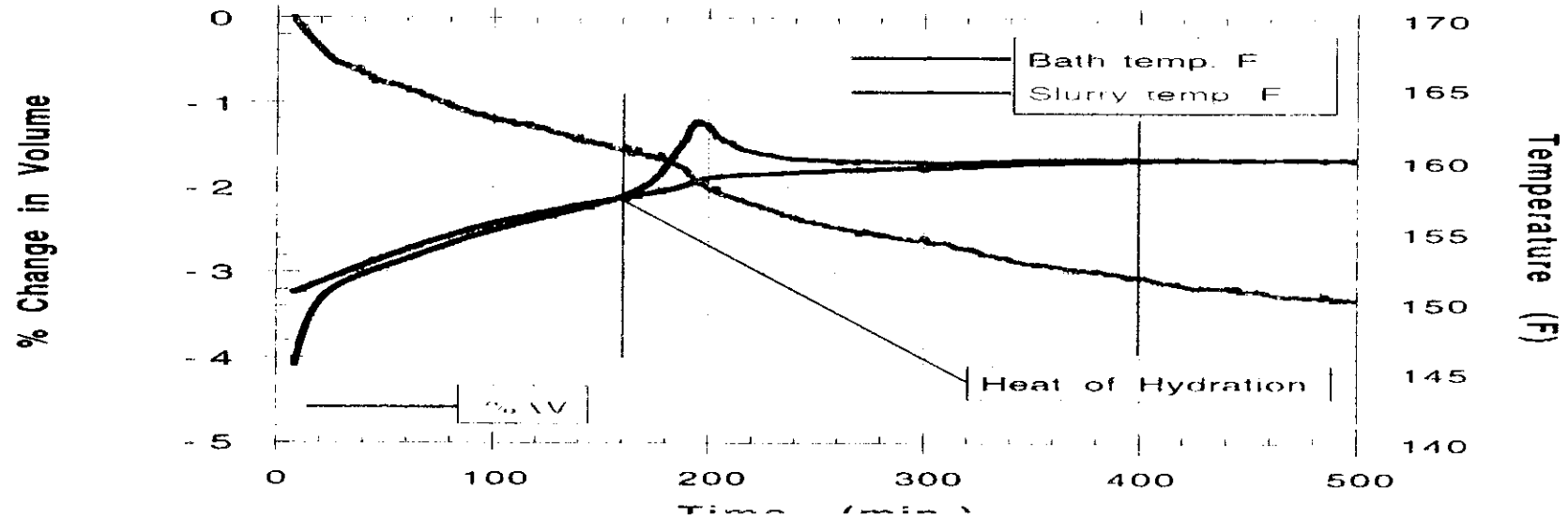

Figure 3.10
BFS with PHPA Test 8.
Open to water uptake. 3000 psi.

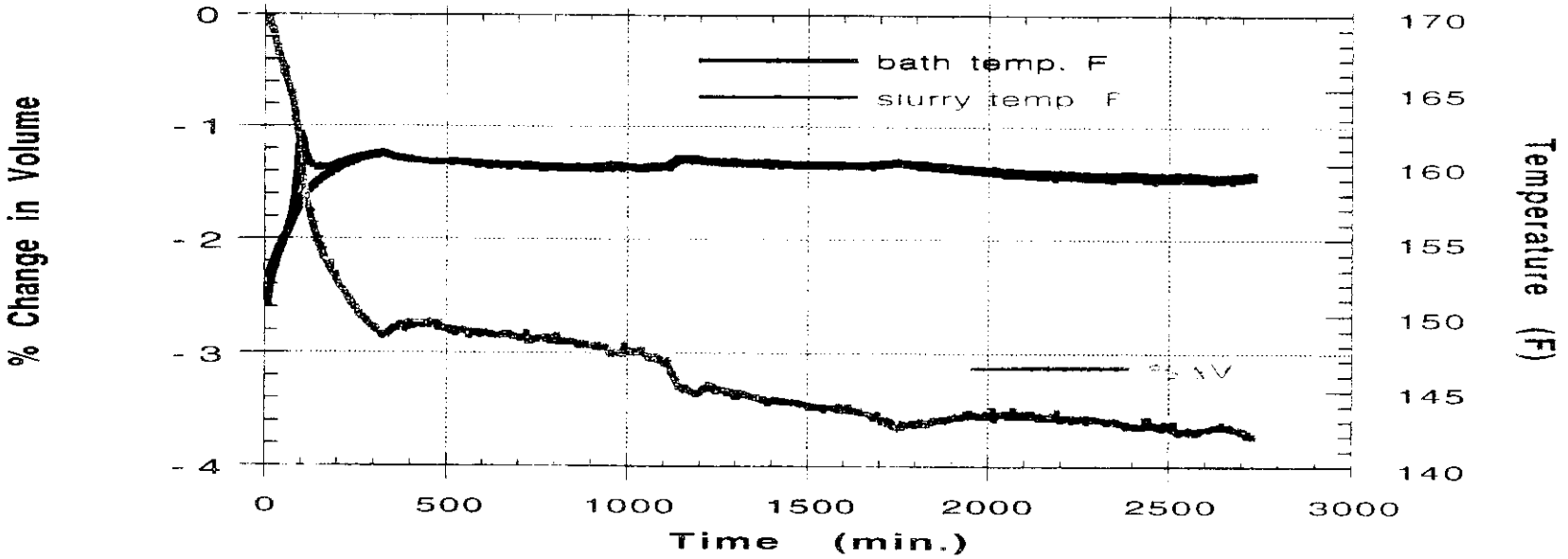

BFS with PHPA Test 8.
(Expanded time scale)

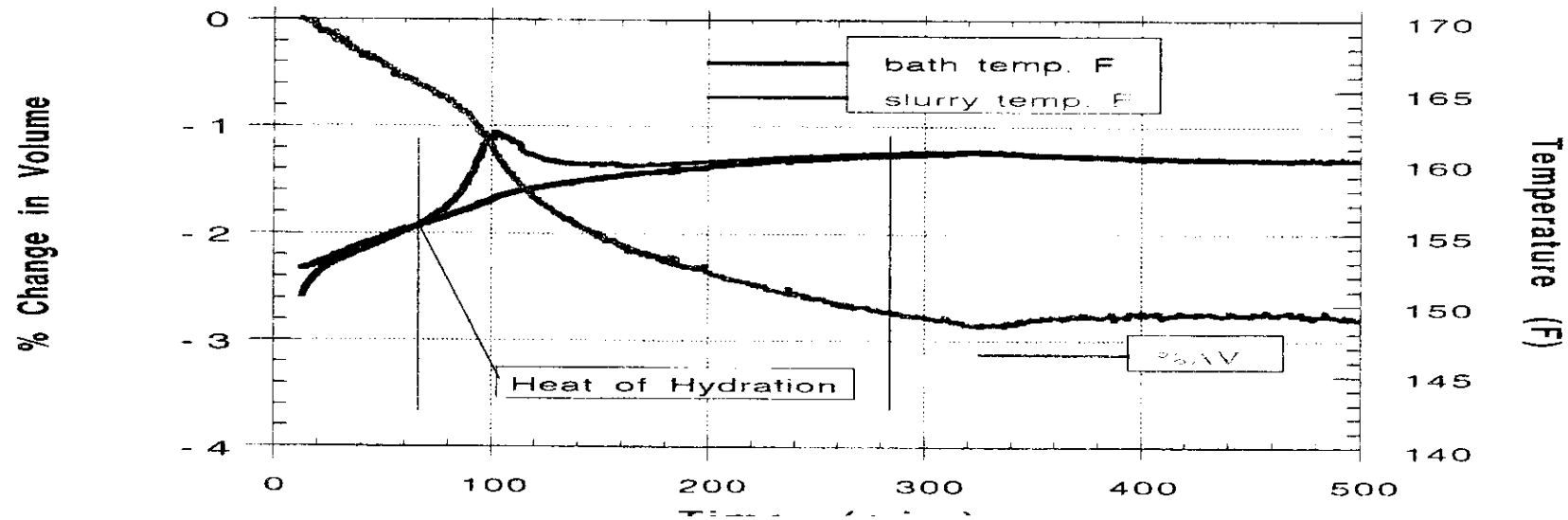

Figure 3.11
BFS with PHPA Test #9
Bulk and Internal Volume Change with Time

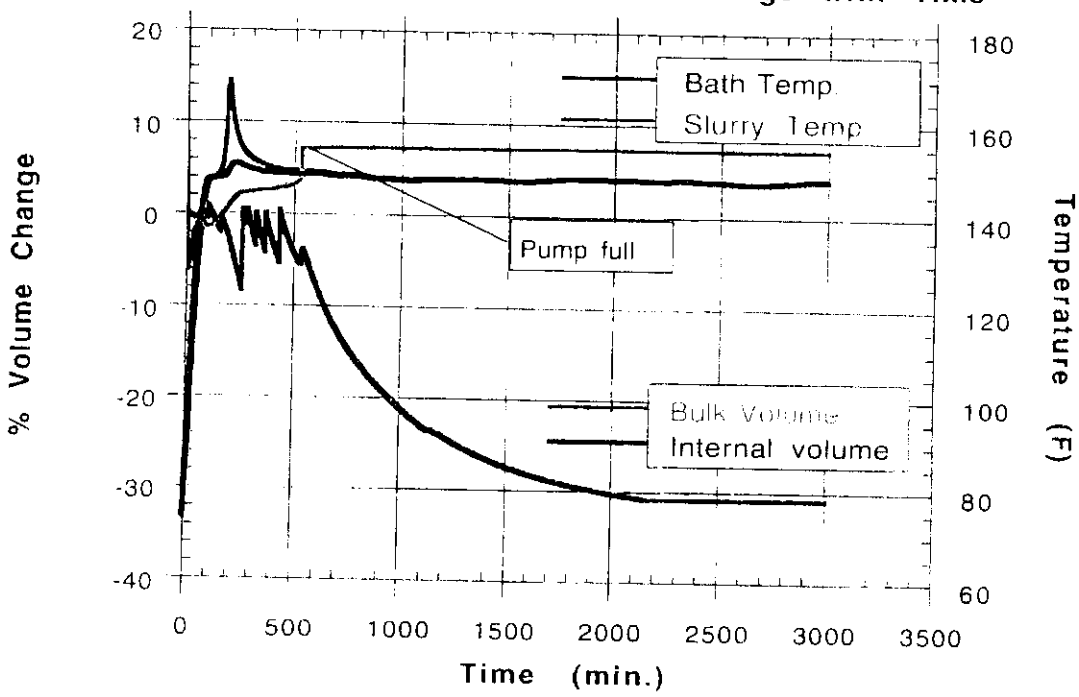

BFS with PHPA Test #9
Pressures vs. Time

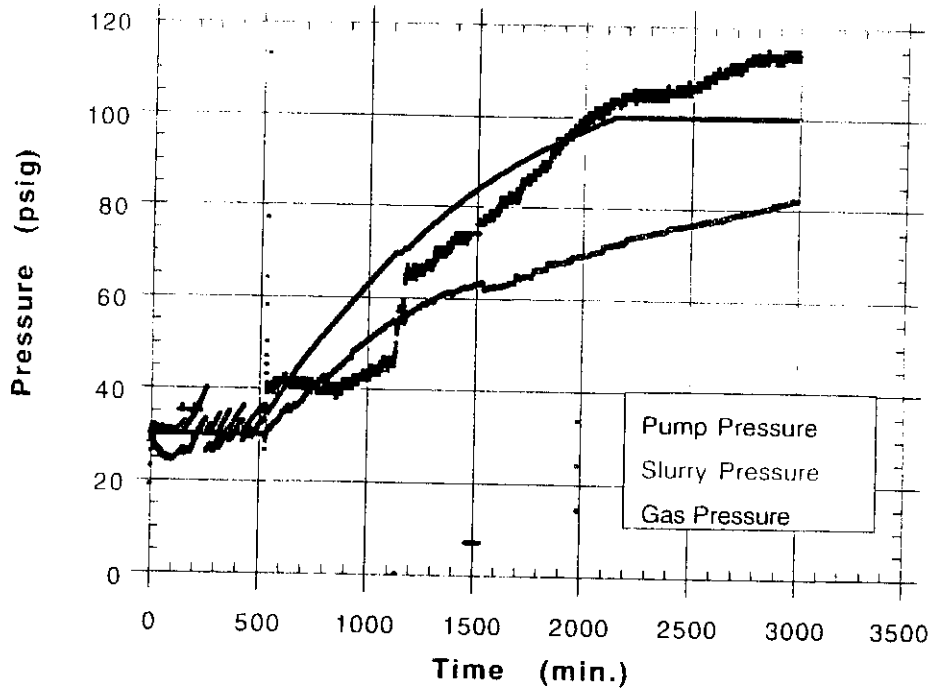

Figure 3.11b
BFS with PHPA Test #9
Expanded Time Scale

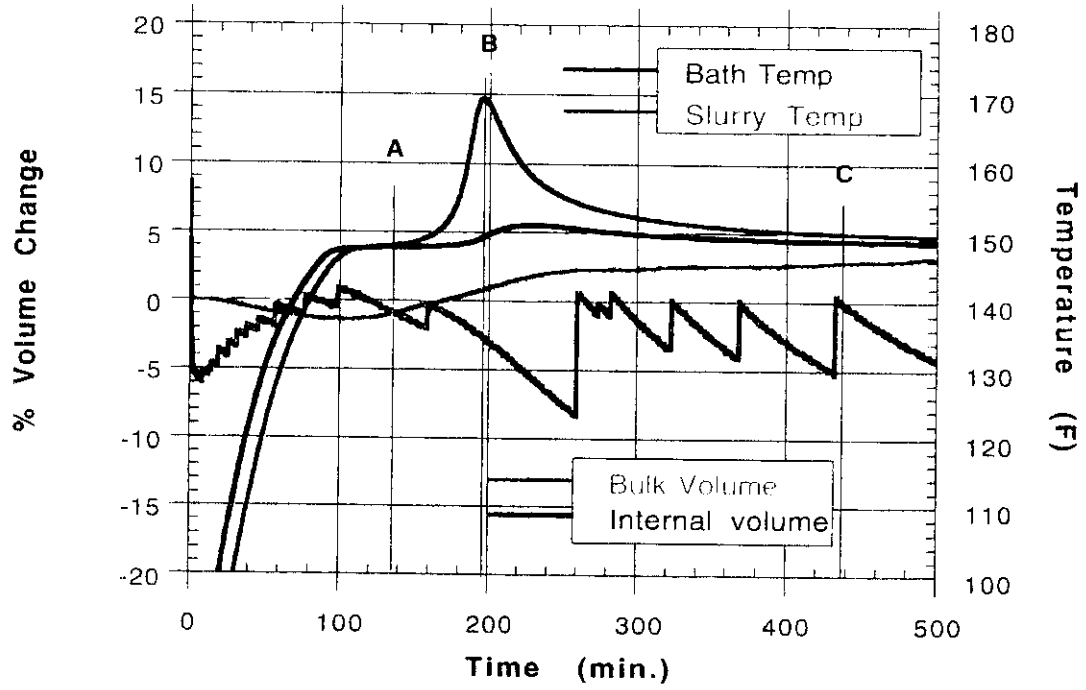

BFS with PHPA Test #9
Expanded time scale

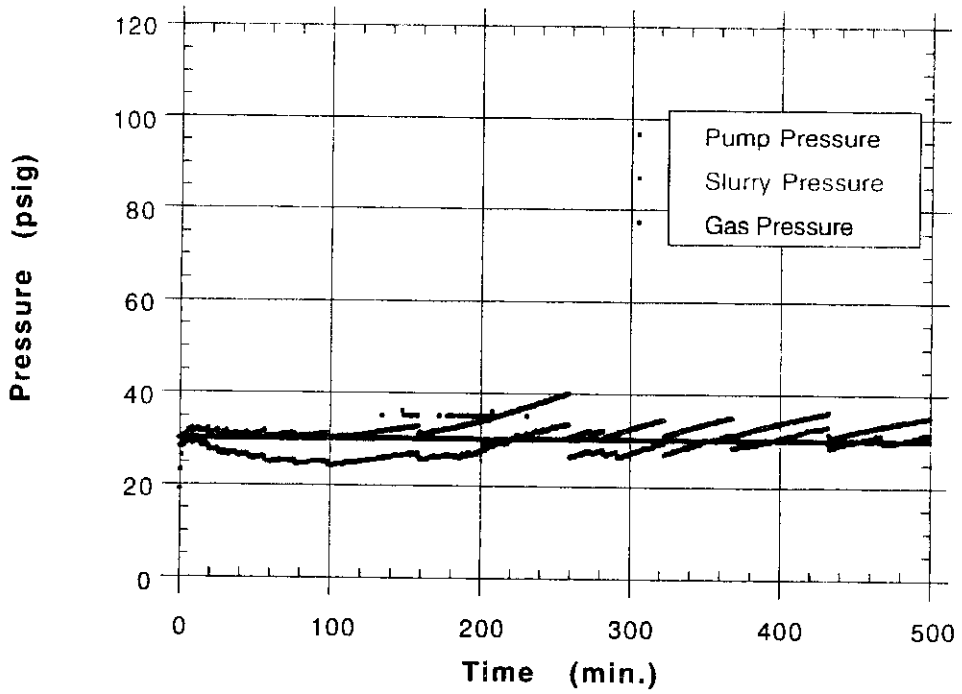

Figure 3.12
BFS with PHPA Test #9
Changes in Pump and Helium Reservoir Volumes

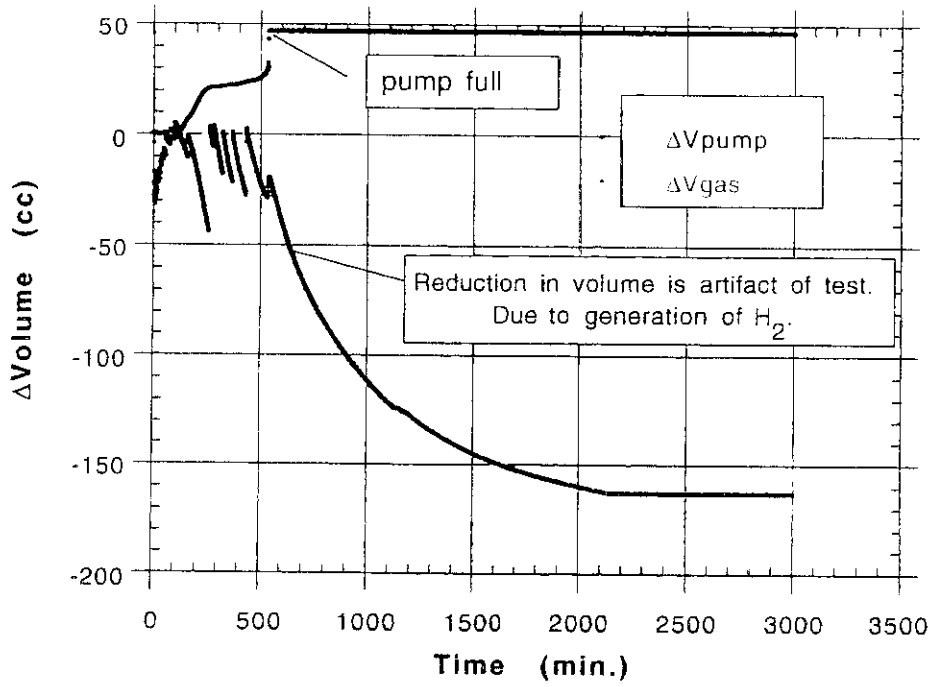

Figure 3.13
BFS with PHPA Test #10
Bulk and Internal Volume Change with Time

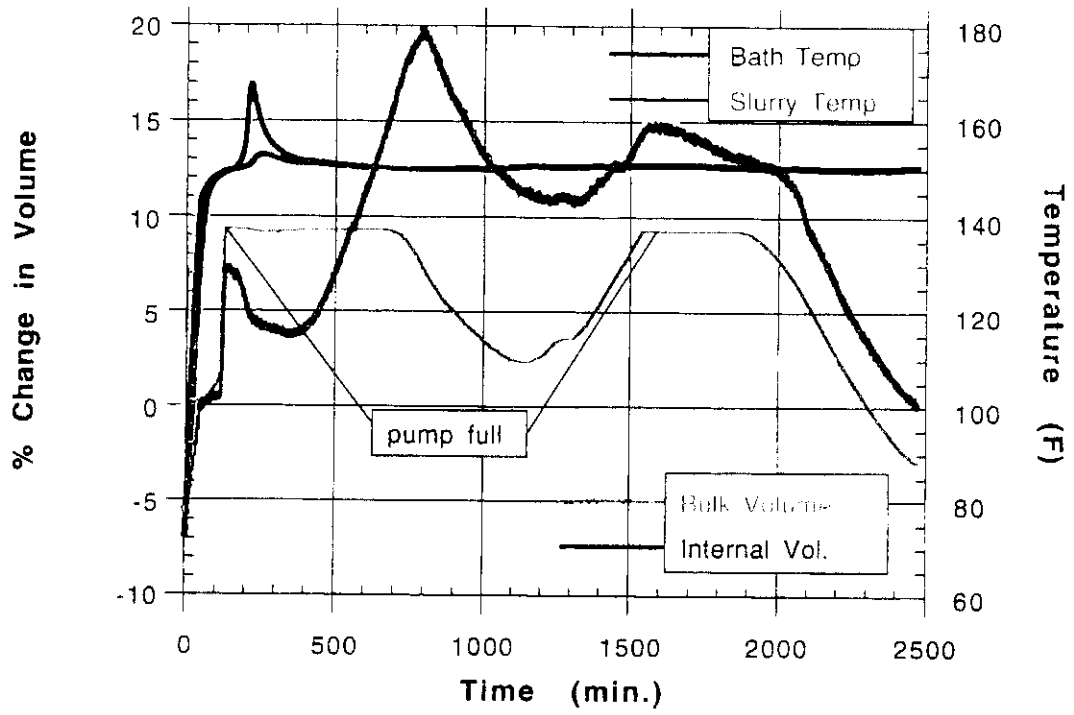

BFS with PHPA Test #10
Pressures vs. time

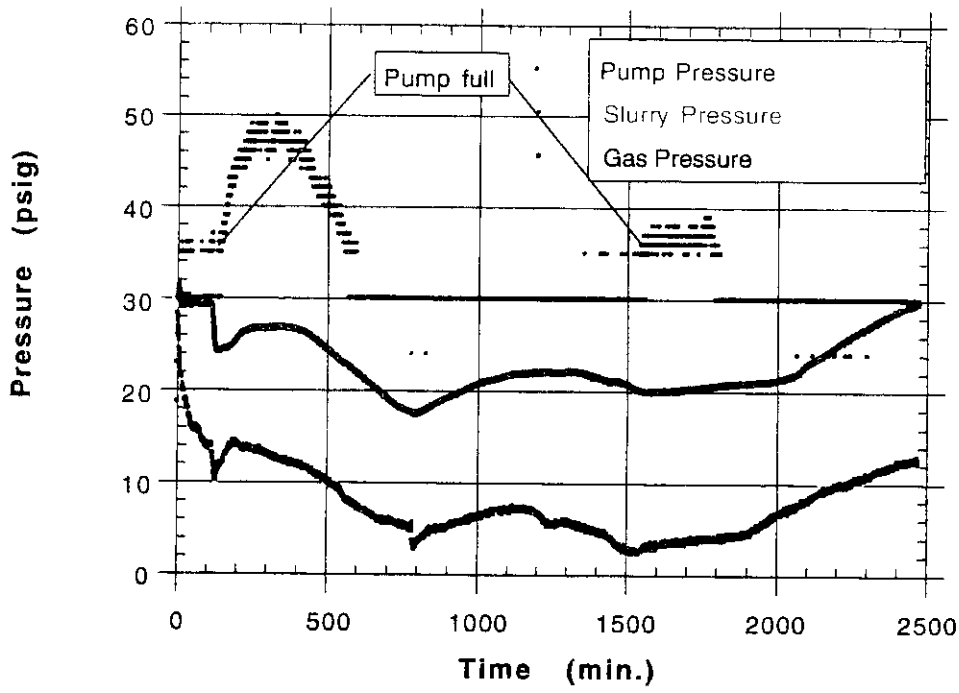

Figure 3.13b
BFS with PHPA Test #10
Expanded Time Scale

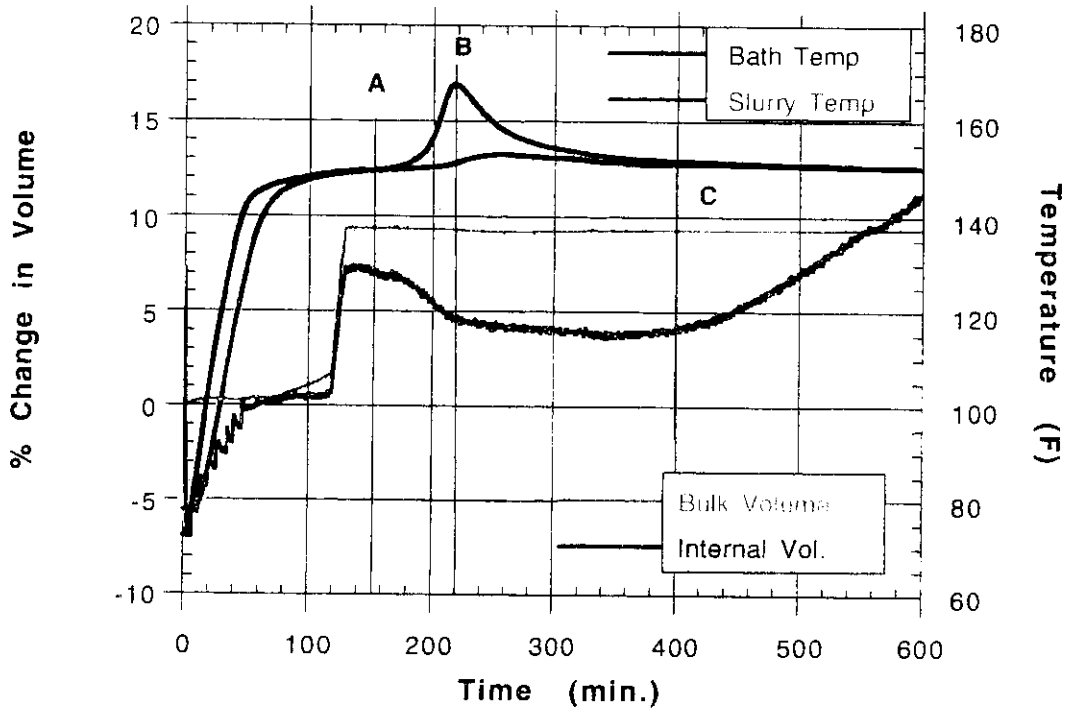

BFS with PHPA Test #10
Expanded Time Scale

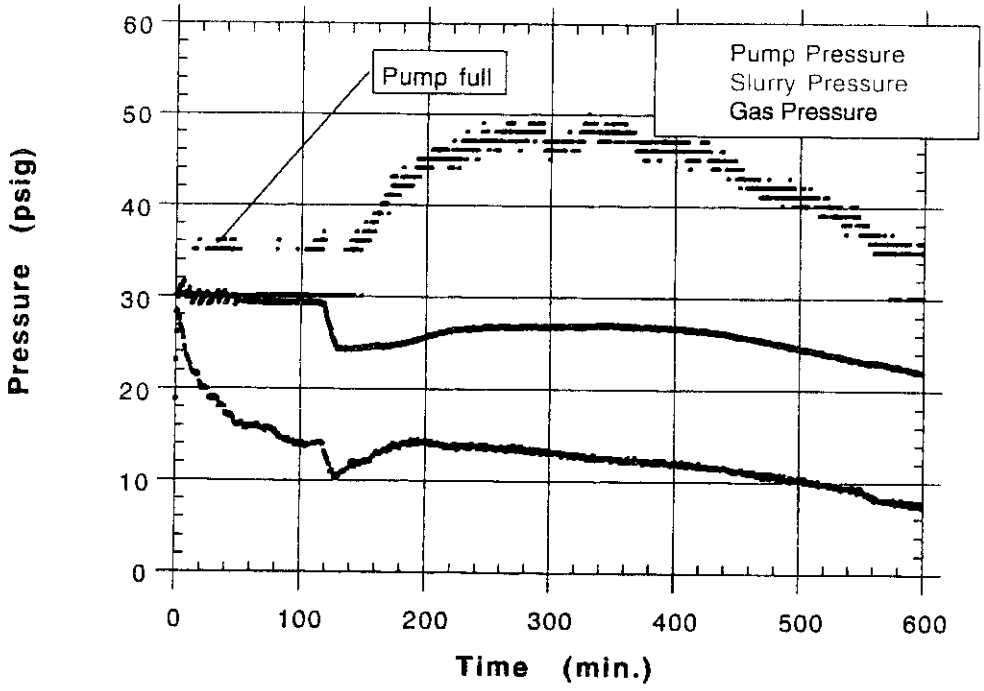

Figure 3.14
BFS with PHPA Test #10
Changes in Pump and Helium Reservoir Volumes

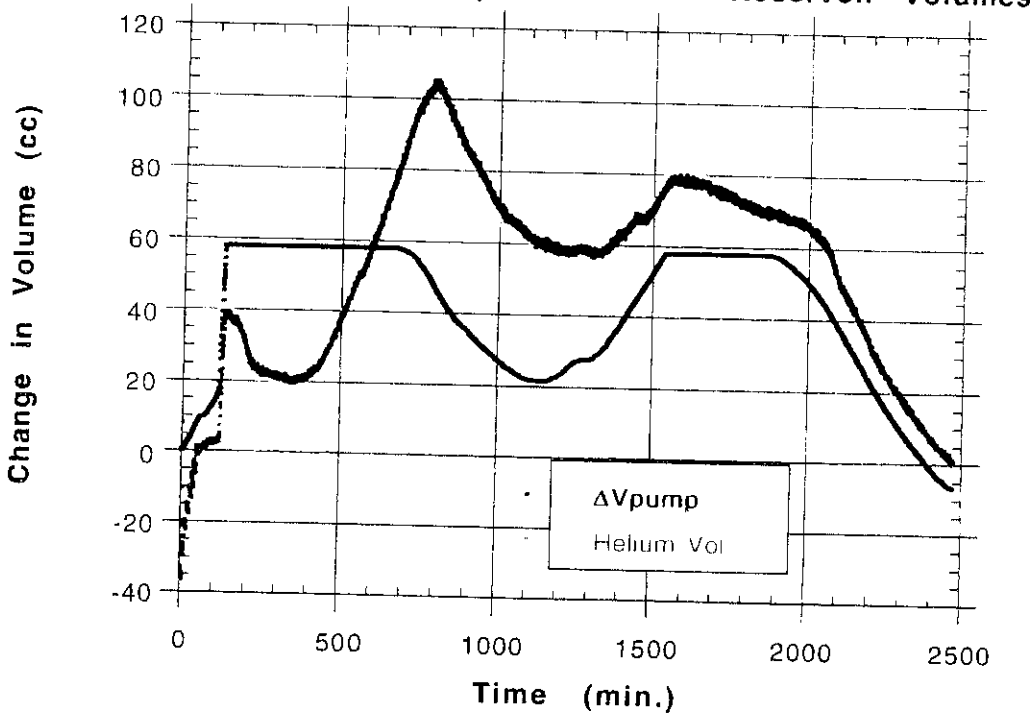

Figure 3.15
Portland Class G Cement Test #11
Bulk and Internal Volume Changes with Time

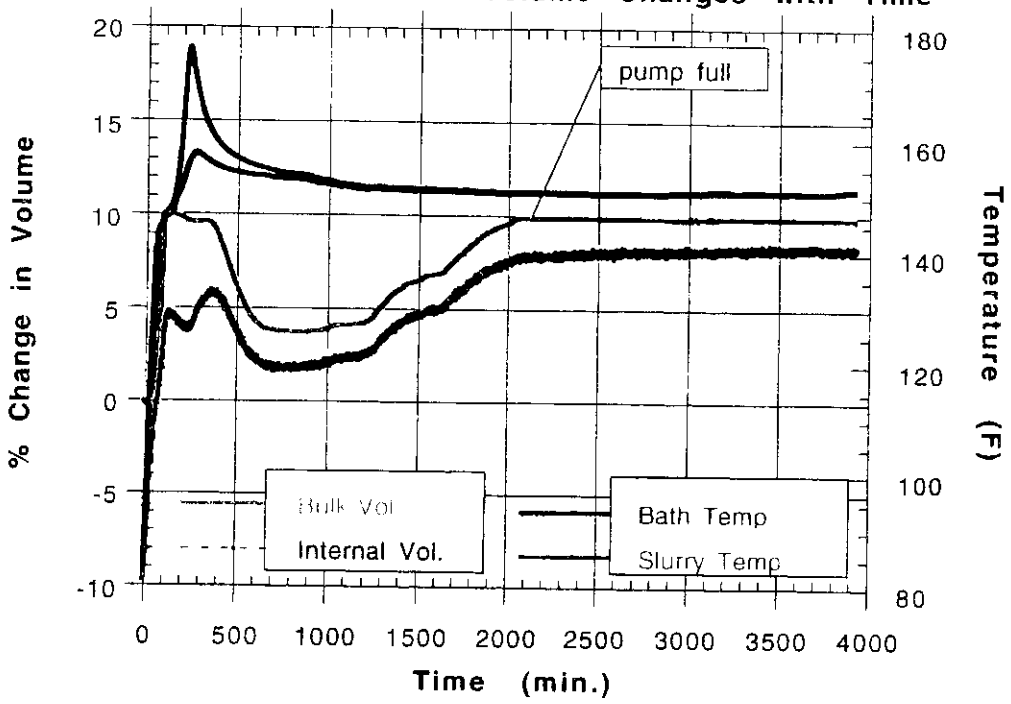

Portand Class G Cement Test #11
Pressures vs. Time

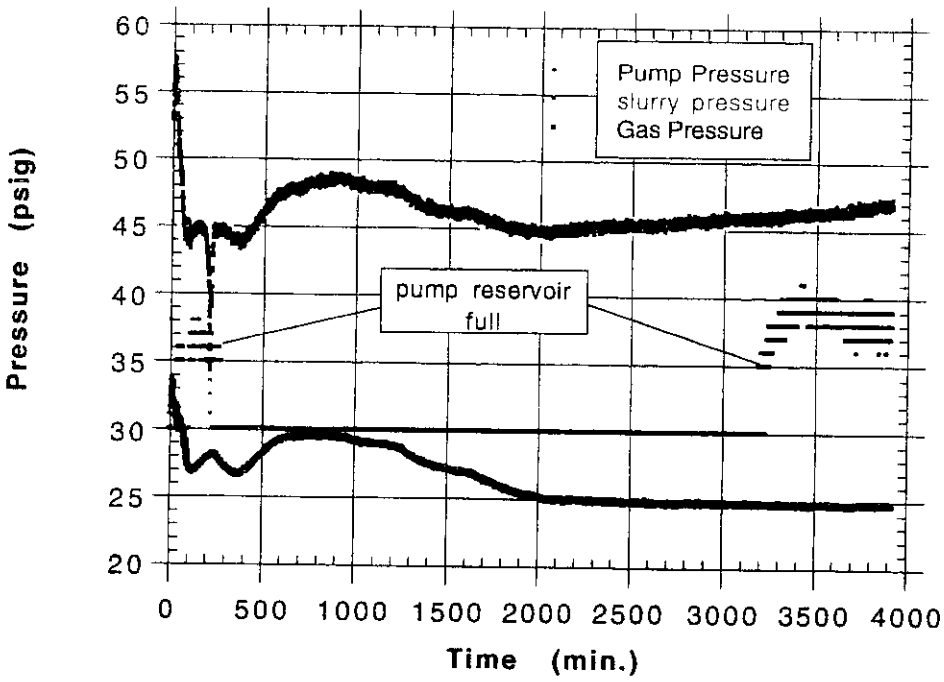

Figure 3.15b
Portland Class G Cement Test #11
Expanded Time Scale

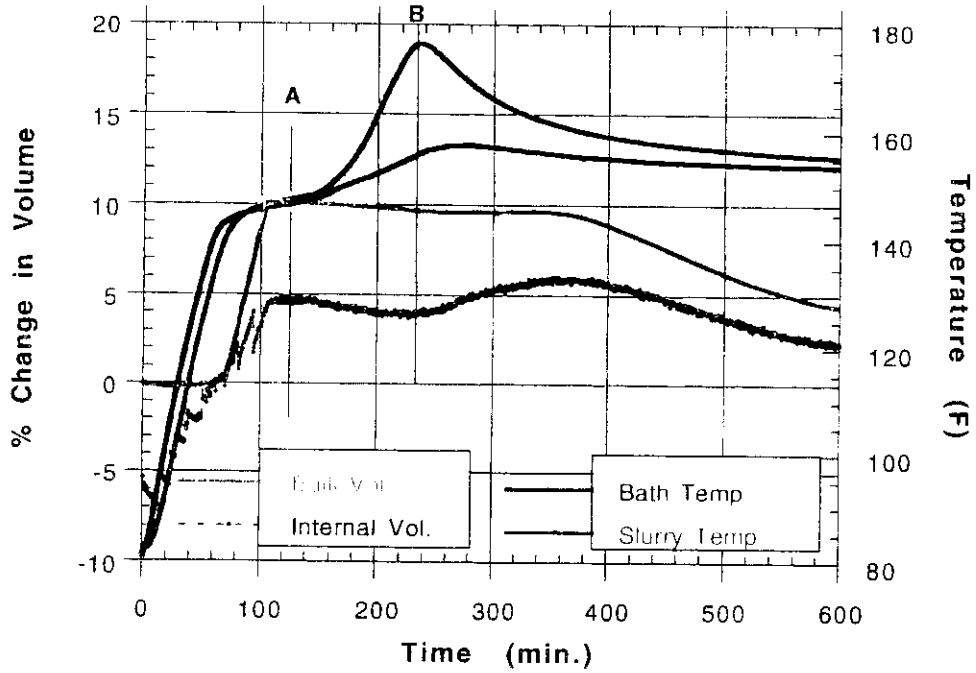

Portand Class G Cement Test #11
Expanded time scale

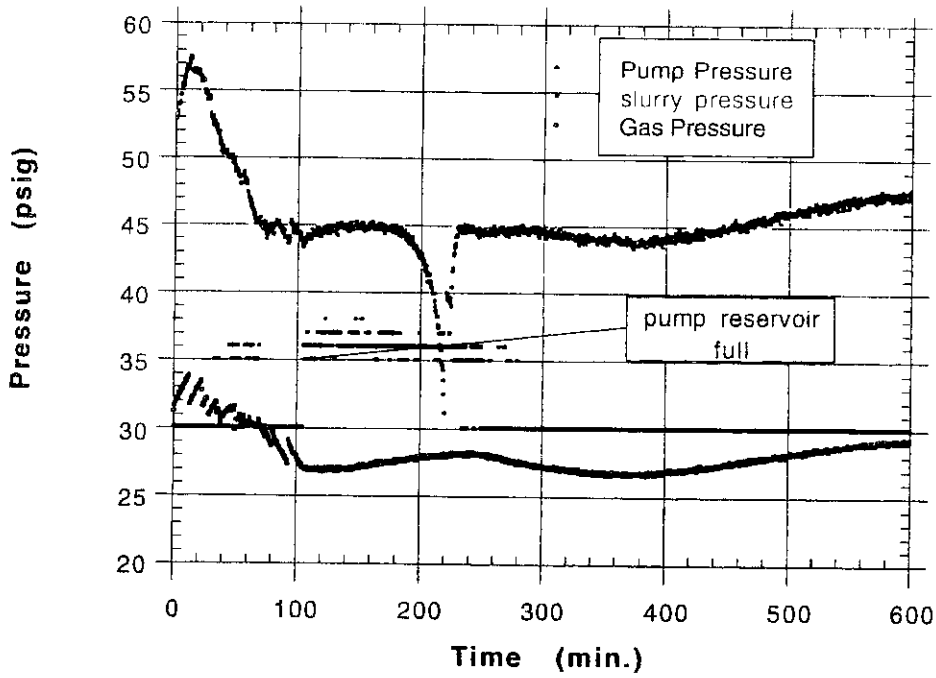

Figure 3.16
Portland Class G Cement Test #11
Pump and Helium Volume Changes vs. Time

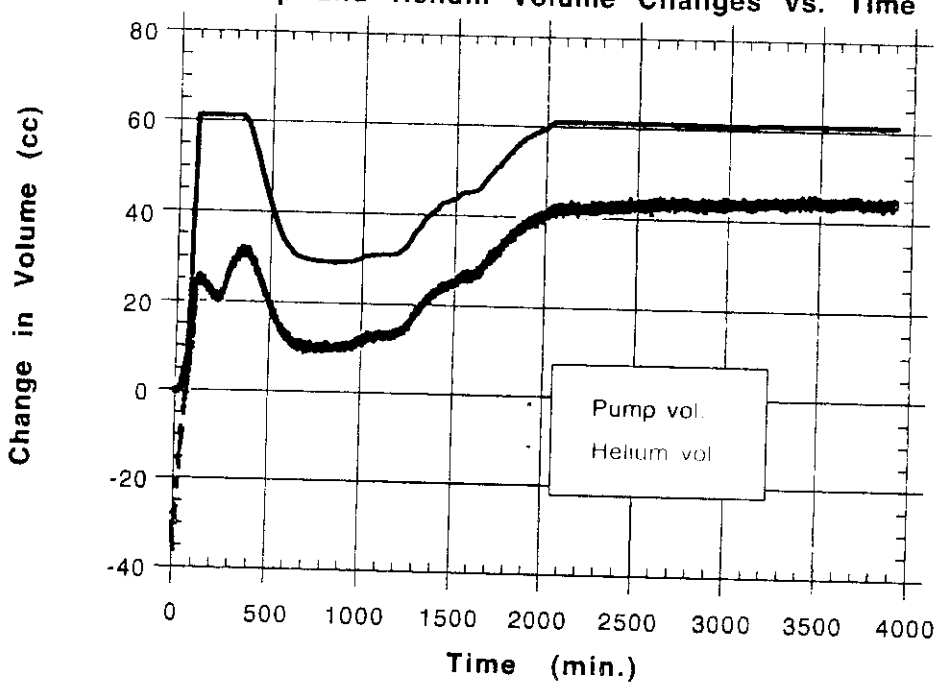

Figure 3.17
BFS with Dispersed Mud Test #12
Bulk and Internal Volume Changes vs. Time

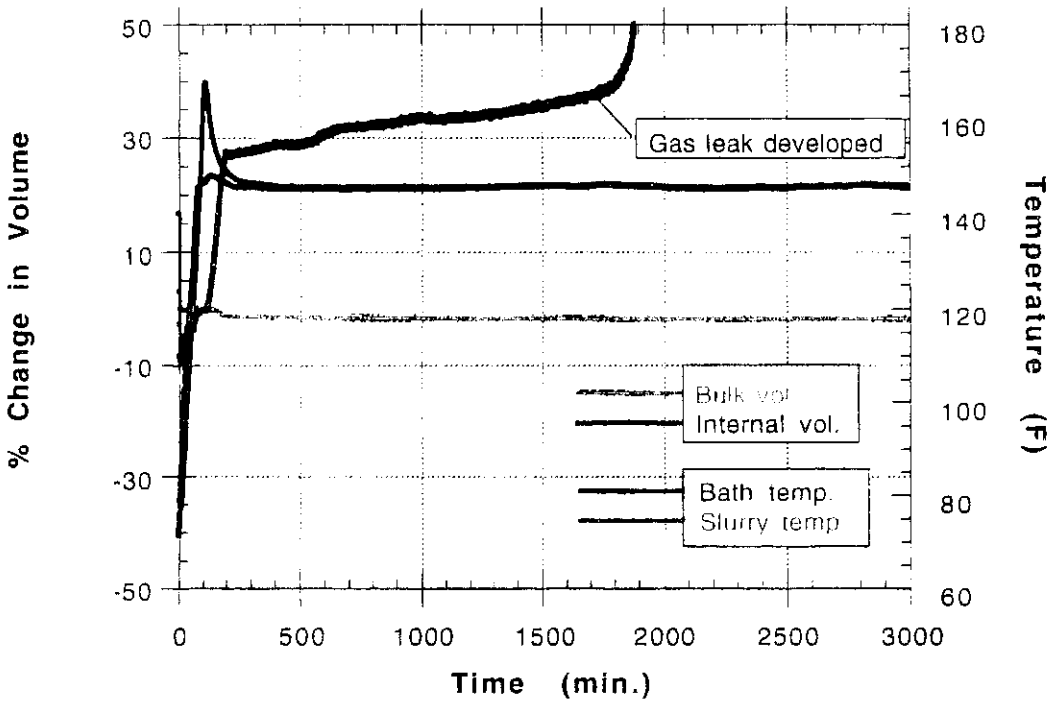

BFS with Dispersed Mud Test #12
Pressures vs. Time

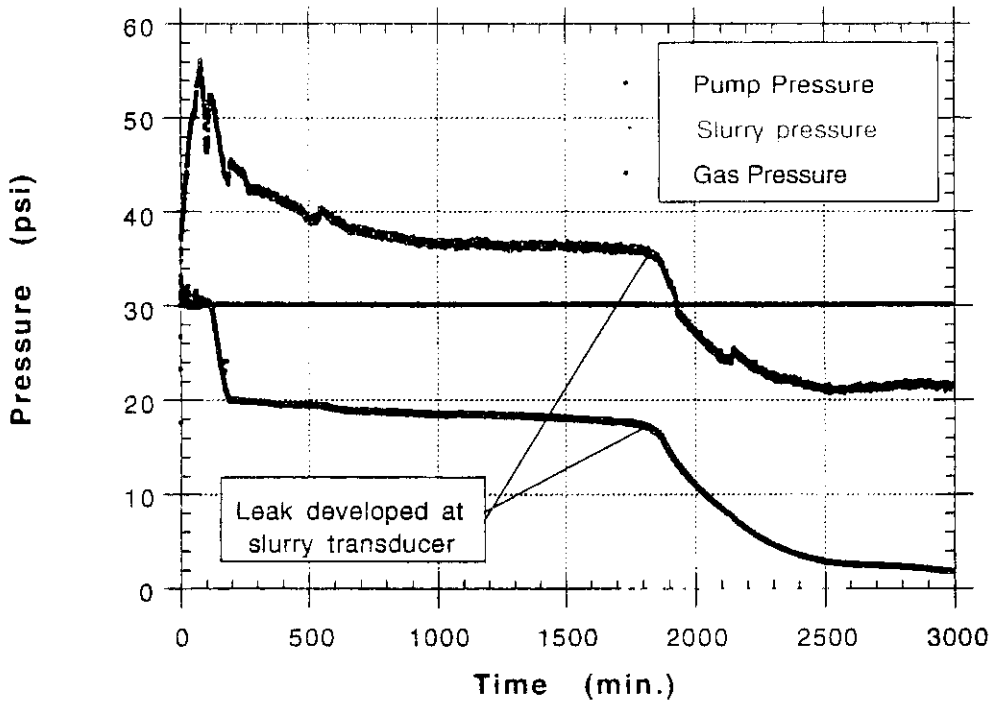

Figure 3.17b
BFS with Dispersed Mud Test #12
Expanded time scale for ΔV and T

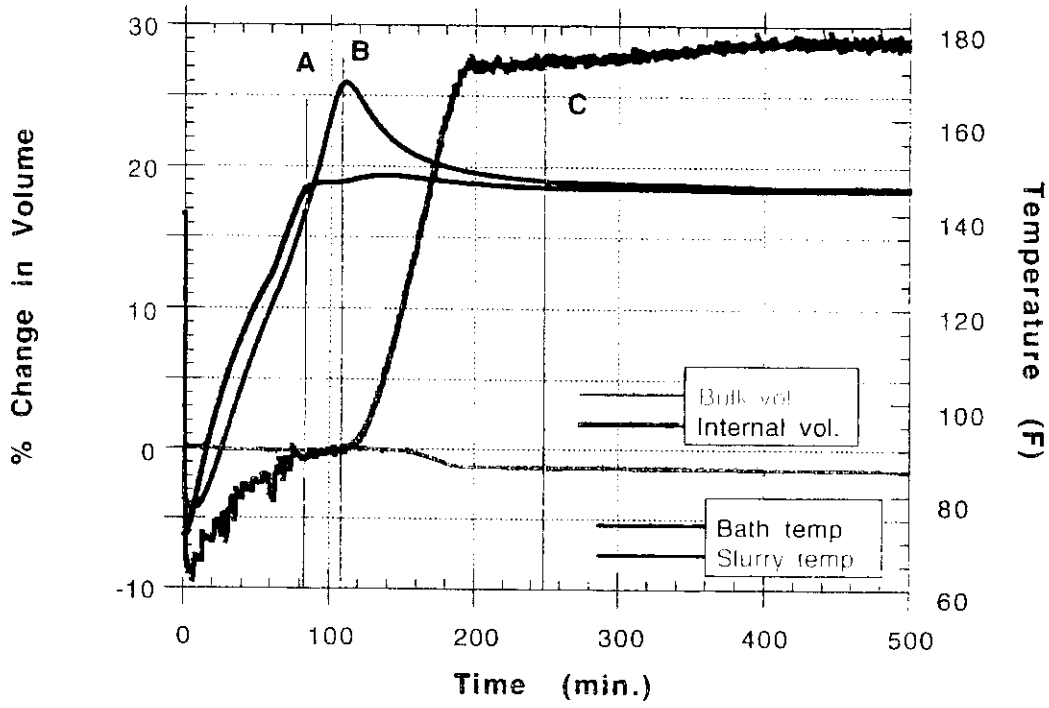

BFS with Dispersed Mud Test #12
Expanded time scale

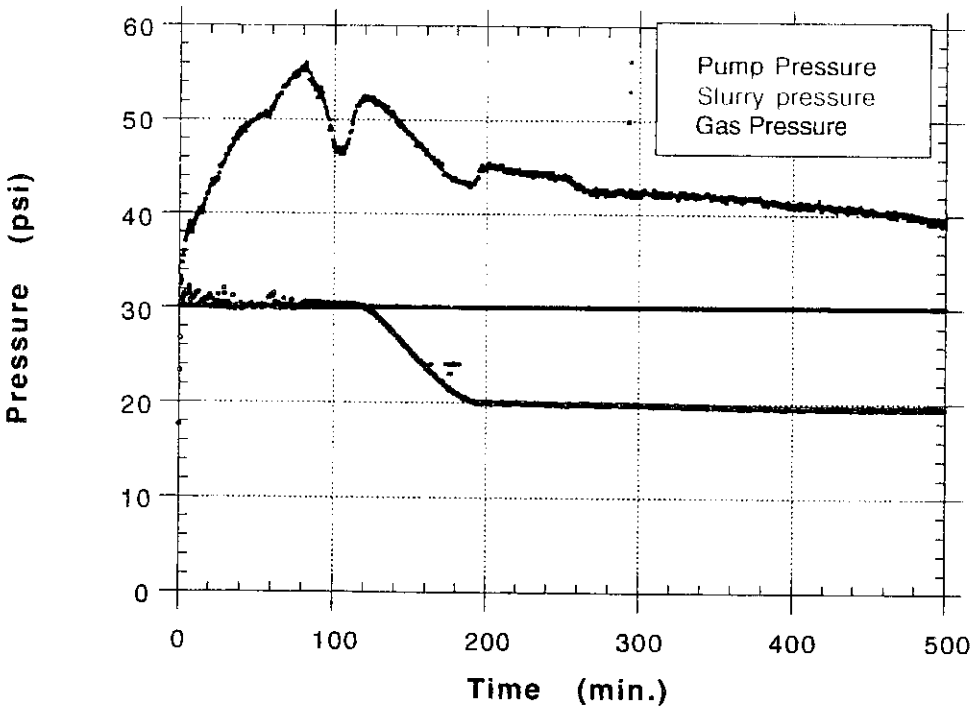

Figure 3.18
BFS with Dispersed Mud Test #12
Pump and Helium Volume Changes vs. Time

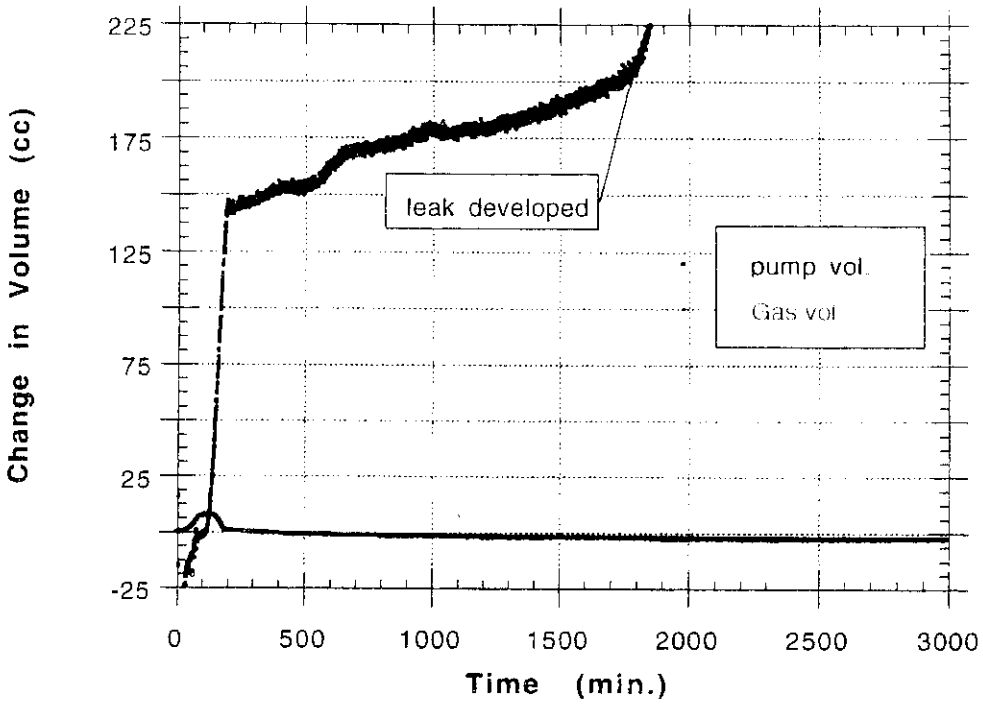

Figure 3.19
BFS with PHPA Test 13
Bulk and Internal Volume Changes with Time

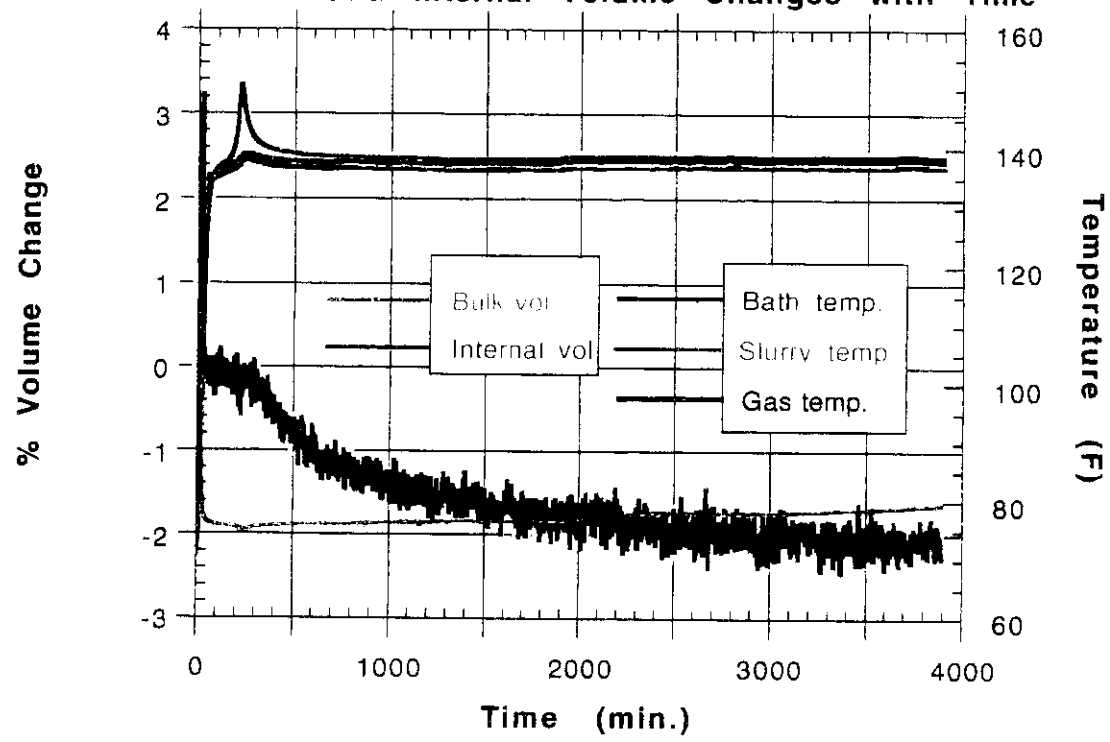

BFS with PHPA Test #13
Pressures vs. Time

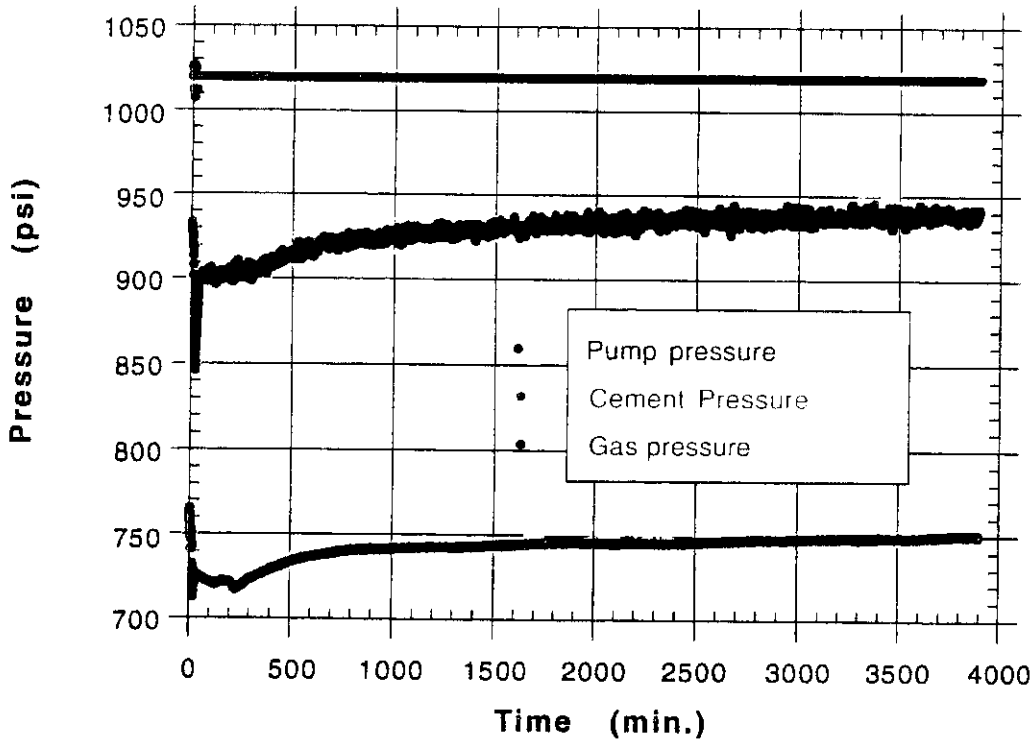

Figure 3.19b
BFS with PHPA Test #13
Expanded time scale for ΔV and T

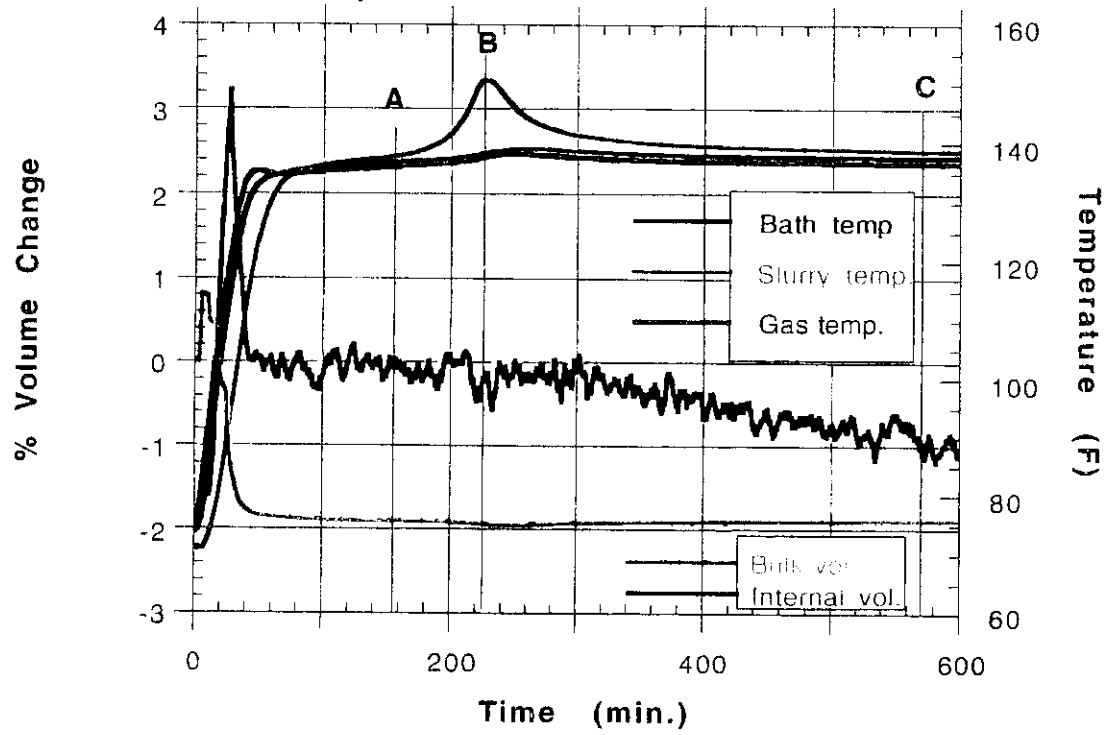

BFS with PHPA Test #13
Pressure vs. Time: Expanded Time Scale

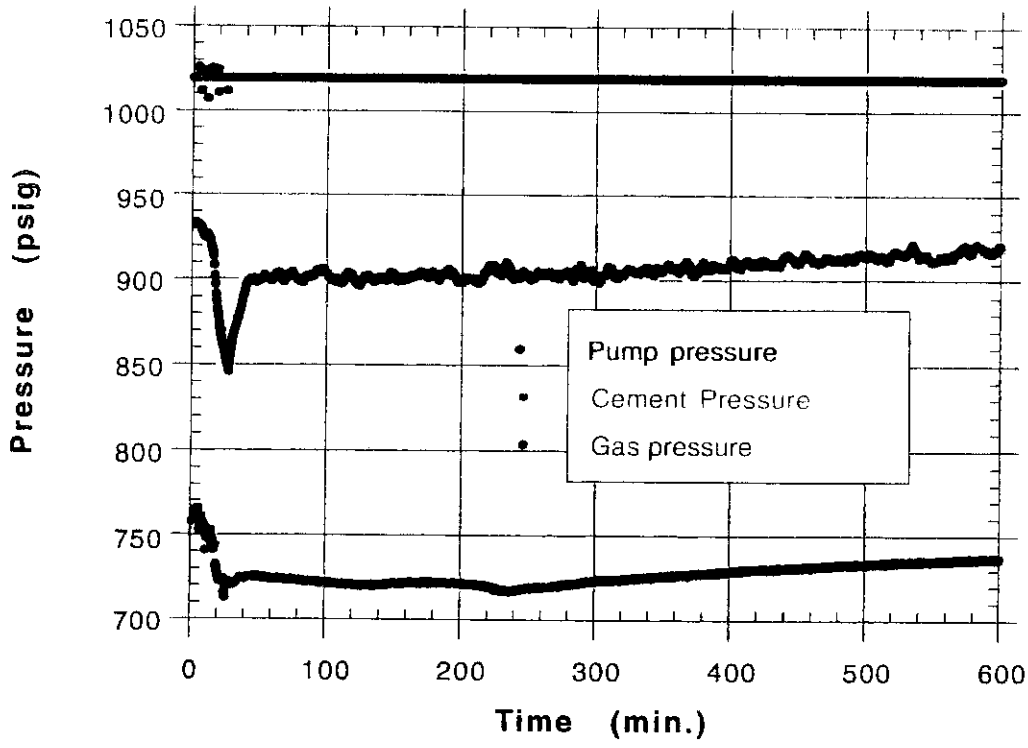

Figure 3.20
BFS with PHPA Test #13
Pump volume change vs. time

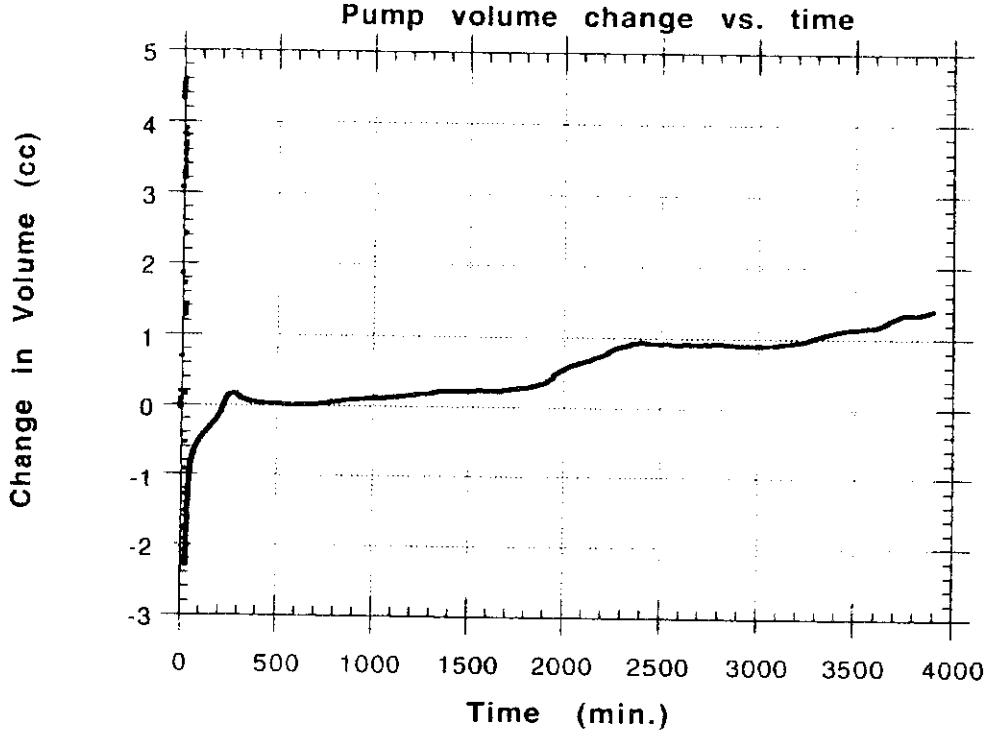

Figure 3.21
"Open" System Container Calibration
Volume-Temperature Curve for Water

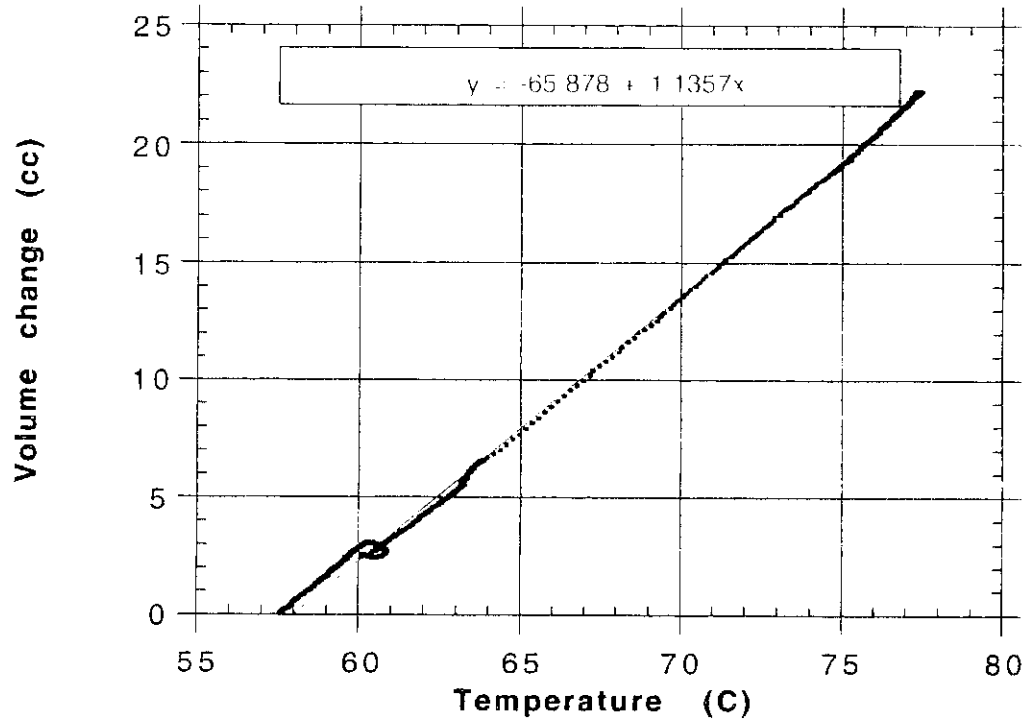

Figure 3.22
Thermo-couple Calibration

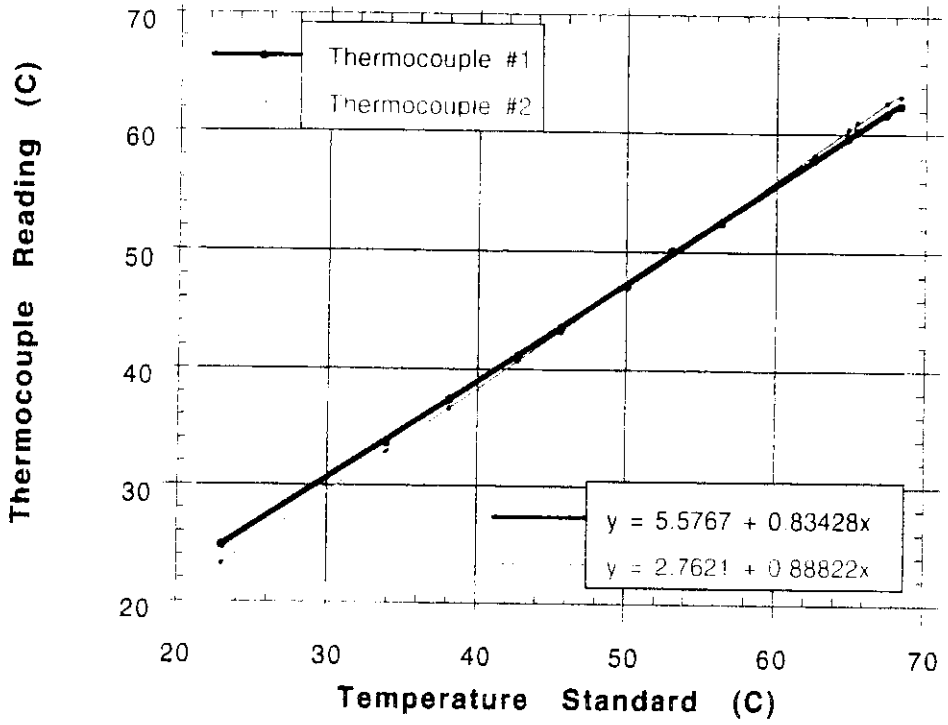

Figure 3.23
Tri-Cell Calibration
Water Volume vs. Temperture

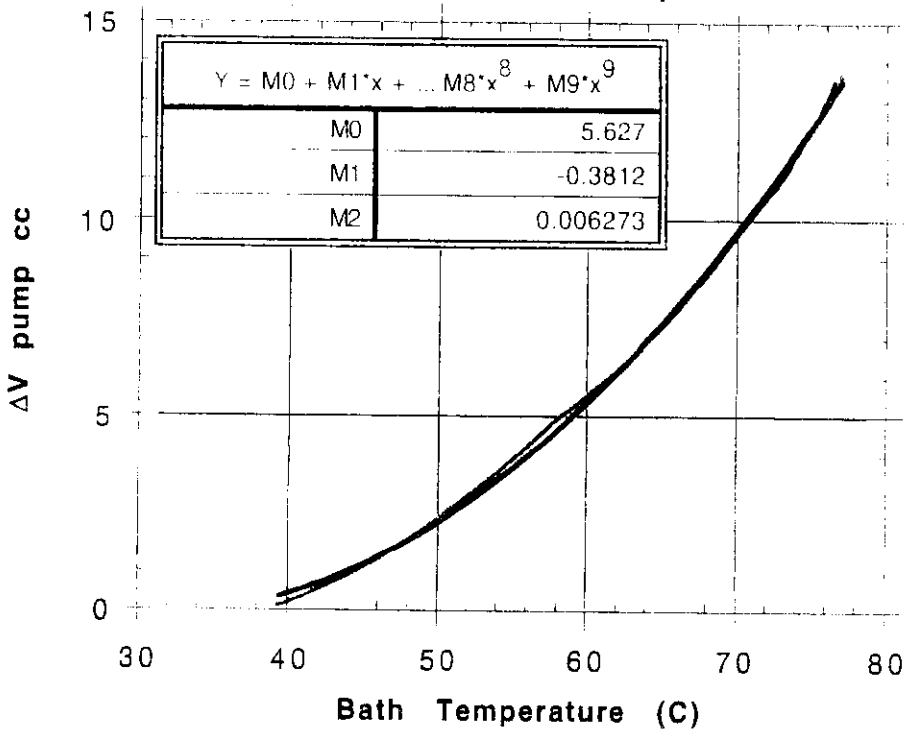

Figure 3.24
Tri-cell Helium Calibration
Pressure-Temperature Curve for Helium

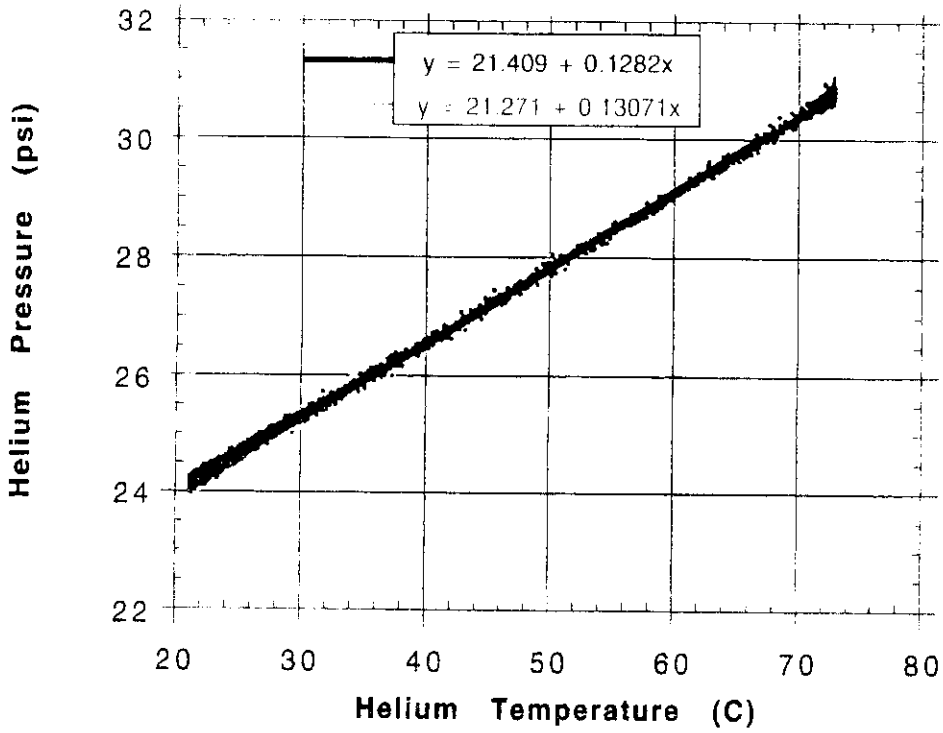

Figure 3.25

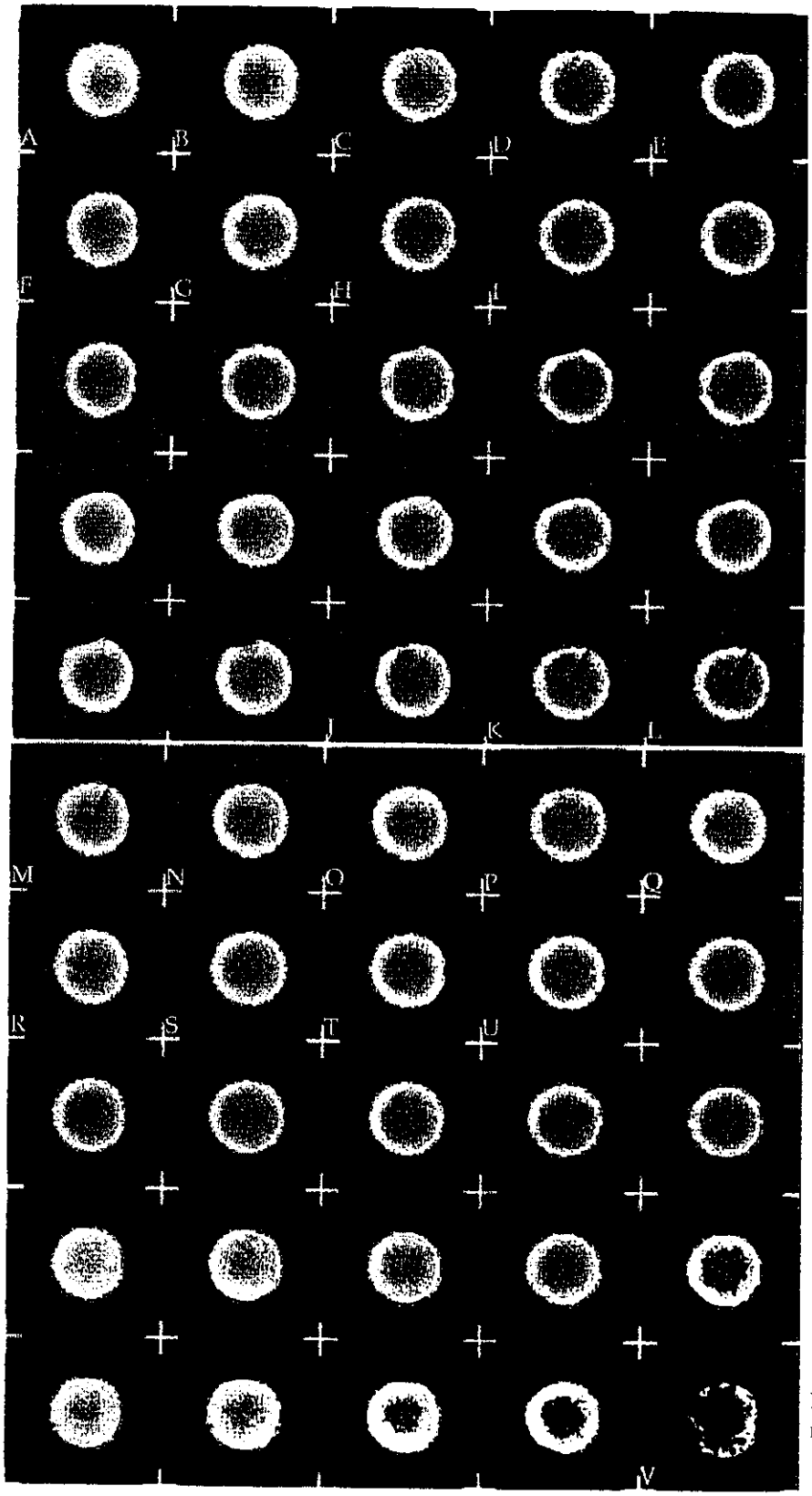

Images of CT scans of BFS with PHPA (test 10). Images A-I show a liquid filled void. Images J-M show the location of the thermocouple. Images J-U show another liquid filled void. The total void volume is approximately 2ml. Image V shows the sample/ hydromechanical restraint interface. The images are 0.125 inches apart.

Figure 3.26

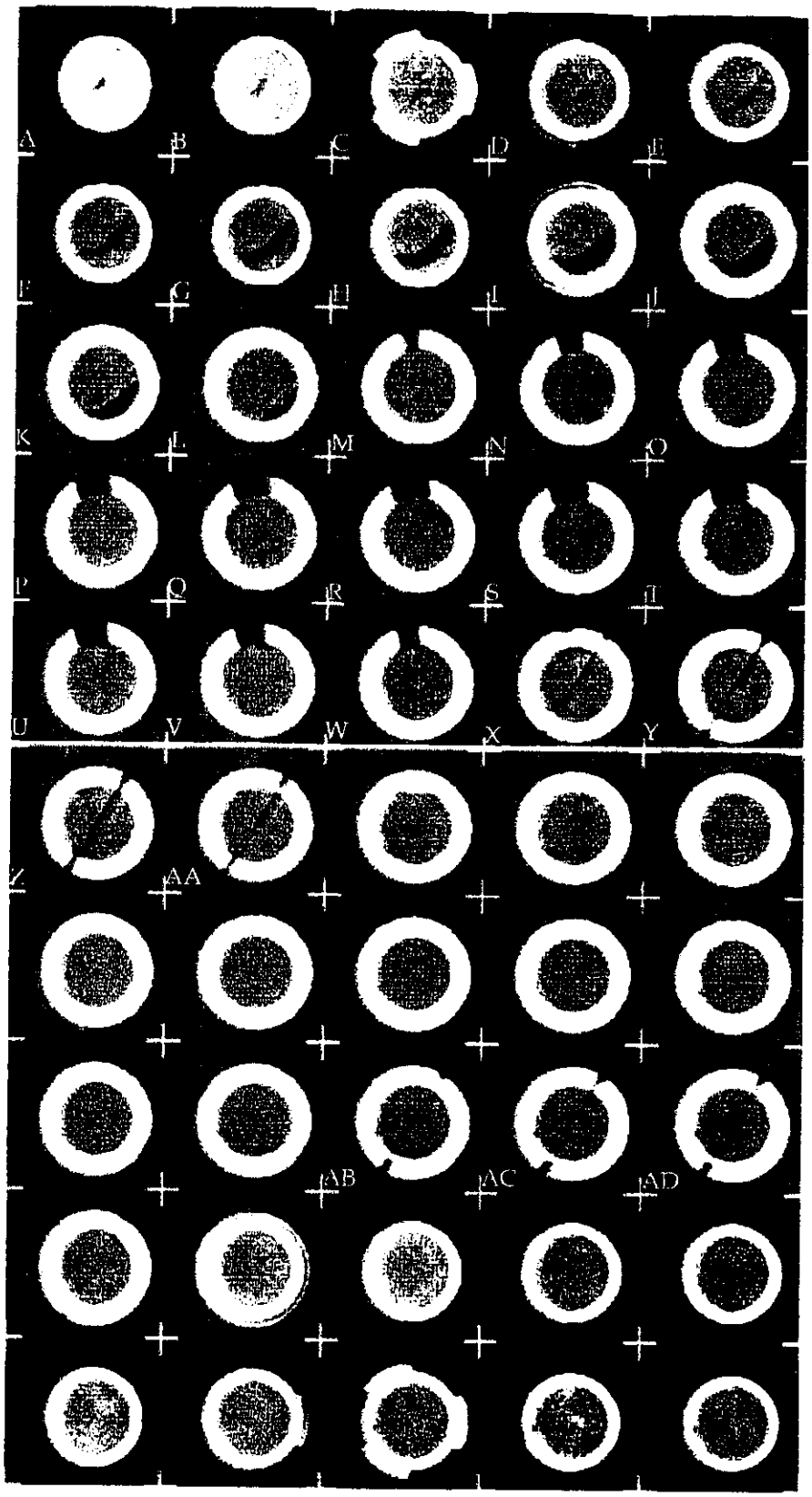

Images of CT scans of the Portland class G cement (test 11). Images A-M show a liquid filled void with an approximate volume of 8ml. The space in the white ring in images M-W show the location of the pressure transducer. Images X-AA show the location of the thermocouple. Images AB-AD showthe location of additional pressure ports. The images are 0.125 inches apart.

Figure 3.27

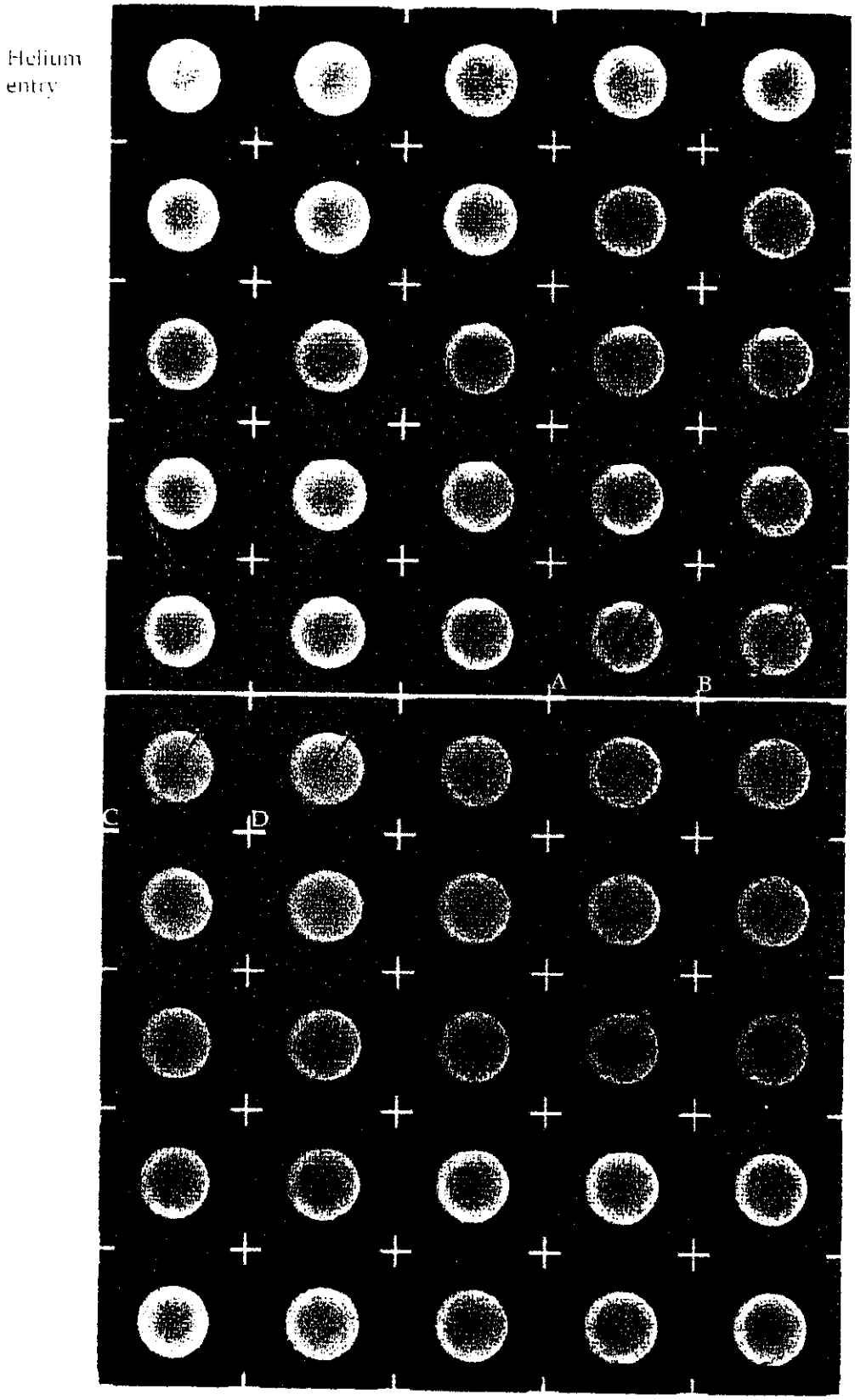

Images of CT scans of BFS with dispersed mud (test 12). Images A-D show the location of the thermocouple. The images are 0.125 inches apart.

Figure 3.28

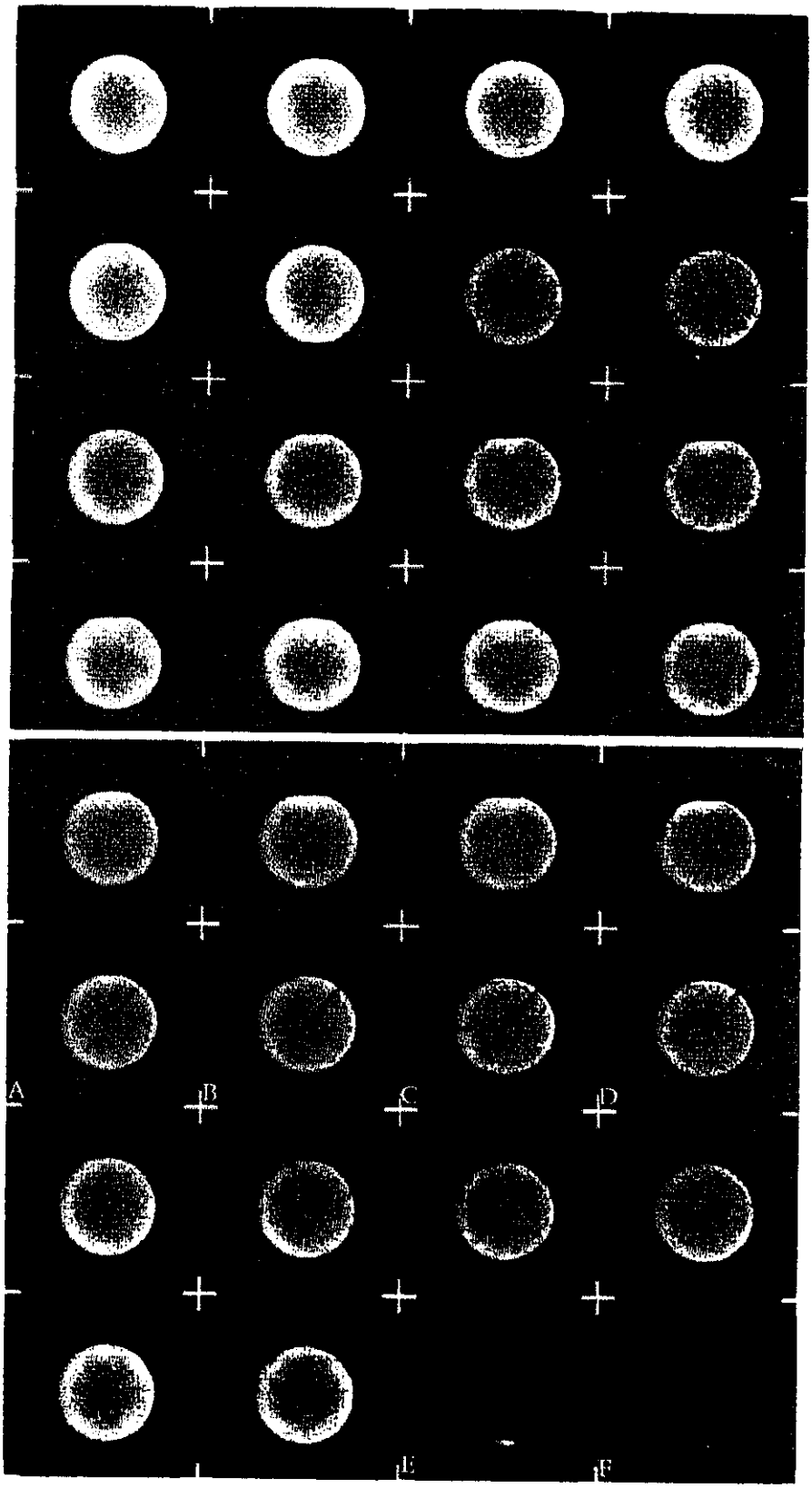

Images of CT scans of BFS with PHPA tested at 1000 psi (test 13). Images A-D show the location of the thermocouple. Images E-F show the beginning of a 70ml void which was probably formed during cell disassembly. The images are 0.125 inches apart.

Section 4 - Mechanical Stability

4.1 Summary

The compressive and tensile strengths of Blast Furnace Slag were compared with Portland Class G cement. For the BFS compositions used in this study, three out of eleven BFS samples showed comparable tensile strengths with Portland. The average tensile strength of Portland cement was 436 psi compared to 290 psi in the three PHPA prepared BFS. However, eight out of the eleven BFS samples failed at lower than 15 psi tensile stress.

The compressive strength of Portland cement was found to be approximately 15% greater than BFS with dispersed mud. The Portland cement also displayed a brittle-ductile transition, while BFS displayed only brittle behavior. The shear strength of Portland cement was slightly greater than BFS. Shear strength increased with increasing confining stress in the Portland cement, but remained constant in the BFS.

Long-term creep tests demonstrated all three systems exhibited axial "creep" phenomena over a 38 day period. Axial strain did not reach equilibration after 38 days. The axial strain rates of all the samples were low, but the BFS rates were approximately 50% lower than the Portland. Total axial strains after this time were between 1% - 1.5%. None of the samples failed as a result of the "creep" response.

Attempts to compare fracture toughness failed because of the inability to extract BFS specimens from their molds. All ten BFS samples broke apart upon removal, while the Portland samples did survive extraction from their molds.

4.2 Objectives

The purpose of this section of the project is the measurement and comparison of the final set, load-bearing elastic and "creep" properties of BFS to Portland cement. The tests involve measurements of the compressive and tensile strengths of prepared specimens. "Creep" tests were performed to compare the long term response of BFS with Portland cement that were subjected to stresses close to the yield point of the materials.

4.3 Experimental Procedures

4.3.1 Tensile Strength

ASTM standard briquette samples were prepared for these tests. The samples were prepared by pouring a slurry mixture into a mold and allowing it to cure in a water bath at temperature. The mold was coated with a non-reactive grease that reduced adhesion of the final set cement to the surface of the mold. Sample dimensions were nominally three inches long by one inch thick. The samples were allowed to reach final set for at least 30 hours before removal from the mold. All samples prepared for these tests survived removal from the mold. Once removed, the samples were stored in water until time of testing.

The tensile strength was measured using an Instron 4507 tensile machine. The tests were performed by Huntingdon Engineering & Environmental, Inc. The tests were conducted at room temperature. Once mounted in the jaws of the tensile machine, a constant strain rate of 0.2 inches/min. was applied to the sample and the tensile stress and displacement recorded on strip chart recorder. The test terminated at failure.

A total of three Portland cement, five BFS with dispersed mud, and six BFS with PHPA samples were tested.

Attempts were made to measure fracture toughness using a standard "notch" test on bar-shaped samples. This part of the study had to be abandoned after all ten BFS samples broke apart upon removal from their molds. All Portland samples did survive the extraction process.

4.3.2 Compressive Strength and Shear Failure

The compressive strengths of each cement type were measured using a rock mechanics load frame and confinement vessel. Right cylindrical samples were prepared from nylon molds. The sample dimensions were nominally three inches in length by 1.5 inches in diameter. The samples were cured for at least thirty hours in a water bath at 150 °F and 3000 psi. The samples were pressed from their molds and stored in water until time of testing. A CT scan of the samples were made to screen samples for internal flaws.

Each sample was first sleeved in viton rubber before placing the sample between two stainless steel platens. The viton serves as an impermeable barrier to the confining pressure fluid. Three axial and two radial Linear Variable Differential Transformers (LVDT's) were mounted and used to measure the axial and radial displacements. Samples were stressed at a constant strain rate of 10×10^{-6} per second. Even though the stainless steel platens, that contacted the cement samples and used to apply the axial load, had fluid distribution ports open to the atmosphere, the low permeability of these samples probably prevented true drained condition tests. Axial displacement and stress were recorded every two seconds.

Three identical samples for each cement type were prepared so that the Mohr-Coulomb envelope for compressive strength could be generated. Each sample was first loaded under hydrostatic pressure to a specified test confining load. Afterward, the confining stress was held constant, while continuing to apply the axial load. The confining stress for each sample was different. The set of confining stresses were nominally 500 psi, 1000 psi, and 3000 psi.

4.3.3 Long Term "Creep" Tests

These tests were undertaken to determine whether the BFS exhibits excessive "plastic" deformation (compared to Portland cement) under changing or long term loads. These tests involved measuring the change in length of each sample over time at a constant stress.

One sample of each slurry system were prepared in an identical manner to the samples prepared for compressive strength. Each sample was trimmed and its ends polished to ensure flatness and parallelism. The samples were maintained in a wet condition throughout the sample preparation process.

Each sample was placed inside a Viton sleeve and loaded into a triaxial stress confinement vessel. Each end of the sample was placed in contact with a stainless steel flow distributor. The pore lines of these vessels were open and allowed the "creep" test to proceed under drained conditions, even though fluid production was not expected. Each sample was loaded under an identical stress path. Initially, the stress was increased from ambient pressure to 1000 psig under a hydrostatic load. Once at 1000 psig, the radial stress was held constant while the axial load was increased to 4000 psig. The stress rate in each case was increased at about 7 psig per minute. The stresses were then maintained constant while the axial displacements of each sample were monitored and recorded. The length changes were measured with dial indicator gauges that have a precision of 0.0005".

This choice of stress state was based on the results of the compressive strength tests. At 1000 psig confining and 4000 psig axial stress, this stress state is close, but does not exceed, the yield point of either the BFS or Portland samples. The "creep" test was conducted over a 38 day period.

4.4 Results

4.4.1 Tensile Strength

Tables 4.1 through 4.3 contain the results of the tensile tests on the Portland Class G cement and the BFS cements. The Portland cement samples are designated with "P", the BFS samples with dispersed mud with "SD", and BFS samples with PHPA with "SPH". These tables contain the dimensions of each sample, the maximum load at failure and the tensile strength. The tensile strength was calculated by dividing the maximum load by the cross-sectional area of the sample.

All BFS and Portland cement samples survived extraction from the mold.

The Portland cement exhibited the greatest tensile strength. The average value was 436 psi with a standard deviation of 45 psi. All BFS with dispersed mud samples exhibited very low tensile strengths ranging from less than 3 psi to 13 psi. The first batch of the BFS with PHPA samples exhibited tensile strengths comparable with the Portland cement. Their average value was 290 psi. The second batch failed at less than 3 psi.

Figure 4.1 displays all the samples after failure. Many samples did not break apart at their narrowest dimension. These samples also tended to fail at low stress.

TABLE 4.1
Tensile Strength in Portland Cement
30 hour curing time at 150 °F & atmospheric pressure.

ID	Width in.	Height in.	Length in.	Area sq. in.	Max. Load, lbs.	Tensile Strength psi
P1	1.001	1.003	3.077	1.004	486.7	484.8
P2	1.003	1.013	3.078	1.016	402.7	396.3
P3	1.002	1.033	3.070	1.035	443.6	428.6

TABLE 4.2
Tensile Strength in BFS with Dispersed Mud
30 hour curing time at 150 °F & atmospheric pressure

ID	Width in.	Height in.	Length in.	Area sq. in.	Max. Load, lbs.	Tensile Strength psi
SD1	1.000	1.025	3.070	1.025	<3	<2.93
SD2	1.001	1.035	3.074	1.036	<3	<2.88
SD3	1.001	1.035	3.075	1.036	8.27	7.99
SD4	1.000	1.030	3.070	1.030	<3	<2.91
SD5	0.998	1.057	3.072	1.054	13.62	12.91

TABLE 4.3
Tensile Strength in BFS with PHPA
30 hour curing time at 150 °F & atmospheric pressure

ID	Width in.	Height in.	Length in.	Area sq. in.	Max. Load, lbs.	Tensile Strength psi
SPH1	1.003	0.964	3.072	0.967	269.9	279.1
SPH2	1.004	0.992	3.070	0.996	303.4	304.6
SPH3	1.000	1.004	3.073	1.004	298.3	297.1
SPH4	1.003	0.989	3.073	0.992	<3	<3
SPH5	0.999	1.019	3.070	1.080	<3	<3
SPH6	0.997	0.885	3.079	0.882	<3	<3

4.4.2 Compressive Strength

Only compressive strength tests on the BFS with dispersed mud were completed because of the inability to either remove the BFS with PHPA samples from their molds or once removed they fell apart in their water bath.

The results for the BFS with dispersed mud are shown in Figures 4.2 and 4.3. The first figure displays the axial stress vs. axial strain for all three samples. The confining stress (Pc) is shown in the legend. The compressive strength is defined here as the point of maximum axial stress. These values are also displayed in the figure. The compressive strength increased with confining stress as expected.

The second figure (4.3) displays the differential stress vs. axial strain. The differential stress is the difference between axial and confining stresses. The differential stress is also equal to twice the maximum shear stress in the sample. It is interesting to note that the differential stress at failure did not increase with confining stress but remained relatively constant with an average value of 4420 psi. All BFS samples exhibited brittle behavior, characterized by the material's inability to resist increasing load. The region of brittle behavior is observed along the stress-strain curve past the yield point where stress decreased with increased strain.

For comparison, the results of the Portland Class G cement are shown in Figures 4.4 and 4.5. These figures display the same information as shown in Figures 4.2 and 4.3. Like BFS, the compressive strength increased with confining stress. Unlike BFS, the Portland cement samples display a brittle-ductile transition somewhere near a confining stress of 1075 psi. Ductile behavior is characterized by a material's ability to resist increasing load beyond its yield point. At a confining stress of 555 psi, Portland cement exhibited brittle behavior. At a confining stress of 3140 psi, Portland cement exhibited ductile behavior and work hardening. Work hardening is seen as the positive slope portion of the stress-strain curve beyond the yield point.

The maximum differential stress also increased slightly with confining stress, in contrast to the BFS. The maximum differential stress ranged from 5100 psi to 6260 psi.

4.4.3 Long Term "Creep" Tests

The lengths and diameters of each sample are shown in Table 4.4.

Table 4.4 Sample Dimensions

Sample ID	Length (in.)	Diameter (in.)	Strain Rate
BFS-Dispersed Mud	1.540	1.560	1.39×10^{-6}/hr.
BFS-PHPA	1.870	1.538	1.58×10^{-6}/hr.
Portland	1.331	1.545	2.36×10^{-6}/hr.

The history or profile of the change in length of each sample is displayed in Figures 4.6 and 4.7. Most of the deformation occurs during the initial increase in axial and radial stresses and is attributed to the elastic response of the material. After the axial load reaches 4000 psig, the profiles shows "creep" behavior occurring in all the samples. Figure 4.6, which displays the displacement profile of each sample, seems to imply that Portland and BFS with PHPA are more similar in properties than the BFS with dispersed mud. This is misleading because the lengths of each sample were different. Because length contraction of a material is dependent on sample dimensions, axial strain (change in length per sample length) is the appropriate quantity for comparing the effects of loads on deformation.

Figure 4.7 shows the axial strain history of each sample. Each strain profile is divided into three regions: (A) region of linear response to stress; (B) short-term non-linear creep region; (C) long-term linear creep region. The long-term strain rates of each sample are displayed in Table 4.4. The strain rates were calculated from the slope of a fitted linear function through data from region C. This figure shows that all samples exhibit long-term creep behavior. Also, note the BFS profiles are more similar in magnitude and slope than the Portland cement. Upon inspection of the samples when removed from the vessel, no sample failed. The continual deformation of each sample never reached equilibrium, even after 38 days.

The magnitude of the total axial strains in BFS were lower than that for Portland cement and implies that the BFS was stiffer than the Portland cement under these stress conditions.

Figure 4.1
Post Failure Photos of Tensile Strength Samples

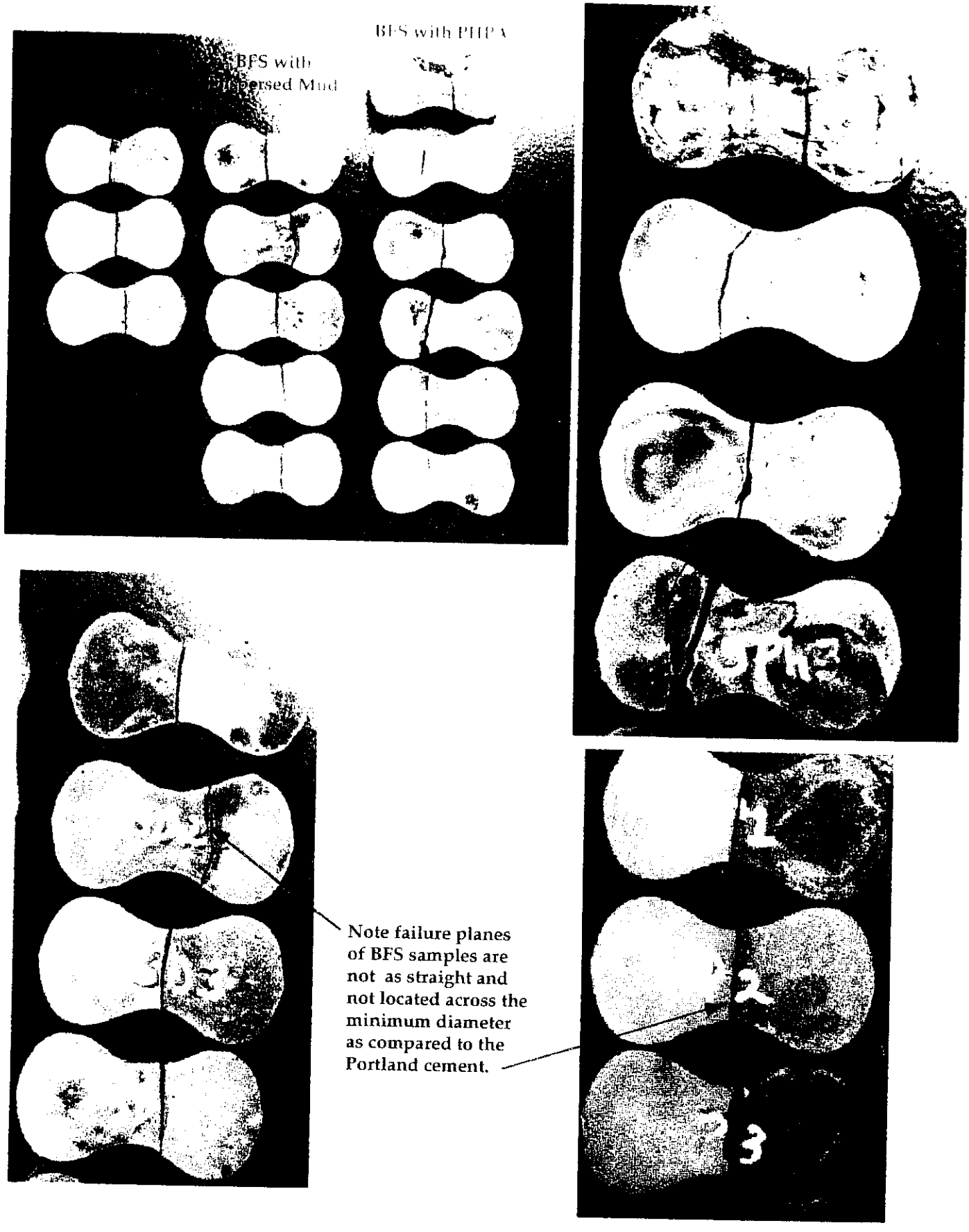

Figure 4.2
BFS with Dispersed Mud
Compressive Strength Tests

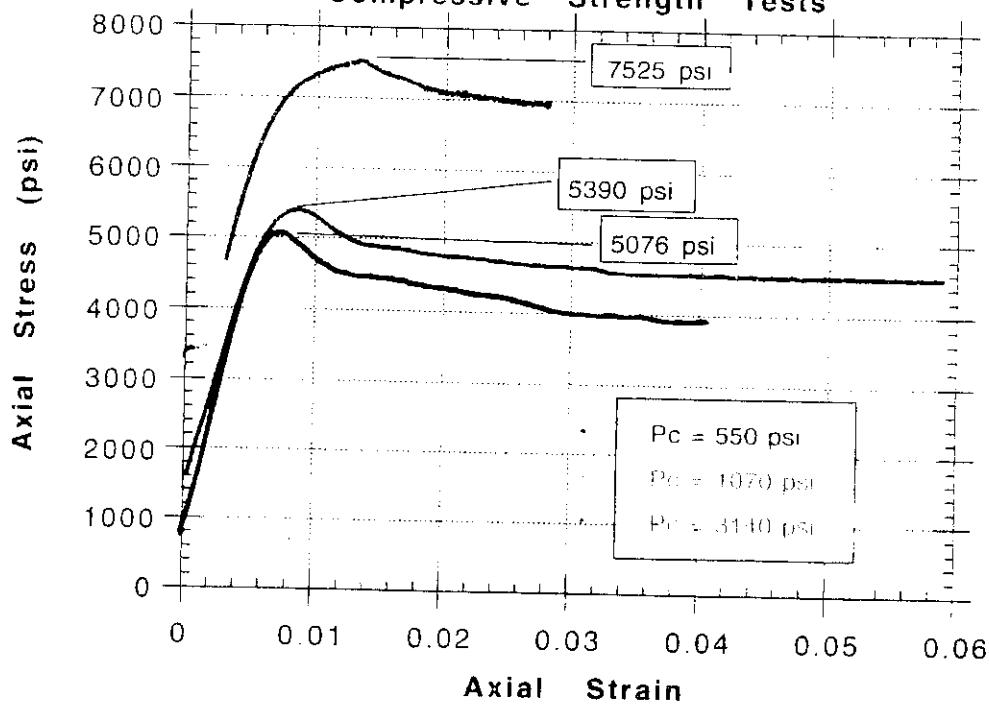

Figure 4.3
BFS with Dispersed Mud
Differential Stress vs. Axial Strain

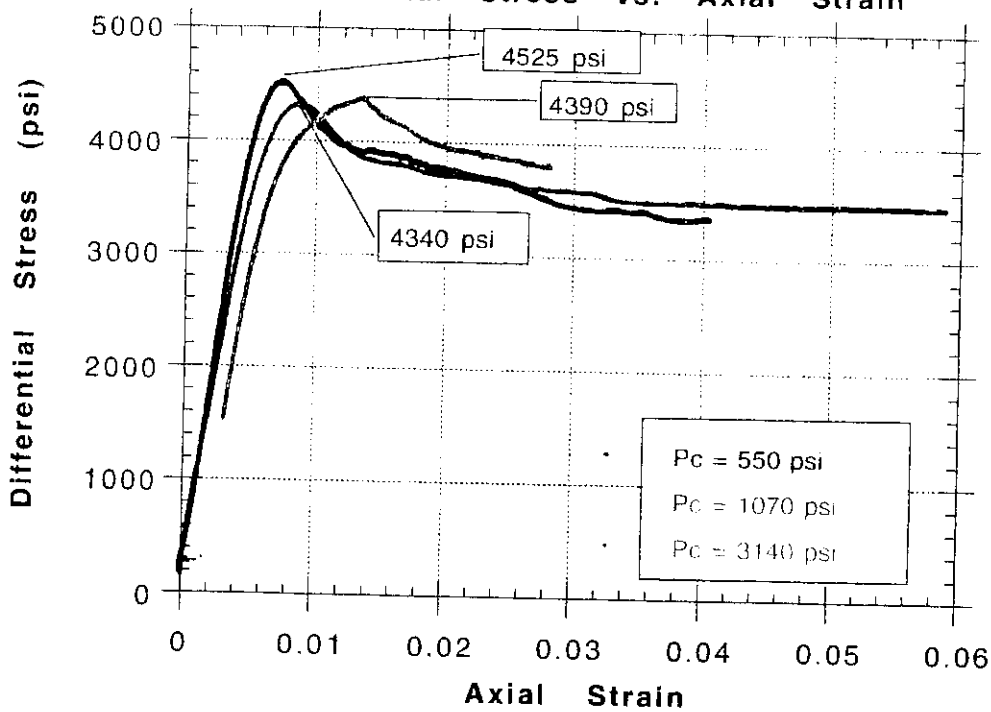

Figure 4.4
Portland Class G Cement
Compressive Strength Tests

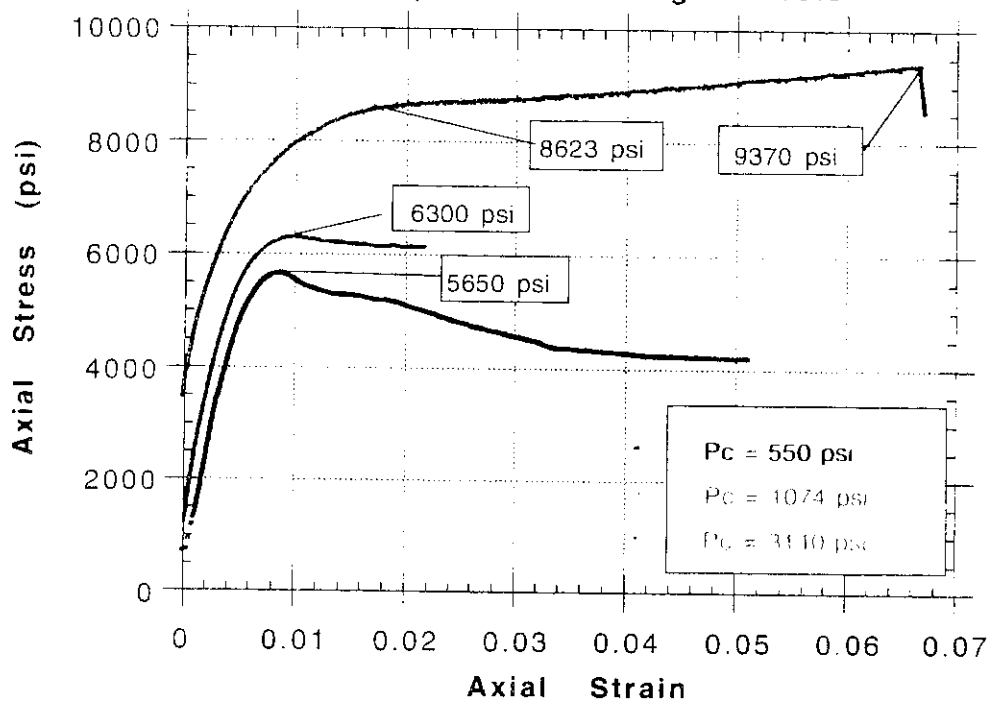

Figure 4.5
Portland Class G Cement
Differential stress vs. Axial Strain

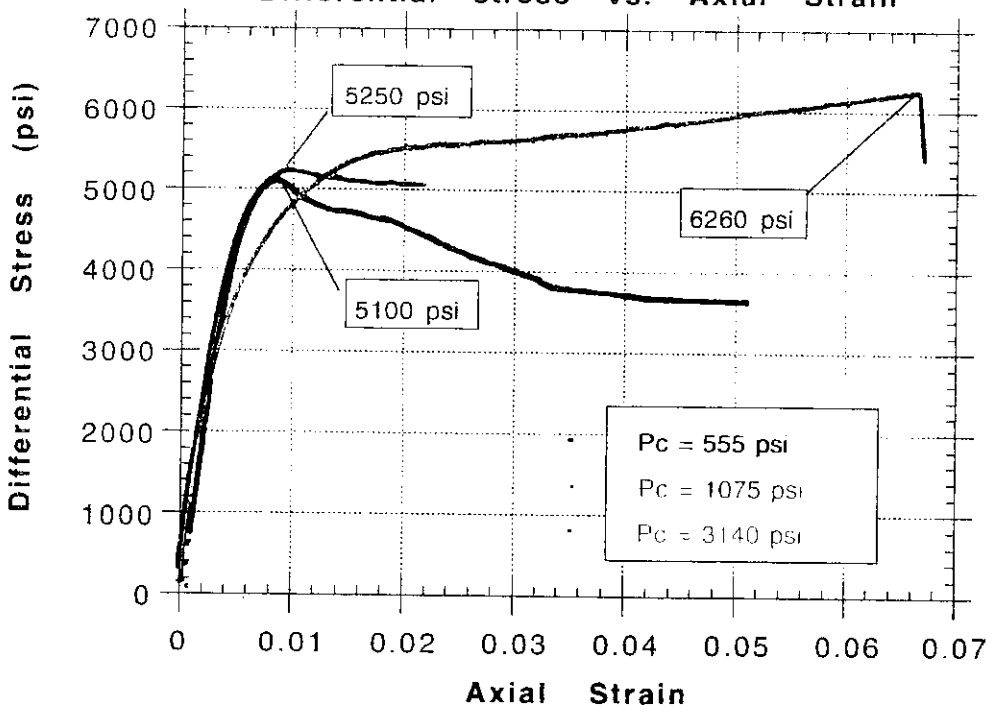

Figure 4.6 Long Term "Creep" Test
Comparison of length contraction between
BFS and Portland Cement

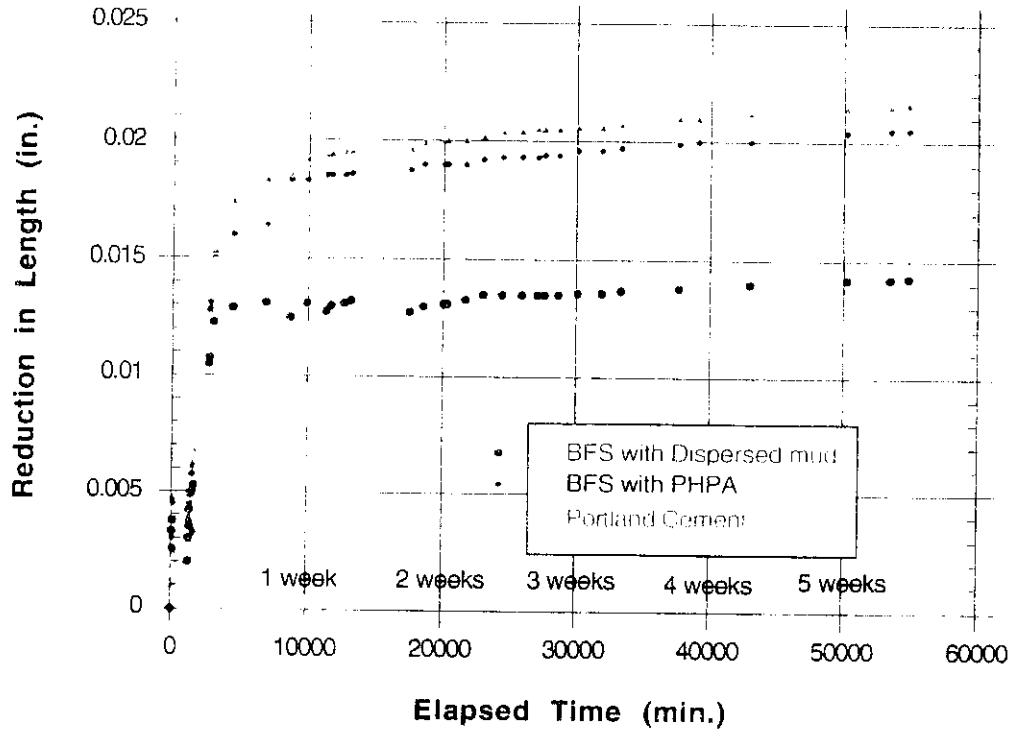

Figure 4.7 "Creep" Test
Comparison of axial strains between
BFS and Portland Cement

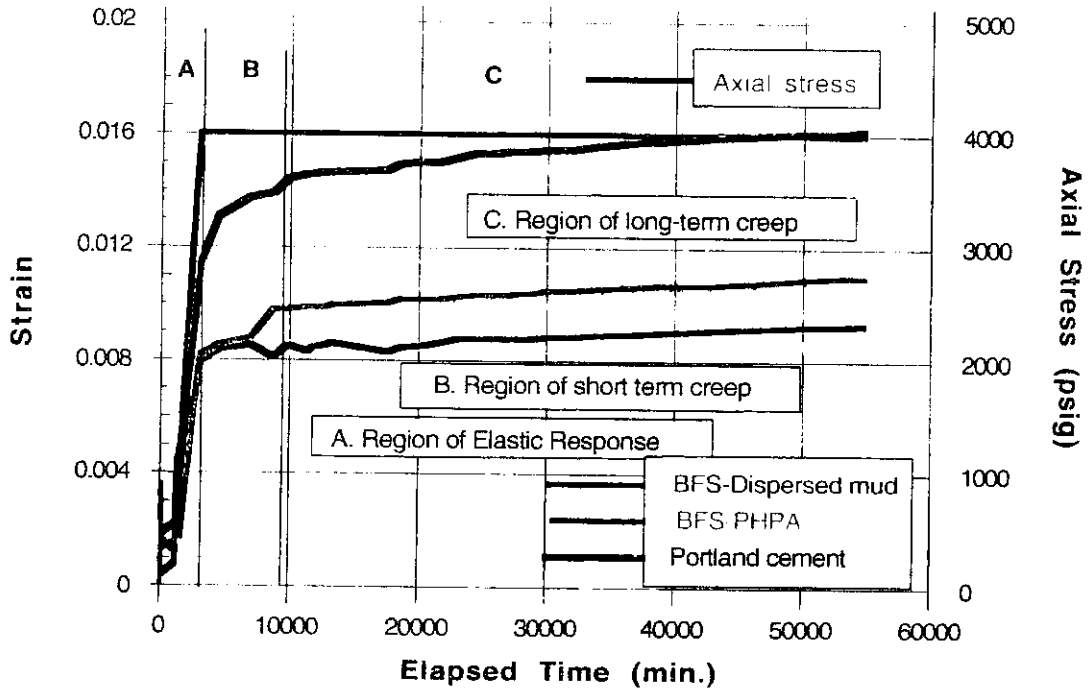

5.3 Technical Approach

The data base provided by the research program "Performance Studies of Mud Converted to Cement (BFS)" has been processed by aid of multivariate regression analyses. The aim of the analyses was to find relationships between the amount of slag added and such parameters as base mud density, diluted density, dispersant, MBT, plastic viscosity, yield point, gel strength, and mud solids.

The purpose of the multivariate approach was to achieve the narrowest possible confidence interval by elimination and (or) grouping of the above parameters. A standard regression analysis software package has been used.

5.4 Results

The ability to develop an advisory or expert system is based on having a large amount of data drawn from, in this instance, field condition results and laboratory data, including extensive interaction with those experienced in the 'art'. Little success has been achieved in meeting the objective of developing an advisory system applicable to BFS cements. The amount of data anticipated and made available by the members skilled in the 'art' of BFS cements has been insufficient to develop a meaningful data set as the basis of an advisory system.

However, even with the paucity of data made available by members and by the process of elimination of the "noisy" parameters, three parameters were deduced as having relevant relationships to a rudimentary system using regression analysis. These were namely: mud base density, dilution to base mud (% volume), and the amount of dispersing. This process resulted in relationships among these three parameters and the amount of slag added. In the equations below the following notations used were:

Y = the amount of slag added to 1 bbl of B, lbs

X_1 = mud base density, lbs/gal

X_2 = dilution to base mud, % volume

X_3 = dispersant added to 1 bbl's of B, lbs

The following equations have been obtained for the various mud systems:

Sea Water Lime Mud

$$Y = 22 X_1 + 1.9 X_2 + 76 X_3 \quad (1)$$

Fresh Water Lime Mud

$$Y = 10 X_1 + 3.7 X_2 + 86 X_3 \quad (2)$$

Sea Water Gel/Chemical Mud and Sea Water PHPA Mud

$$Y = 20 X_1 + 2.2 X_2 + 63 X_3 \quad (3)$$

Fresh Water Gel/Chemical Mud and Fresh Water PHPA Mud

$$Y = 11.3 X_1 + 2.14 X_2 + 105 X_3 \quad (4)$$

Salt (NaCl) Saturated Mud

$$Y = 14.7 X_1 + 1.2 X_2 + 44 X_3 \quad (5)$$

These equations predict the amount of slag to be used in a slurry may give an indication on the combination of mud base density (X_1), amount of dilution (X_2), and dispersant (X_3).

5.5 Recommendations

In our view the above results should not be used as a statistical predictive tool for a slurry design for two reasons: (a) the confidence interval for some of the coefficients in the equations listed above can be fairly wide (up to 50% of the value of the coefficient for 95% of probability), and (b) a number of important parameters had to be eliminated to reduce the noise to a manageable level.

However, as the amount of data available increases with time it is expected that an improvement in the multivariate regression analysis approach will become feasible.